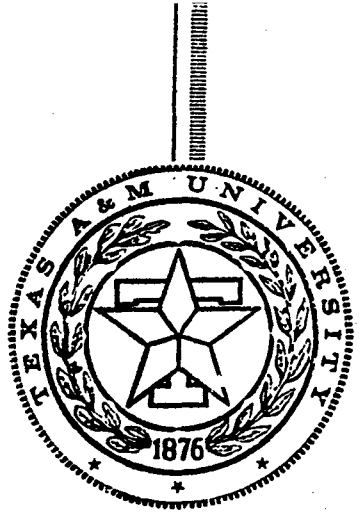

TEXAS
TRANSPORTATION
INSTITUTE

TEXAS
HIGHWAY
DEPARTMENT

COOPERATIVE
RESEARCH

DESIGN PROCEDURE COMPARED TO FULL-SCALE TESTS OF DRILLED SHAFT FOOTINGS

in cooperation with the
Department of Transportation
Federal Highway Administration
Bureau of Public Roads

RESEARCH REPORT 105-3

STUDY 2-5-67-105

DESIGN OF FOOTINGS FOR MINOR SERVICE STRUCTURES

DESIGN PROCEDURE COMPARED TO FULL-SCALE TESTS OF DRILLED SHAFT FOOTINGS

By

Don L. Ivey

and

Wayne A. Dunlap

Research Report Number 105-3

Design of Footings for Minor Service Structures

Research Study Number 2-5-67-105

Sponsored by

THE TEXAS HIGHWAY DEPARTMENT

in cooperation with

The U.S. Department of Transportation
Federal Highway Administration
Bureau of Public Roads

February 1970

TEXAS TRANSPORTATION INSTITUTE

Texas A&M University

College Station, Texas

ACKNOWLEDGEMENTS

This research was conducted under an interagency contract between the Texas Transportation Institute and the Texas Highway Department. It was sponsored jointly by the Texas Highway Department and the Bureau of Public Roads. Liason was maintained through Mr. H. D. Butler, contact representative for the Texas Highway Department, and through Mr. Robert J. Prochaska of the Bureau of Public Roads.

The analysis of footings using the IBM 7094 was carried out by Mr. Harry L. Smith. The fabrication and instrumentation of all tests reported was accomplished by Mr. Bill D. Ray and Mr. M. B. Robertson.

The opinions, findings, and conclusions expressed in this publication are those of the authors and not necessarily those of the Bureau of Public Roads.

IMPLEMENTATION STATEMENT

The results of this research have now reached the point at which full implementation can be achieved. The study was begun because of the belief among some Texas Highway Department engineers that the present method of designing drilled shaft footings to resist overturning loads was overly conservative. This belief has now been confirmed.

Research Report 105-3, the last of the reports dealing exclusively with the effects of relatively short term, static overturning loads, compares the theory developed and correlated in Research Reports 105-1 and 105-2 with full-scale tests of drilled shaft footings. A new design procedure is presented which is extremely easy to apply, since it is based on the use of design curves rather than the cumbersome application of equations. The "Tentative Design Procedure" is given in Research Report 105-3 on pages 45 and 46 and an example problem is worked on page 49.

The design curves, also included in the report, allow the selection of a particular size footing as a function of the loads acting on the footing and the characteristics of the soil. The methods of determining the desired soil parameters limit to some degree the full application of the design curves by some Texas Highway Department Districts. The design must be based on an estimate of the cohesion and angle of shear resistance of the soil. The most desirable way of determining these parameters is by use of the triaxial test. Since only a few THD Districts make wide use of this test method, a section of Research Report 105-3 has been devoted to more approximate methods which include THD and Standard penetrometer tests. The use of these tests will probably dictate some conservatism on the part of the designer, but will still represent a considerable improvement in our current methods. Under the direction of Mr. Leon Hawkins, engineers in D-18 are presently studying this report, and the use of penetrometer tests to estimate the necessary soil parameters.

TABLE OF CONTENTS

LIST OF FIGURES

LIST OF TABLES

ABSTRACT

This report brings together the results of model tests, full-scale tests, and a theoretical development; and proposes a usable design procedure for drilled shaft footings subjected to overturning loads. The theory is significantly more sophisticated than the older more conservative theory, but is adapted to allow a very simple design procedure. It is applicable for static load conditions and is based on the soil parameters of cohesion, angle of shear resistance, and unit weight.

SUMMARY

A theory which will predict the ultimate resistance of a drilled shaft footing to overturning loads was presented in Research Report 105-1 and was correlated with model tests reported in Research Report 105-2. In this report the results of full-scale tests on drilled shaft footings are presented and compared to a "Tentative Design Procedure" based on the previously published theory. Design curves are given as a part of the design procedure, which result in easy application of the theory. The report also includes an example problem and a section on estimating the soil parameters necessary for the design of these footings. The results of this study have now reached the stage where full implementation can be achieved.

INTRODUCTION

The ultimate test of any theoretical solution of an engineering problem is the adaptation of the theory to a usable design procedure and the correlation of this theory with the characteristics of real structures. A theory which would predict the ultimate resistance of a drilled shaft footing to overturning loads was presented in Research Report 105-1[1]. This theory was correlated with model tests which were reported in Research Report 105-2[2].

In this report the results of full-scale tests in soils of widely varying properties are presented. The actual test loads are compared with the loads predicted by the theory. The relative accuracy of these predictions indicates that a design procedure based on this theory would be substantial improvement over the older, more conservative design methods. Such a design procedure has been developed and is presented in this report. Although based on rather complex equations, the IBM 7094 has been used to construct design curves which are extremely simple for the practicing engineer to use. As an additional aid in using this design procedure, methods for the determination of the necessary soil parameters are given.

---

1 and 2 These numbers refer to selected references found at the end of this report.

TESTING PROGRAM

In order to check the validity of the theory presented in Research Reports 105-1 and 105-2, three full-scale pullover tests were conducted. The sites were selected to represent the large range of soil conditions and types that might be encountered in practice. These soils were a natural sand having an extremely low cohesion, a clay of relatively high cohesion, and a very soft clay.

Footing Test Configuration

The footings were nominally 2 feet in diameter by 6 feet in depth. The bottom of the footings were not belled. Bolted to the top of the footing was a 2-inch thick anchor plate which supported a 13-foot segment of 12 WF 120. Photographs of the footing cage and wide flange support column are shown in Figures 1 and 2.

Installation Procedure

The test footings were poured in place using the same installation procedures that would normally be used in the field. A drilling rig using a 24-inch Auger bit drilled the holes in the various test sites. The wallow of the Auger resulted in holes approximately 26 inches in diameter. The holes were drilled 6 feet 6 inches deep so that the top surface of the footing was approximately 6 inches below the ground surface. The footing reinforcement cage was lowered into place, centered and leveled. Ready-mixed concrete was then placed in the hole and vibrated. At the same time the test footings were installed, an anchor

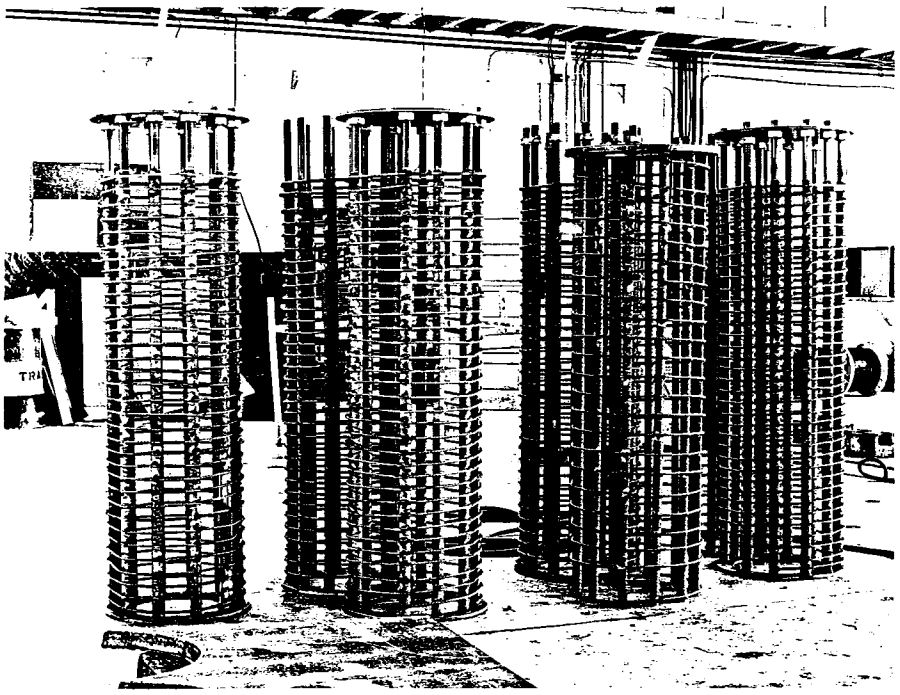

Figure 1, Footing Reinforcement Cages.

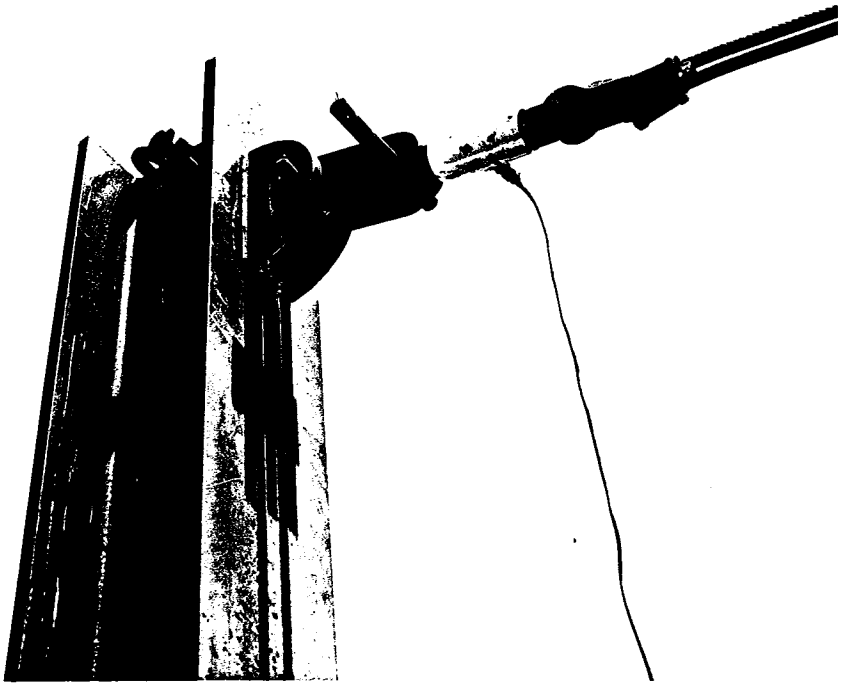

Figure 2, Wide Flange Support Column (12 WF 120).

footing was placed approximately 100 feet away. This footing was the same size as the test footing but was belled at the bottom to provide additional anchorage. It was necessary to support the tackle blocks which would be used to supply an overturning load to the footing. After 2 weeks, the support column was bolted to the test footing and the system was ready to test.

Loading System

The load necessary to overturn the footing was applied through a cable system by either a fork lift or a winch. The cables ran directly from a point 12 feet above the top of the footing to the anchor footing. This resulted in both a horizontal and vertical component of force at the point of application. The vertical component of load is taken into account in the analysis as a simulated structural load. This loading system is shown in Figures 3 and 4.

Instrumentation

The loads applied to the footing during testing were measured by a load cell attached to the top of the support column (Figure 5). The output of this strain-guage load cell was recorded continuously during each test by a Honeywell Visicorder. The rotation of the footing as the load increased was measured by means of the pendulum arrangement which is shown in Figure 6. As the support column tilted, the pendulum rotated with respect to the support column, activating the Linear Differential Transformer (LDT). The movement of the LDT was also recorded on the Honeywell Visicorder (Figure 7). Thus simultaneous

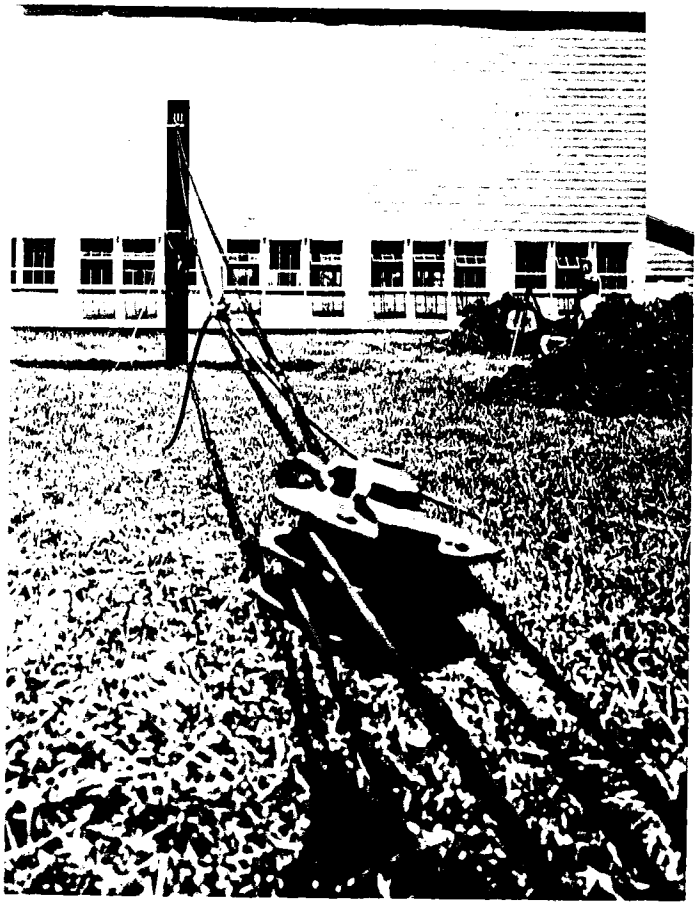

Figure 3, From Anchor Footing to Test Footing.

Figure 4, Fork Lift Over Anchor Footing.

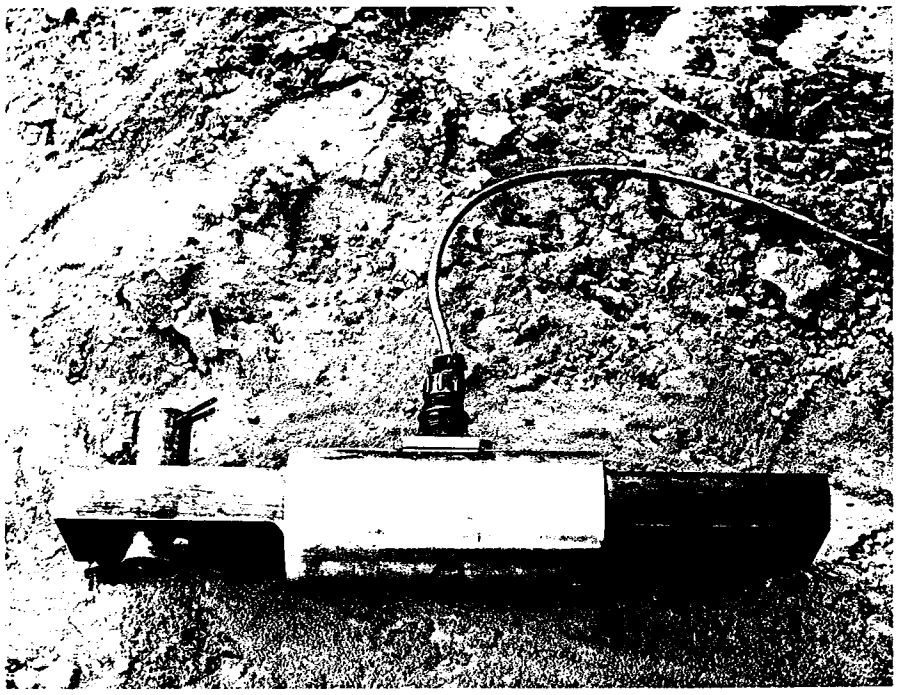

Figure 5, Load Cell.

Figure 6, Pendulum Arrangement Used for Measurement of Footing Rotation.

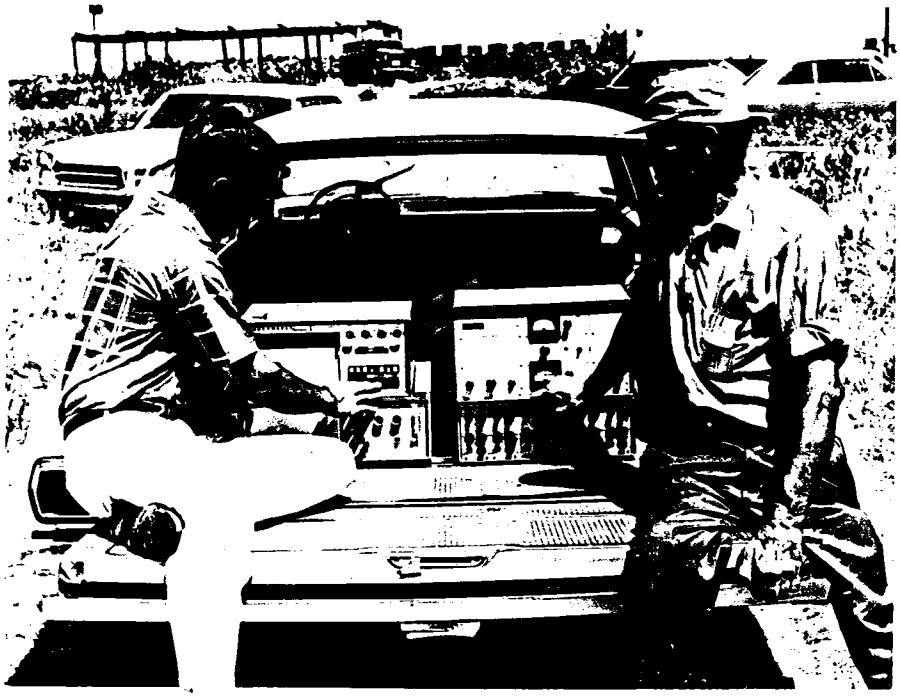

Figure 7, Amplifier and Recorder System Used for Recording Load and Footing Rotation.

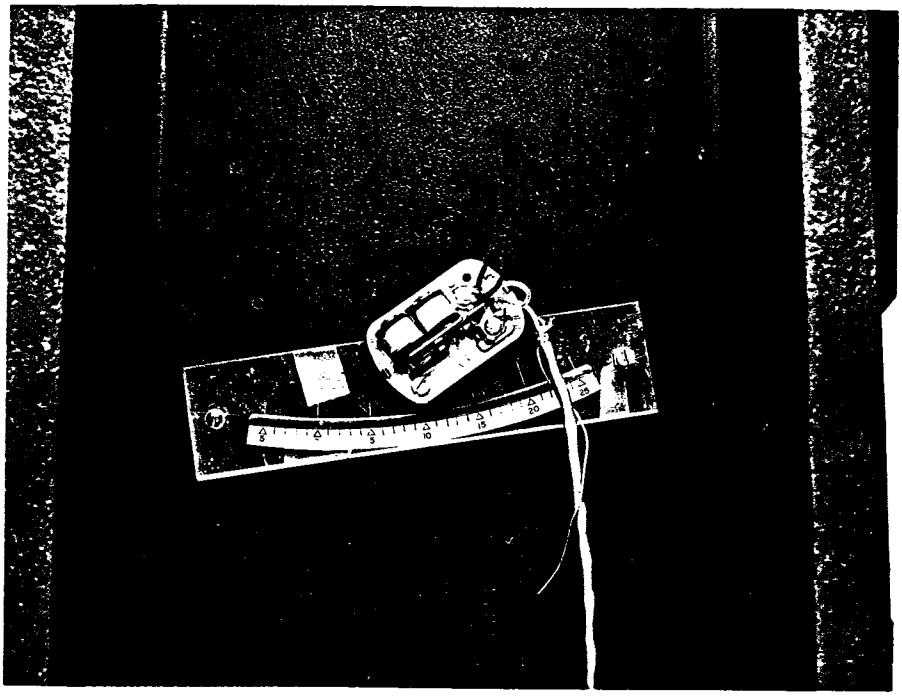

Figure 8, Ball Bearing Inclinometer.

readings of load and footing rotation were available throughout the progress of the test.

As an additional rough check of footing rotation, ball bearing inclinometers were attached to the side and back of the support column. The movement of the ball bearings in the circular slot, as shown in Figure 8, was recorded by a technician during the test.

In order to determine the absolute value of the movement of any point on the footing with respect to the surrounding soil from the determinations of footing rotation, it was necessary to determine the lateral movement of one point on the footing. As a test progressed, the change in the distance from the top of the footing to a point approximately 20 feet behind the footing was recorded using a steel tape (see Figure 9).

Figure 9, Lateral Movement of Top of Footing.

SOIL PARAMETERS

Before presenting the soil parameters, it is cogent to briefly discuss those parameters which are of importance to this particular report.

The theory used is based on earth pressure theories, and solution of the problem requires knowledge of the shear strength of the soil and its unit weight. With respect to shear strength, use is made of the well-known Mohr-Coulomb expression as given below:

$$\tau = c + \sigma \tan\phi$$

where: τ = shearing strength

c = apparent cohesion

σ = applied normal stress

ϕ = apparent angle of shearing resistance.

Thus, the two shear strength parameters needed are c and ϕ. These are generally obtained from triaxial tests on undisturbed specimens or--in the case of sands not recoverable from borings--by Standard Penetration Tests on the material in situ.

It is important to recognize the influence of drainage and consequently the pore water pressures on the shear strength parameters. It is known, for example, that if a saturated soil is sheared so slowly that the induced pore pressures have dissipated at failure, then it will have a definite, observable angle of shearing resistance, ϕ_d, which is generally termed the "drained" angle of shearing resistance. On the other hand, the same soil, if sheared too rapidly to allow any

dissipation of pore pressures will exhibit a cohesion and no angle of shearing resistance (the $\phi = 0$ case). Thus, the operative shear strength in situ is a function of the drainage characteristics of the soil as related to rate at which the soil is sheared. Selection of the appropriate strength test requires knowledge of both the drainage characteristics (or permeability) and the rate at which the soil will be sheared.*

If the soil is free-draining, such as a sand, the appropriate laboratory test would be a "drained" test since it is virtually impossible to prevent drainage of the pore pressures under normal rates of loading. Clays, which are not free-draining, will have little, if any, opportunity to dissipate excess pore pressures during rapid shearing, and the appropriate laboratory test in this case would be an undrained test. The triaxial test terminology "slow" and "quick" often used in lieu of "drained" and "undrained" is considered misleading: a drained test on a free-draining sand may be carried out as quickly as an undrained test on an impervious clay.

Navasota Sand

This site was located in the borrow ditch on S. H. 30 approximately 4.6 miles south of the intersection of S. H. 30 and F. M. 158 in Brazos County.

Visually, the soil can be classified as a gray fine sand, uniformly graded with a trace of silt. It is overlain by a thin layer of tan clayey sand which was stripped from the immediate test area just prior to installation of the test footing. Within the depth influenced by

*The alternative solution is an effective stress type of analysis which requires a prediction of the pore pressures during shear.

the footing (approximately 8 feet) the sand was remarkably uniform.

Before the test footings were installed, Standard Penetration Tests were performed at depths of 1, 3, 5 and 7 feet below the stripped ground surface. Although the results are somewhat suspect at shallow depths, the Standard Penetration Test does provide an excellent indication of the relative density of a sand, and can also be used to estimate the angle of shearing resistance of a sand (see page 37).

To provide a more reliable estimate of shear strength than is normally obtained from a Standard Penetration Test, undisturbed samples were taken of the sand at the same depths as the penetration tests. This sampling procedure was made possible by the use of special sampling equipment plus the slight apparent cohesion exhibited by the moist sand. A flat bottomed auger was used to advance a 6-inch diameter hole to the sampling depth. Three sampling tubes, 1-5/8-inches I. D. and 1/32-inch wall thickness with a slightly beveled cutting edge, were then forced into the sand. After all three sampling tubes were in place, they were extracted with a special tool.

In the laboratory, the ends of the samples were trimmed, they were carefully extruded from the tubes, and then placed on the pedestal of a triaxial cell. The specimens maintained their shape during this operation although they were so fragile that they collapsed if jarred even slightly.

As this was a free-draining material, it was felt that consolidated, drained triaxial tests would give the most appropriate shear strength parameters. The test results are summarized in Figure 10, while results showing Mohr circles and failure envelopes are given in Appendix C.

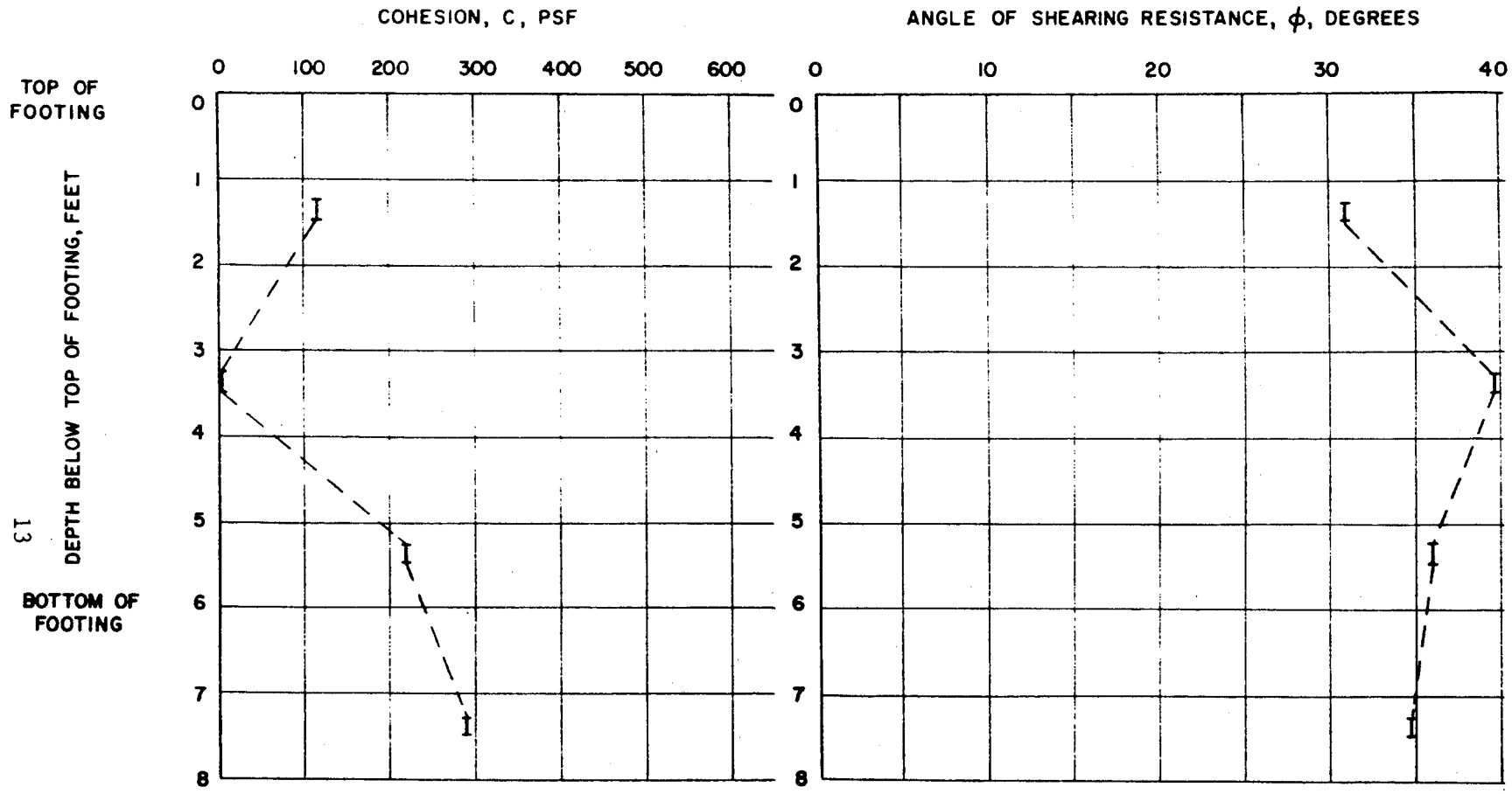

FIGURE 10, SOIL COEFFICIENTS OF NAVASOTA SAND.

As expected, the sand exhibited a small amount of apparent cohesion thought to be primarily the result of thin moisture films around the grains of the partly saturated soil. This cohesion undoubtedly was acting during the pullover test, but it would disappear with either complete saturation or drying of the mass.

A comparison of the Standard Penetration Test and triaxial test results is presented in Figure 24 on page 39.

Galveston Clay

This site was located on property owned by Texas A&M University on Pelican Island approximately 1/4 mile east of the bridge linking Pelican Island and Galveston Island. Pelican Island is an old mudflat which has been built up by man-made fill. At the test site, the original surface is overlain with approximately 9 feet of soft to plastic brown clay which appears to be derived from the deeper Beaumont Clay formation. It is believed that this was spoil from the dredging operations when the adjacent ship channel was widened and deepened. Inclusions of bituminous material and recent shells in the borings support this premise.

Two shallow borings were made adjacent to each of the three test footings constructed at this site. Undisturbed samples were taken at each foot of depth with 3 inch diameter thin wall Shelby tubes. The samples were extruded in the field, wrapped and coated with paraffin, and returned to the laboratory for testing.

The highly plastic nature of this soil indicated that it had a very low permeability and consequently little, if any, dissipation of excess pore pressures could be expected during the short period

over which the pullover tests would be conducted. Consequently, unconsolidated, undrained triaxial tests were used to determine the strength parameters. For the most part, each triaxial test series used three 1.5-inch diameter specimens which were trimmed from a single undisturbed core. The shear strength parameters obtained from the triaxial tests are shown in Figure 11.

The test results are typical of a recently deposited, normally consolidated clay. The shear strength in the surface "drying crust" is relatively high, but it decreases with depth, reaching a minimum between 3 and 4 feet. Below this depth, the shear strength first remains constant, then shows a slight increase near the bottom of the test footing. The slight angle of shearing resistance obtained in the upper 3 feet is a manifestation of the compressibility of a partly saturated soil under an all round confining pressure. If the soil were saturated, the angle of shearing resistance for an unconsolidated, undrained triaxial test should be zero.

Bryan Sandy Clay

The third site was located on the Texas A&M Research Annex about 50 yards south of the hangar housing the Terramechanics Laboratory. Visual observation of a nearby deep test pit indicated a formation of relatively uniform soil to a depth of 9-10 feet. Unfortunately, the strength parameters showed the soil to be anything but uniform.

One boring was made adjacent to each of the three test footings. Equipment and procedures were as described previously for the Galveston

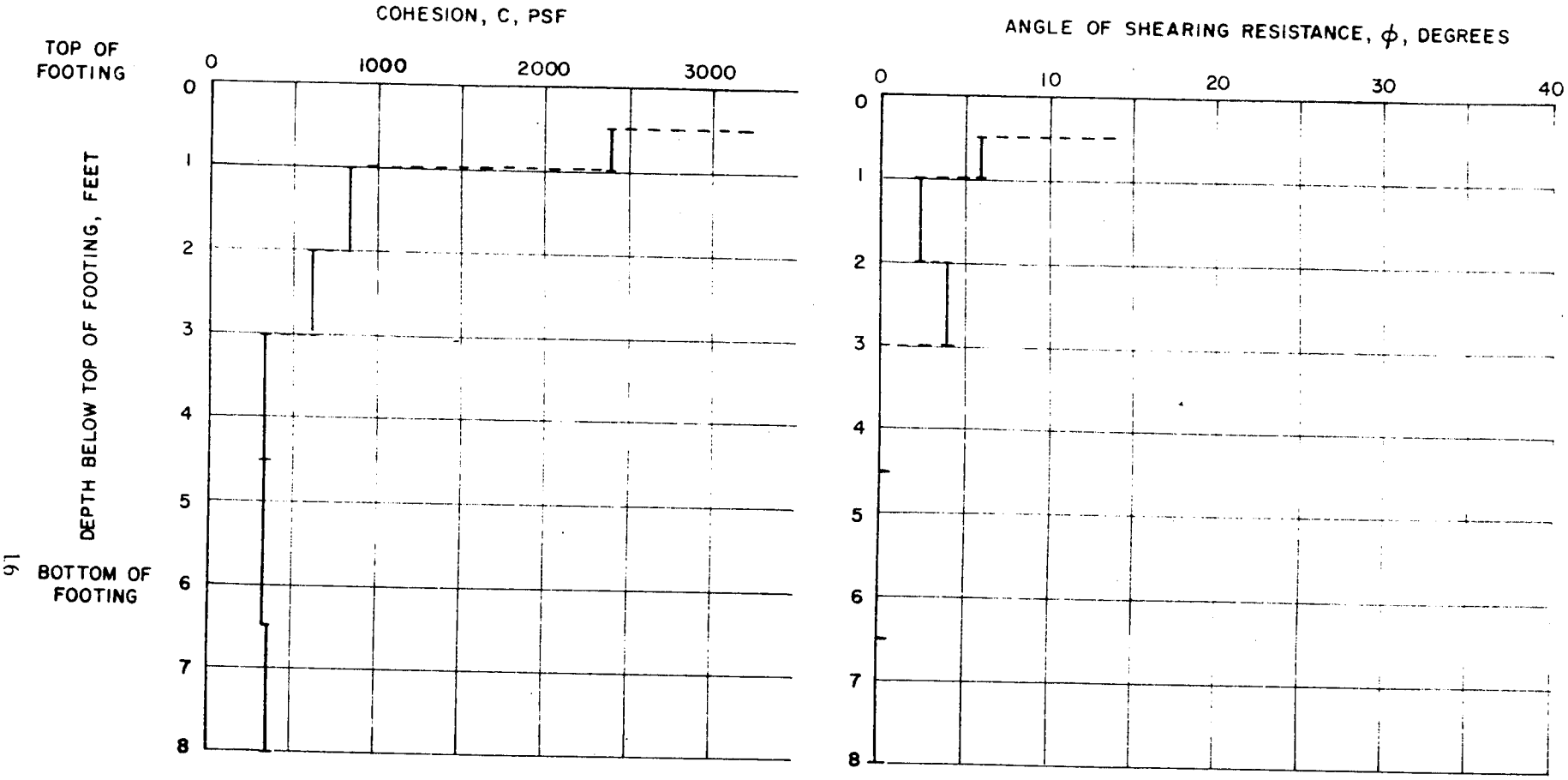

FIGURE 11, SOIL COEFFICIENTS OF GALVESTON CLAY.

Clay. The general descriptive soil profile obtained from the boring logs and visual observation of the specimens is as follows:

0 - 6"	Firm tan silty fine sand with roots
6" - 42"	Stiff gray clay
42" - 60"	Very stiff gray clay
60" - 75"	Very stiff tan and gray clay with occasional calcareous nodules
75" - 90"	Very stiff tan and gray clay with numerous calcareous nodules
90" -	Firm tan and red silty fine sand

Owing to unseasonable rainfall, a significant period of time elapsed between construction and testing of the footing. To check for any significant changes in soil properties during this time, another boring was made adjacent to the test footing just prior to the pullover test. Final strength parameters and other pertinent properties of the upper layers were obtained from this boring. Below a depth of 3-4 feet, no significant moisture changes occurred in the interval between the initial and final sampling, so the major amount of triaxial testing was done on cores from all borings.

The soil below a depth of 3-4 feet was comparatively dry and stiff, and also contained a significant amount of calcareous nodules. Considerable difficulty was encountered in trimming smaller specimens so a triaxial test series could be conducted on at least three specimens obtained from a single core. As an alternate, multi-stage triaxial tests were performed on single specimens. Also, three or more specimens from the same stratigraphic position, but in different borings, were combined for a triaxial test series. The latter gave rather poor results due to the variability of supposedly similar

specimens.

Again, because of the relatively low permeability of the soils involved, unconsolidated, undrained triaxial tests were considered as giving the most appropriate shear strength parameters. As shown in Figure 12 , the strengths were very erratic. Fairly high angles of shearing resistance were obtained in the lower portion of the boring, and this is again considered to be the consequence of partly saturated specimens.

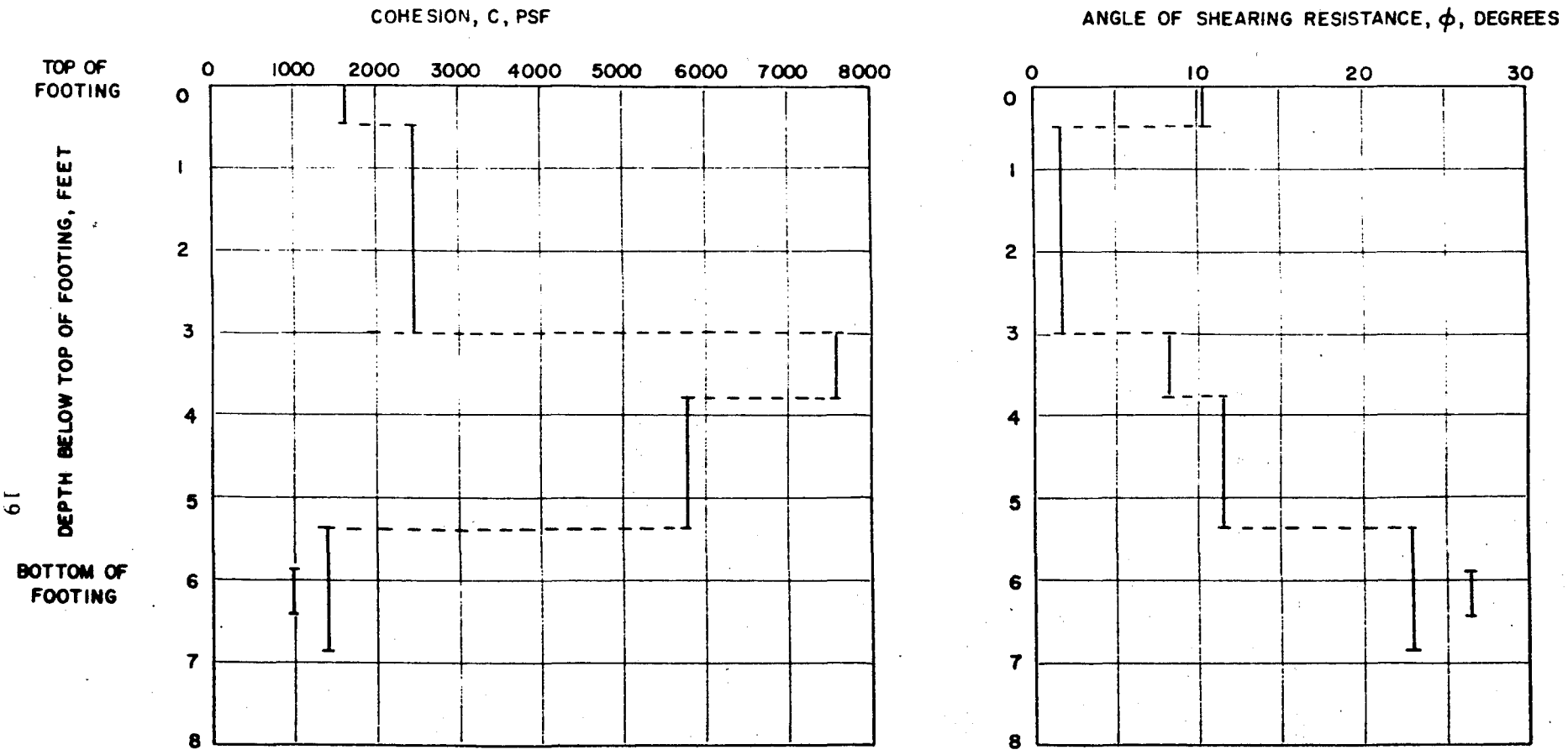

FIGURE 12, SOIL COEFFICIENTS OF BRYAN SANDY CLAY.

TEST PROCEDURE

The test sites are shown in Figures 13, 14, and 15. After the necessary instruments and cable arrangements were secured, initial readings were recorded before any load was applied. The slack was then taken out of the cables until an initial load of 500 lbs was on the footing. Readings of all instruments were taken at this point and the test was begun.

The load was applied in increments of 500 pounds by observing the Visicorder line beam. After the application of each increment of loading, readings of the ball bearing inclinameters, the steel tape and the level rod were made. A continuous record of the load and the footing rotation was recorded on the Visicorder. This procedure was followed until the maximum load had been reached. After the ultimate load had been reached, the points of observation were determined by footing rotation. The test was discontinued after a footing rotation of approximately 20° had been reached.

Figure 13, Bryan Sandy-Clay Test Site.

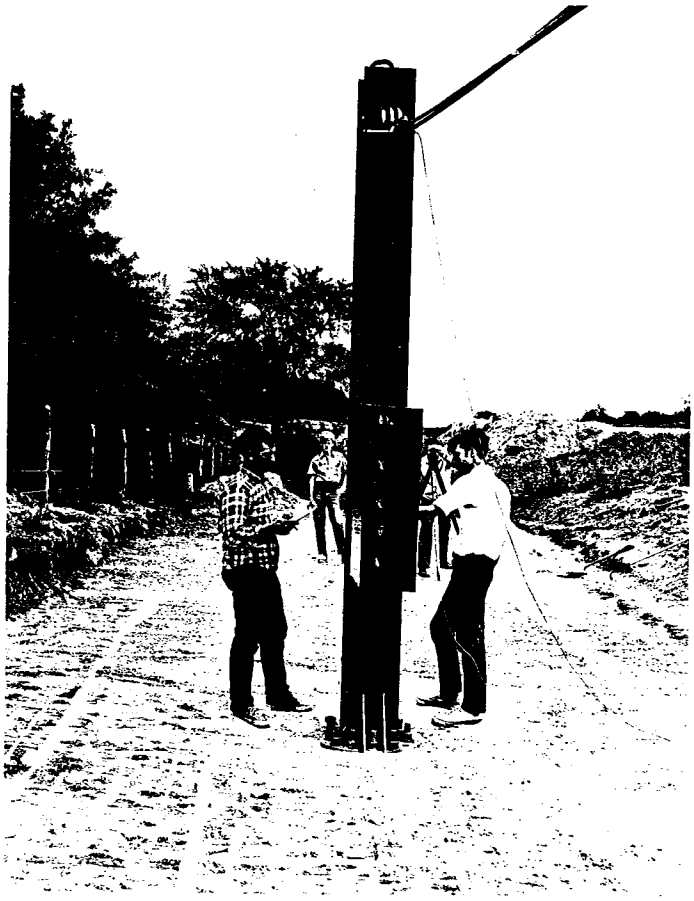

Figure 14, Navasota Sand Test Site.

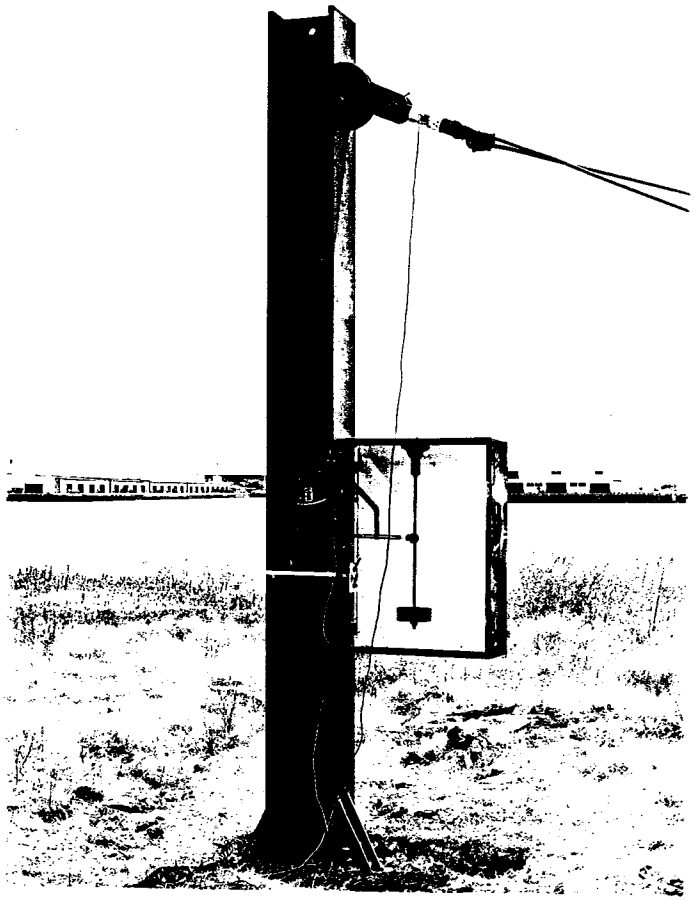

Figure 15, Galveston Clay Test Site.

TEST RESULTS

These footing tests were designed so that there would be a failure of the soil surrounding the footing rather than a structural failure in some portion of the footing. Footings which have been built using current design procedures are over-designed with respect to the soil so that the failure would probably occur in the structure above the footing, in the connection to the footing, or in the footing itself if a failure load was applied. A summary of the three full-scale tests is given by Figures 16, 17, and 18. The corresponding values of horizontal load and footing rotation are plotted in these Figures.

As indicated by the model tests reported in Research Report 105-2[2], the ultimate load which these footings can resist occurs at a footing rotation of approximately 5°. This check on the behavior of large footings as compared to the behavior of model footings was considered extremely important if the theory was to be extrapolated to full-scale tests. The failure patterns of the soil surrounding each footing are given in the sequential photographs shown by Figures 19, 20, and 21. Comparison of these photographs with those given for the model tests[2] show that the failure modes are very similar. The exception to this was the Galveston Clay Test. In this test, the footing rotated through the soil, displacing a wedge of material precisely the width of the footing. In the Navasota and Bryan Tests, and in all of the model tests,

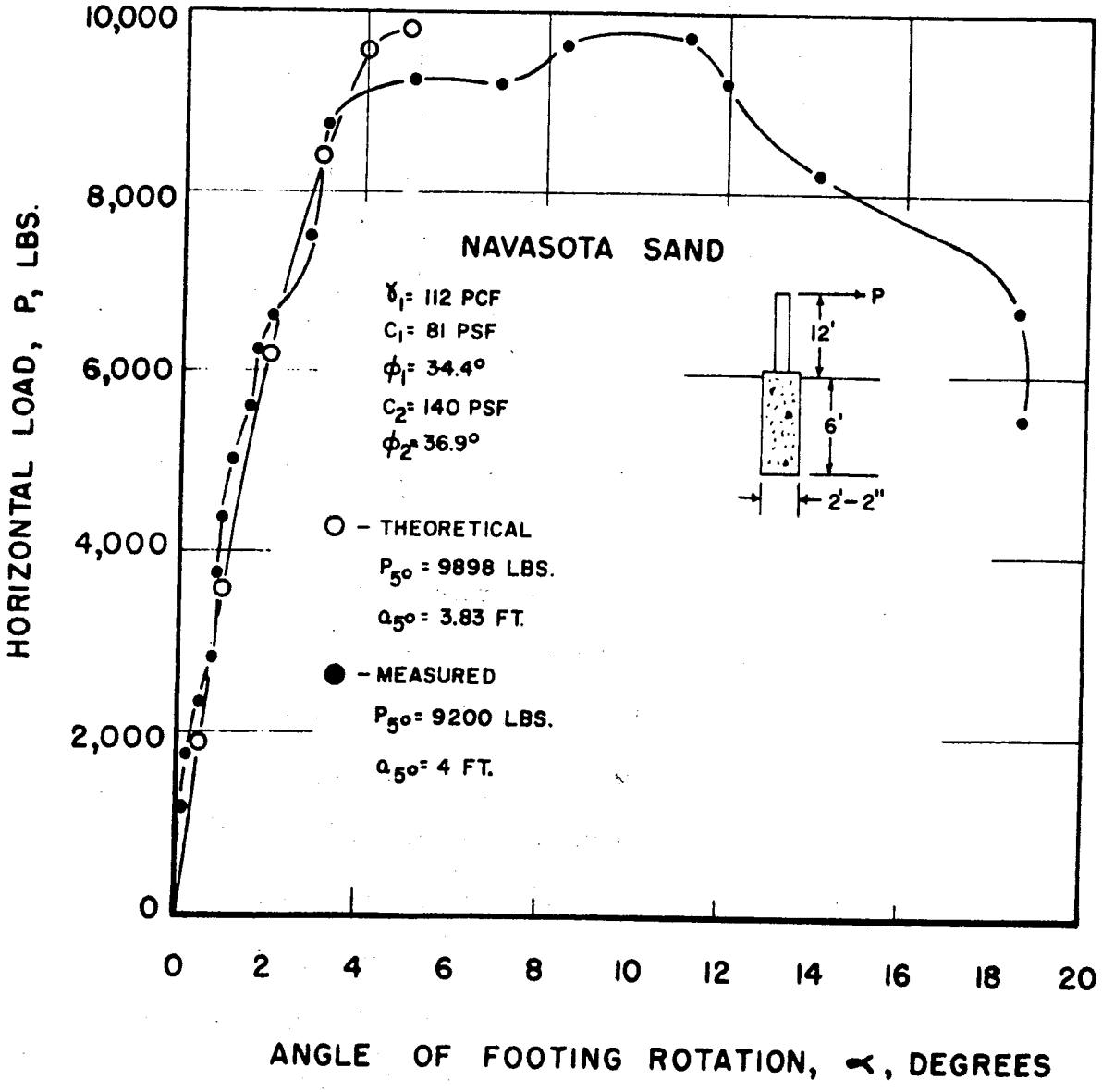

FIGURE 16, COMPARISON OF LOAD TEST AND THEORY, NAVASOTA SAND.

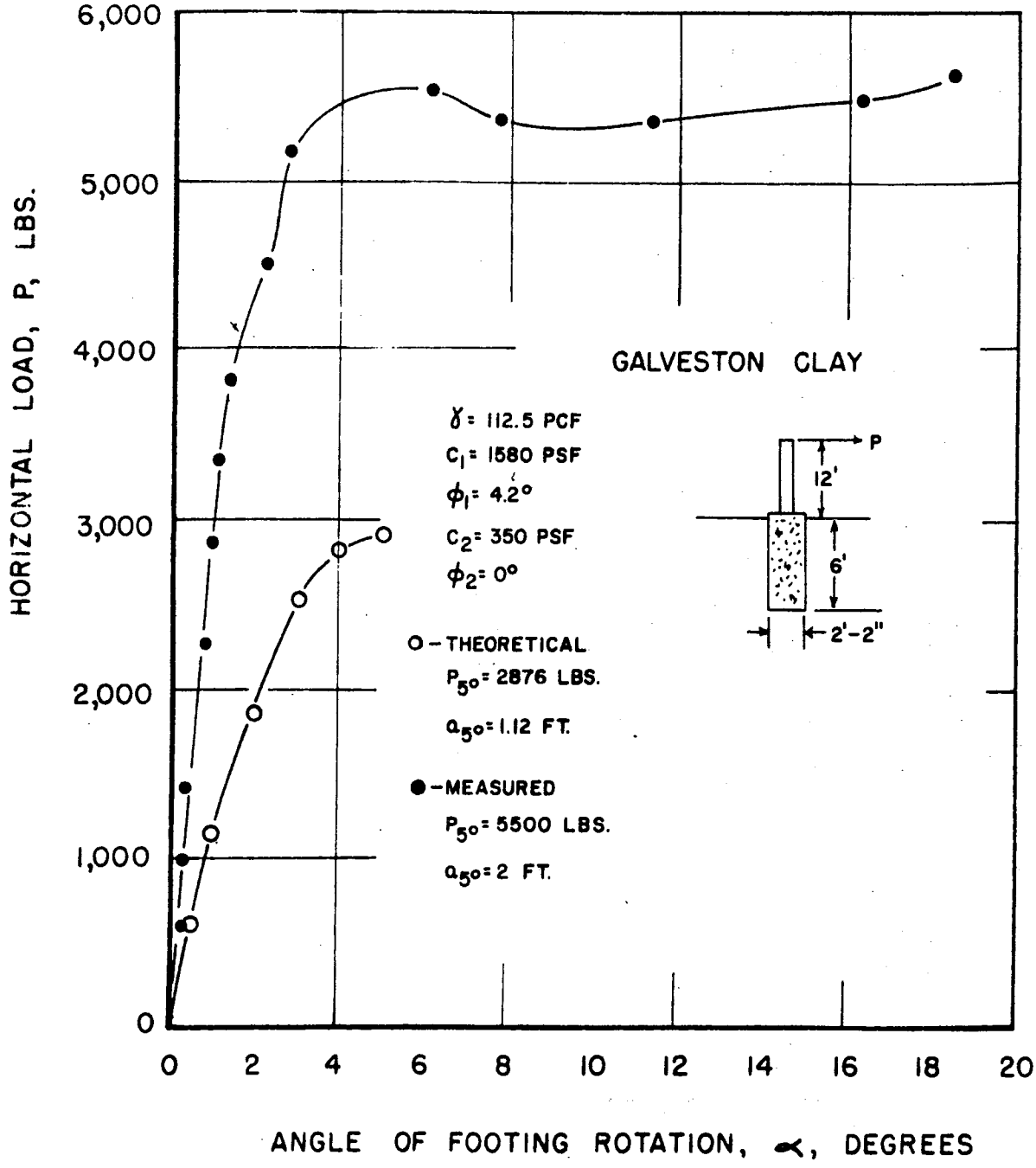

FIGURE 17, COMPARISON OF LOAD TEST AND THEORY, GALVESTON CLAY.

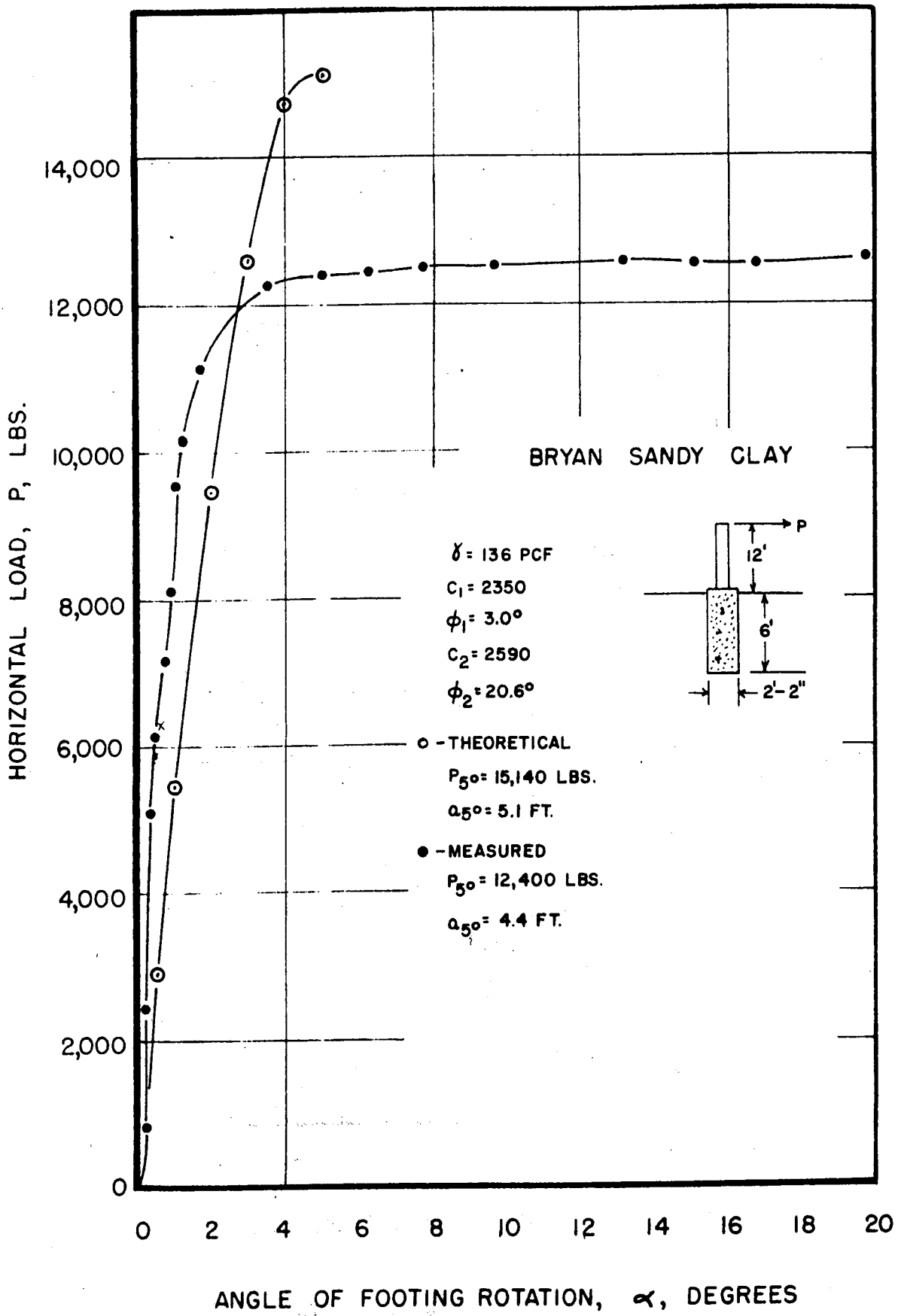

FIGURE 18, COMPARISON OF LOAD TEST AND THEORY, BRYAN SANDY CLAY.

1

2

3

3
(Top view.)

4

4
(Top view.)

Figure 19, Sequential Photographs of Navasota Sand.

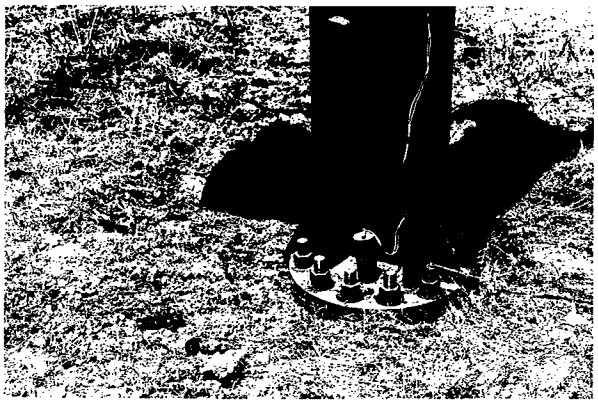

1

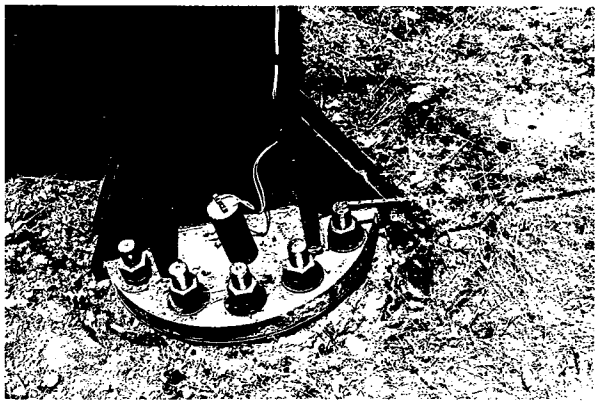

2

3

4

(From other side.)

5

(Hole after removal of footing.)

Figure 20, Sequential Photographs of Galveston Clay Test.

1

2

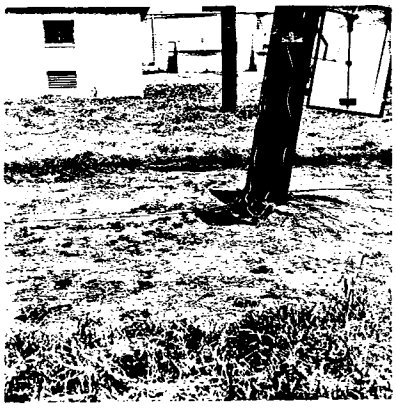

3

4

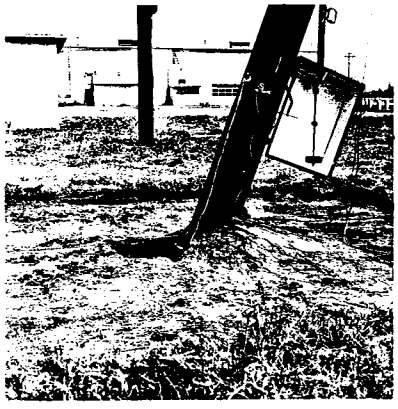

5

6

Figure 21, Sequential Photographs of Bryan Sandy-Clay Test.

a larger segment of soil, as compared to the individual footing size, was kicked out behind the footing. The reason for this difference is probably the extremely low strength and high plasticity of the Galveston Clay. It was the softest of all materials tested and could easily be remolded by hand. In all three tests the plot of horizontal load versus rotation is fairly linear up to a load of approximately 60% of the maximum load. In the two tests of cohesive soil, the Bryan Test and the Galveston Test, approximately 60% of the maximum load is achieved at footing rotation of 1°. In the Navasota Sand Test, the load at a rotation of 1° is 52% of the maximum. This reinforces the previous assumption based on model tests that one-half of the maximum load would result in a footing rotation of 1° or less.

COMPARISON OF TEST RESULTS WITH THEORETICAL RESULTS

The comparison of observed values of load and footing rotation with those values predicted by the theory[2] is the ultimate test in determining whether the theory is of practical value. Figures 16, 17, and 18 show both test values of horizontal load versus footing rotation and theoretical values. In order to apply the theory with some degree of accuracy it was necessary to determine the values of cohesion and angle of shearing resistance for each soil throughout the depth of the footing. The values determined by triaxial tests were shown previously in Figures 10, 11 and 12 . In order to determine the average values of c_1, ϕ_1 (cohesion and friction angle above the rotation point) and c_2, ϕ_2 (cohesion and friction angle below the rotation point) the soil values within $\pm$ 1 foot of the rotation point were not considered. This procedure will be discussed at greater length in the section on design procedure.

In the Navasota Sand Test, the theoretical and test curves coincide to a remarkable degree. The load predicted by the theoretical procedure was 9,998 lbs. while the actual load measured at a rotation of 5° was 9,200 lbs. This observed load is 7% below the theoretical maximum load. It would appear that the coefficients of soil pressure which were developed in the laboratory model study using Ottawa Sand extrapolate extremely well to the Navasota Sand Test.

The Galveston Clay Test gave the largest difference between the theoretical curve and the test curve. The predicted curve is 48% low

for the value of footing resistance at 5° rotation. Several points can be brought out which may help to explain this discrepancy. First, the failure mode of the Galveston Clay was different from that of any other material tested. Considerable suction forces may have been present on the face of the footing which was moving away from the soil. This possibility occurs because of the extreme softness and plasticity of this clay. Second, it was not possible to determine the soil parameters of the material in contact with the top six inches of the footing. This was due to a high content of grass roots and other organic materials. As was shown previously in Figure 11, the cohesion of this material was extremely low except for that portion close to the desiccated ground surface. Between the depth of 1 foot 6 inches and 0 feet 9 inches, the cohesion rose from 850 to 2,380 PSF. It is probable that the cohesion became significantly higher in the material above the first testable depth. It should be observed that when the soil becomes lower in strength with increasing depth, the footing point of rotation will shift upward from the center of the footing instead of the usual case when the rotation point is approximately two thirds of the footing depth down from the top of the footing. The observed rotation point was two feet below the top surface of the footing and the theoretical rotation point was only 1.12 feet below the top surface. Where this large discrepancy between observed strength and theoretical strength exists, it is reassuring that the theory is conservative. That is, that it predicts loads less than the loads the materials can actually sustain. It is also probable that if this hard crust becomes saturated during the rainy season the load the footing could resist would decrease and approach the theoretical load more closely.

The footing constructed and tested in the Bryan Sandy Clay shows a good correlation between observed and theoretical maximum loads. The theoretical load is 15,140 lbs. as compared to an observed load of 12,400 lbs. This observed load is 18% below the theoretical value. Although the theory is on the unconservative side at the ultimate load, the curves show that the theory is still conservative up to a rotation of approximately 3^{o}.

The theory gives only a predicted load for the footing at a rotation of 5^{o}. The intermediate points between zero and 5^{o} are the result of arbitrarily selecting a parabola to express these intermediate points. This parabola is given by the following equation:

$$P_i = P_{5o}\left[1 - \frac{(5 - \alpha_i)^2}{25}\right]$$

P_i is any intermediate load, and α_i is any corresponding intermediate rotation between 0 and 5^{o}. P_{5o} is the load at a rotation of 5^{o}. The justification for the use of this parabola is given by Figure 22. This figure includes the data from the model tests* and full-scale tests conducted in this study. If the load at 5^{o} rotation for each test is arbitrarily assigned the value of 100%, and each intermediate load between 0 and 5^{o} rotation is expressed as a percentage of the 5^{o} load, the resulting values can be plotted as shown. This figure illustrates that the parabola is a conservative approximation of the load versus rotation curve up to 5^{o} rotation, and approximates the Galveston and Navasota tests rather well.

---

* All model tests are included except numbers 8 and 9 which were non-compacted sand tests.

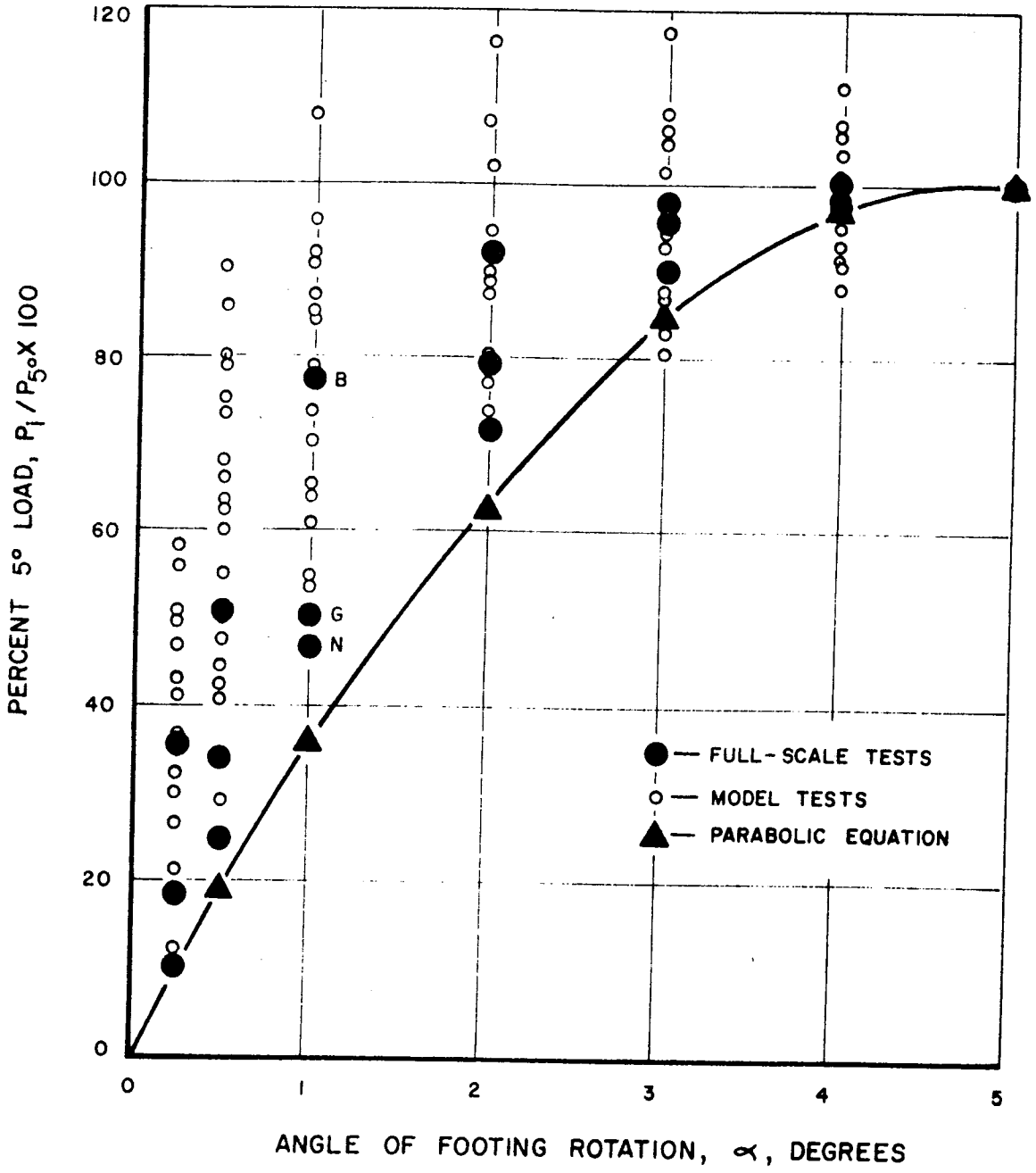

FIGURE 22, TEST DATA COMPARED WITH PARABOLIC CURVE.

Summarizing the results of the three full-scale tests, the theoretical plot of load versus footing rotation is conservative in all cases up to a footing rotation of approximately 3^{o}. In both the Navasota Sand Test and the Bryan Sandy Clay Test, the theory then becomes slightly unconservative from 3 to 5^{o}. The theory is conservative for all rotations in the Galveston Clay Test.

APPROXIMATE METHODS OF DETERMINING SOIL PARAMETERS

The application of the theory described in this paper is dependent on the determination of the soil parameters, c and ϕ. An accurate way of determining these parameters is by the triaxial test methods described previously on page 10. Although this type of testing was necessary for research purposes, it is not feasible for the design of service structures of minor importance from the point of view of public safety or installation costs. In such cases, it would be helpful if the appropriate soil parameters could be estimated or if they could be determined by expedient methods in the field.

The estimation of these soil parameters becomes a difficult problem for two reasons:

a) Suitable methods for estimating soil properties with any degree of accuracy are nearly non-existent. This is particularly true when it is necessary to separate the components c and ϕ.

b) Account must be made of the fact that the soil properties may--and probably will--change with time owing primarily to climatic changes.

With actual structures of the type being considered, the latter problem is acute because the structure offers no protection to the underlying soil as would a slab, for example. Thus, the appropriate design parameters are not necessarily those found at the time of sampling or construction, but rather those occurring when the soil is at its most weakened condition.

For example, moist sands generally exhibit some apparent cohesion which disappears with saturation or complete drying. Obviously, this contribution to the shear strength cannot be considered for long-term conditions. In the same manner, partly saturated clays will exhibit an angle of shearing resistance which disappears with subsequent saturation. Thus, regardless of the method used to determine shear strength parameters, engineering judgments must be made concerning the long-term adequacy of these parameters. Several methods for estimating the shear strength parameters are discussed in the following paragraphs.

Standard Penetration Test [3]

In the case of relatively cohesionless materials (clean sands, for example), the Standard Penetration Test (S.P.T.) has been used successfully for many years. The relationship between the S.P.T. blow count and angle of shearing resistance is presented in Figure 23 . This relationship has been generally considered to be somewhat conservative. The ability to procure undisturbed specimens from the Navasota Sand Site presented a unique opportunity to verify the relationship between the drained angle of shearing resistance as measured in triaxial tests and that predicted from the S.P.T. blow count for this particular soil. This comparison is shown in Figure 24 . In general, it is seen that the triaxial tests gave results which were 1.5° to 10.5° higher than S.P.T. results, thus confirming the somewhat conservative nature of the S.P.T. for sands.

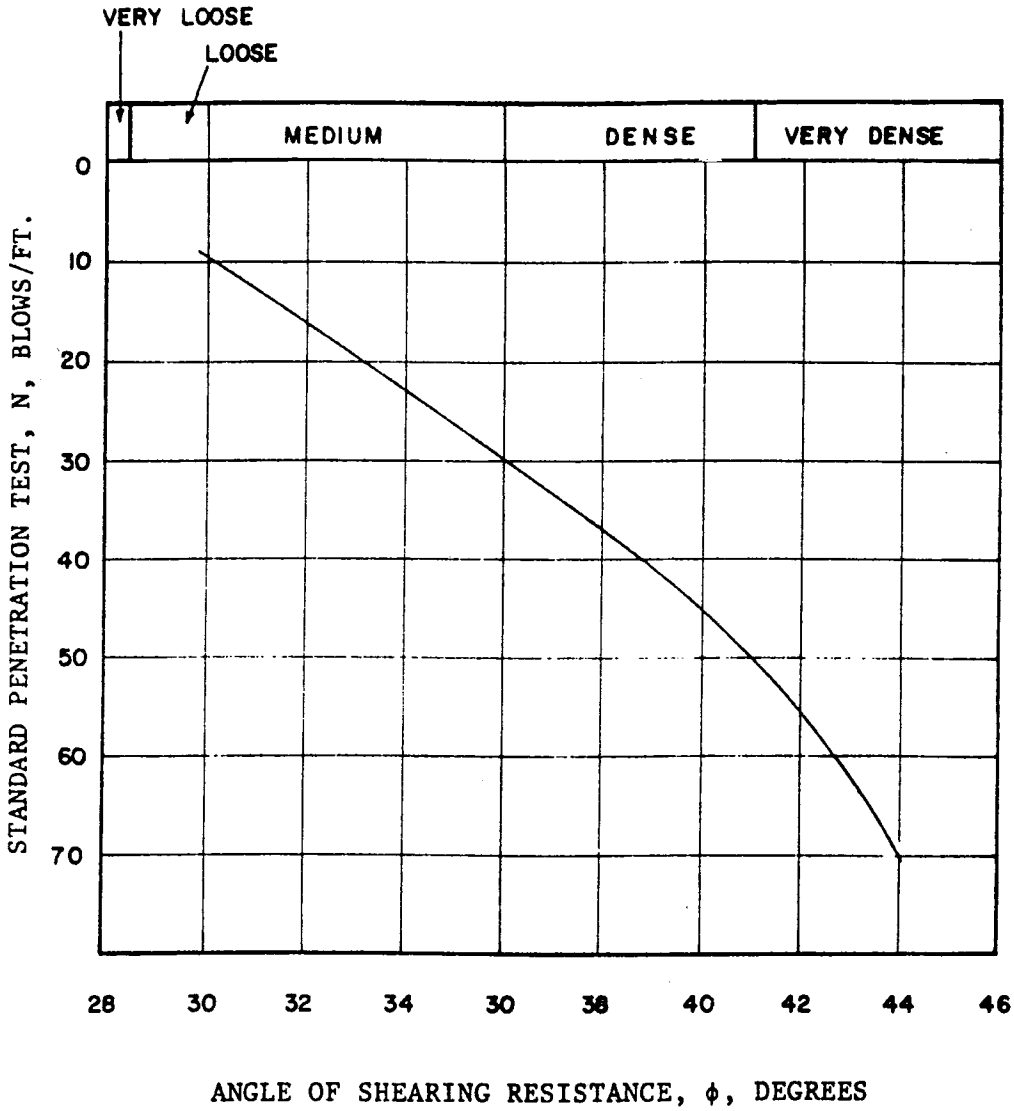

Figure 23, Standard Penetration Test, Relationship With Angle of Shearing Resistance (After Peck, Hanson and Thornburn, Reference 3).

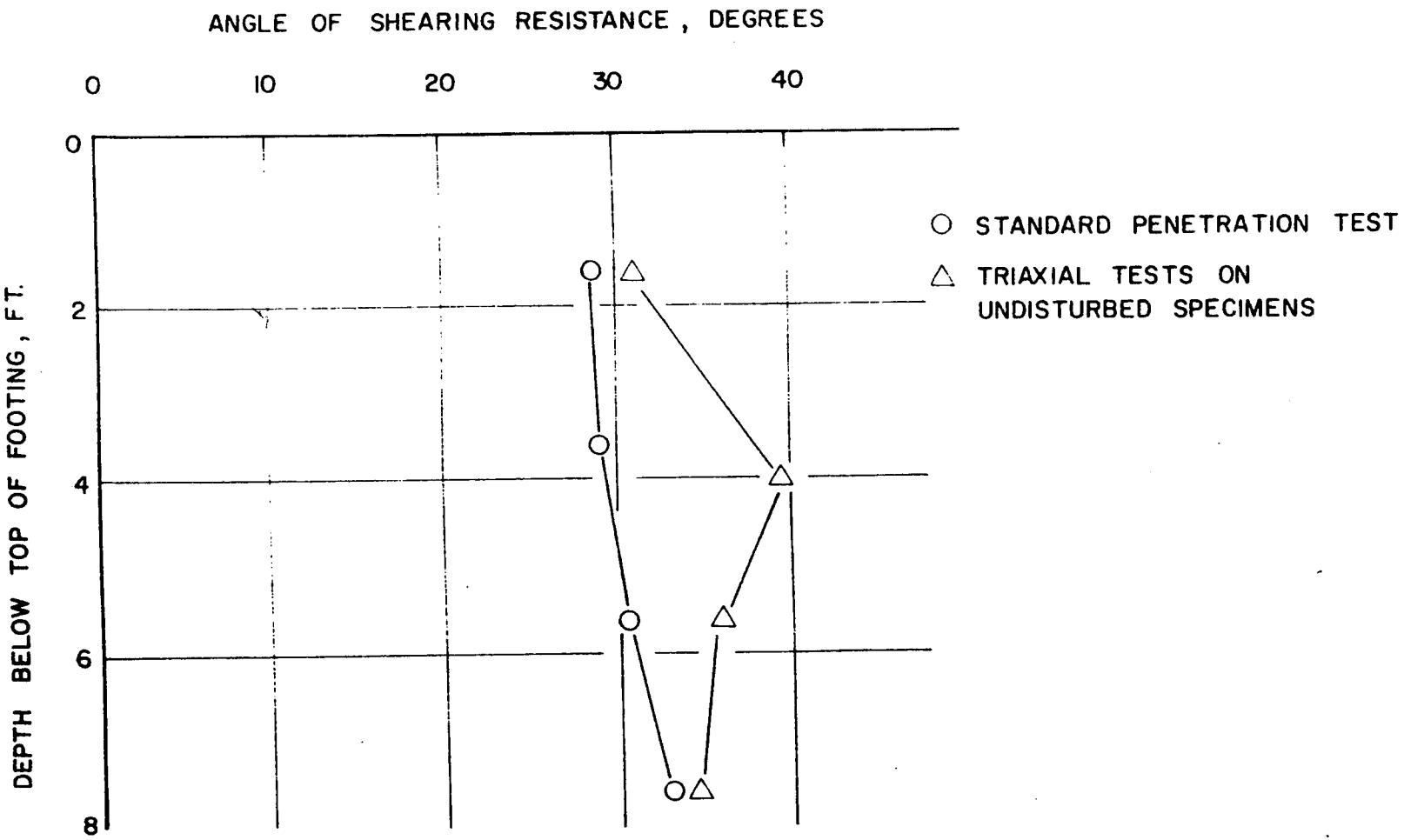

Figure 24, Comparison of the Angles of Shearing Resistance as Predicted by Standard Penetration Tests and by Triaxial Tests.

It should be noted that the Standard Penetration Test cannot distinguish between cohesive and frictional components of strength if both are present. In the Navasota Sand, which had some apparent cohesion at the time of sampling, this was basically "read" by the Penetration Test as a contribution to the angle of shearing resistance.

The above does not detract from the use of the Standard Penetration Test in predicting the angle of shearing resistance for sands. The results are conservative, but not unduly so, and while it does not provide values for apparent cohesion, the latter is transient as explained previously.

The Standard Penetration Test has also been used for estimating the shearing resistance of clays, although it is generally considered to provide conservative and erratic data. Figure 25 shows the relationship between blow count and cohesion. A problem arises here analogous to that with sands: there is no way of arriving at an angle of shearing resistance should one be present. In addition, whereas the angle of shearing resistance remains relatively constant with sands regardless of climatic conditions, the cohesion of clays varies widely during different seasons of the year, particularly with the more plastic clays.

Vane Shear Tests[4]

For soft cohesive materials, the vane shear test is an ideal method of determining shear strength. Either in-place vane shear or miniature vane shear on undisturbed samples may be used with confidence. The results are expressed in terms of cohesion only and are unsuitable for stiff clays or cohesionless materials.

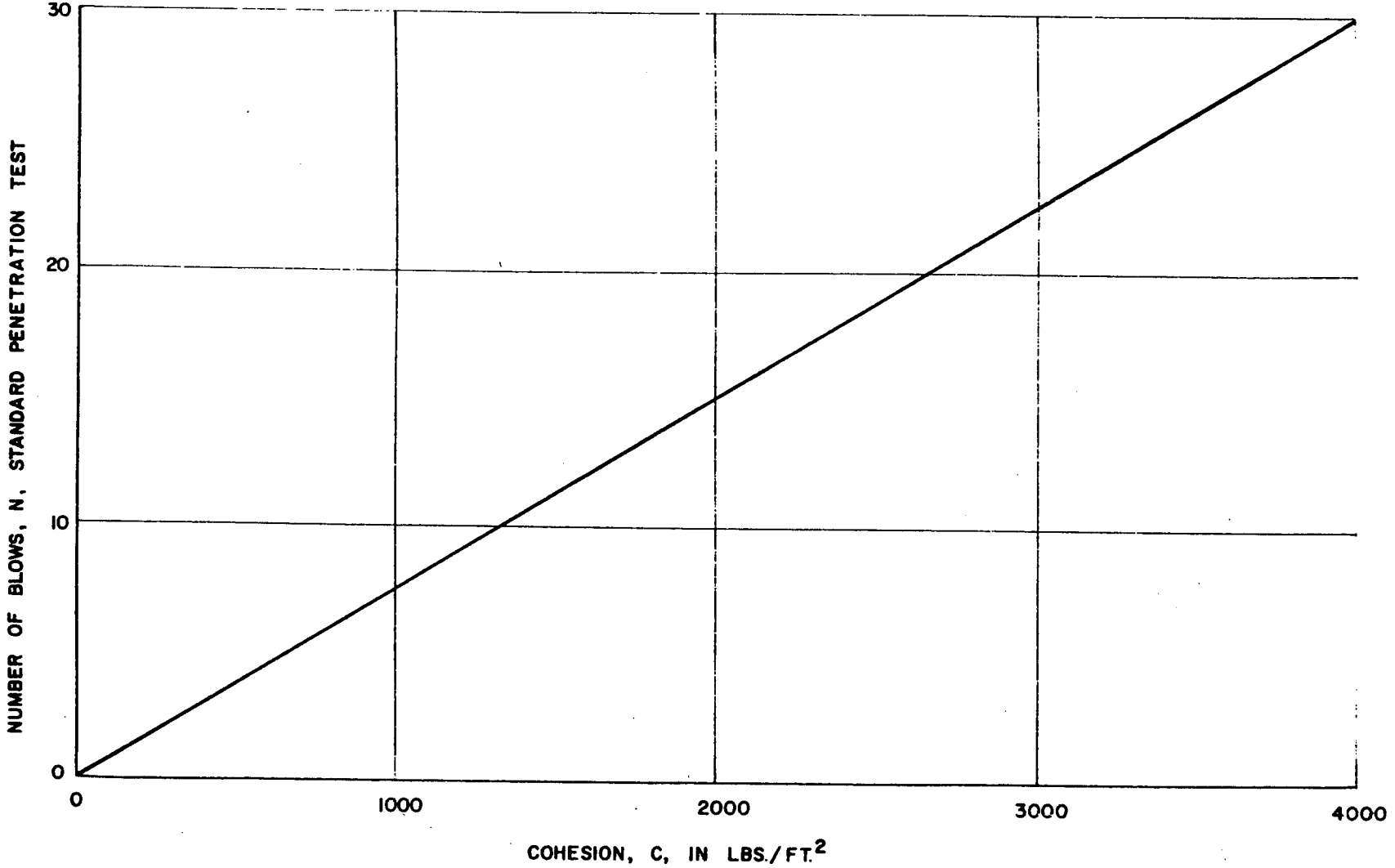

FIGURE 25, STANDARD PENETRATION TEST, RELATIONSHIP WITH COHESION (AFTER TERZAGHI & PECK, REF. 5).

THD Cone Penetrometer Test [4]

The Texas Highway Department has developed a cone penetrometer test which, in many respects, is similar to the Standard Penetration Test. The results of this test have been correlated to triaxial shear test data and presented in graphical form. As with the Standard Penetration Test, the angle of shearing resistance cannot be separated from the cohesion, so for purposes of this design it must be assumed that only cohesion can be obtained.

Cohron Sheargraph [6,7]

The Cohron Sheargraph is a relatively new instrument for determining soil shear strength. It was devised primarily for determining shear strength parameters for mobility calculations on off-road and earth-moving equipment. It has many of the characteristics of the vane shear device with this important variation: the normal stress applied to the soil can be varied during application of torsion to the apparatus. The end result of the test, which takes only a few minutes to perform, is a graph representing the Mohr-Coulomb failure envelope. Thus, both the cohesion and angle of shearing resistance are found if they exist under the drainage conditions obtained during the period of the test.

Summary

The various tests that can be used to estimate the shear strength parameters of c and ϕ are given in Table 1. Each test is listed directly across from the soil type and condition to which it is applicable. All five tests which were discussed will give an approximate value of cohesion for soft or saturated clays ($\phi \approx 0$). Only the Standard Penetration Test and the Cohron Sheargraph is capable of estimating ϕ for clean sands ($c = 0$) and only the Cohron Sheargraph is capable of estimating both c and ϕ for all other soils.

Table 1

SUMMARY OF METHODS
OF
ESTIMATING SHEAR STRENGTH

General Soil Type or Condition	Means of Estimating Shear Strength
Soft Clays or Saturated Clays (ϕ = 0 case)	1. In-place vane shear test. 2. Miniature vane shear test on undisturbed specimens. 3. Standard Penetration Test. 4. T.H.D. Penetration Test. 5. Cohron Sheargraph.
Clean Sands (c = 0 case)	1. Standard Penetration Test. 2. Cohron Sheargraph.
Other Soils* (c, ϕ case)	1. Cohron Sheargraph.

* Clays and silts which are likely to become saturated for significant periods during the life of the structure should be evaluated as described in the ϕ = 0 case.

TENTATIVE DESIGN PROCEDURE

Determination of Magnitude and Position of Chart Load

Assume that analysis of a particular structure dictates that the most critical short term load conditions that will exist at the top of the footing are the shear and moment shown in Figure 26a. Then an equivalent P_d and H, shown in Figure 26b, may be calculated from the following equations of statics. Determination of the necessary factor

$$P_d = V \qquad H = \frac{M}{P_d}$$

of safety should be based on the importance of the particular structure and considerations of public safety. If, for example, the design of a highway sign is considered, its useful life is probably limited. Slight tilting would pose no problem and the failure of such a structure would not endanger the public. Therefore, a 50-year wind might be used with a factor of safety of as little as 1.2.

Therefore use a chart load, $P_c = 1.2\ P_d$.

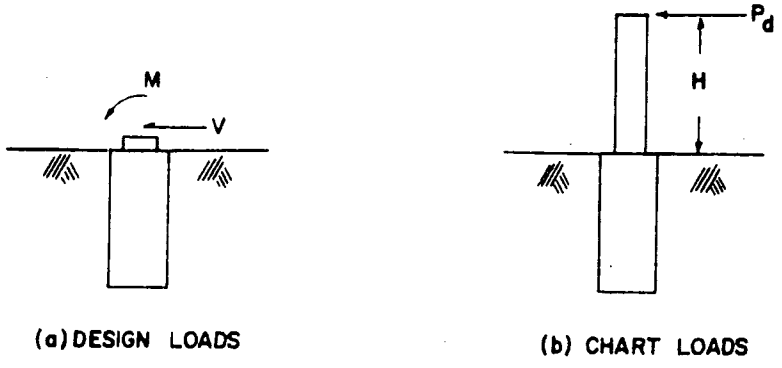

Figure 26, Equivalence of Two Loading Systems.

If a relatively high cost structure were to be built which would become unusable if an angle of rotation above 2° were encountered, it might be desirable to have a factor of safety of 2 against having a rotation of 2°. Therefore use the following equations to determine the chart load:

$$P_{2^\circ} = \frac{P_d}{1 - \frac{(5 - \alpha_d)^2}{25}}$$

$$P_c = 2\, P_{2^\circ}$$

Where:

P_{2° = load acting at height, H, necessary to rotate the footing two degrees.

α_d = the critical rotation in degrees; in this example 2°.

P_c = the load to be entered into the design charts.

Selection of Soil Parameters

Selection of appropriate values of the soil parameters, c and ϕ, is of major importance. Of the two parameters ϕ is the one that has the greatest influence on the size of footing selected. Figure 27 shows that as ϕ doubles (from 5° to 10°) the value of B goes from 1.4 to 2.1 (for a cohesion of 2000 psf) while doubling cohesion from 2000 to 4000 psf only raises B from 0.7 to 0.8 (for $\phi = 0$). Roughly, the size of footing selected for given load conditions is inversely proportional to B.

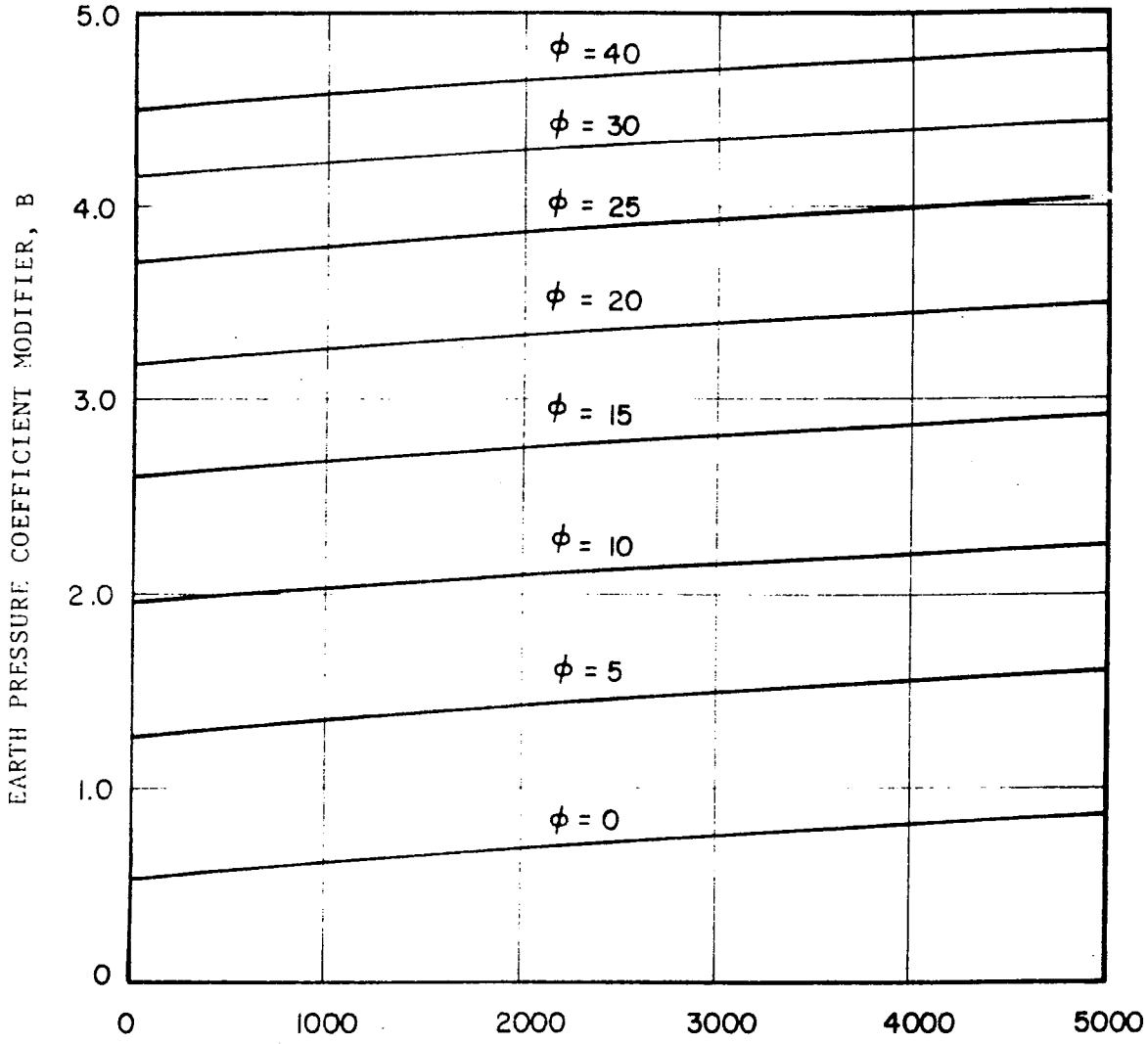

B EQUATION

$$B = 0.0000673\ c + 10.25 \tan \phi + 2.686 \tan(45 + \phi/2) - 2.141 \tan^2 (45 + \phi/2)$$

Figure 27, Solution of Earth Pressure Coefficient Modifier (From Research Report 105-2).

The testing program conducted in this study encompassed soils of widely varying shear strengths and angles of shear resistance. However, in neither the laboratory model tests or the full-scale tests were soils encountered possessing angles of shear resistance in excess of 15° in combination with cohesions in excess of 500 psf. Since rather high values of B are predicted by the theory for soils outside this range, users of the theory should be cautious in their use of this prediction equation in the untested range. The problem is minor, since relatively few soils will have combinations of soil parameters in this range. A conservative way of treating this problem would be to arbitrarily reduce the value of ϕ to 15° for any value of cohesion over 500 psf.

Selection of Footing

The Index to Design Curves on page 60 of Appendix B is an easy way of finding the proper curve sheet for the selection of a footing. The use of these curves will be demonstrated by the following example:

Given: $c = 1000$ psf

$\phi = 10°$

$P_c = 10{,}000$ lbs

$H = 14$ ft

By scanning the Index to Design Curves on page 60, the combination of $c = 1000$ psf and $\phi = 10°$ is listed as being on page 95. Referring to page 95, the values of P_c and H are plotted. Any footing having a curve lying to the right or above this point will provide the necessary resistance. Economic factors may dictate the choice of one footing geometry over another, when both would provide the same resistance to overturning. In this example, a 3'x6' footing (3 feet in diameter by 6 feet in depth) might be chosen. Others that would also suffice would be the 7'x8' and the 2.5'x7' footing. The footing, 2'x7' (2 feet in diameter by 7 feet in depth), has a curve lying below and to the left of the plotted point, and would therefore not meet the design criteria.

SUMMARY AND CONCLUSIONS

The full scale tests for the resistance of drilled shaft footings to overturning loads have confirmed that the theory developed in research report 105-1 and correlated with model tests in research report 105-2 can give a good approximation of actual overturning loads. This was confirmed in soils ranging from sands to soft clays. In the full scale test in sand, the predicted load was 10,000 pounds, while the actual load measured at a rotation of 5° was 9,200 pounds. This observed load is 7% below the theoretical maximum load. The Galveston clay test gave the largest difference between the theoretical load and the test load. The predicted load is 48% below the actual value that was necessary to give the footing a rotation of 5°. Fortunately, this discrepancy is on the conservative side. The footing constructed and tested in a sandy clay shows a predicted maximum load of 15,100 pounds compared to an observed load of 12,400 pounds. This observed load is 18% below the predicted value. Although the predicted load is higher than observed at a 5° rotation, the curves of load vs. rotation show that the predicted loads are lower than observed up to a rotation of approximately 3°.

Summarizing the results of the three full scale tests, the theoretical plot of load vs. footing rotation is conservative in all tests up to a footing rotation of approximately 3°. By conservative we mean that it gives a value of load which is below the value actually observed in the test. In both the sand test

and the sandy clay test, the predicted load becomes slightly unconservative from 3 to 5°. The theory gives values of load below those actually observed for all rotations in the Galveston clay test.

In order to apply the theory developed in this study, it is necessary to approximate the soil strength parameters of cohesion (c) and angle of shear resistance (Ø). Although triaxial testing is the best way of determining these parameters, it is not economically feasible for the design of many footings. For this reason, a section of this report is devoted to approximate methods of determining these strength parameters. The Cohoron Sheargraph seems to offer the only quick method of determining both c and Ø.

Design curves are presented in Appendix B of this report, which allow a very quick selection of an appropriate footing when the approximate values of the soil strength parameters are known. The use of these design curves, along with a tentative design procedure, is given in the preceding section of this report. The use of the design procedure developed in this study along with reasonable safety factors will result in significant savings in the costs of drilled shaft footings used to support highway service structures.

SELECTED REFERENCES

1. Ivey, Don L., "Theory, Resistance of a Drilled Shaft Footing to Overturning Loads," Research Report No. 105-1, Texas Transportation Institute, August, 1967.

2. Ivey, Don L., Koch, Kenneth J., and Raba, Carl F. Jr., "Resistance of a Drilled Shaft Footing to Overturning Loads, Model Tests and Correlation with Theory," Research Report No. 105-2, Texas Transportation Institute, July, 1968.

3. Peck, Hanson, and Thornburn, Foundation Engineering, Wiley & Sons, New York, 1953.

4. Foundation Exploration and Design Manual, Texas Highway Department, January, 1964, p. 4-51.

5. Terzaghi and Peck, Soil Mechanics in Engineering Practice, 2nd edition, John Wiley and Sons, 1967, p. 347.

6. Operation Manual for the Cohron Sheargraph, Model D-250, Soiltest, Incorporated, Evanston, Illinois.

7. Cohron, G. T., "The Soil Sheargraph," ASAE Technical Paper No. 62-133, June, 1962.

APPENDIX A

ALGEBRAIC ANALYSIS

The use of the various equations necessary to analyze a drilled shaft footing problem will be demonstrated in this section. When equations from Reference 1 are used, they will be referenced by the equation number given in Reference 1 (e.g. Ref. 1 (6)). When equations from Reference 2 are used, they will be referenced by page number (e.g. Ref. 2 pg. 13).

Given: Footing Diameter, d = 2.16 ft (25 in diameter hole produced by a 24 in auger)

Footing Radius, R = 1.08 ft

Footing Depth, D = 6 ft

Height of Load, H = 12 ft

Average cohesion in the soil surrounding the top two-thirds of the footing, c_a* = 200 psf

Average cohesion in the soil surrounding the bottom one-third of the footing, c_b* = 200 psf

Angles of Shear Resistance,

$\phi_a = \phi_b = 30°$

Coefficients of shear stress,

$J_1 = J_2 = 0.7$ Ref. 2, pg. 14

Coefficients of earth pressure at rest,

$K_o = 0.5$ Ref. 2, pg. 14

Unit weight coefficient,

$k = 0.5$ Ref. 2, pg. 14

Unit weight of soil,

$\gamma = 100$ lb/ft^3

Find: P, the load that will cause a footing rotation of 5°.

---

* Wherever the subscripts a or b are used, they refer to a condition in the top two-thirds (a) or the bottom one-third (b) of the footing installation.

Approach:

(1) Assume a value of "a", the distance down to the rotation point.

(2) Calculate the value of P, the maximum (5° rotation) load the footing can resist using equation (17') Ref. 1.

(3) Put this value of P into equation (18') and see if this moment equation is satisfied.

(4) If equation (18') is not satisfied, select a new value of "a" and repeat steps 1 through 4.

(5) If equation (18') is satisfied, the value of P computed by equation (17') is the correct one.

This is a trial and error solution which will be demonstrated by this example:

Calculations:

$B_a = B_b = .0000673\ (200) + 10.25 \tan 30° + 2.686 \tan (45° + 30°/2) - 2.141 \tan^2 (45° + 30°/2)$ Ref. 2, pg. 15

$B_a = B_b = 4.17$

$K_{1a} = K_{1b} = 4.17 \tan^2 (45° + 30°/2) = 12.51$ Ref. 2, pg. 13

$K_{2a} = K_{2b} = 2\ (4.17) \tan\ (45° + 30°/2) = 14.46$ Ref. 2, pg. 13

$T_a^* = T_b = 0.5\ [1 - 3.14/4 + 0.577\ (3.14/4 - 0.333)] + 12.51\ (3.14/4 + 0.192)$ Ref. 1, pg. 8

$T_a = T_b = 12.46$

$V_a^* = V_b = 0.786 + 14.46\ (0.786 + 0.192)$

$V_a = V_b = 14.94$ Ref. 1, pg. 8

$\gamma_a = 100\ [1 + 0.5\ (0.577)] = 128.8$

$\gamma_b = 100\ [1 - 0.5\ (0.577)] = 71.2$ } Ref. 2, pg. 14

$L_a = K_o\ \gamma_a = 0.5\ (128.8) = 64.4$

$L_b = K_o\ \gamma_b = 0.5\ (71.2) = 35.6$

---

* Same as E and G in Ref. 1, pg. 8.

$M_a = K_{2a}\, c_a = 14.46\ (200) = 2892$

$M_b = K_{2b}\, c_b = 14.46\ (200) = 2892$

$N_a = (K_{1a} - K_o)\, \gamma_a = (12.51 - 0.5)\ 128.8 = 1547$

$N_b = (K_{1b} - K_o)\, \gamma_b = (12.51 - 0.5)\ 71.2 = 854$

Assume $a = (0.5\ D) = 3$ feet

$F_{xa} = 2.166\ [128.8\ (9/2)\ (12.46) + 200\ (14.94)\ 3]$

$F_{xa} = 35{,}100$ lbs Ref. 1, (5)*

$F_{xb} = 2.166\ [71.2\ (\frac{36-9}{2})\ 12.46 + 200\ (14.94)\ 3]$

$F_{xb} = 45{,}500$ lbs Ref. 1, (6)*

V_{za} and V_{zb} are presented here in slightly different form than in Ref. 1. e.g.:

$$V_{za} = 2\, J_1\, R \left\{\left[\frac{a^2}{2} \tan \phi_a \left[\frac{\pi\, L_a}{2} + N_a\right]\right] + a \left[M_a \tan \phi_a + \frac{c_a\, \pi}{2}\right]\right\}$$

$$V_{za} = 0.7\ (2.166) \left\{\left[\frac{9}{2}\ (0.577) \left[1.57\ (64.4) + 1547\right]\right] + 3 \left[2892\ (0.577) + 200\ (1.57)\right]\right\} = 15{,}600 \text{ lbs}$$

$$V_{zb} = 2\, J_1\, R \left\{(D^2 - a^2) \tan \phi_b \left[\frac{\pi\, L_b}{2} + N_b\right] \frac{1}{2} + (D - a) \left[M_b \tan \phi_b + \frac{c_b\, \pi}{2}\right]\right\}$$

$$V_{zb} = 0.7\ (2.166) \left\{(\frac{36-9}{2})\ (0.577) \left[1.57\ (35.6) + 854\right] + 3 \left[2892\ (0.577) + 200\ (1.57)\right]\right\} = 19{,}850 \text{ lbs}$$

$F_{xa}\, Z_1 = 2.166\ [128.8\ (27/3)\ 12.46 + 200\ (14.94)\ 9/2]$

$F_{xa}\, Z_1 = 60{,}400$ ft-lbs Ref. 1, (7)

$F_{xb}\, Z_2 = 2.166\ [71.2\ (\frac{216 - 27}{3})\ 12.46 + 200\ (14.94)\ 27/2]$

$F_{xb}\, Z_2 = 210{,}000$ ft-lbs Ref. 1, (8)

---

* In these equations, E and G are now represented by T and V.

$M_v = 0.74\ R\ (V_{za} + V_{zb})$ Simplified form of Equation (11), Ref. 1.

$M_v = 0.37\ (2.166)\ [15{,}600 + 19{,}850]$

$M_v = 28{,}410$ ft-lbs

$F_s = 5{,}525$ lbs. The weight of the structure plus the weight of the footing.

$F_{zd} = 5525 - 15{,}600 + 19{,}850 = 9{,}775$ lbs Ref. 1, (12)

$$V_{xd} = 0.7 \left[9775\ (0.577) + 200\ \frac{(3.14)\ (2.166)^2}{8}\right]$$ Ref. 1, (13)

$V_{xd} = 4{,}206$ lbs

$P = 35{,}100 - 4206 - 45{,}500$ Ref. 1, (14)

$P = -14{,}606$ lbs

$\sum M_z = (-14{,}606)\ 12 + 60{,}400 - 210{,}000 - (4{,}206)\ 6 - 28{,}410$

$\sum M_z = -378{,}518$ ft-lbs Ref. 1, (15)

Since the summation of moments is not equal to zero (necessary for equilibrium) the choice of "a" is incorrect. Table 2 gives the values of P and $\sum M$ calculated in the way demonstrated for different choices of "a".

Table 2

RESULTS OF CALCULATIONS

Assumed "a"	P lbs	$\sum M$ ft-lbs
0.5D	-14,656	-378,518
0.7D	26,242	309,800
0.61D	9,500	-220*

* Unbalanced by 0.1%.

By plotting the $\sum M_z$ as the ordinate and the assumed value of "a" as the abscissa the plot shown by Figure 28 was constructed. By connecting the first two points calculated (corresponding to 0.5D and 0.7D) by a straight line, the third estimate for "a" was selected. Using this value (0.61D) the moment equation is satisfied for a value of P of 9500 lbs. Thus the correct answer is P = 9500 lbs.

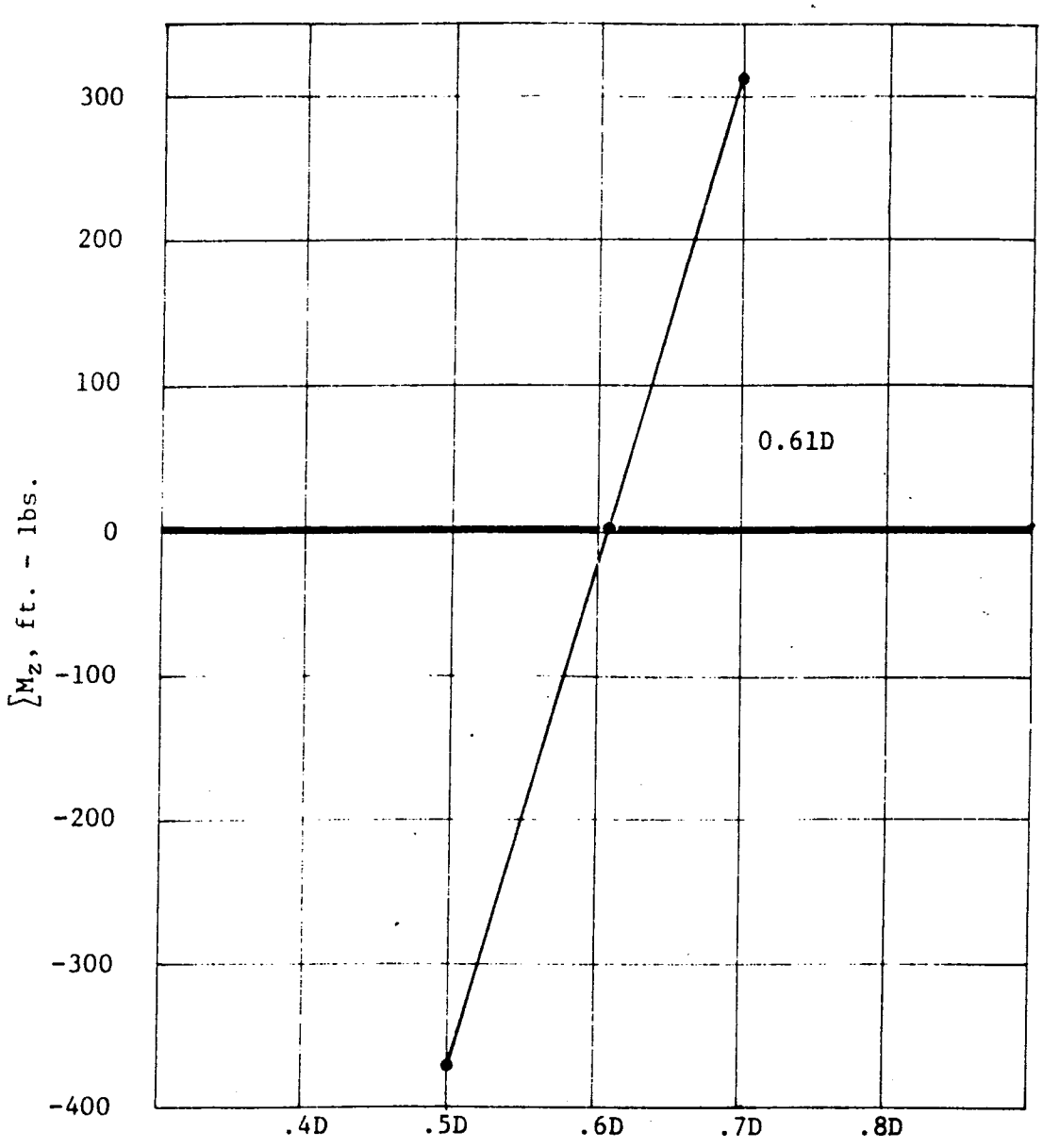

Figure 28, Approximation of "a".

APPENDIX B

INDEX TO DESIGN CURVES*

Cohesion, c (PSF)	Angle of Shearing Resistance, ϕ (Degrees)	Page Nos.
0	5	61,62
0	10	63,64
0	15	65,66
0	20	67,68
0	25	69,70
0	30	71,72
0	35	73,74
500	0	75,76
500	5	77,78
500	10	79,80
500	15	81,82
500	20	83,84
500	25	85,86
500	30	87,88
500	35	89,90
1000	0	91,92
1000	5	93,94
1000	10	95,96
1000	15	97,98
1500	0	99,100
1500	5	101,102
1500	10	103,104
1500	15	105,106
2000	0	107,108
2000	5	109,110
2000	10	111,112
2000	15	113,114
2500	0	115,116
2500	5	117,118
2500	10	119,120
2500	15	121,122
3000	0	123,124
3000	5	125,126
3000	10	127,128
3000	15	129,130
3500	0	131,132
3500	5	133,134
3500	10	135,136
3500	15	137,138
4000	0	139,140
4000	5	141,142
4000	10	143,144
4000	15	145,146
4500	0	147,148
4500	5	149,150
4500	10	151,152
4500	15	153,154
5000	0	155,156
5000	5	157,158
5000	10	159,160
5000	15	161,162

* Footing sizes vary from 1 foot in diameter by 2 feet in depth to 3 feet in diameter by 20 feet in depth.

An example demonstrating the selection of the appropriate footing is given on page 49 of the text.

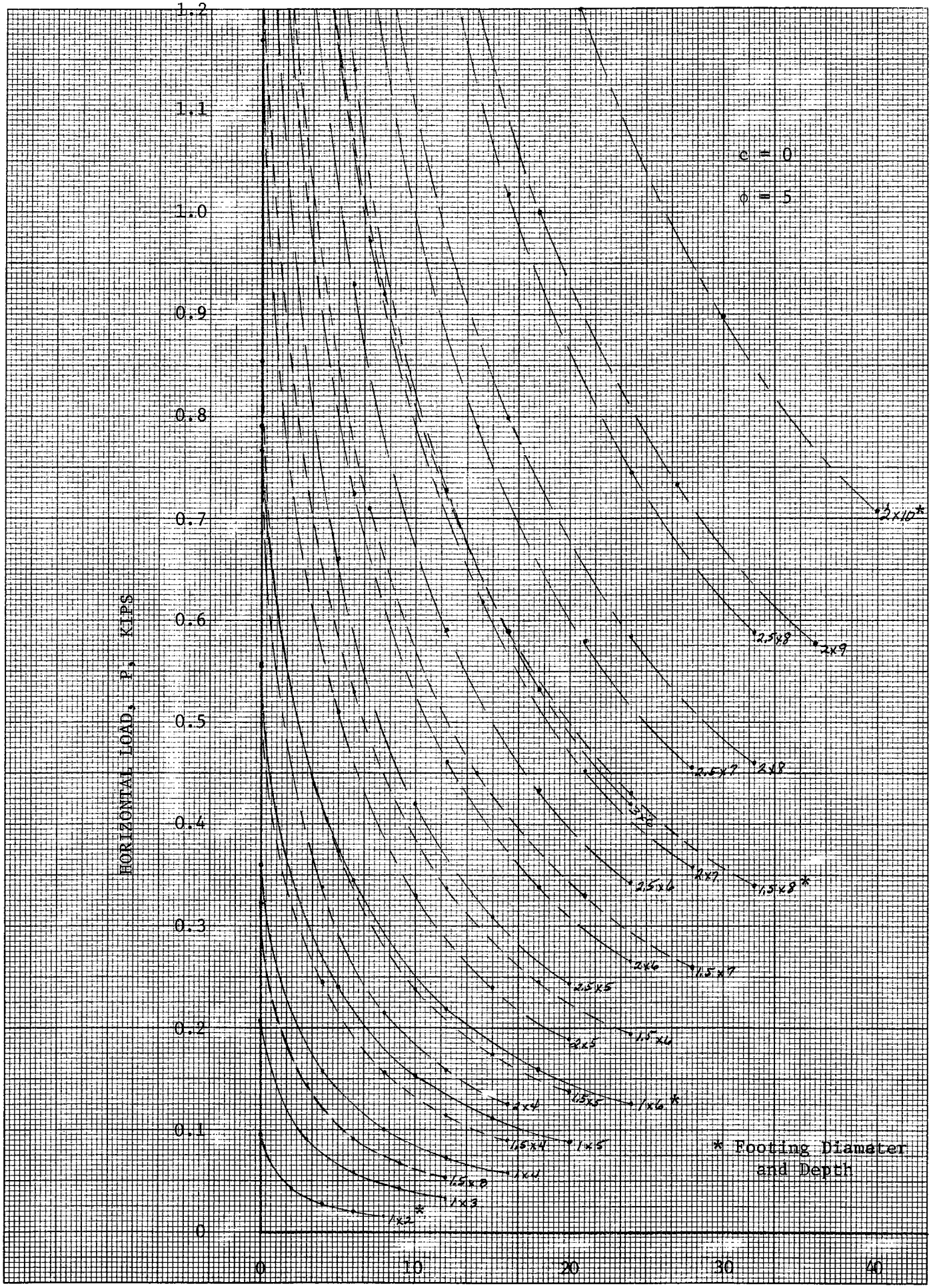

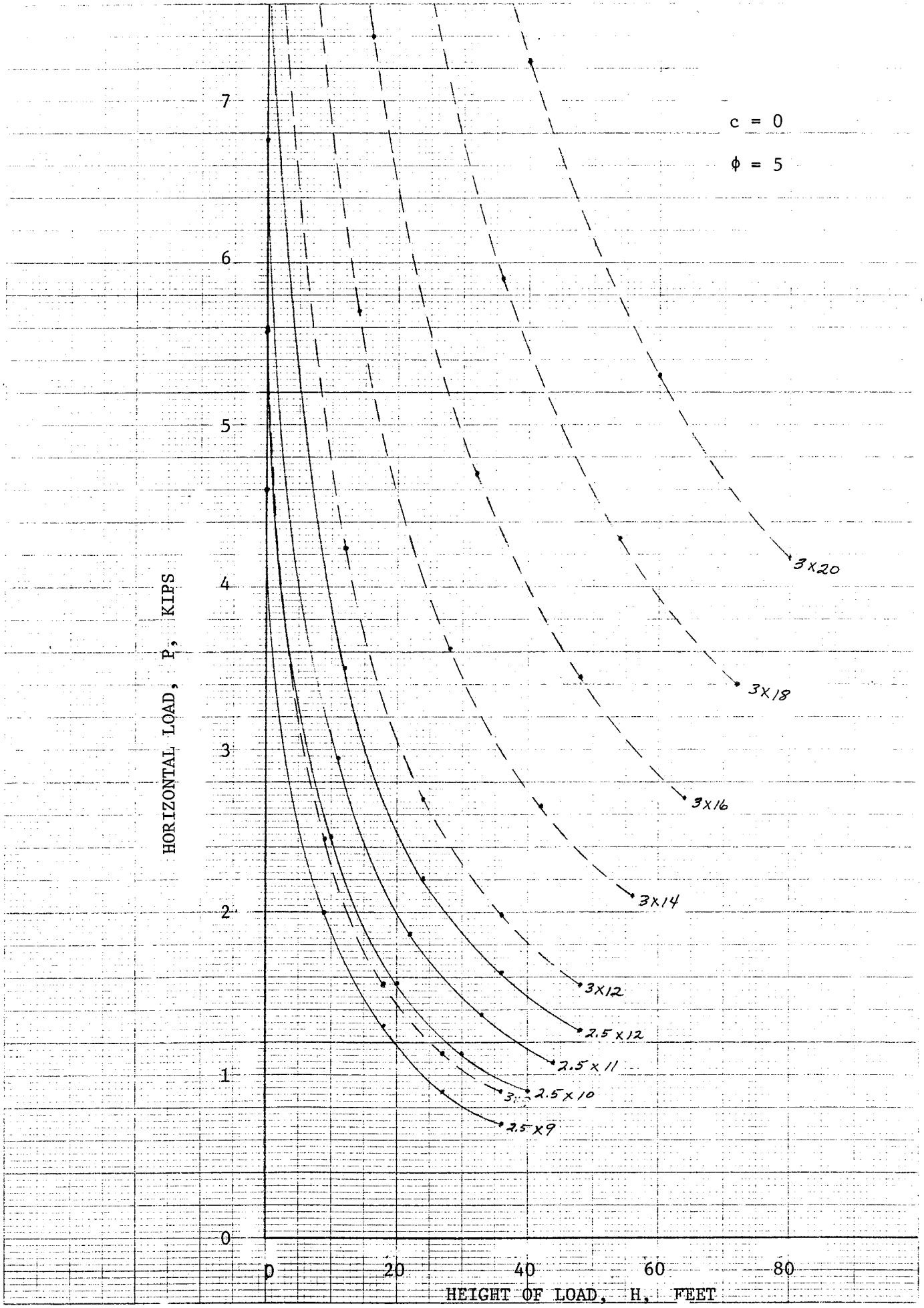
c = 0
ϕ = 5
3X20
3X18
3X16
3X14
3X12
2.5X12
2.5X11
2.5X10
2.5X9
HORIZONTAL LOAD, P, KIPS
HEIGHT OF LOAD, H, FEET
0
1
2
3
4
5
6
7
0
20
40
60
80

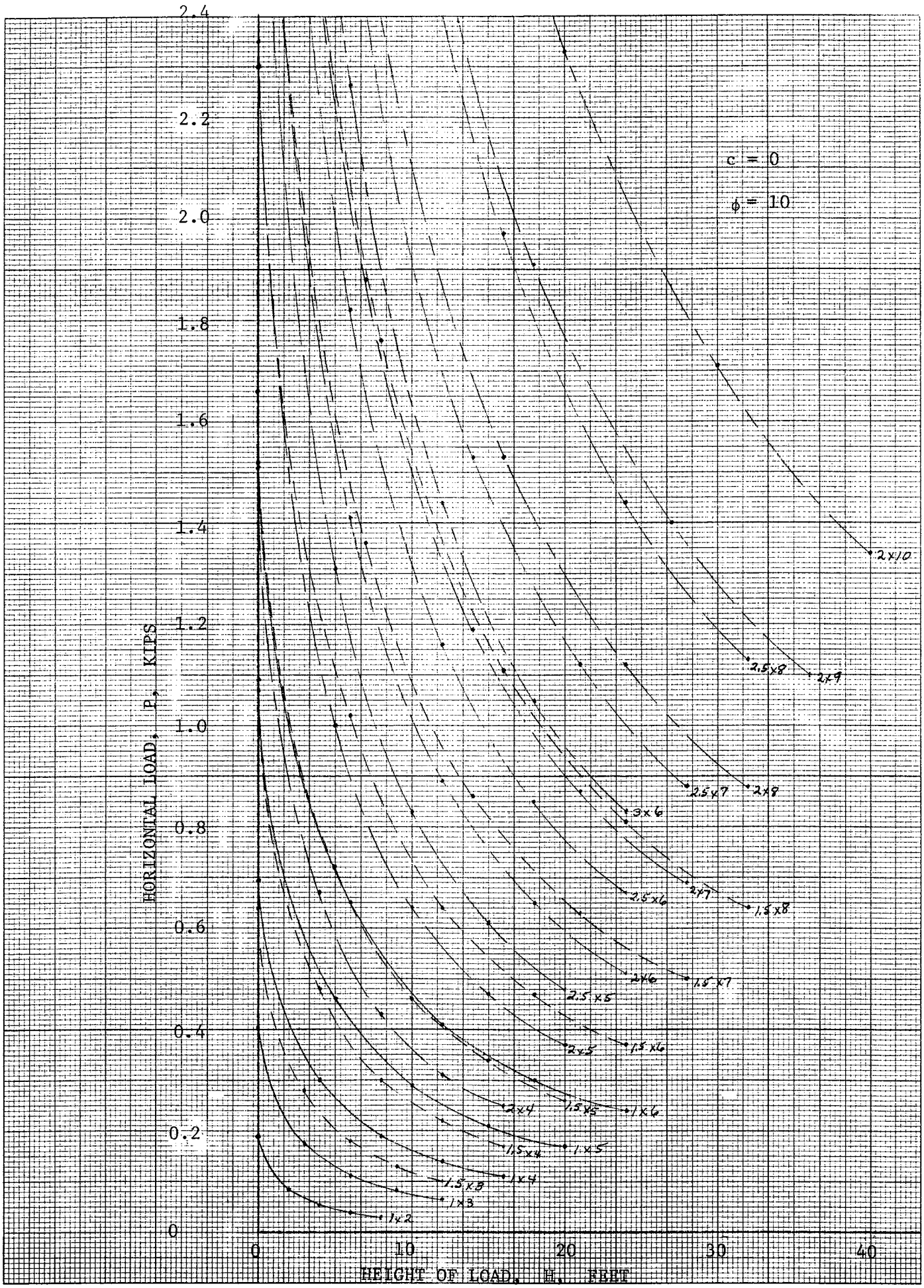

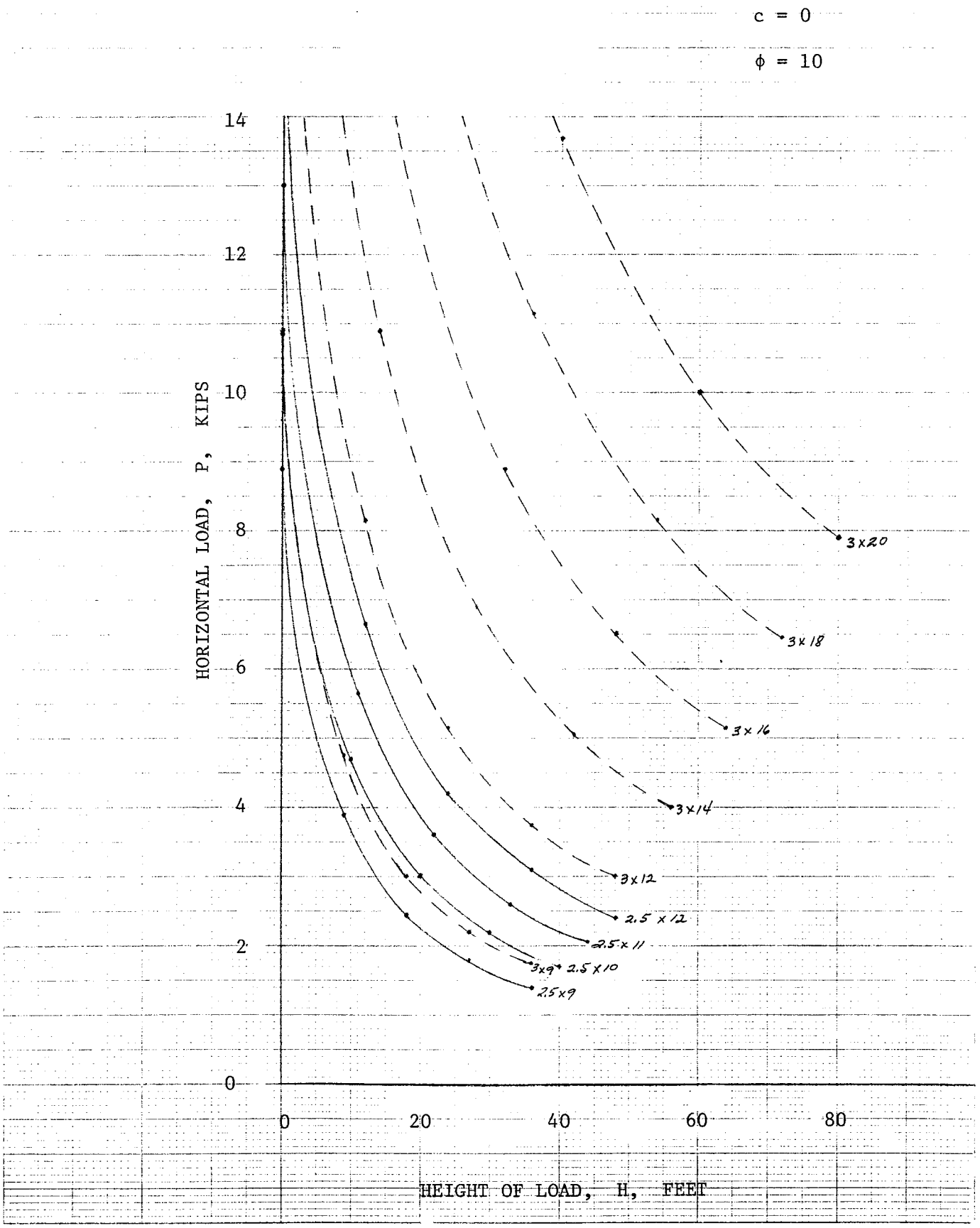
c = 0
ϕ = 10
HORIZONTAL LOAD, P, KIPS
HEIGHT OF LOAD, H, FEET
0
2
4
6
8
10
12
14
0
20
40
60
80
3x20
3x18
3x16
3x14
3x12
2.5x12
2.5x11
3x9
2.5x10
2.5x9

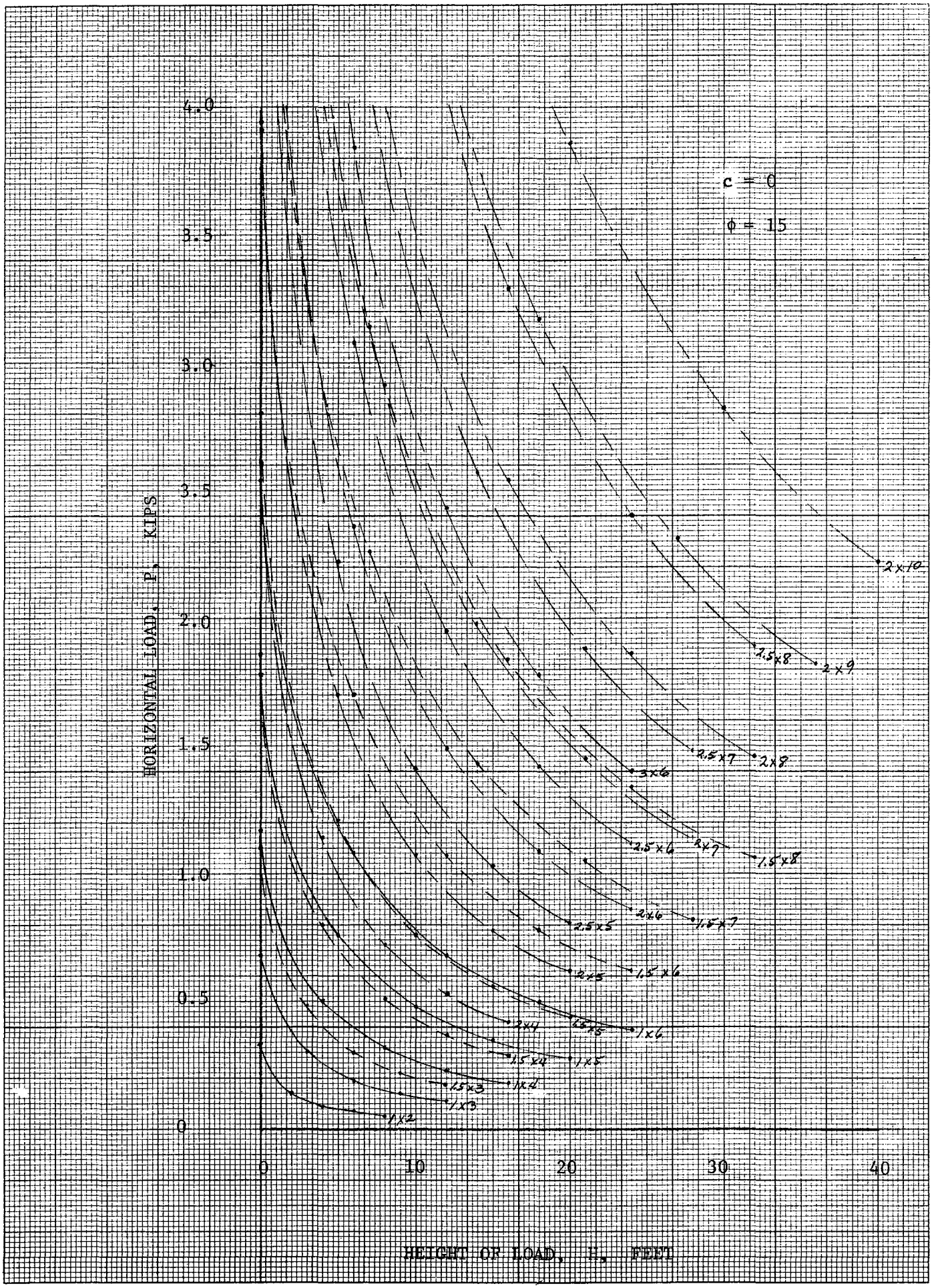

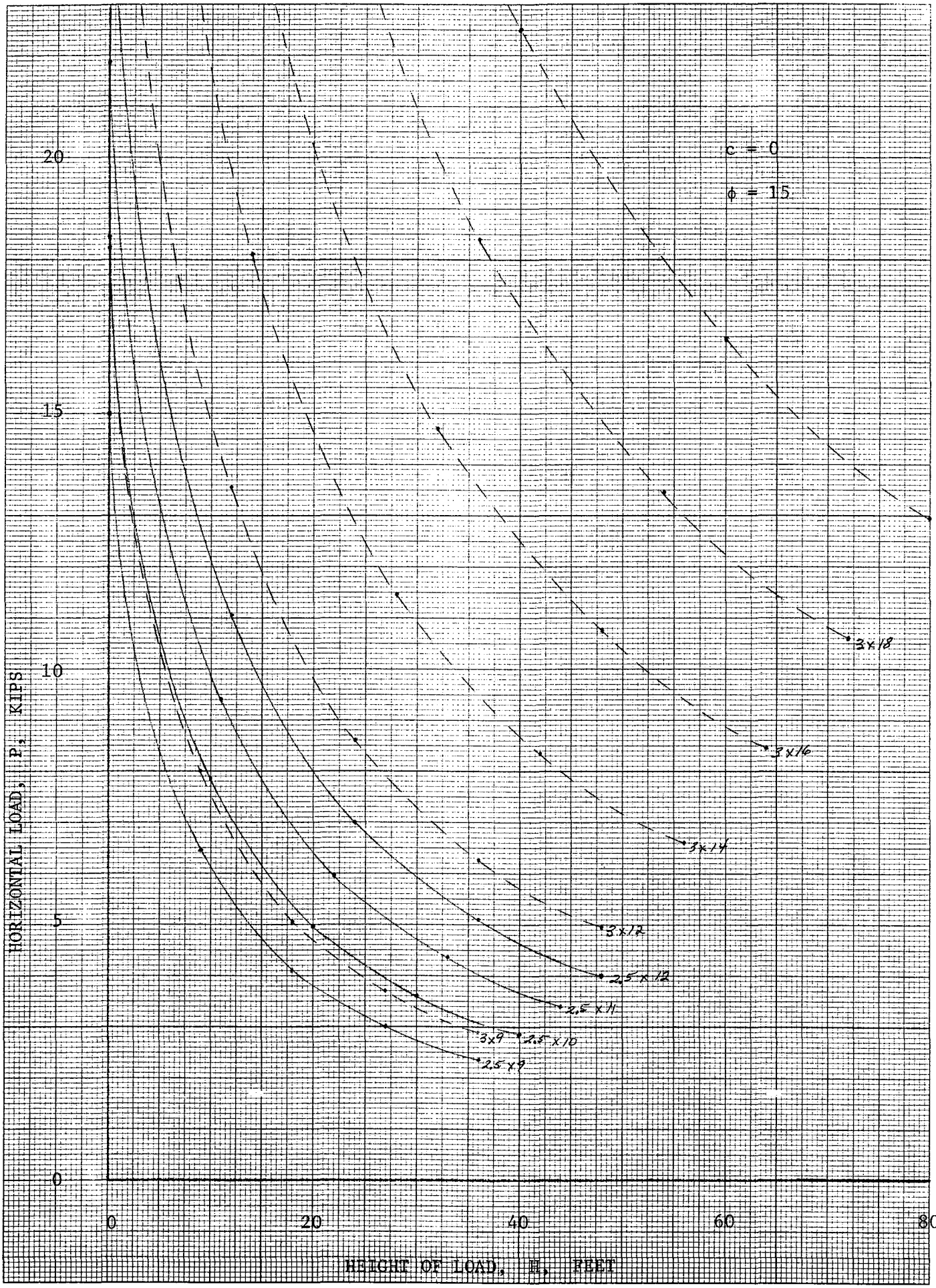

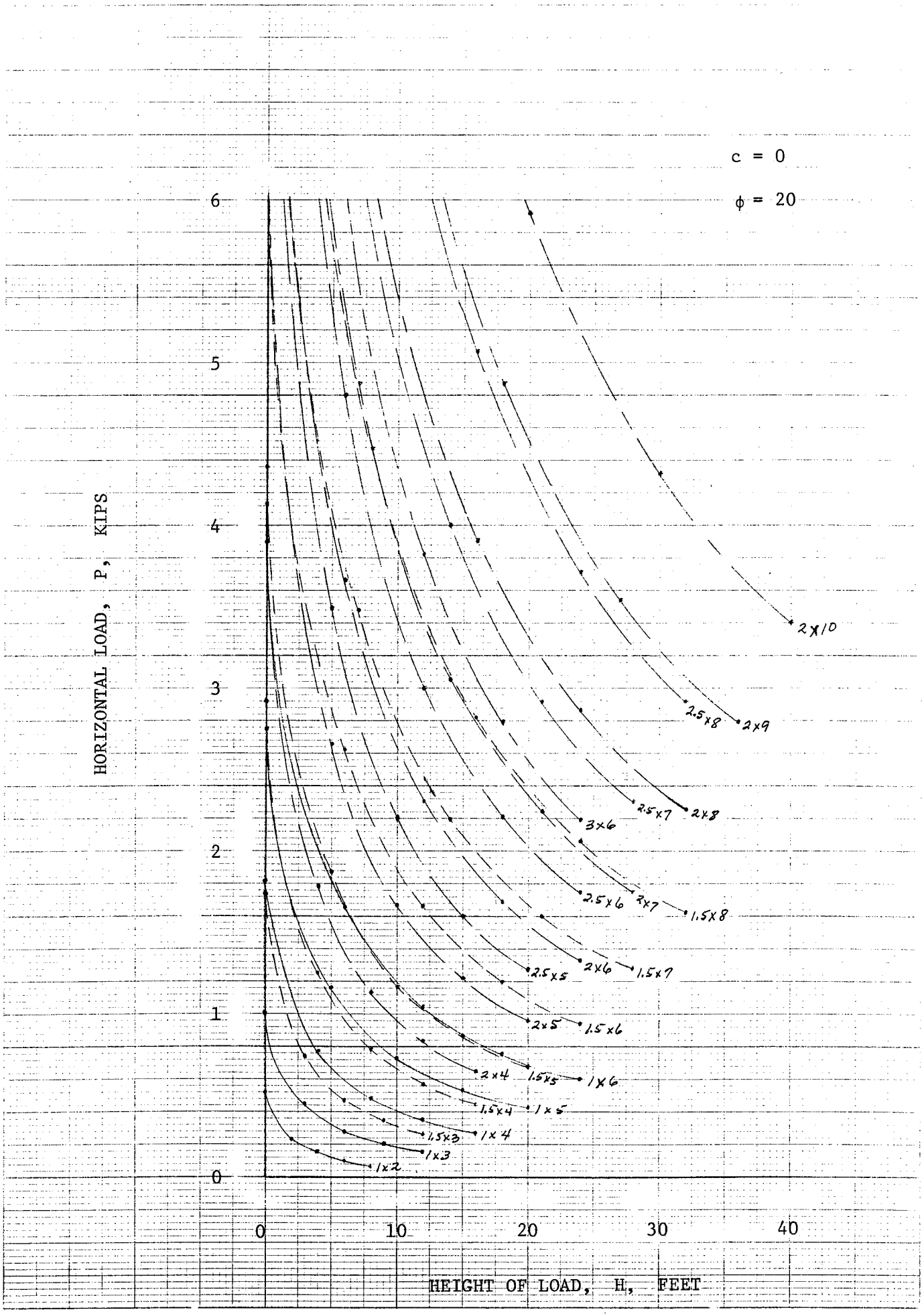
c = 0
ϕ = 20
HORIZONTAL LOAD, P, KIPS
HEIGHT OF LOAD, H, FEET
0
1
2
3
4
5
6
0
10
20
30
40
2x10
2.5x8
2x9
2.5x7
2x8
3x6
2.5x6
3x7
1.5x8
2.5x5
2x6
1.5x7
2x5
1.5x6
2x4
1.5x5
1x6
1.5x4
1x5
1.5x3
1x4
1x3
1x2

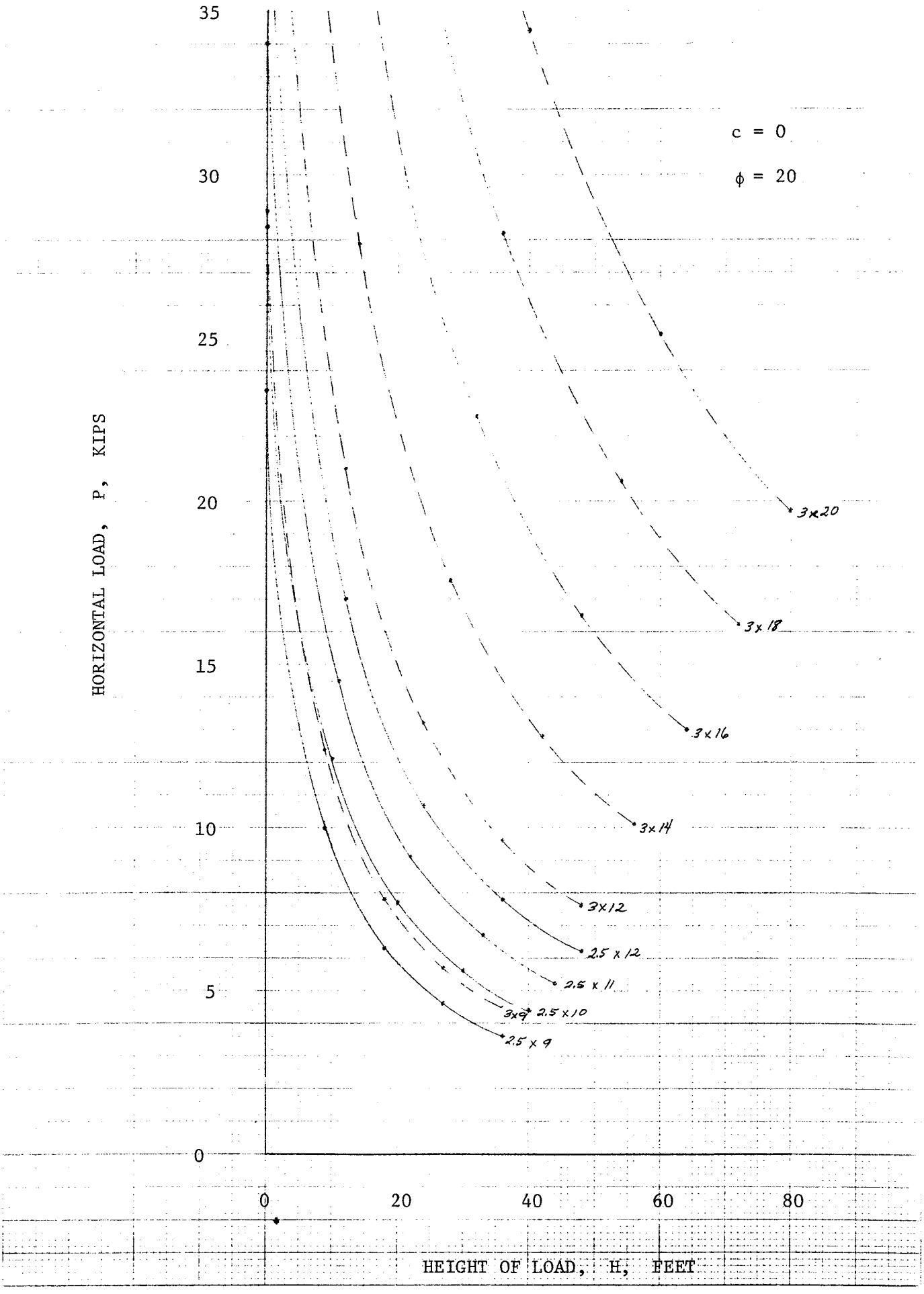
c = 0
ϕ = 20
3x20
3x18
3x16
3x14
3x12
2.5 x 12
2.5 x 11
3x9
2.5 x 10
2.5 x 9
HORIZONTAL LOAD, P, KIPS
HEIGHT OF LOAD, H, FEET
0
5
10
15
20
25
30
35
0
20
40
60
80

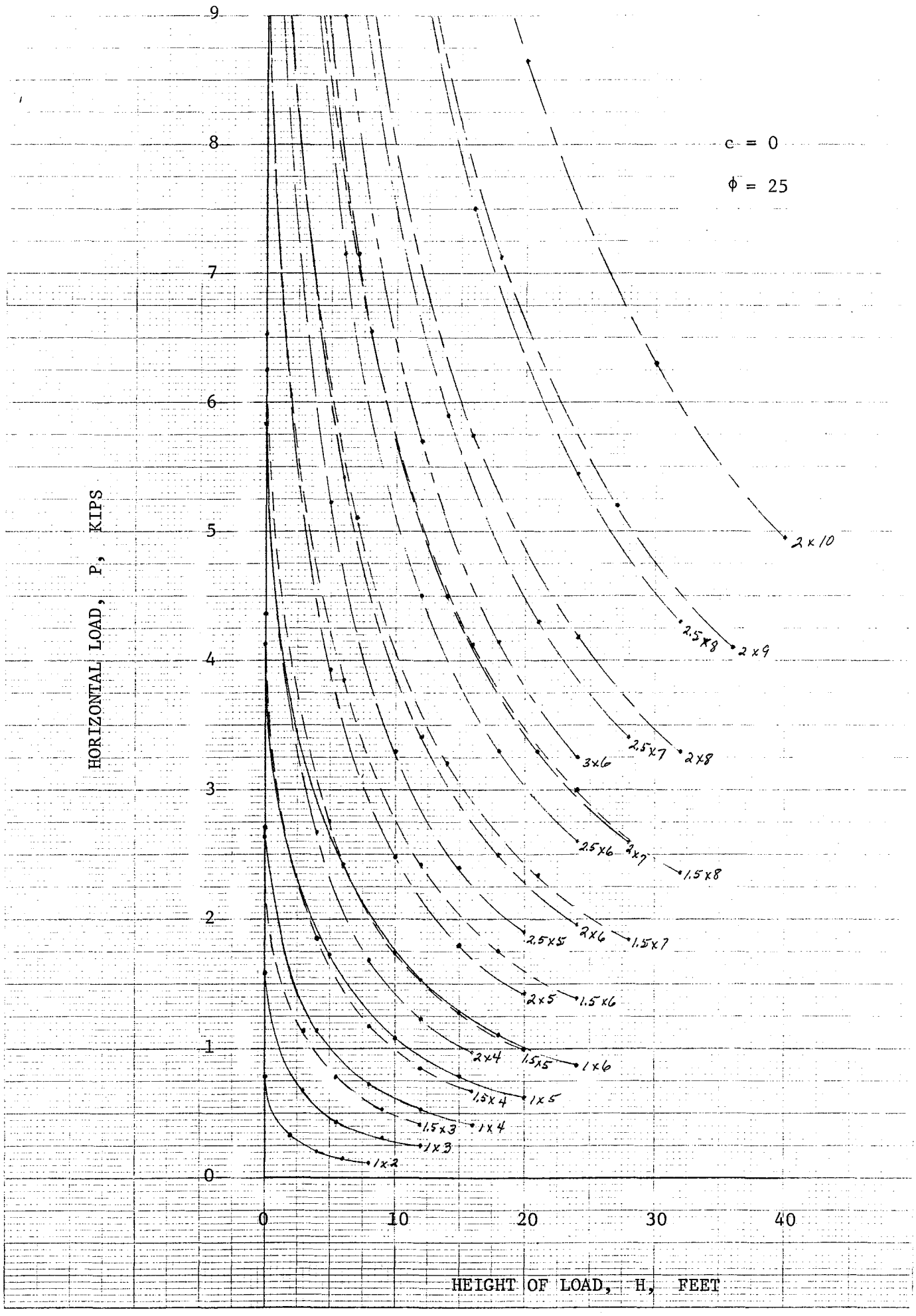
c = 0
ϕ = 25
2 x 10
2.5x8
2 x 9
2.5x7
2x8
3x6
2.5x6
2x7
1.5x8
2.5x5
2x6
1.5x7
2x5
1.5x6
2x4
1.5x5
1x6
1.5x4
1x5
1.5x3
1x4
1x3
1x2
HORIZONTAL LOAD, P, KIPS
HEIGHT OF LOAD, H, FEET
0
1
2
3
4
5
6
7
8
9
0
10
20
30
40

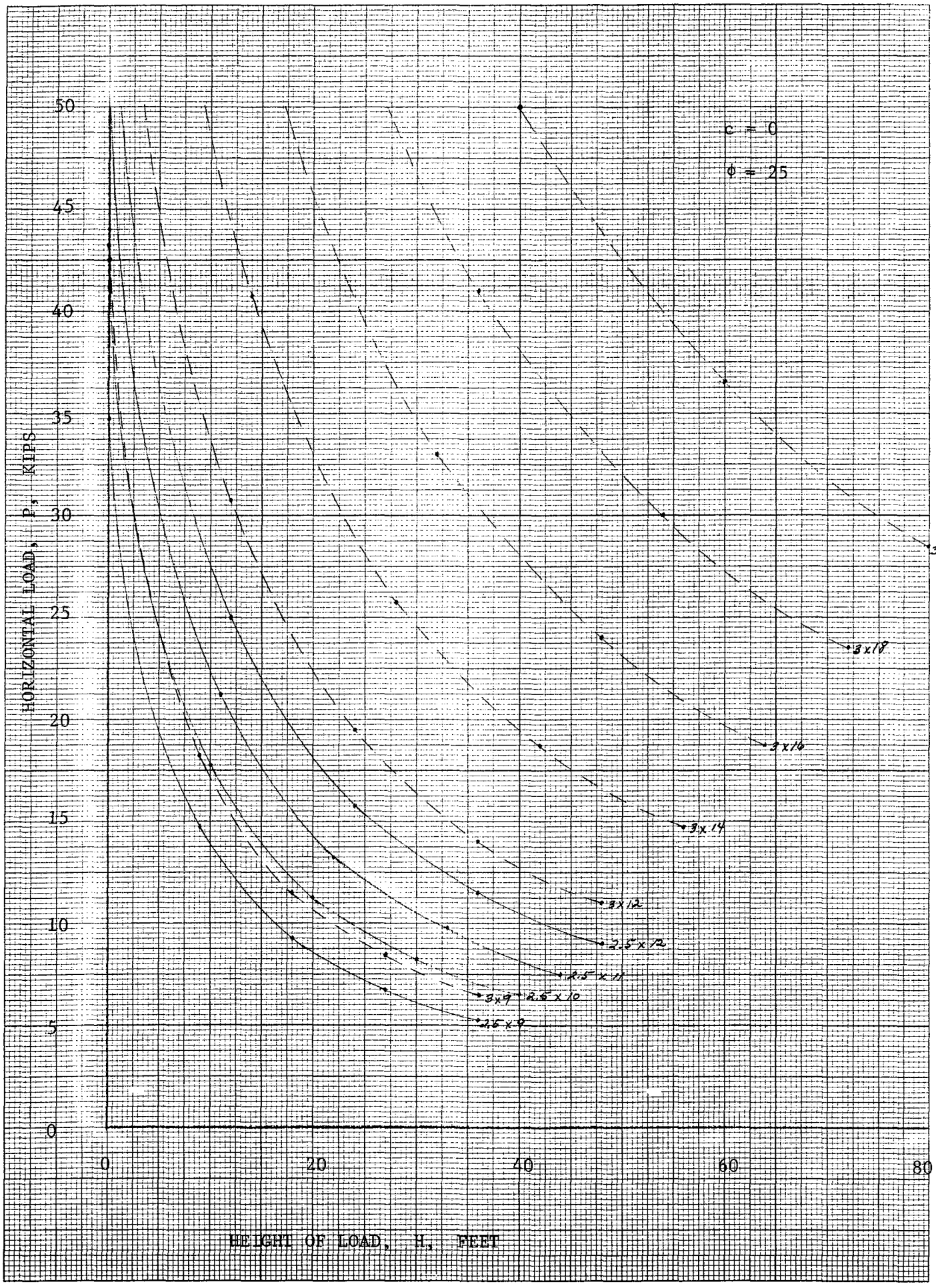

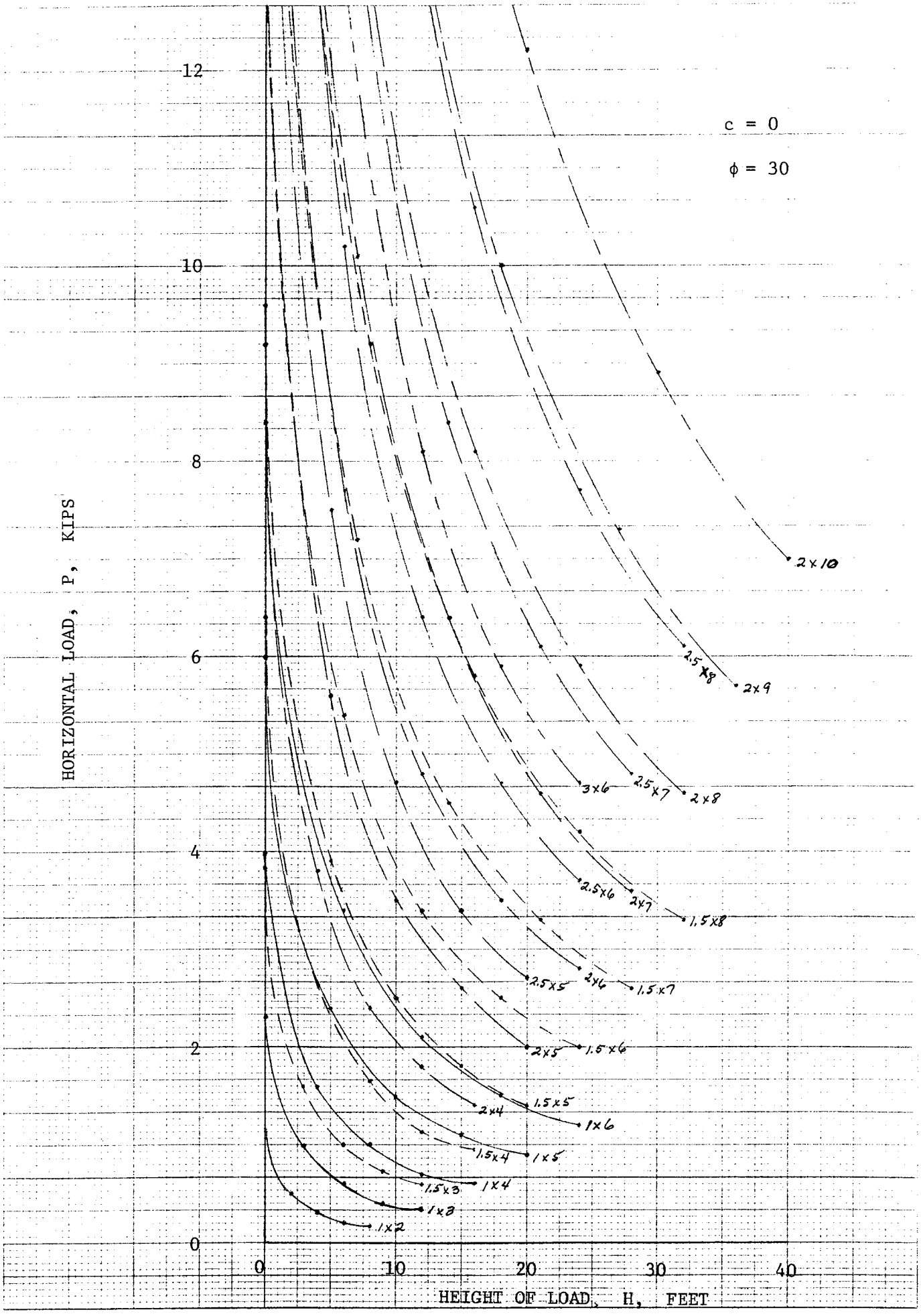
c = 0
ϕ = 30
HORIZONTAL LOAD, P, KIPS
HEIGHT OF LOAD, H, FEET
0
2
4
6
8
10
12
0
10
20
30
40
2x10
2.5x8
2x9
3x6
2.5x7
2x8
2.5x6
2x7
1.5x8
2.5x5
2x6
1.5x7
2x5
1.5x6
2x4
1.5x5
1x6
1.5x4
1x5
1.5x3
1x4
1x3
1x2

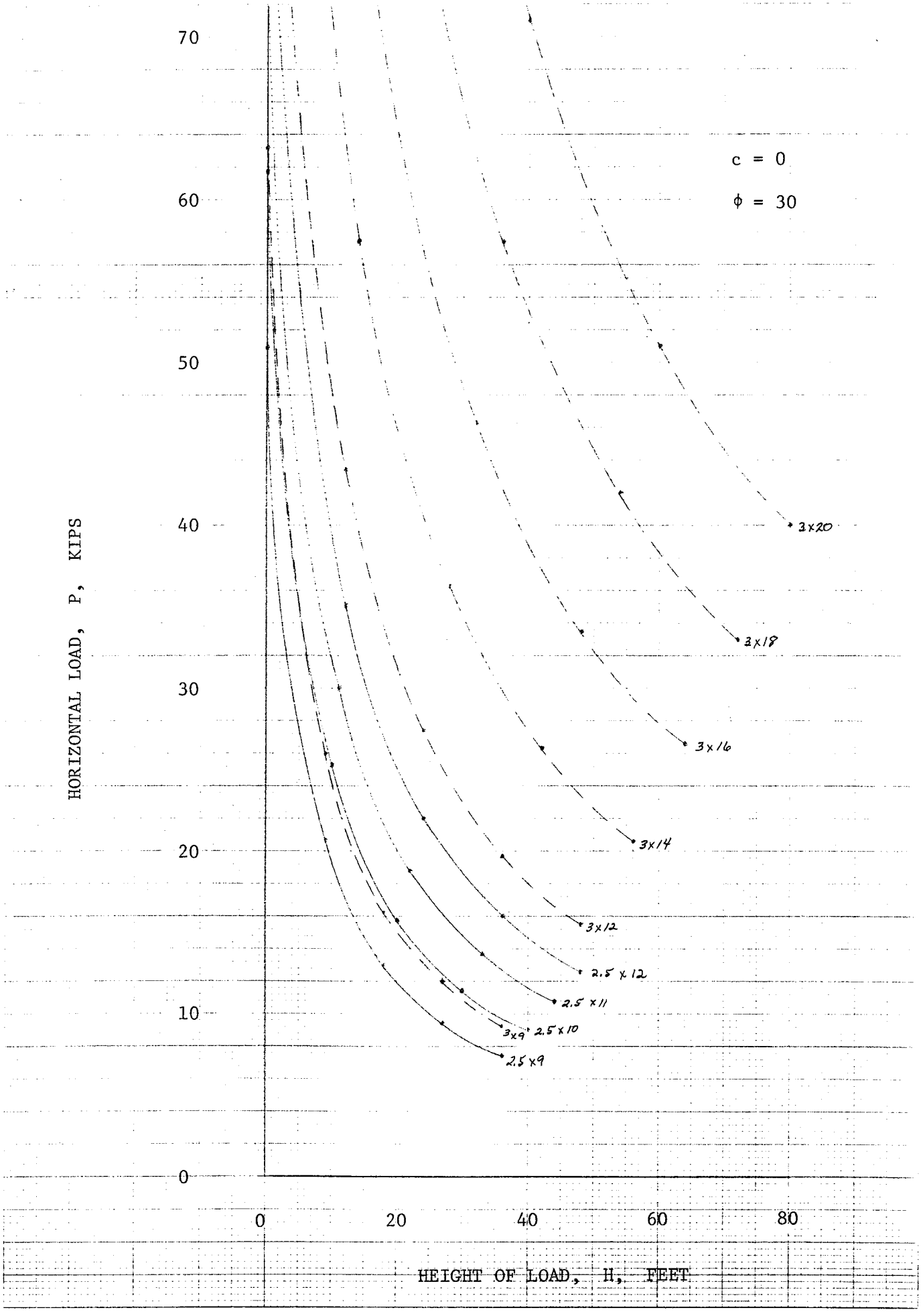
c = 0
ϕ = 30
3x20
3x18
3x16
3x14
3x12
2.5 x 12
2.5 x11
2.5x10
3x9
2.5x9
HORIZONTAL LOAD, P, KIPS
HEIGHT OF LOAD, H, FEET
0
10
20
30
40
50
60
70
0
20
40
60
80

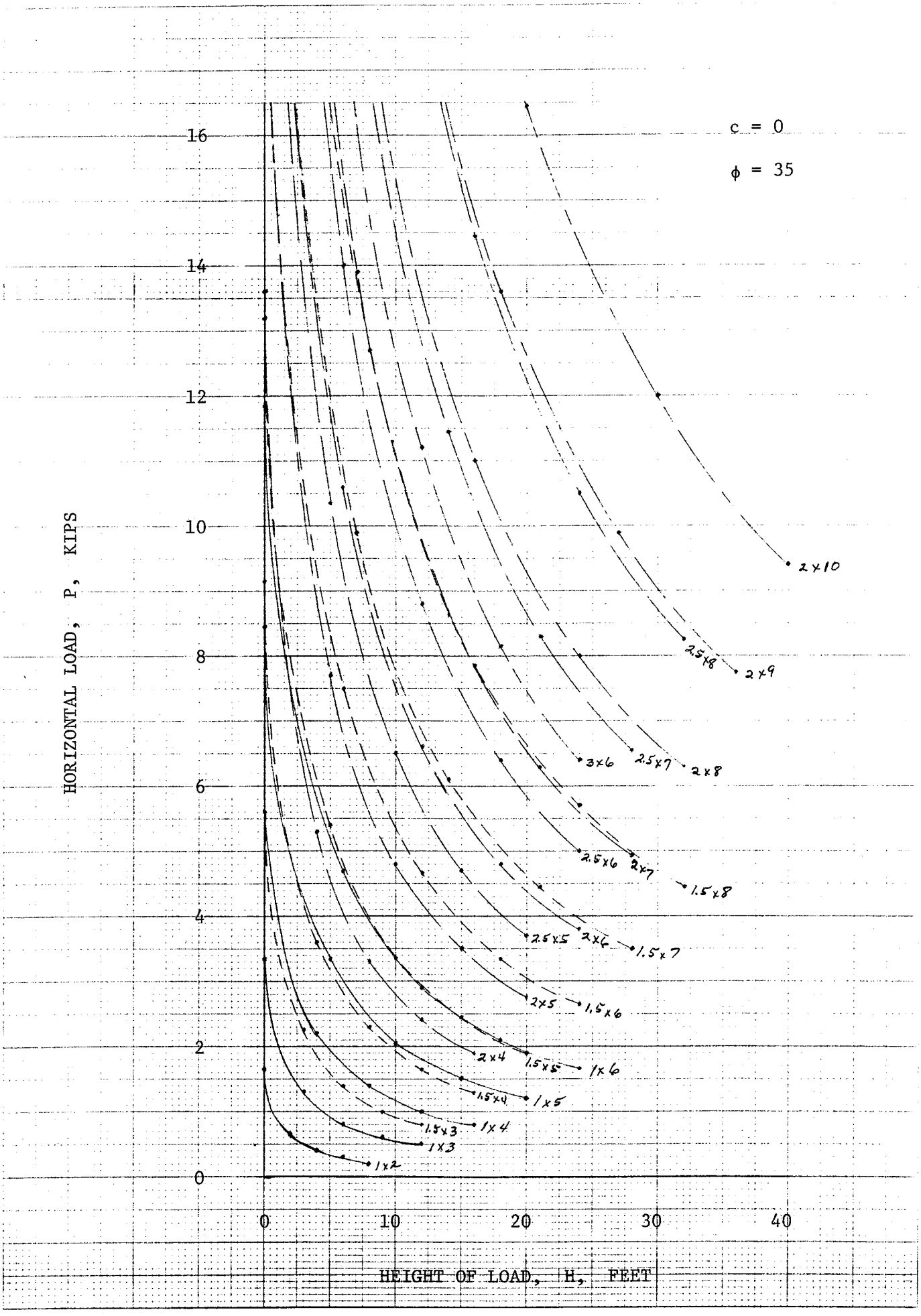
c = 0
ϕ = 35
HORIZONTAL LOAD, P, KIPS
HEIGHT OF LOAD, H, FEET
0
2
4
6
8
10
12
14
16
0
10
20
30
40
2x10
2.5x8
2x9
3x6
2.5x7
2x8
2.5x6
2x7
1.5x8
2.5x5
2x6
1.5x7
2x5
1.5x6
2x4
1.5x5
1x6
1.5x4
1x5
1.5x3
1x4
1x3
1x2

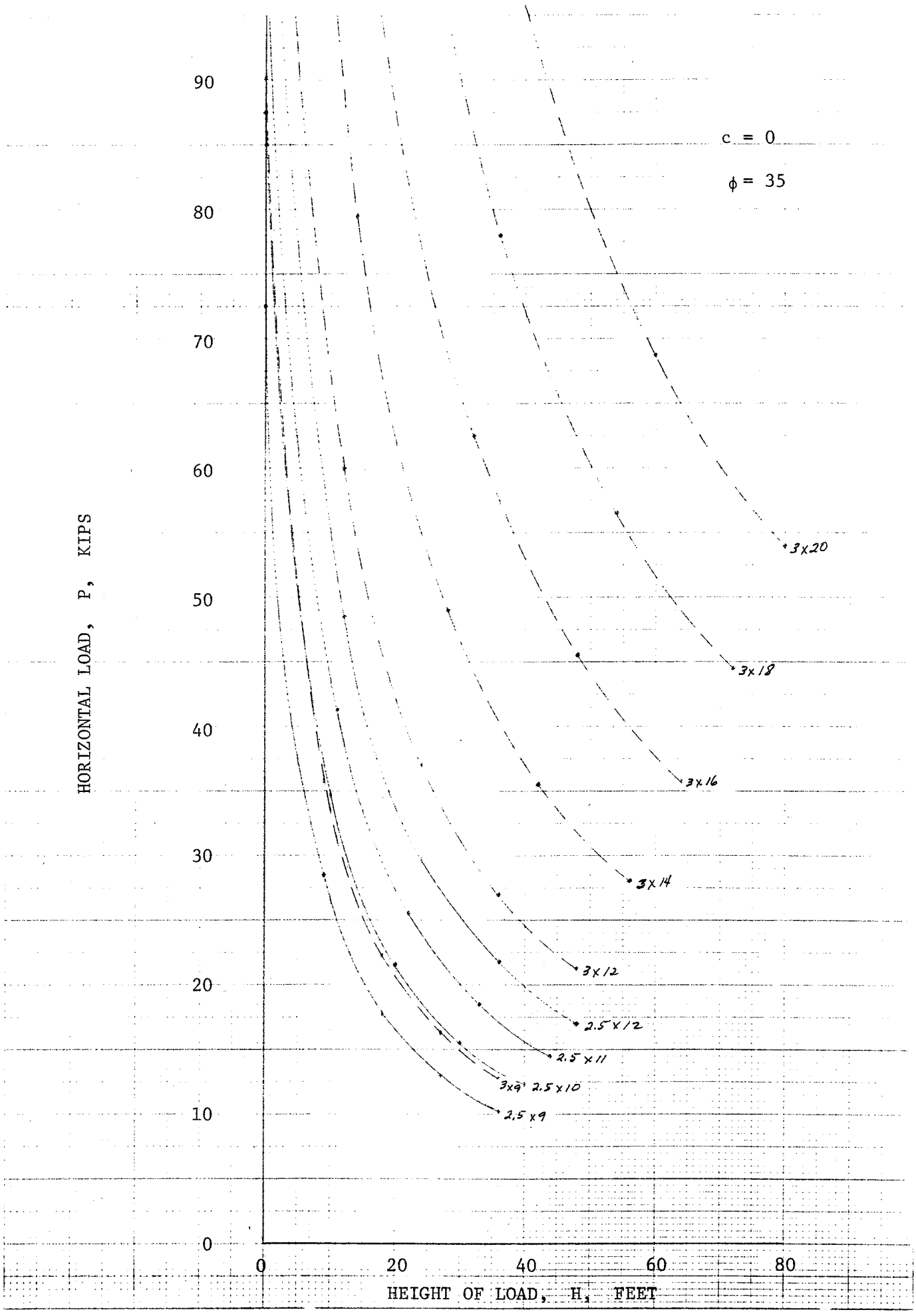
c = 0
ϕ = 35
3x20
3x18
3x16
3x14
3x12
2.5x12
2.5x11
3x9
2.5x10
2.5x9
HORIZONTAL LOAD, P, KIPS
HEIGHT OF LOAD, H, FEET
0
10
20
30
40
50
60
70
80
90
0
20
40
60
80

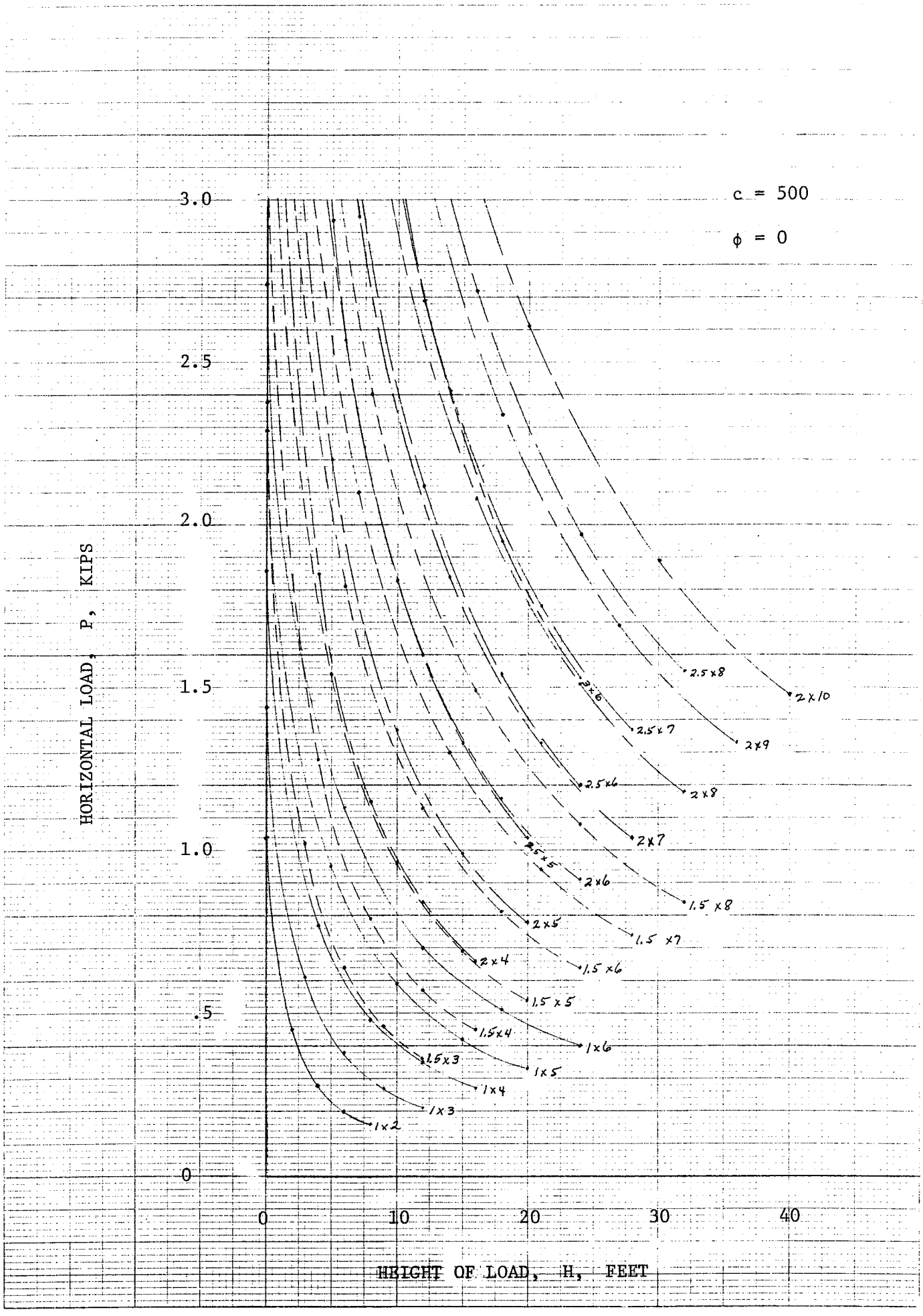
c = 500
ϕ = 0
HORIZONTAL LOAD, P, KIPS
3.0
2.5
2.0
1.5
1.0
.5
0
0
10
20
30
40
HEIGHT OF LOAD, H, FEET
2x10
2.5x8
2x9
2x8
2x7
2.5x7
2x6
2.5x6
2.5x5
2x6
1.5x8
1.5x7
2x5
1.5x6
2x4
1.5x5
1.5x4
1x6
1.5x3
1x5
1x4
1x3
1x2

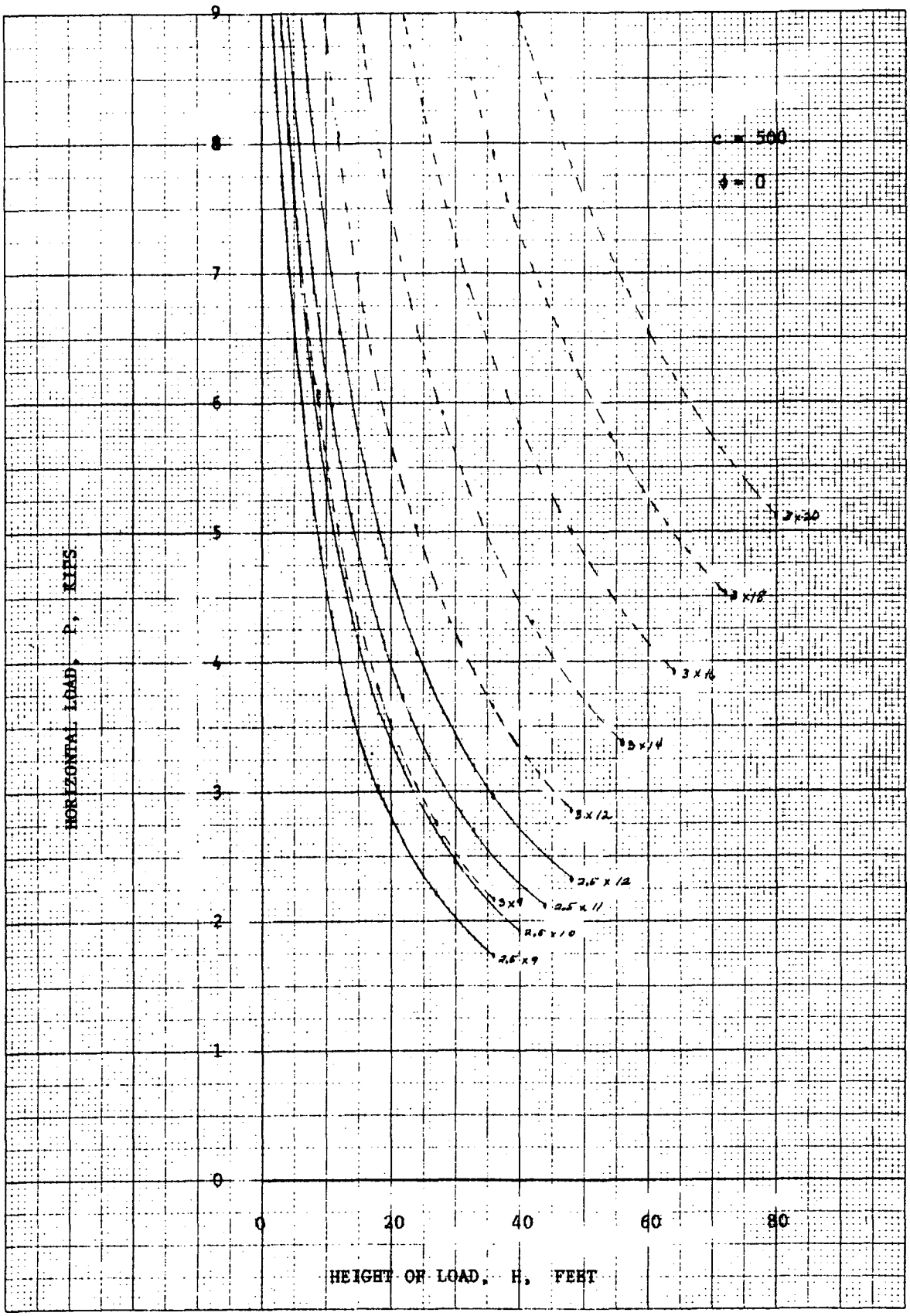
c = 500
φ = 0
3 x 20
3 x 18
3 x 16
3 x 14
3 x 12
2.5 x 12
3 x 11
2.5 x 11
2.5 x 10
2.5 x 9
HORIZONTAL LOAD, P, KIPS
HEIGHT OF LOAD, H, FEET
0
1
2
3
4
5
6
7
8
9
0
20
40
60
80

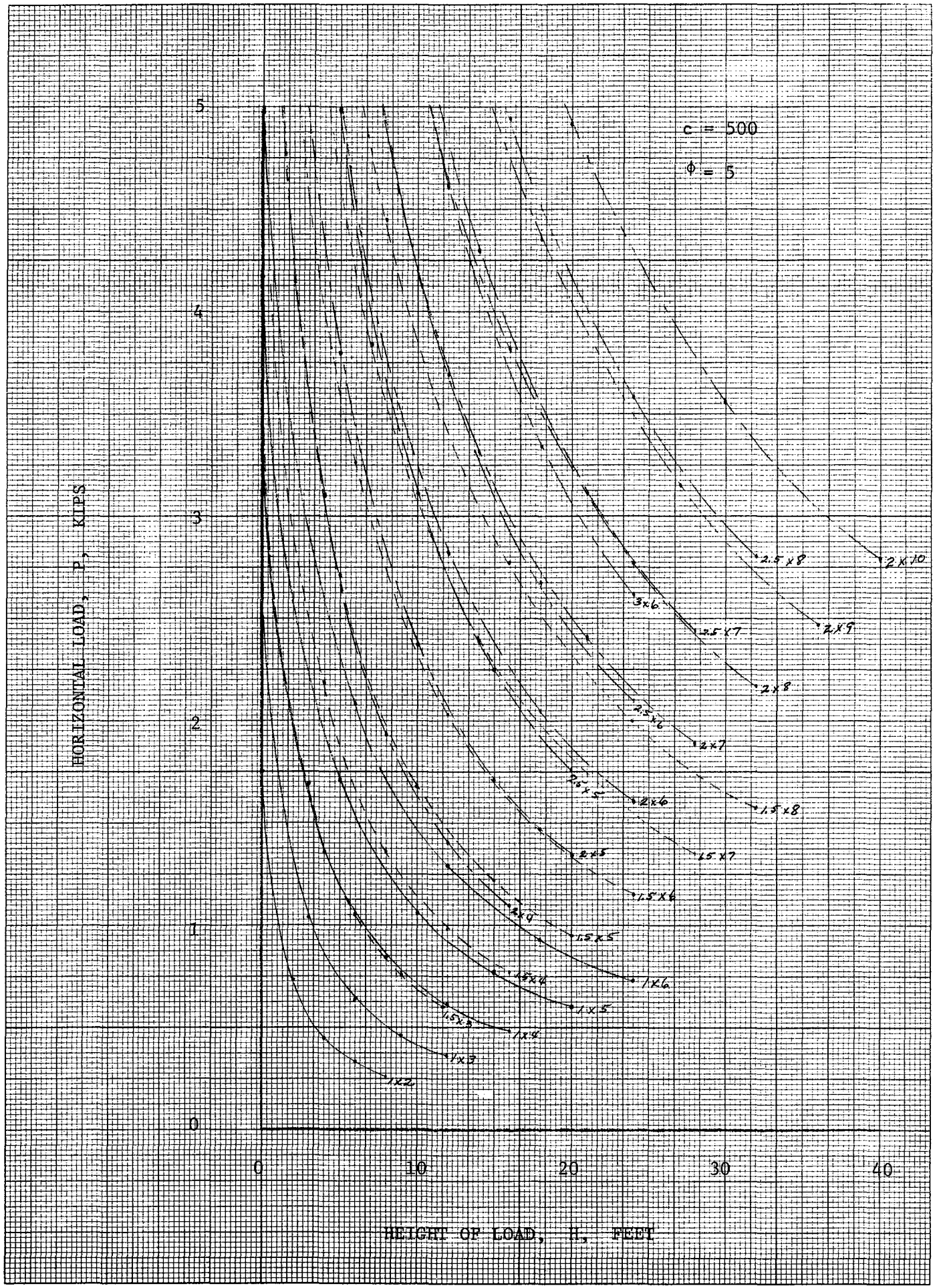

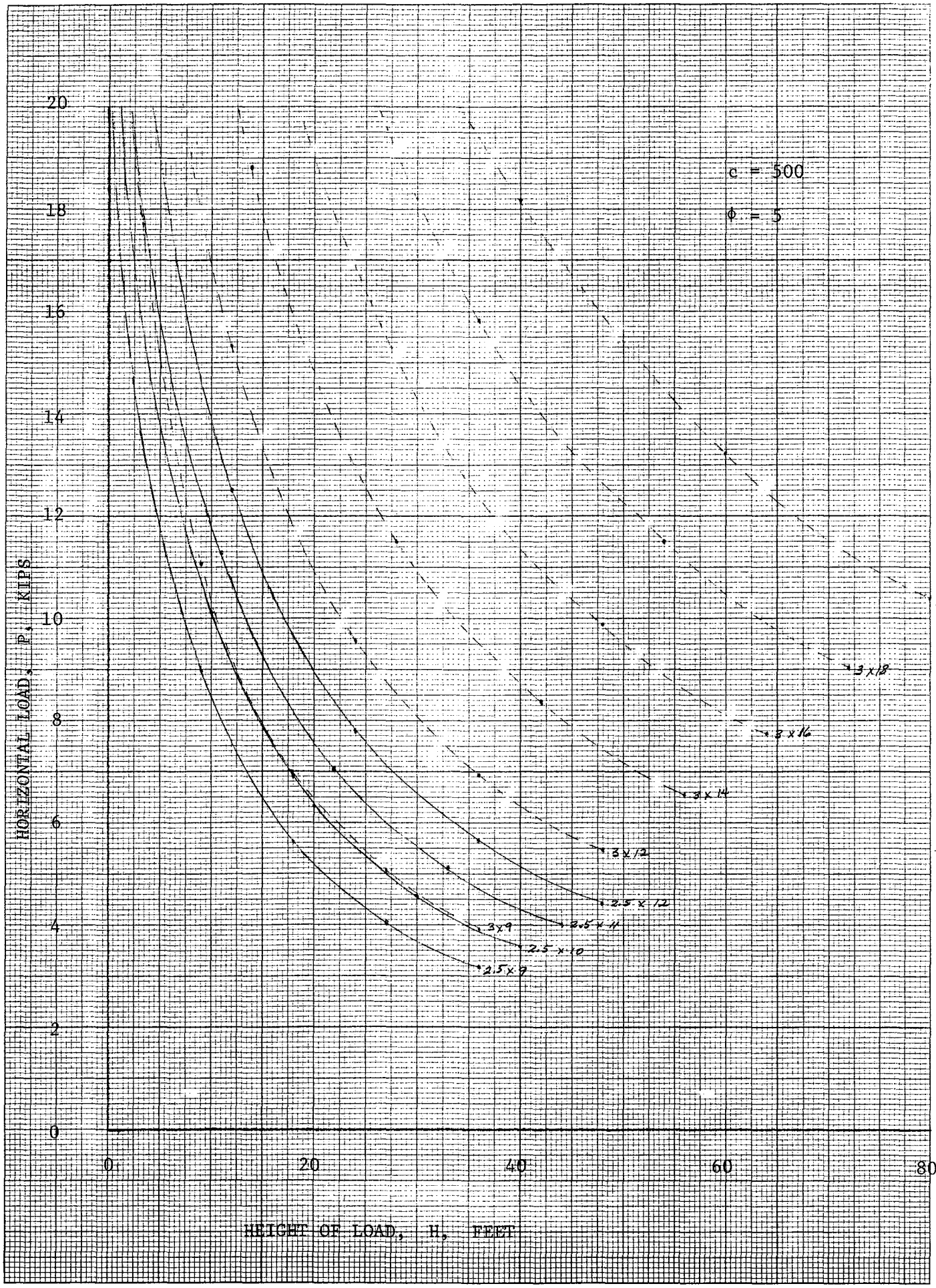

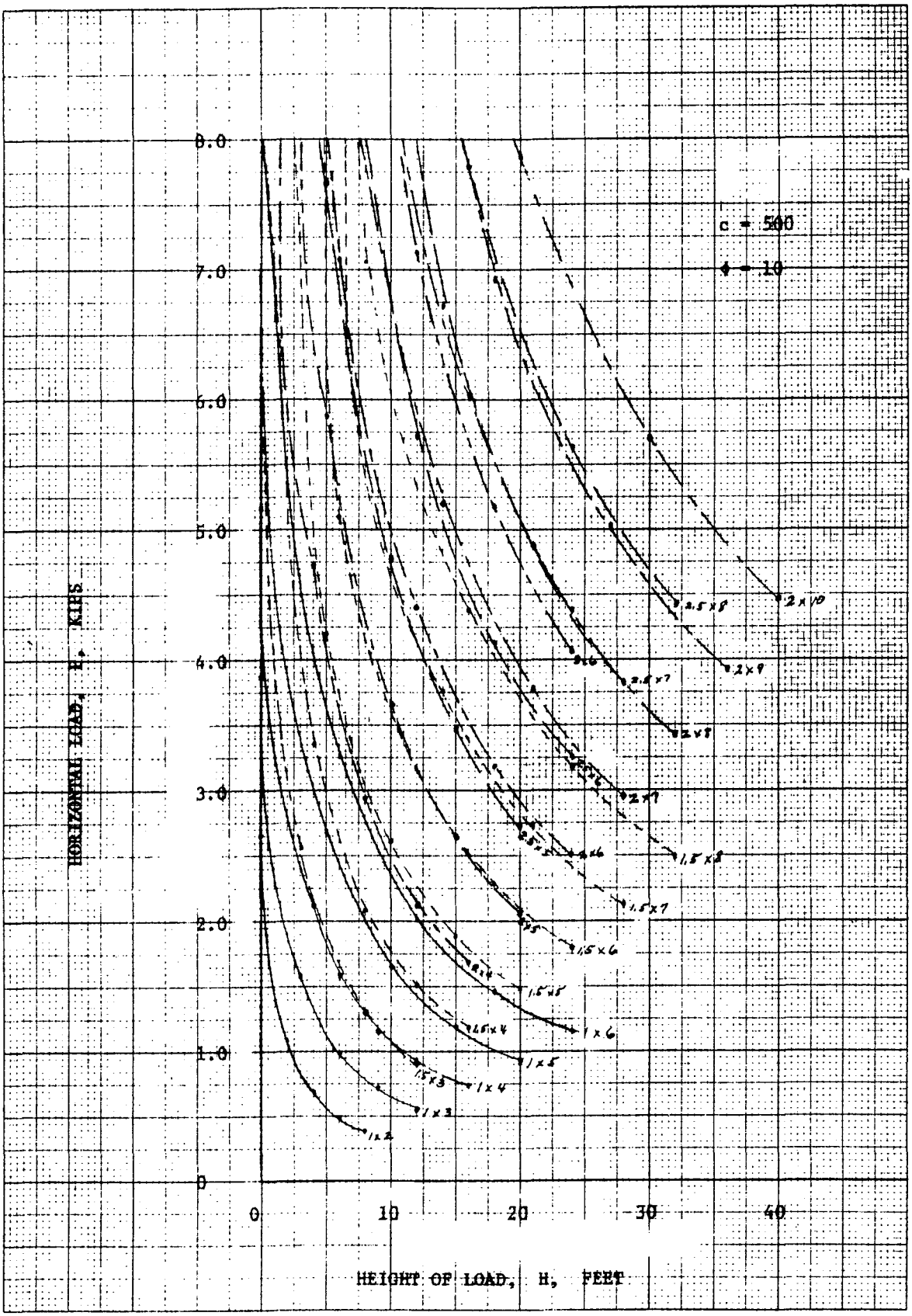
c = 500
ϕ = 10
8.0
7.0
6.0
5.0
4.0
3.0
2.0
1.0
0
0
10
20
30
40
HORIZONTAL LOAD, H, KIPS
HEIGHT OF LOAD, H, FEET
2 x 10
2.5 x 8
2 x 9
2 x 8
2 x 7
1.5 x 8
1.5 x 7
1.5 x 6
1.5 x 5
1 x 6
1 x 5
1 x 4
1 x 3
1 x 2

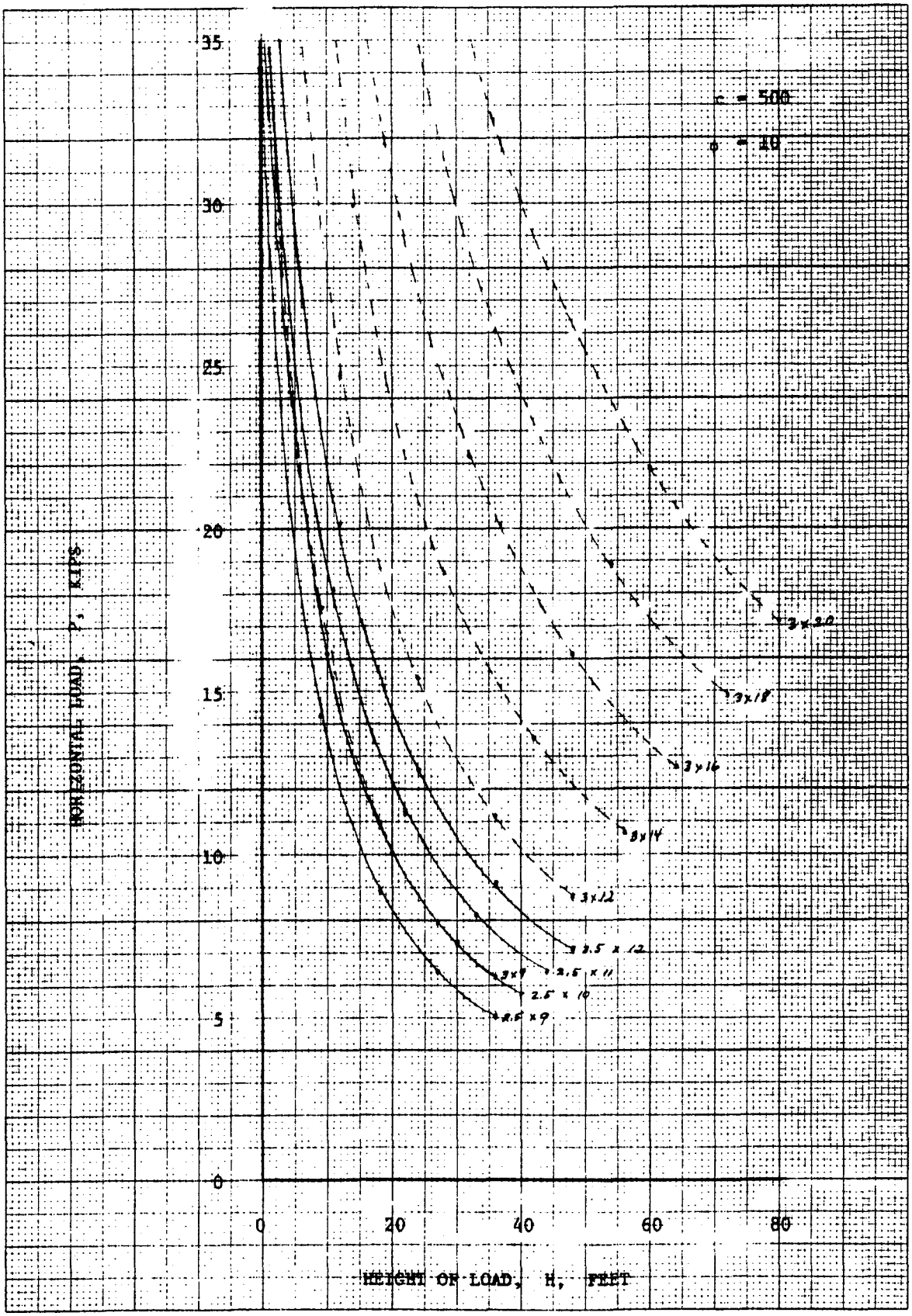
c = 500
φ = 40
35
30
25
20
15
10
5
0
0
20
40
60
80
HORIZONTAL LOAD, P, KIPS
HEIGHT OF LOAD, H, FEET
3x20
3x18
3x16
3x14
3x12
3.5 x 12
3x9
2.5 x 11
2.5 x 10
2.5 x 9

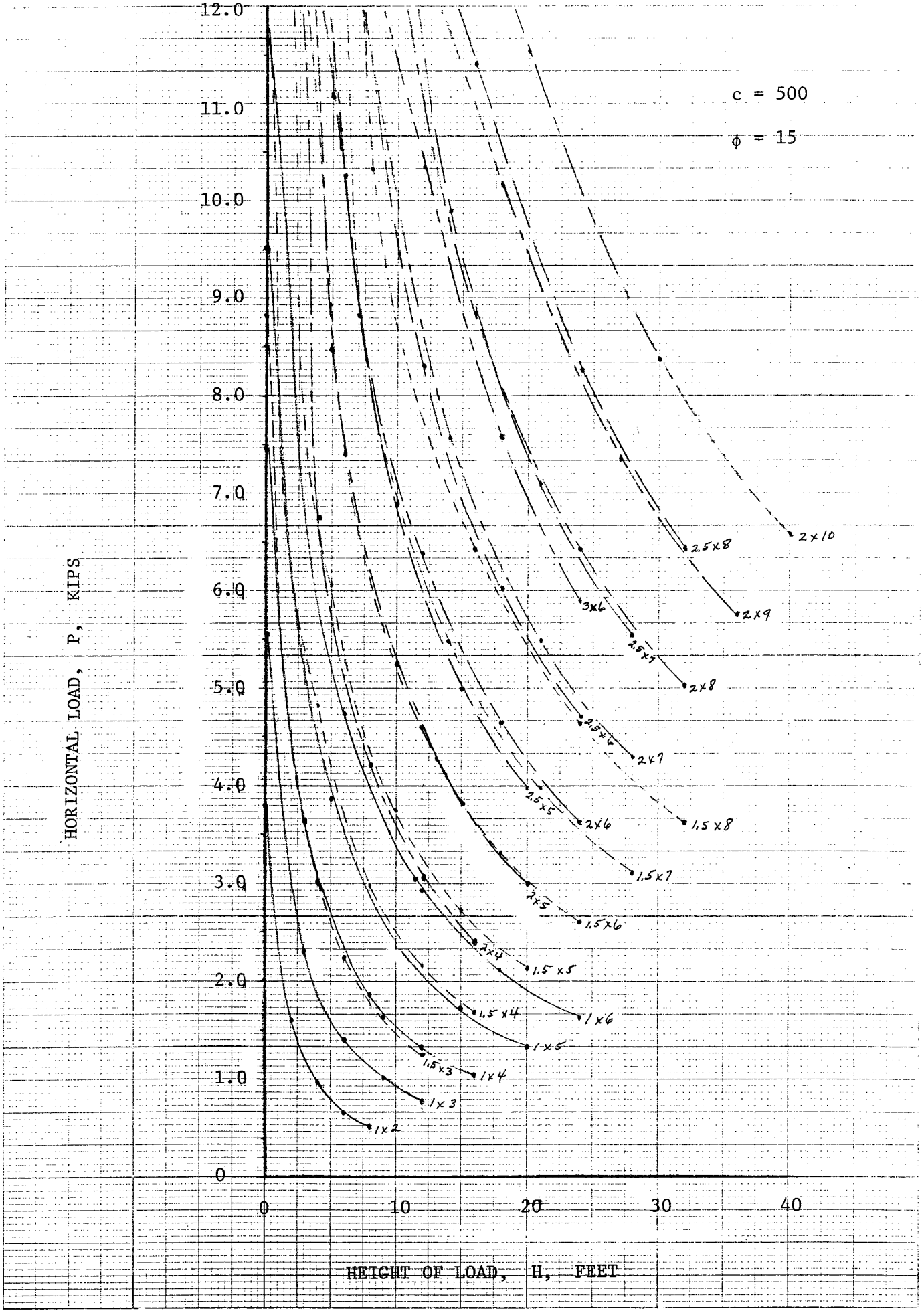
c = 500
ϕ = 15
HORIZONTAL LOAD, P, KIPS
HEIGHT OF LOAD, H, FEET
12.0
11.0
10.0
9.0
8.0
7.0
6.0
5.0
4.0
3.0
2.0
1.0
0
0
10
20
30
40
2x10
2.5x8
2x9
3x6
2.5x7
2x8
2.5x6
2x7
2.5x5
2x6
1.5x8
1.5x7
2x5
1.5x6
2x4
1.5x5
1.5x4
1x6
1x5
1.5x3
1x4
1x3
1x2

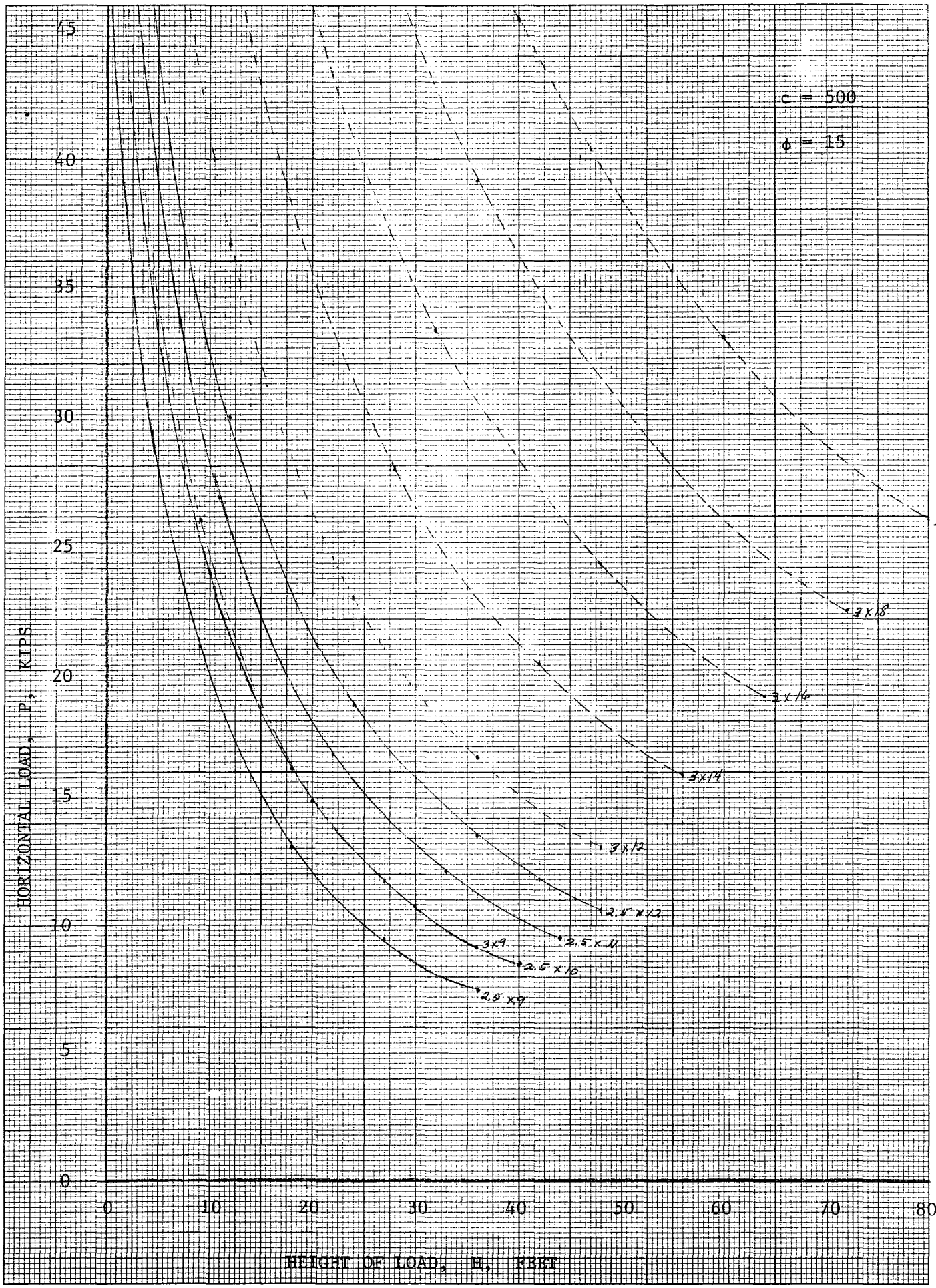

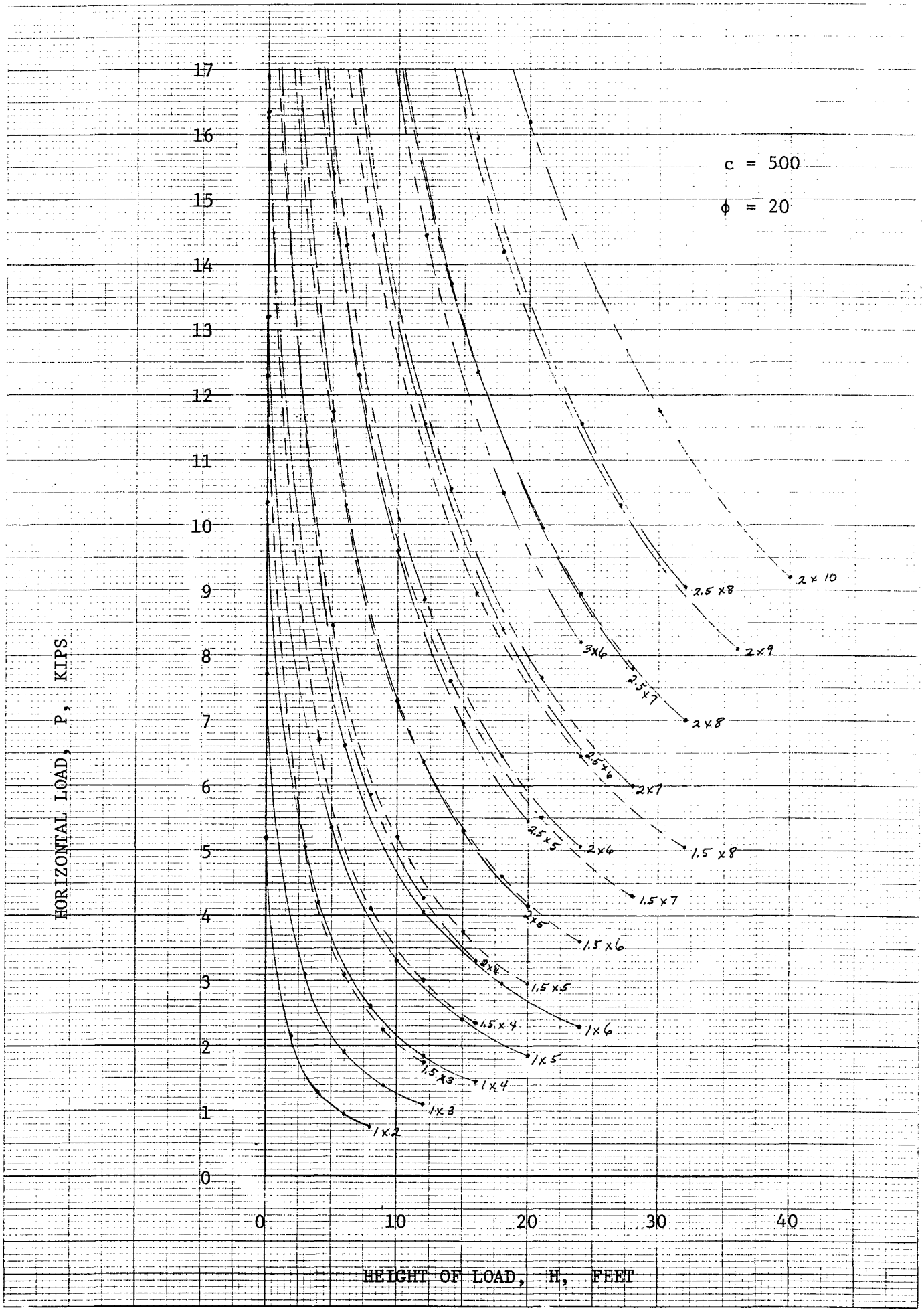
c = 500
ϕ = 20
2 x 10
2.5 x 8
2 x 9
3 x 6
2.5 x 7
2 x 8
2.5 x 6
2 x 7
2.5 x 5
2 x 6
1.5 x 8
1.5 x 7
2 x 5
1.5 x 6
2 x 4
1.5 x 5
1.5 x 4
1 x 6
1 x 5
1.5 x 3
1 x 4
1 x 3
1 x 2
HORIZONTAL LOAD, P, KIPS
0
1
2
3
4
5
6
7
8
9
10
11
12
13
14
15
16
17
0
10
20
30
40
HEIGHT OF LOAD, H, FEET

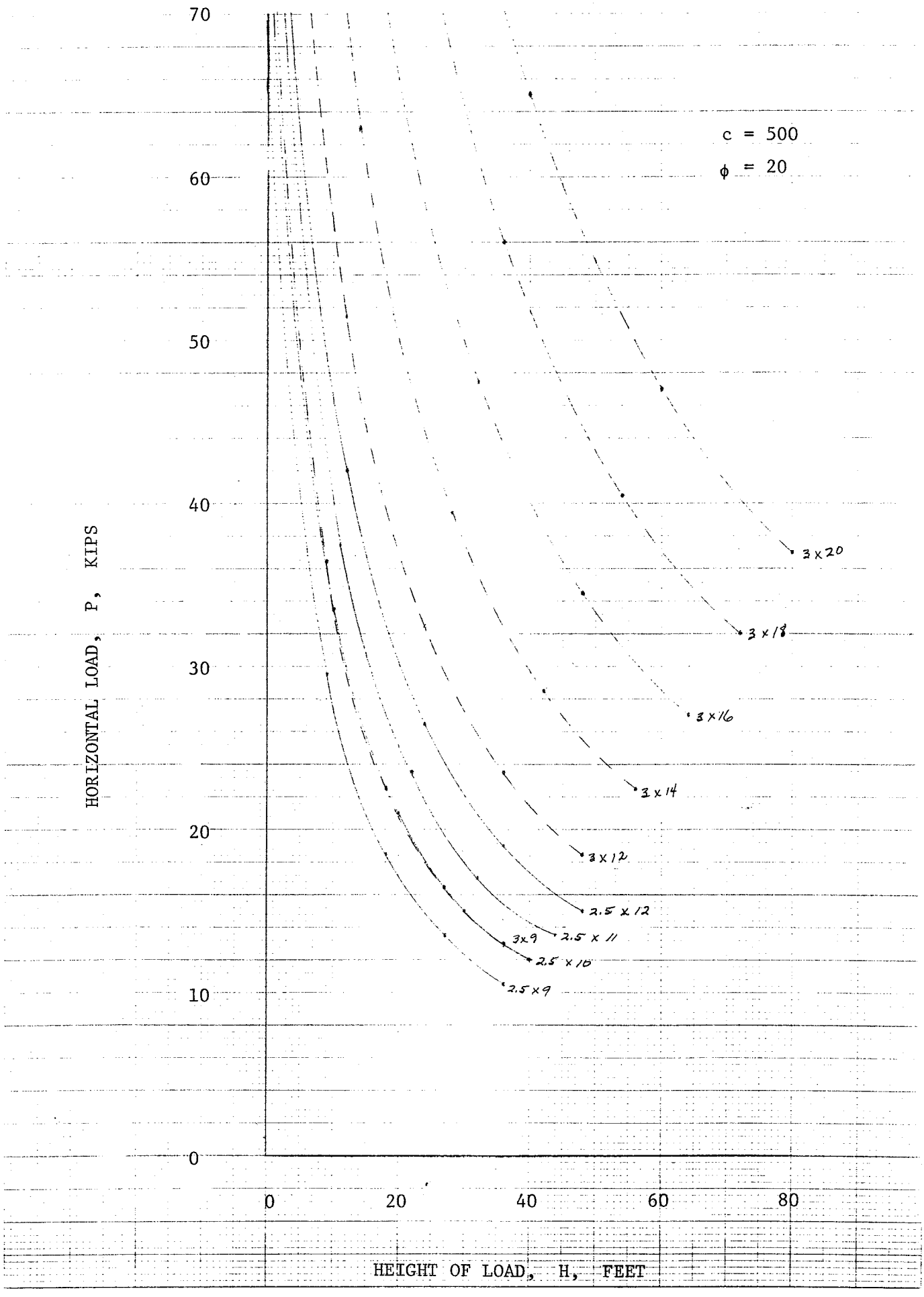
c = 500
ϕ = 20
3 x 20
3 x 18
3 x 16
3 x 14
3 x 12
2.5 x 12
2.5 x 11
3x9
2.5 x 10
2.5 x 9
70
60
50
40
30
20
10
0
0
20
40
60
80
HORIZONTAL LOAD, P, KIPS
HEIGHT OF LOAD, H, FEET

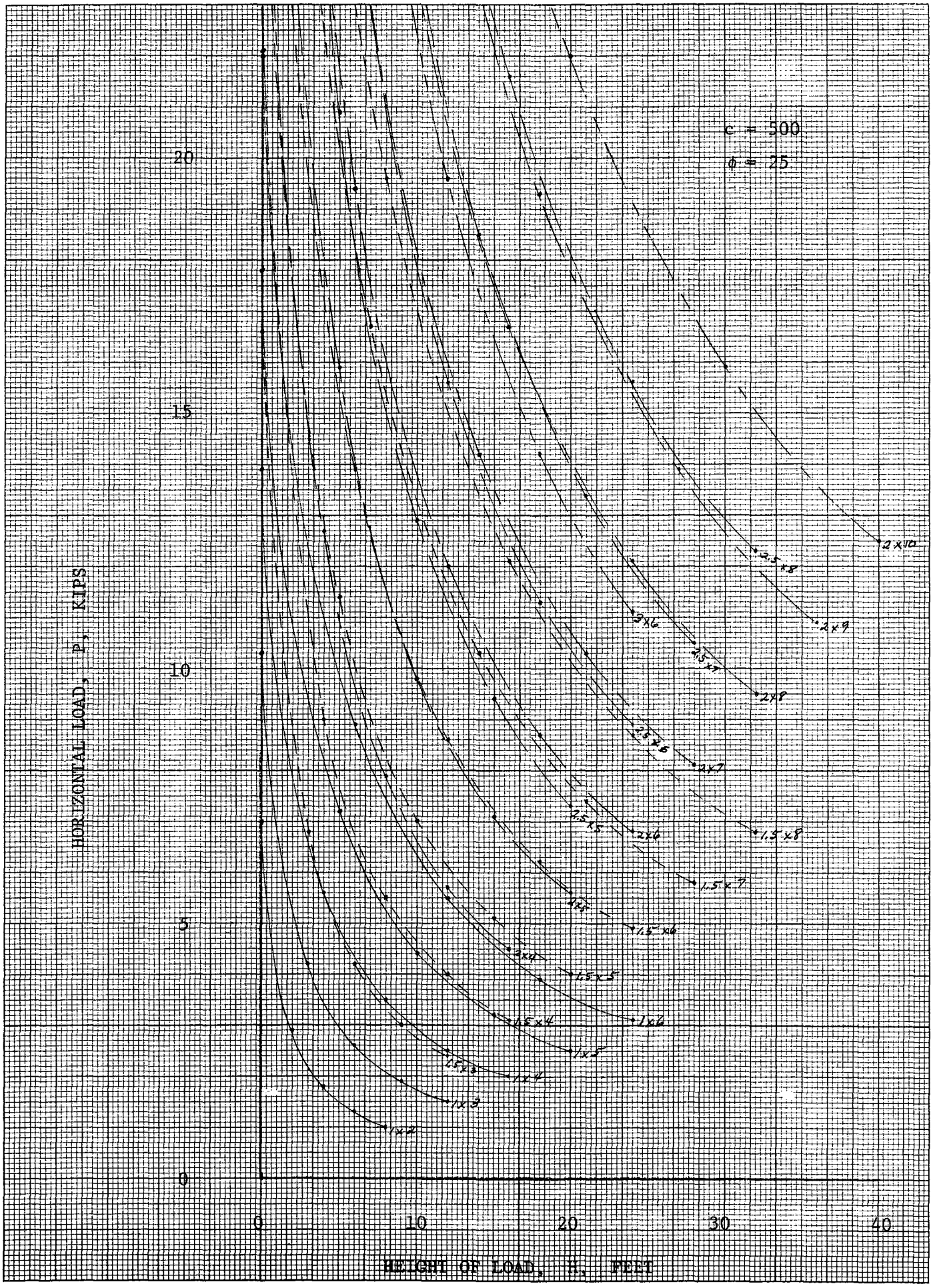

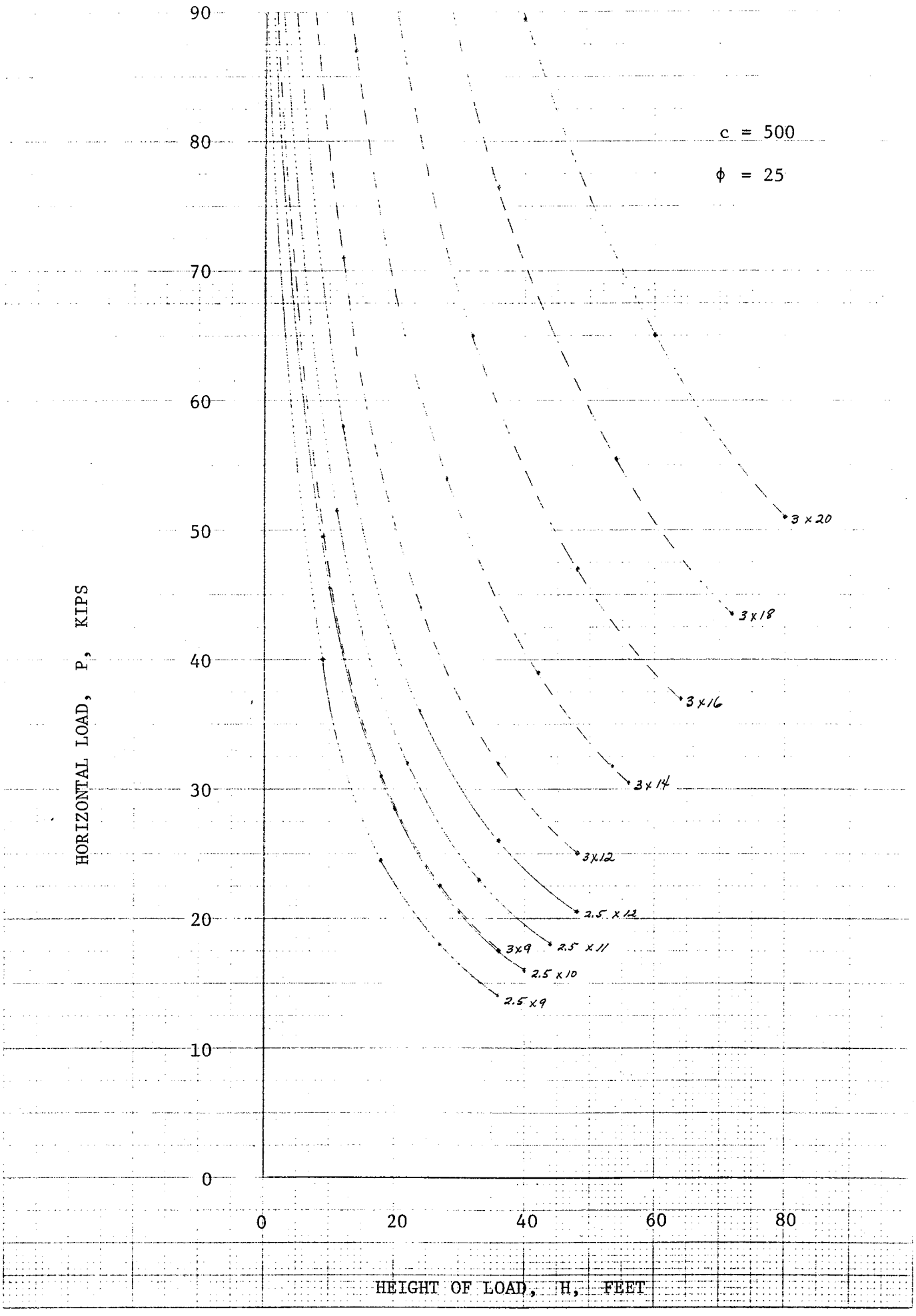
c = 500
ϕ = 25
3 x 20
3 x 18
3 x 16
3 x 14
3 x 12
2.5 x 12
3 x 9
2.5 x 11
2.5 x 10
2.5 x 9
HORIZONTAL LOAD, P, KIPS
HEIGHT OF LOAD, H, FEET
0
10
20
30
40
50
60
70
80
90
0
20
40
60
80

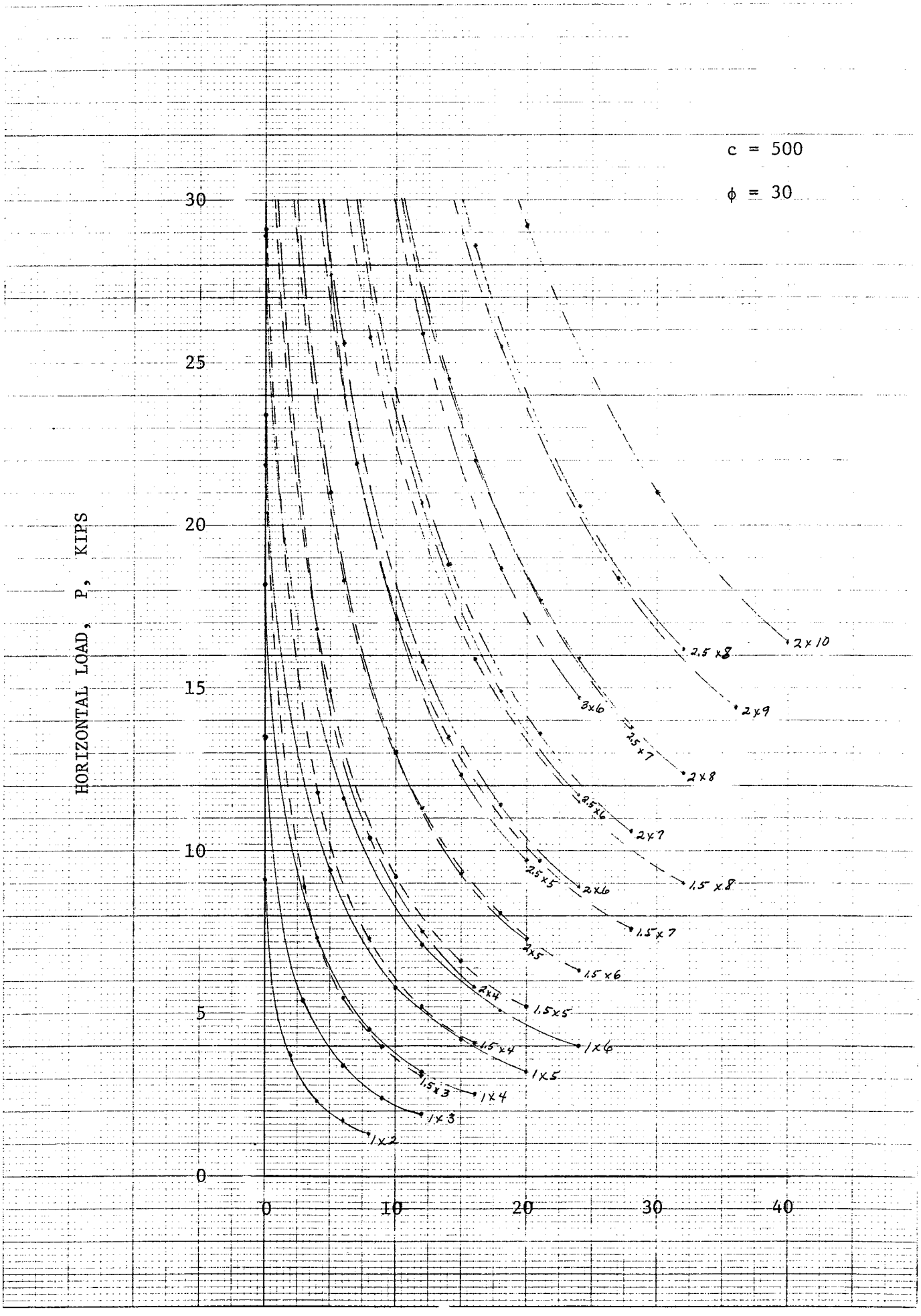
c = 500
ϕ = 30
HORIZONTAL LOAD, P, KIPS
0
5
10
15
20
25
30
0
10
20
30
40
2 x 10
2.5 x 8
2 x 9
3 x 6
2.5 x 7
2 x 8
2.5 x 6
2 x 7
2.5 x 5
2 x 6
1.5 x 8
1.5 x 7
2 x 5
1.5 x 6
2 x 4
1.5 x 5
1 x 6
1.5 x 4
1 x 5
1.5 x 3
1 x 4
1 x 3
1 x 2

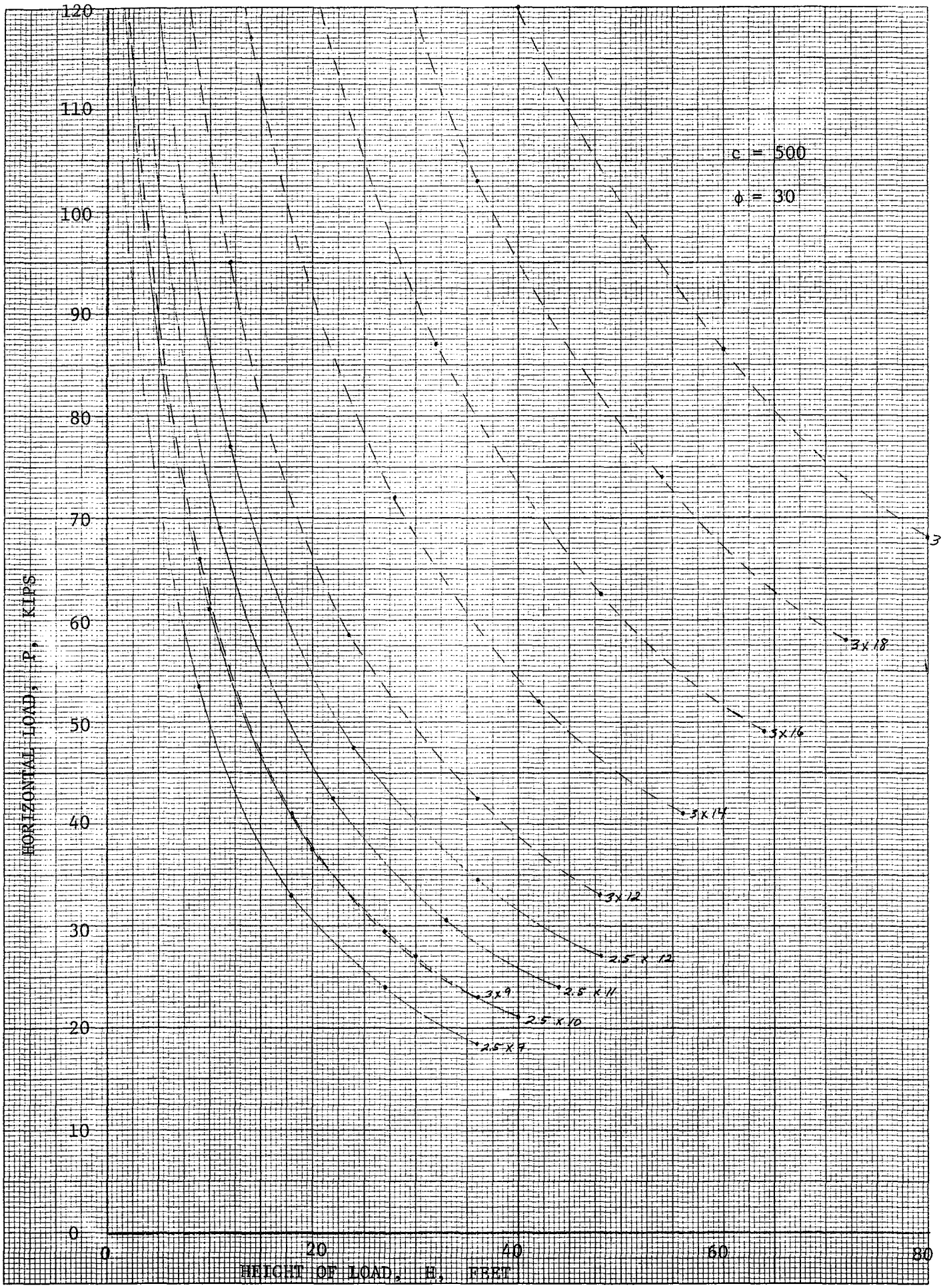

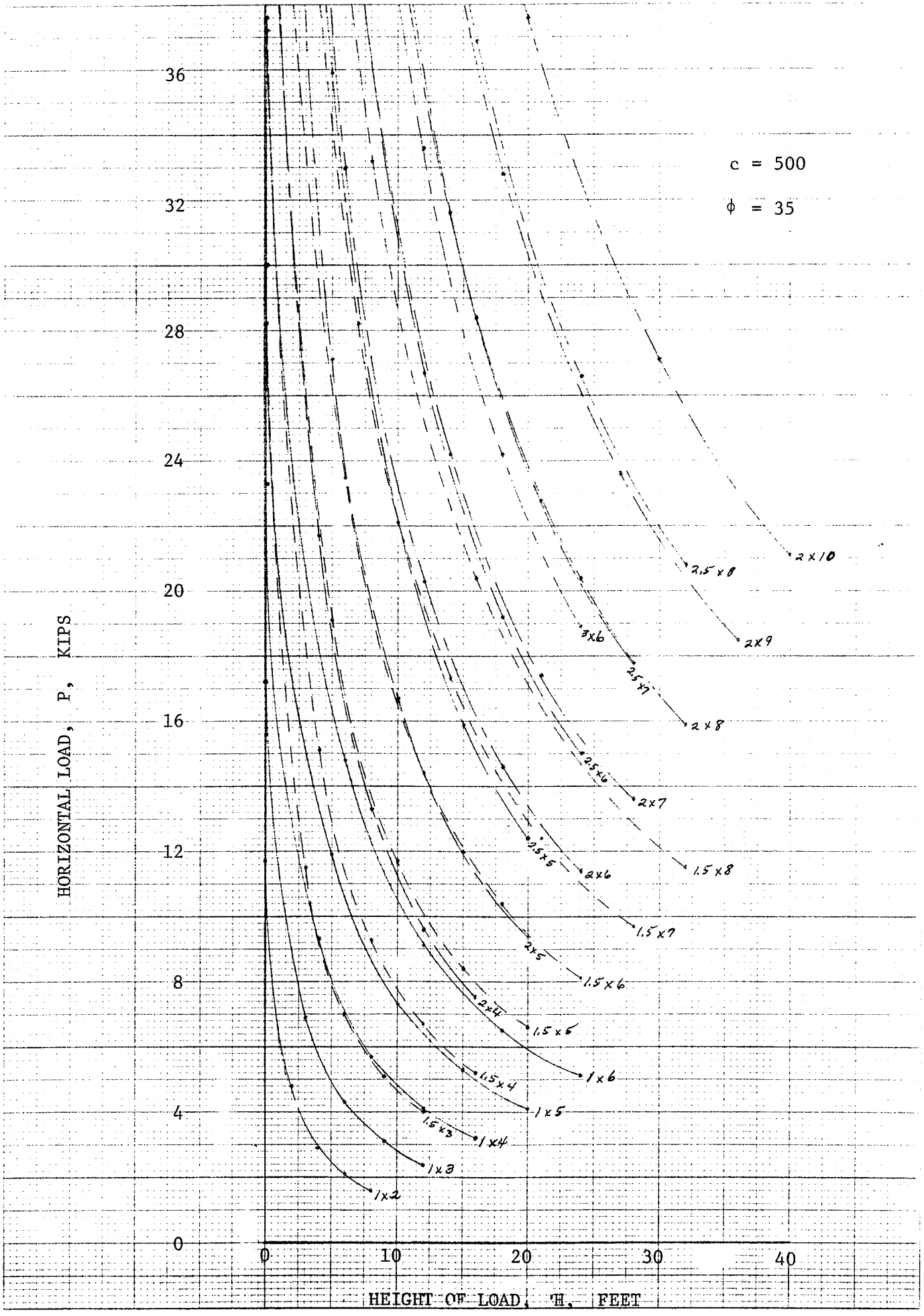
c = 500
ϕ = 35
2 x 10
2.5 x 8
2 x 9
3 x 6
2.5 x 7
2 x 8
2.5 x 6
2 x 7
2.5 x 5
1.5 x 8
2 x 6
1.5 x 7
2 x 5
1.5 x 6
2 x 4
1.5 x 6
1.5 x 4
1 x 6
1 x 5
1.5 x 3
1 x 4
1 x 3
1 x 2
HORIZONTAL LOAD, P, KIPS
0
4
8
12
16
20
24
28
32
36
0
10
20
30
40
HEIGHT OF LOAD, H, FEET

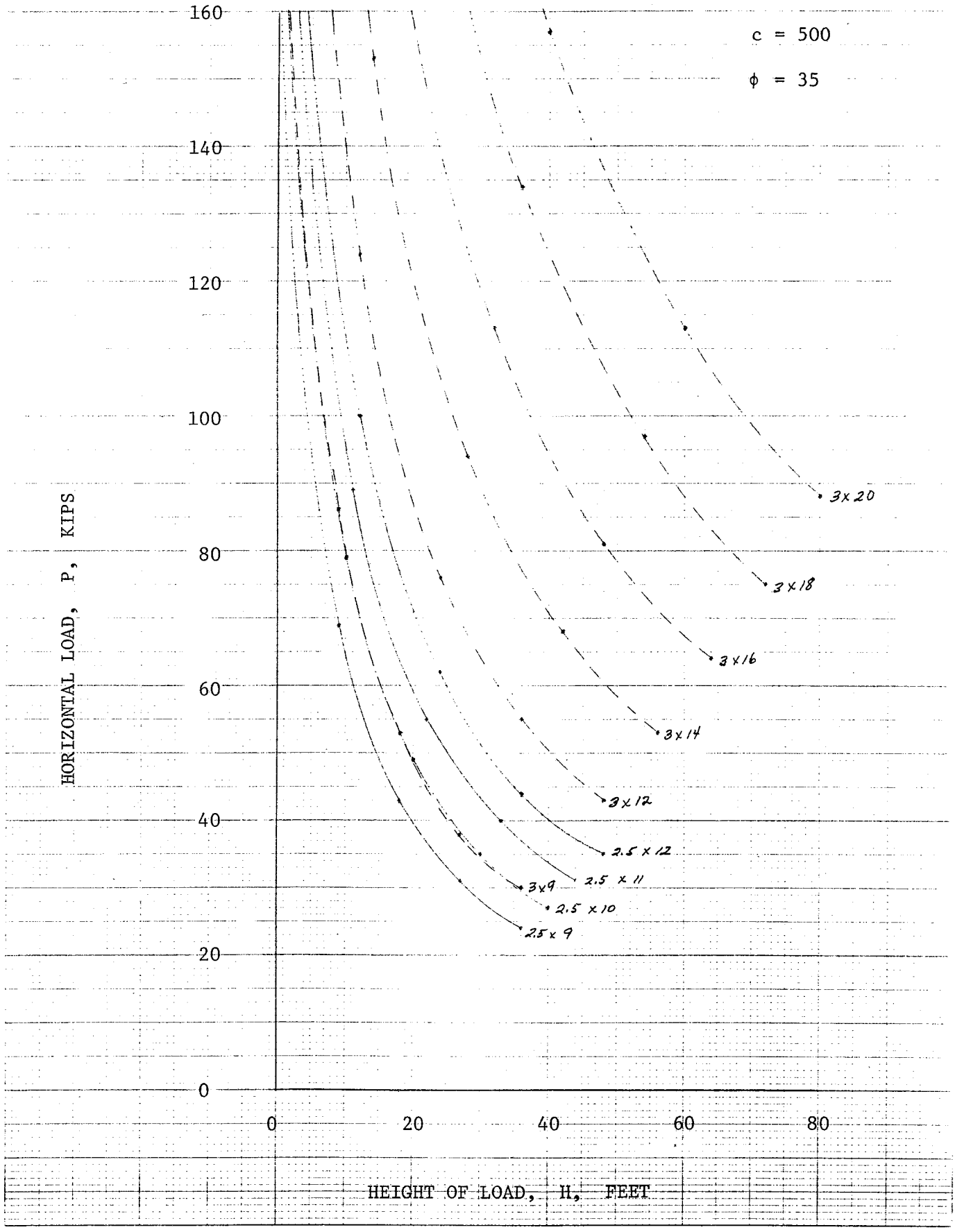
c = 500
ϕ = 35
3x20
3x18
3x16
3x14
3x12
2.5 x 12
2.5 x 11
3x9
2.5 x 10
2.5 x 9
160
140
120
100
80
60
40
20
0
0
20
40
60
80
HORIZONTAL LOAD, P, KIPS
HEIGHT OF LOAD, H, FEET

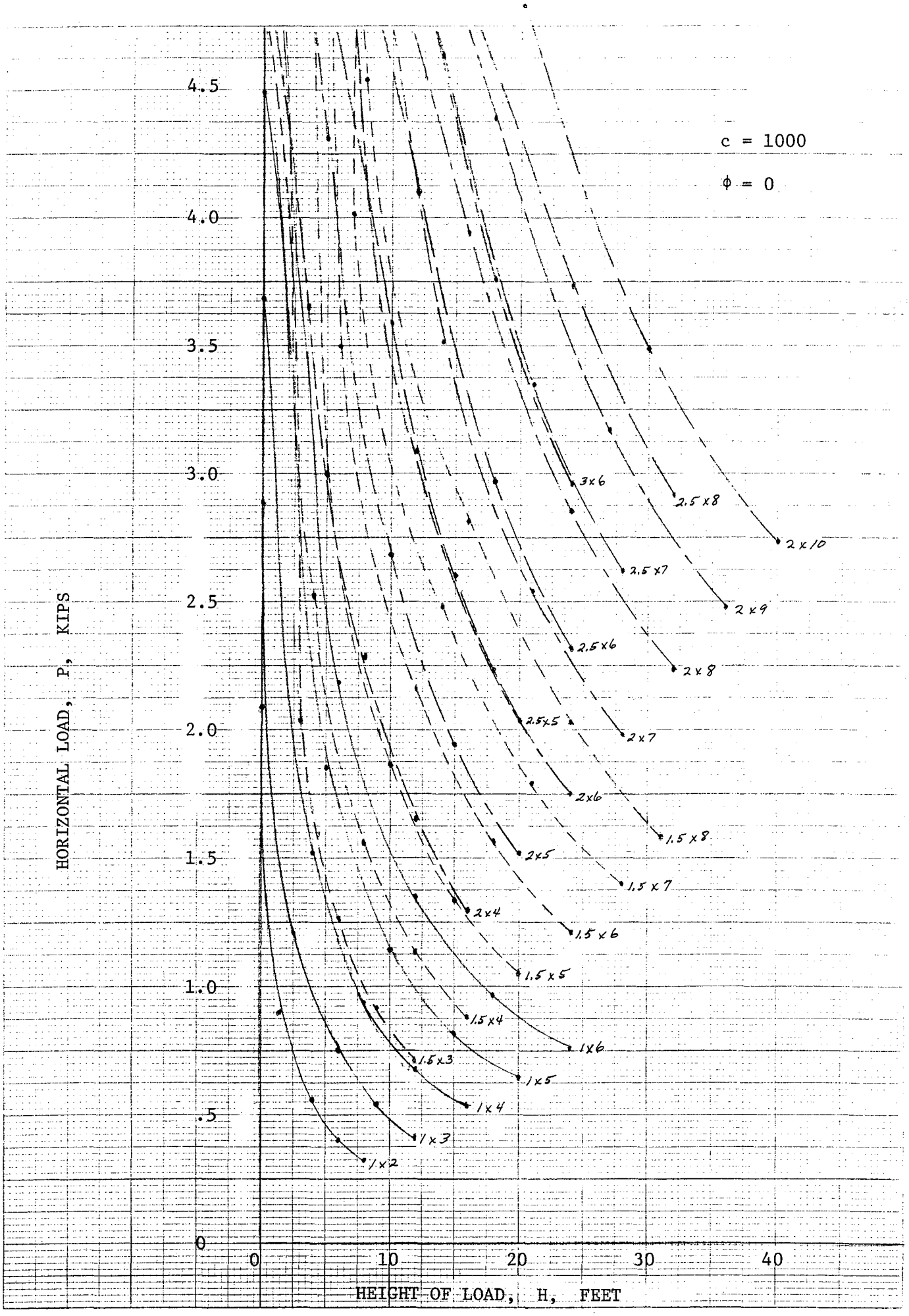
c = 1000
ϕ = 0
HORIZONTAL LOAD, P, KIPS
HEIGHT OF LOAD, H, FEET
4.5
4.0
3.5
3.0
2.5
2.0
1.5
1.0
.5
0
0
10
20
30
40
3x6
2.5x8
2x10
2.5x7
2x9
2.5x6
2x8
2.5x5
2x7
2x6
1.5x8
2x5
1.5x7
2x4
1.5x6
1.5x5
1.5x4
1x6
1.5x3
1x5
1x4
1x3
1x2

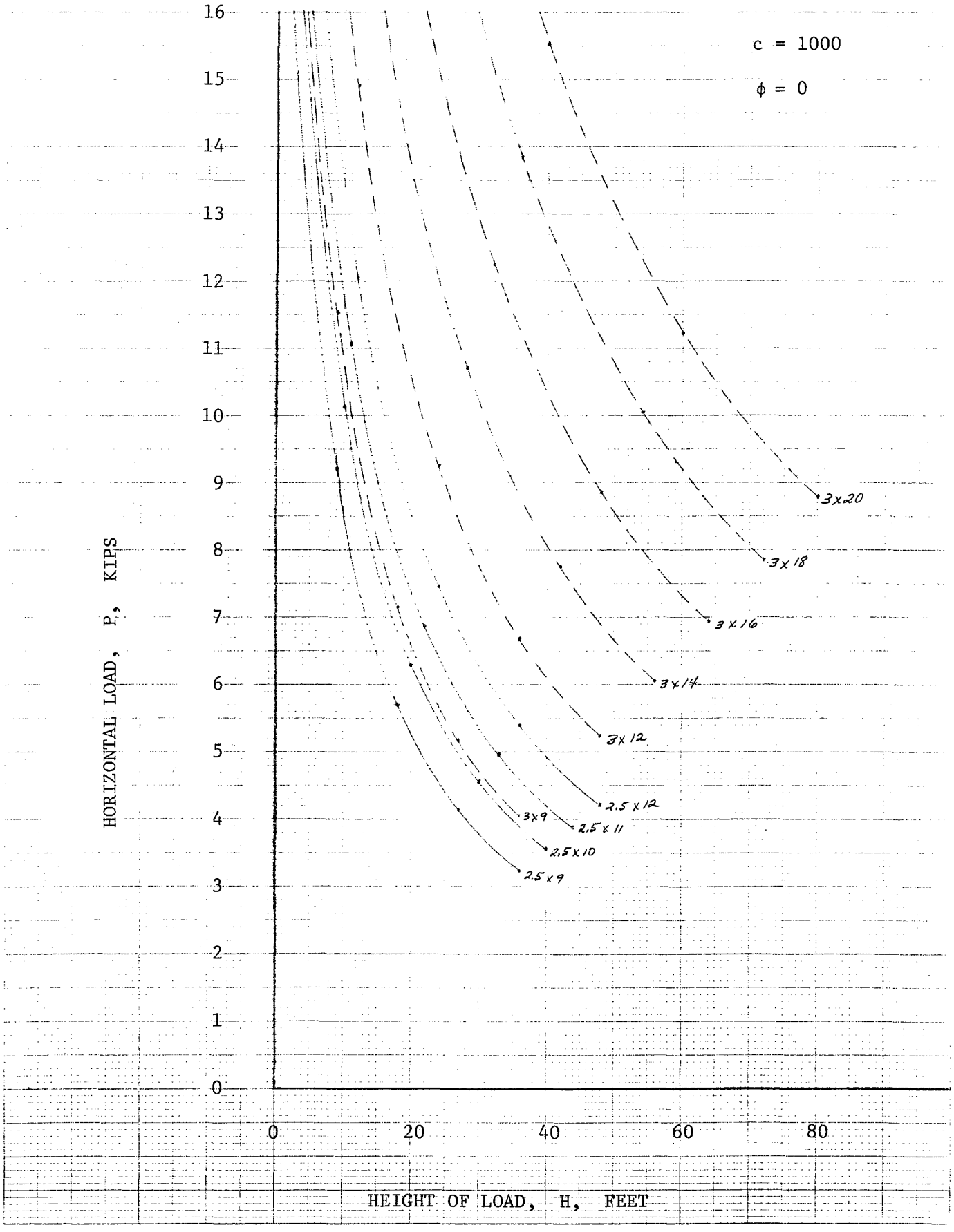
c = 1000
ϕ = 0
3x20
3x18
3x16
3x14
3x12
2.5x12
3x9
2.5x11
2.5x10
2.5x9
HORIZONTAL LOAD, P, KIPS
HEIGHT OF LOAD, H, FEET
0
1
2
3
4
5
6
7
8
9
10
11
12
13
14
15
16
0
20
40
60
80

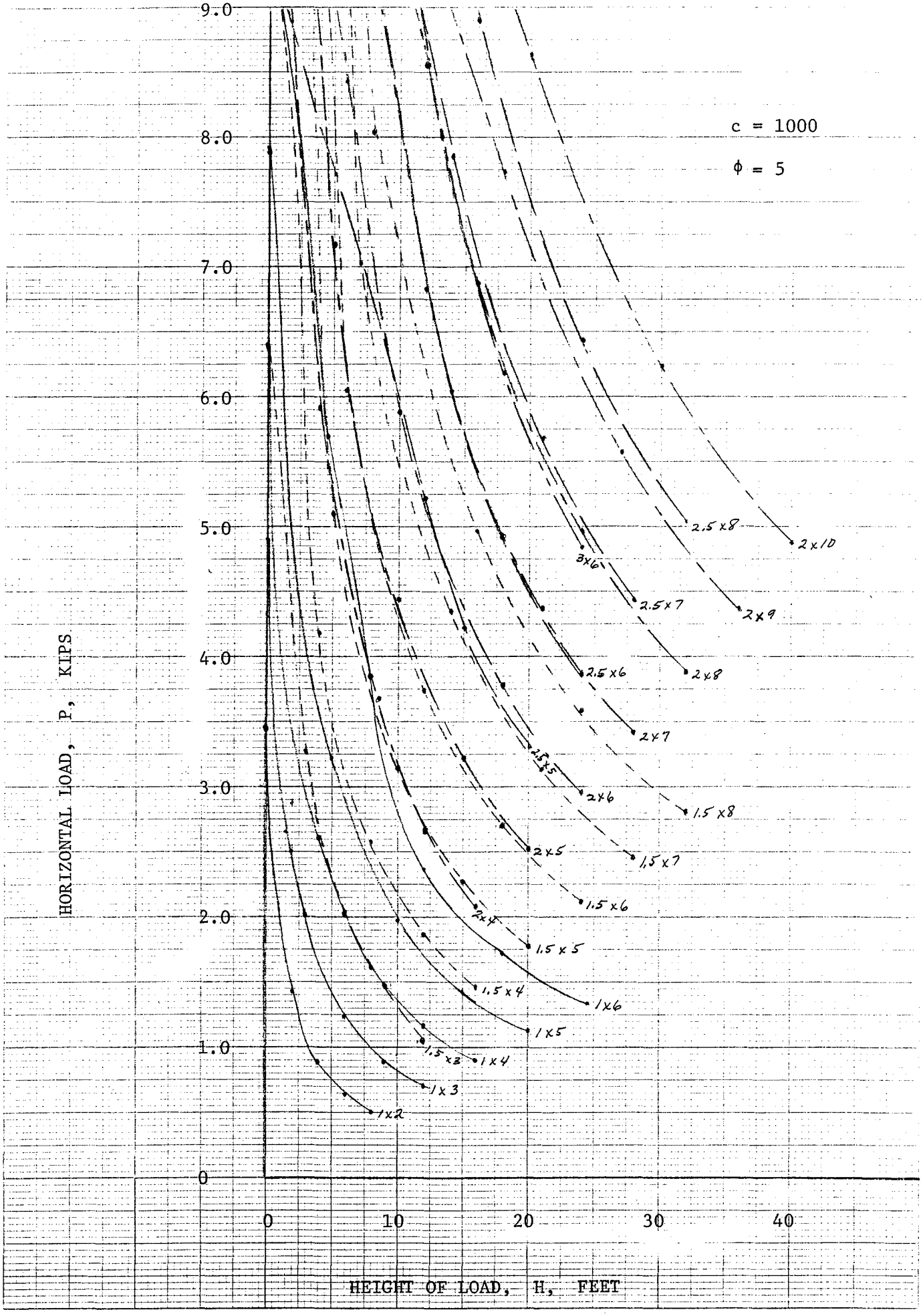
c = 1000
ϕ = 5
HORIZONTAL LOAD, P, KIPS
HEIGHT OF LOAD, H, FEET
9.0
8.0
7.0
6.0
5.0
4.0
3.0
2.0
1.0
0
0
10
20
30
40
2.5x8
2x10
3x6
2.5x7
2x9
2.5x6
2x8
2x7
2.5x5
2x6
1.5x8
2x5
1.5x7
1.5x6
2x4
1.5x5
1.5x4
1x6
1x5
1.5x2
1x4
1x3
1x2

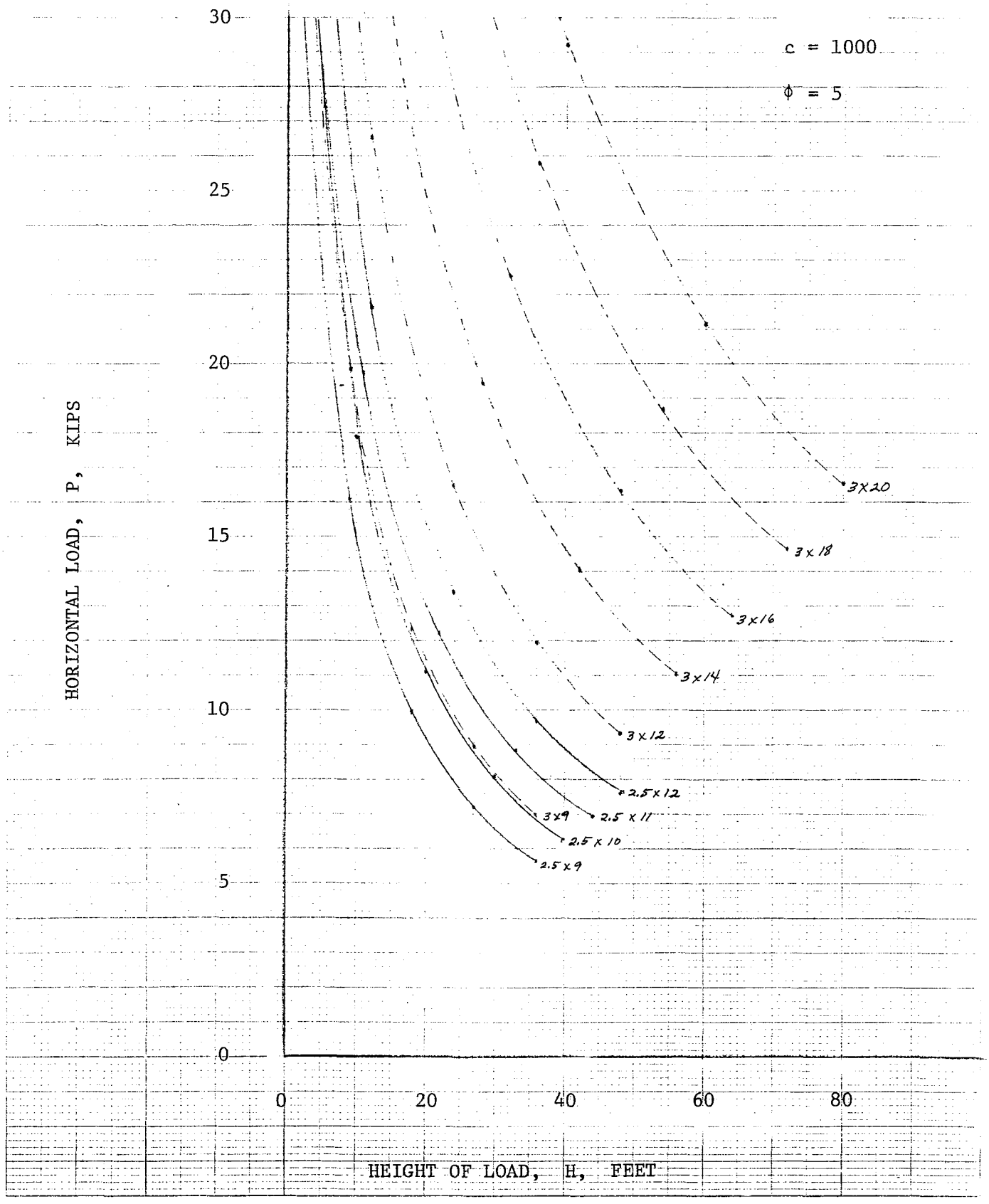
c = 1000
ϕ = 5
3X20
3 x 18
3x16
3x14
3 x 12
2.5 x 12
2.5 x 11
3x9
2.5 x 10
2.5 x 9
30
25
20
15
10
5
0
0
20
40
60
80
HORIZONTAL LOAD, P, KIPS
HEIGHT OF LOAD, H, FEET

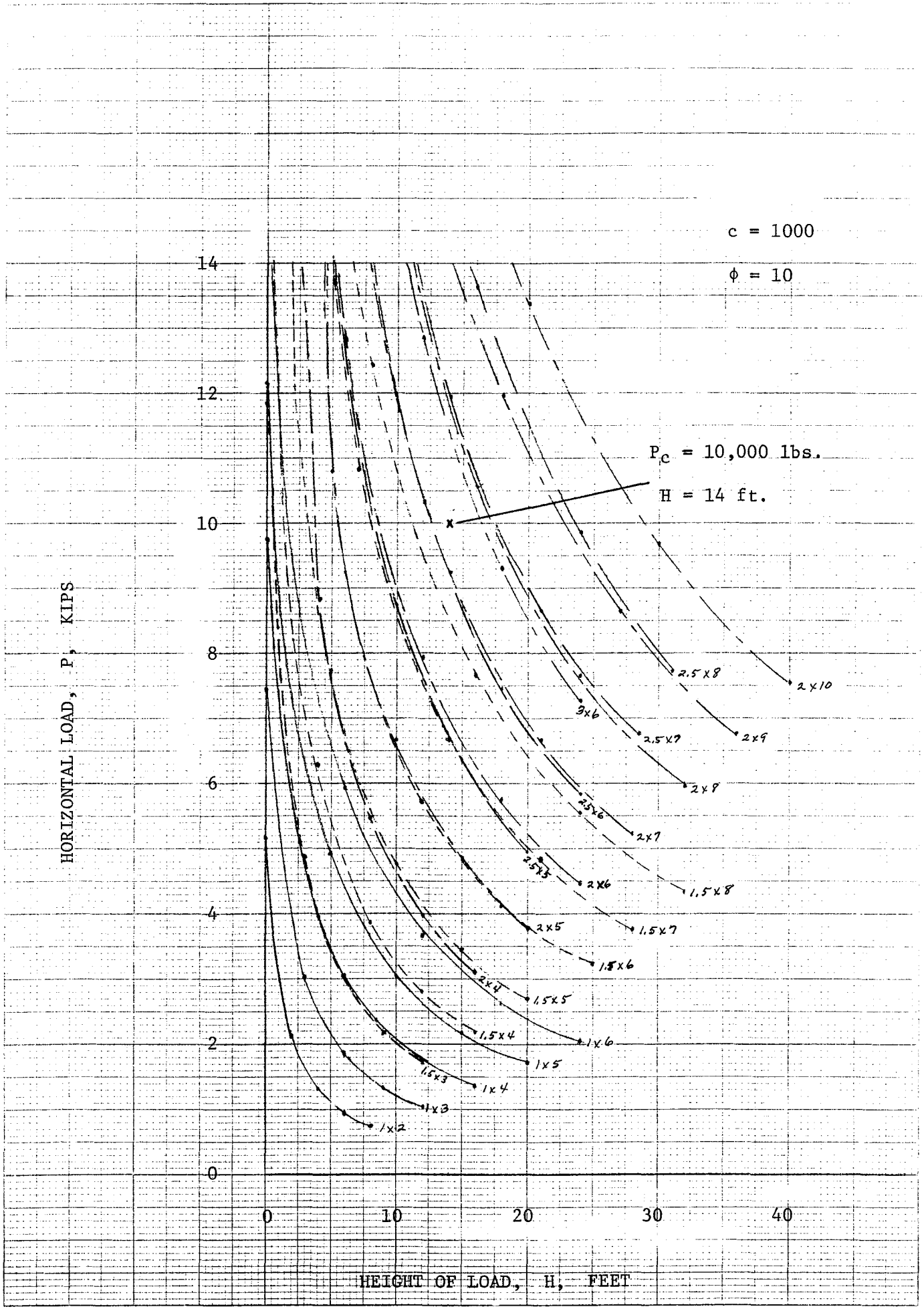
c = 1000
ϕ = 10
P_c = 10,000 lbs.
H = 14 ft.
HORIZONTAL LOAD, P, KIPS
HEIGHT OF LOAD, H, FEET
0
2
4
6
8
10
12
14
0
10
20
30
40
2x10
2.5x8
2x9
3x6
2.5x7
2x8
2.5x6
2x7
2.5x5
2x6
1.5x8
2x5
1.5x7
1.5x6
2x4
1.5x5
1.5x4
1x6
1x5
1.5x3
1x4
1x3
1x2

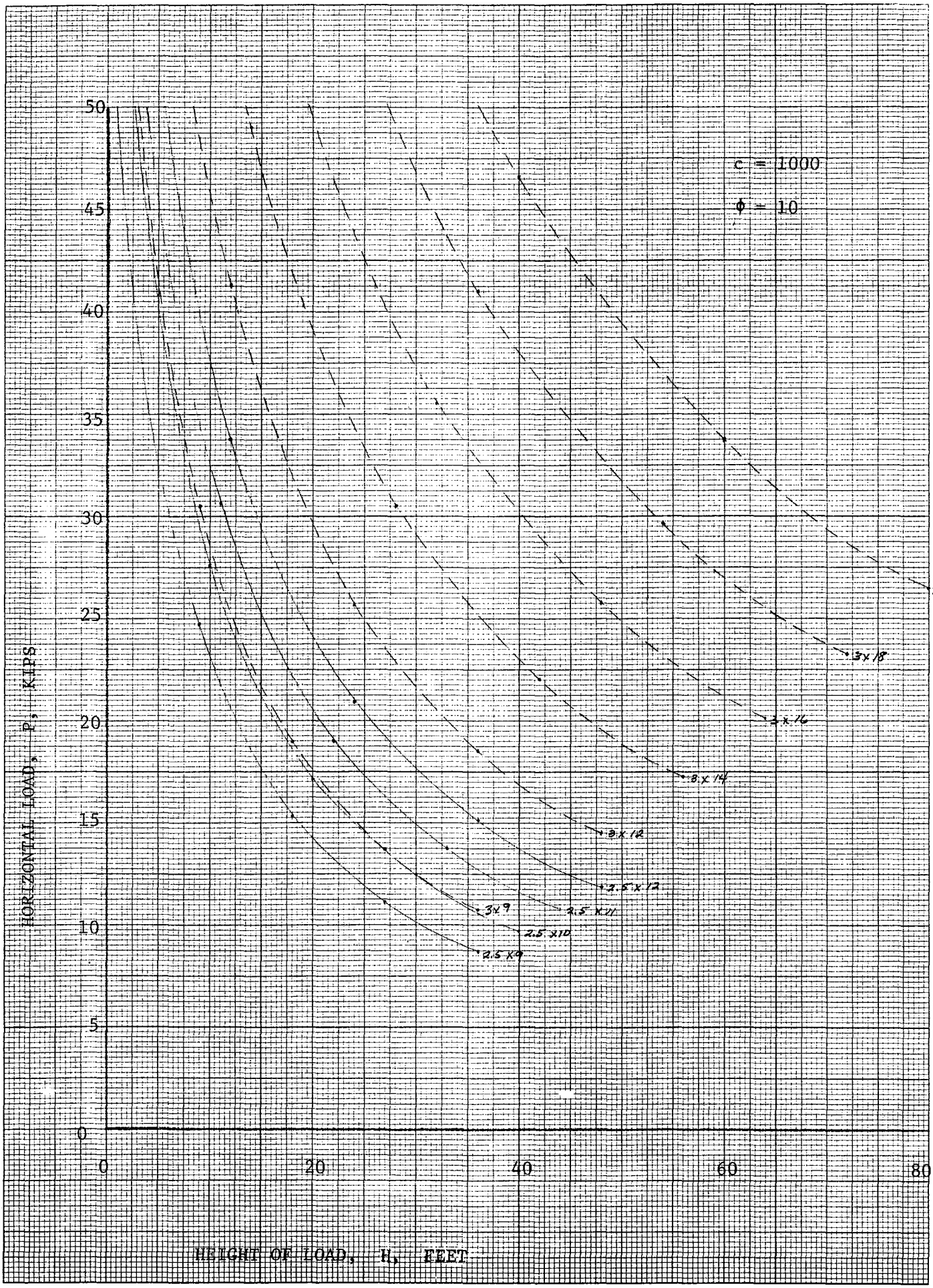

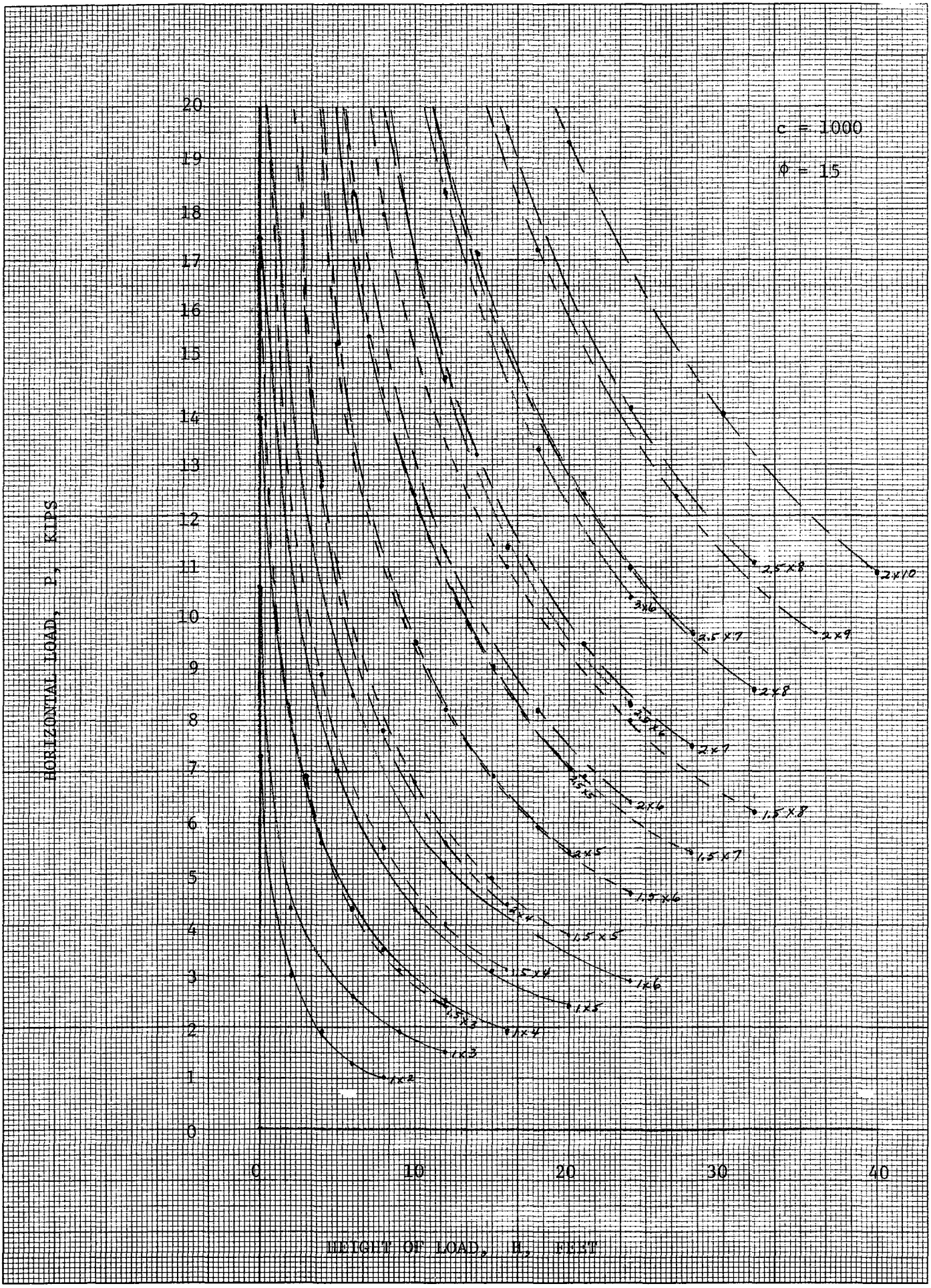

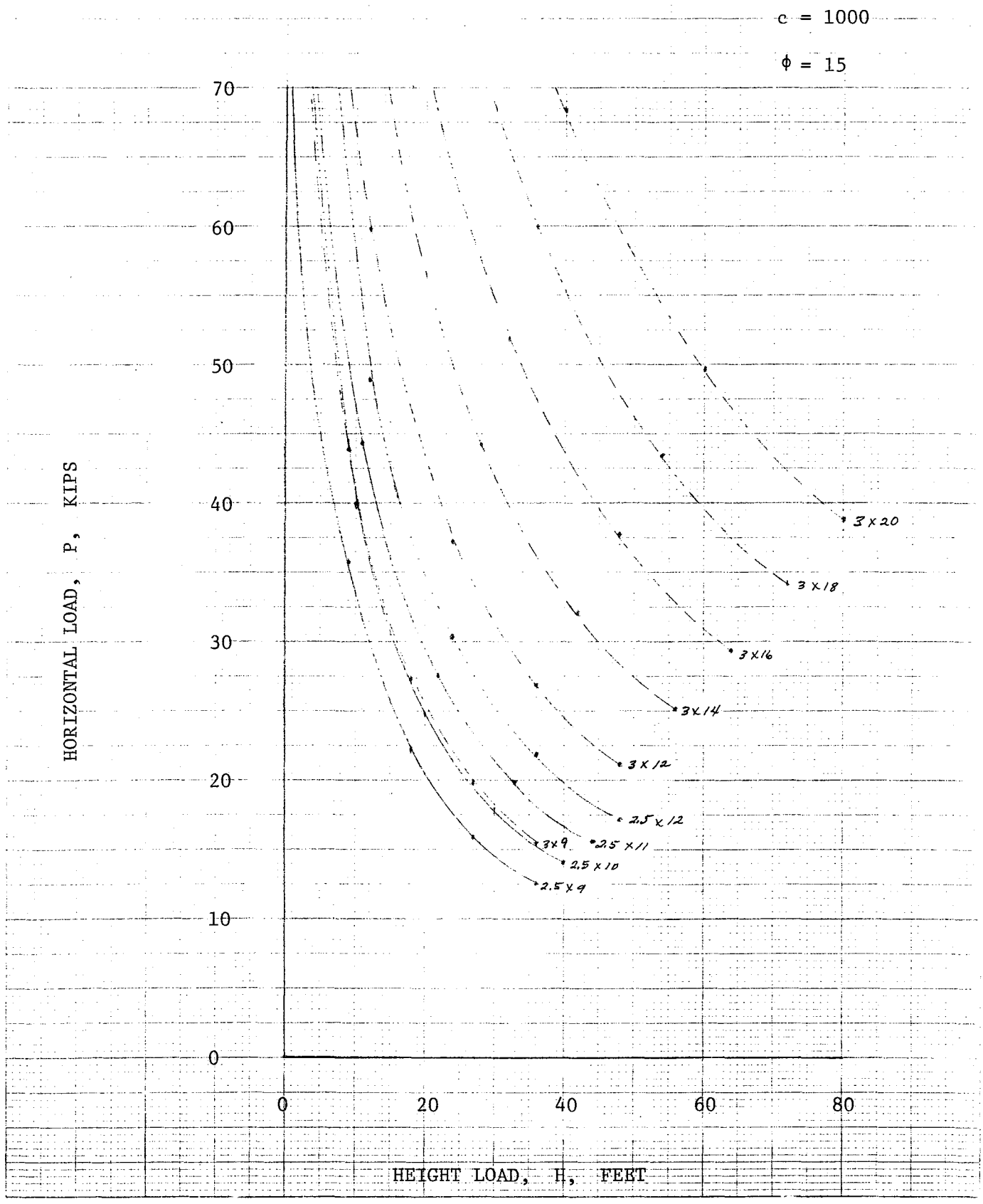
c = 1000
ϕ = 15
70
60
50
40
30
20
10
0
HORIZONTAL LOAD, P, KIPS
3 X 20
3 X 18
3 X 16
3 X 14
3 X 12
2.5 X 12
3 X 9
2.5 X 11
2.5 X 10
2.5 X 9
0
20
40
60
80
HEIGHT LOAD, H, FEET

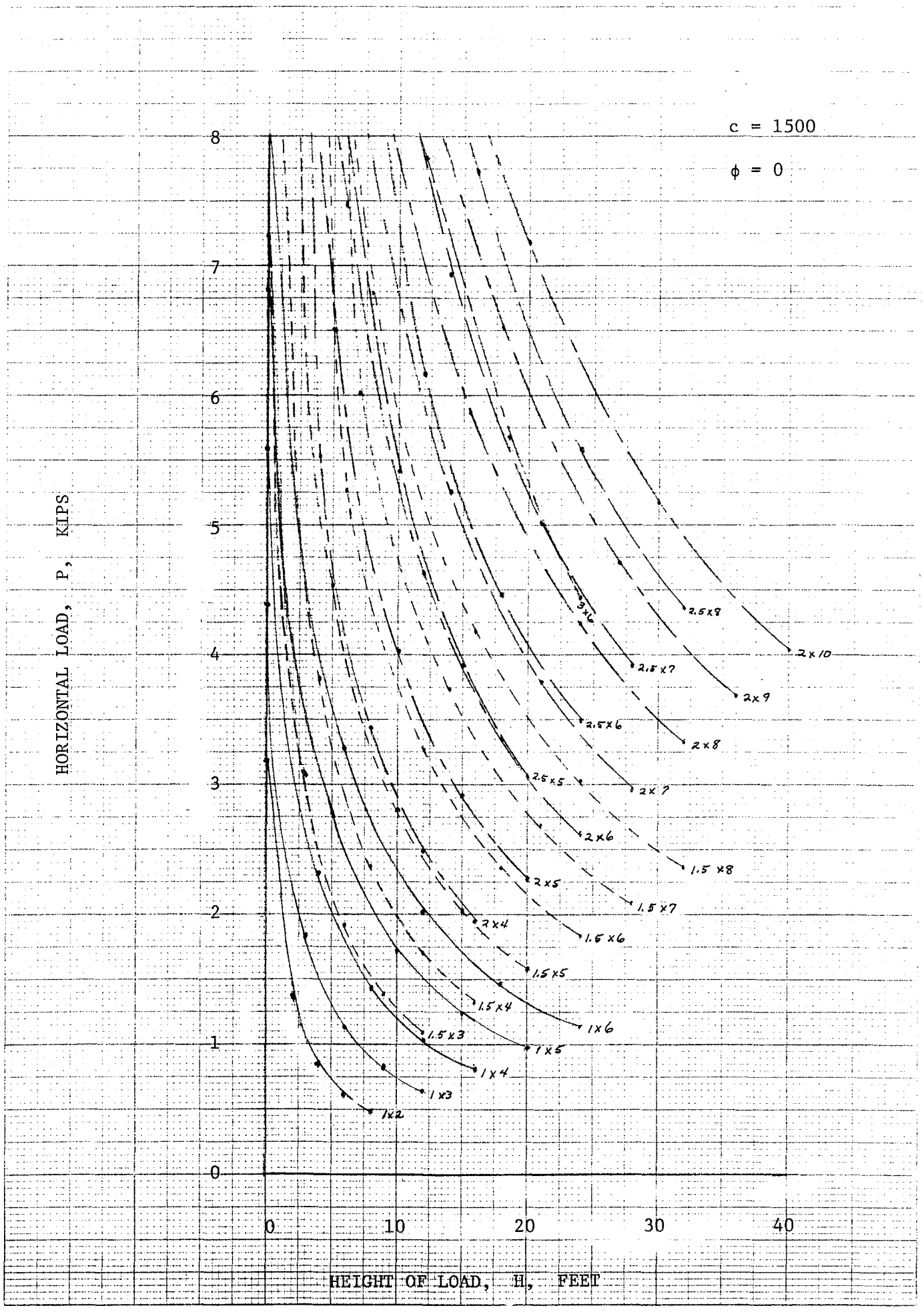
c = 1500
ϕ = 0
HORIZONTAL LOAD, P, KIPS
HEIGHT OF LOAD, H, FEET
0
1
2
3
4
5
6
7
8
0
10
20
30
40
2.5x8
2x10
3x6
2.5x7
2x9
2.5x6
2x8
2.5x5
2x7
2x6
1.5x8
2x5
1.5x7
2x4
1.5x6
1.5x5
1.5x4
1x6
1.5x3
1x5
1x4
1x3
1x2

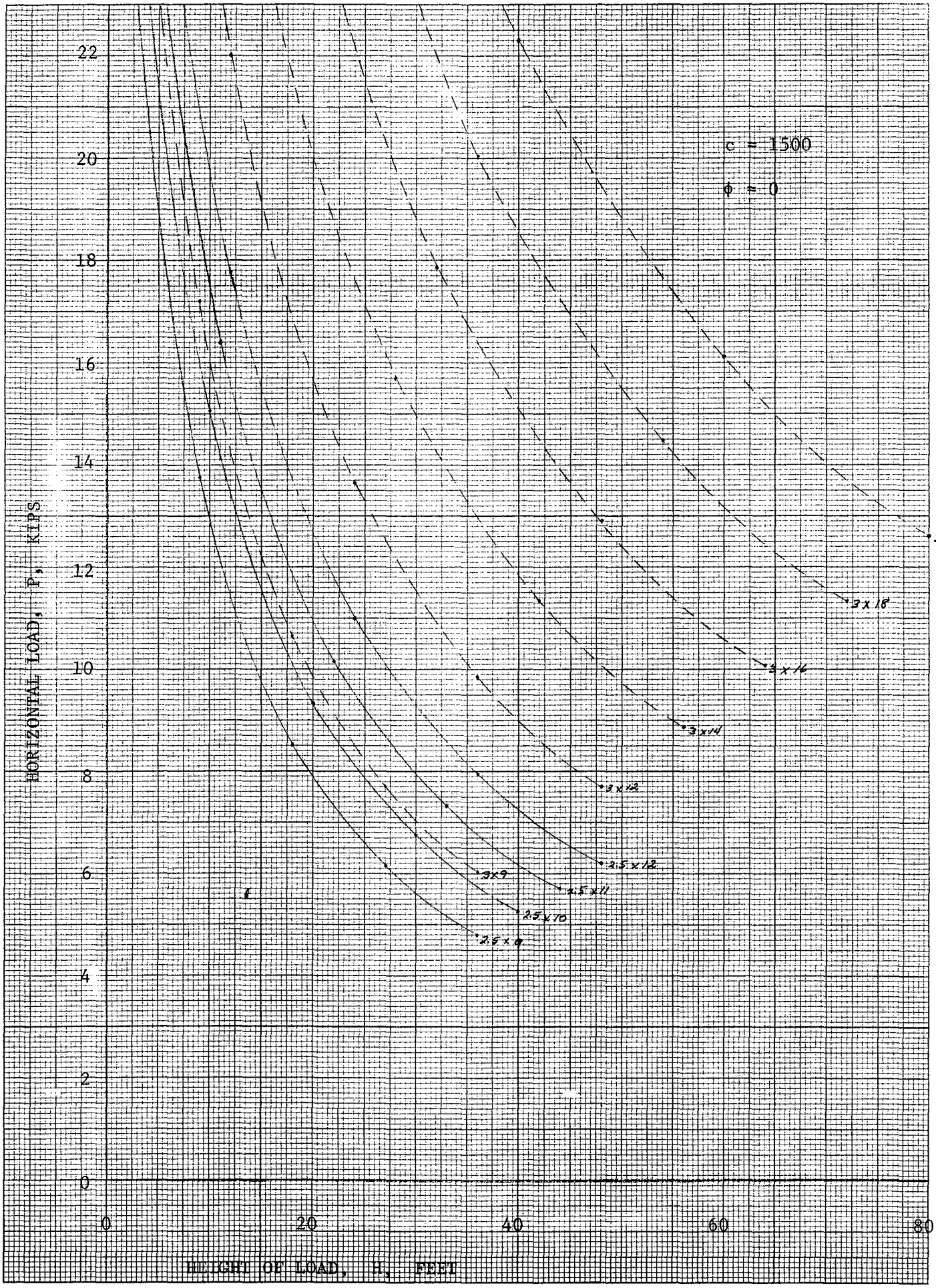

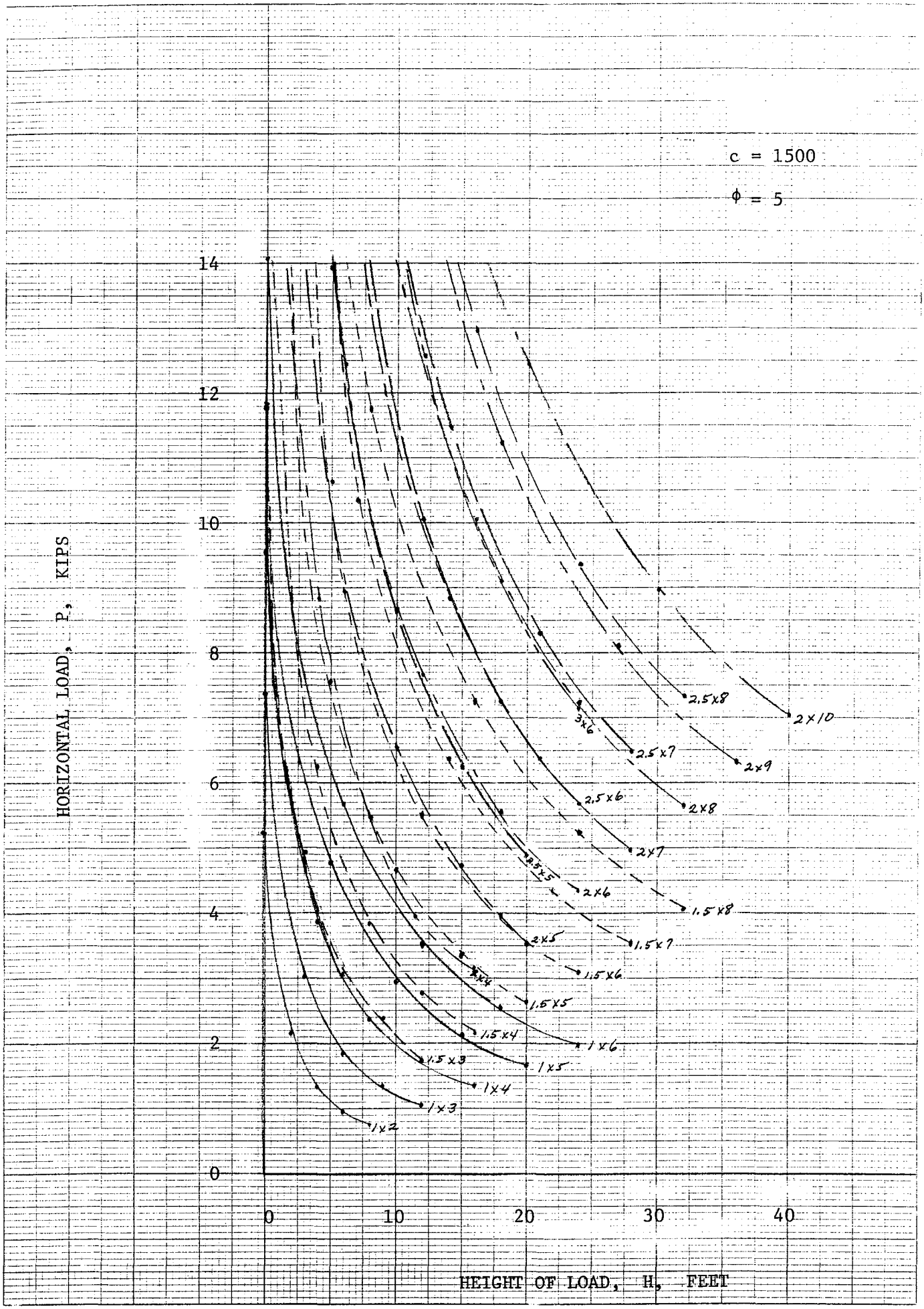
c = 1500
ϕ = 5
HORIZONTAL LOAD, P, KIPS
HEIGHT OF LOAD, H, FEET
0
2
4
6
8
10
12
14
0
10
20
30
40
2.5x8
2x10
3x6
2.5x7
2x9
2.5x6
2x8
2x7
2.5x5
2x6
1.5x8
1.5x7
2x5
1.5x6
3x4
1.5x5
1.5x4
1x6
1.5x3
1x5
1x4
1x3
1x2

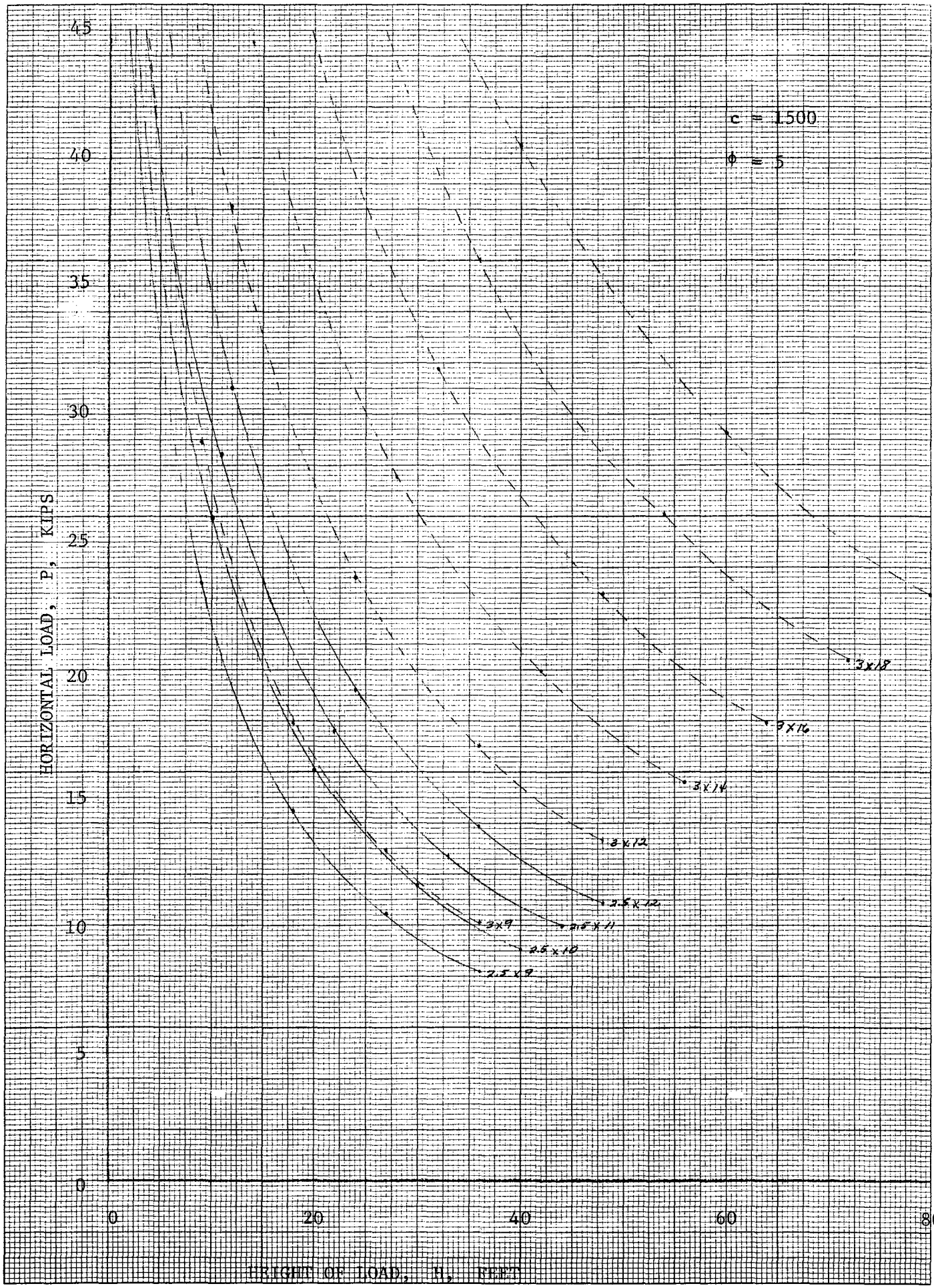

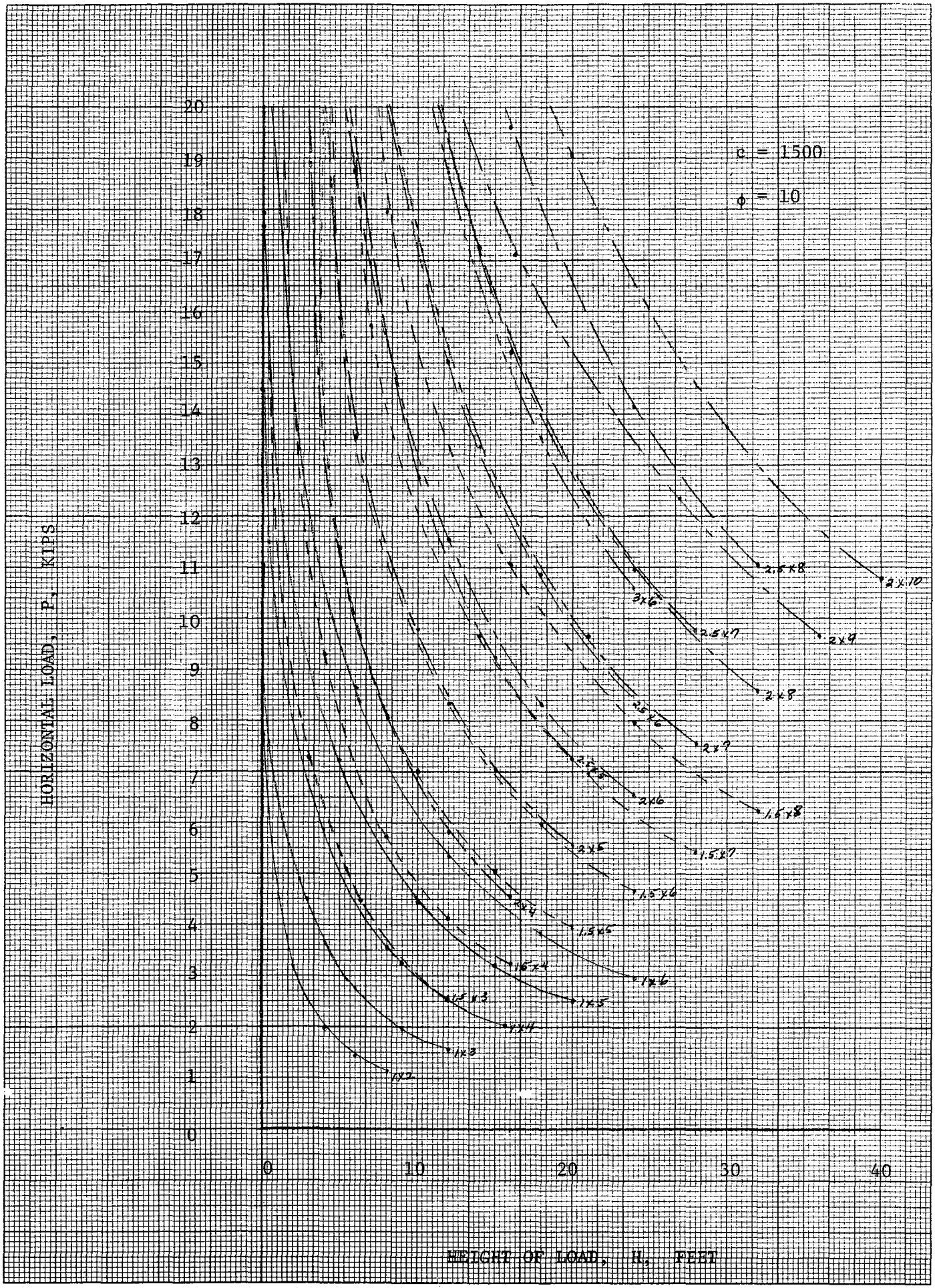

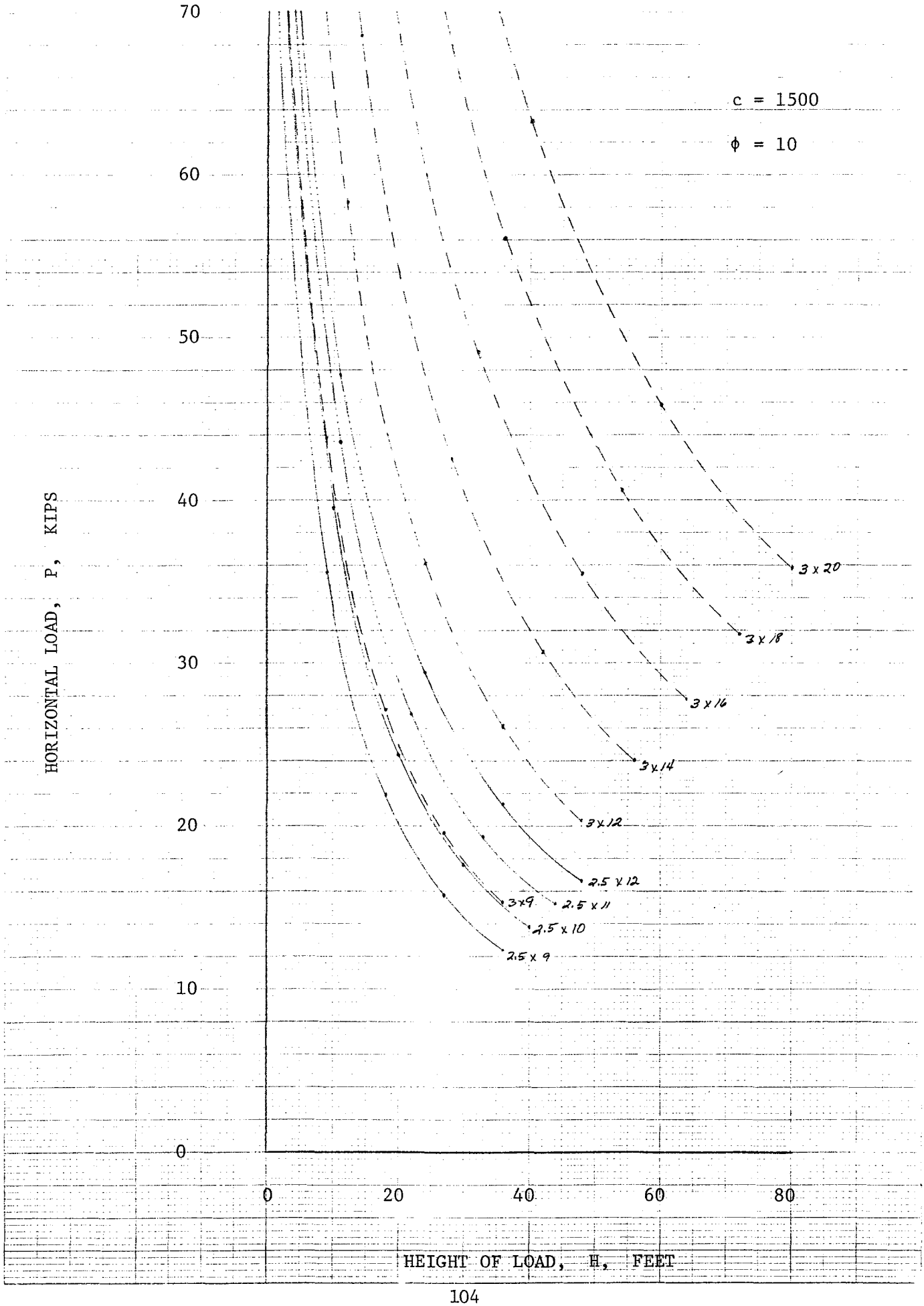
c = 1500
ϕ = 10
3 x 20
3 x 18
3 x 16
3 x 14
3 x 12
2.5 x 12
2.5 x 11
3 x 9
2.5 x 10
2.5 x 9
HORIZONTAL LOAD, P, KIPS
HEIGHT OF LOAD, H, FEET
0
10
20
30
40
50
60
70
0
20
40
60
80

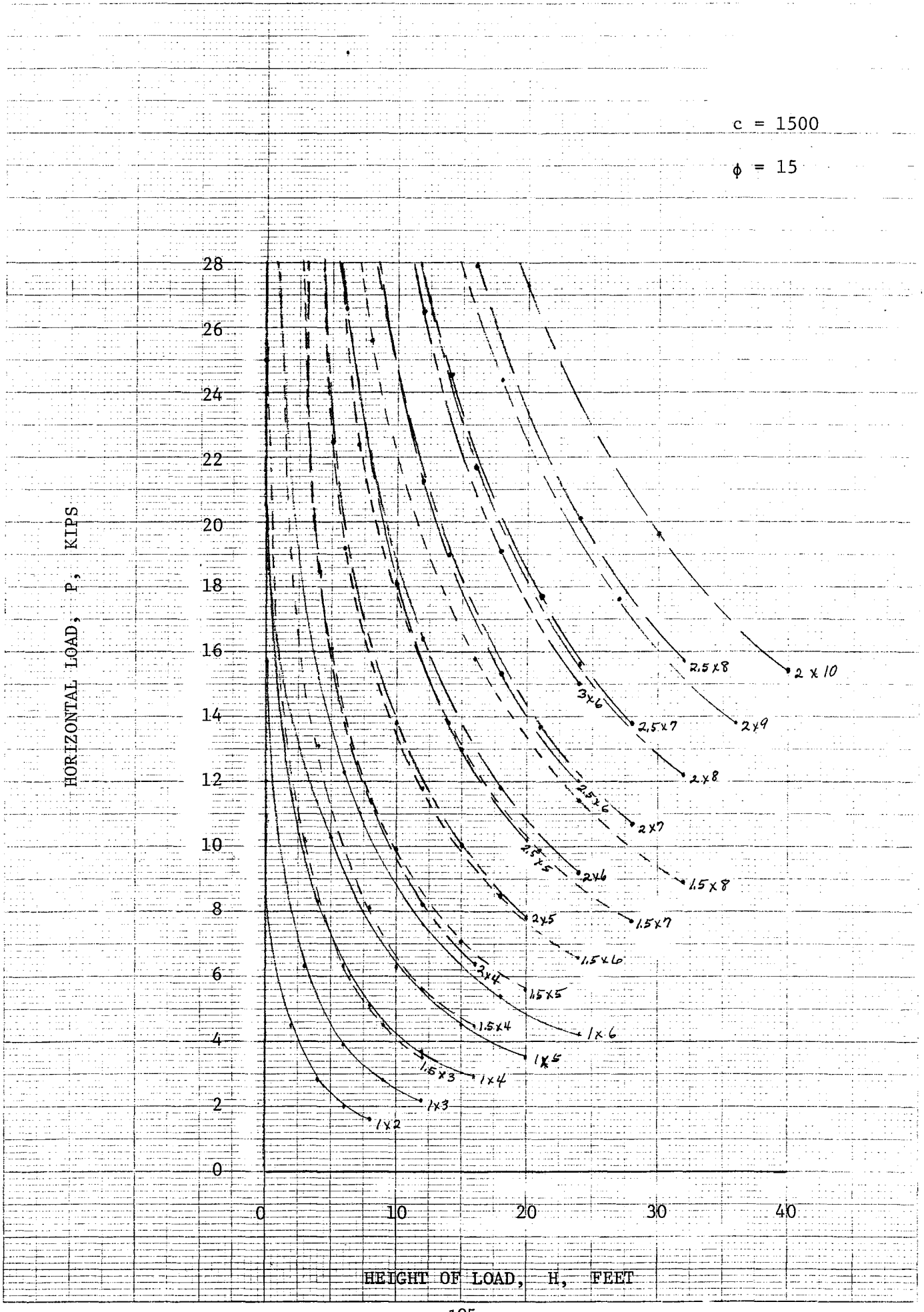
c = 1500
ϕ = 15
HORIZONTAL LOAD, P, KIPS
HEIGHT OF LOAD, H, FEET
0
2
4
6
8
10
12
14
16
18
20
22
24
26
28
0
10
20
30
40
2 x 10
2.5x8
2x9
3x6
2.5x7
2x8
2.5x6
2x7
2.5x5
2x6
1.5x8
2x5
1.5x7
1.5x6
3x4
1.5x5
1.5x4
1x6
1x5
1.5x3
1x4
1x3
1x2

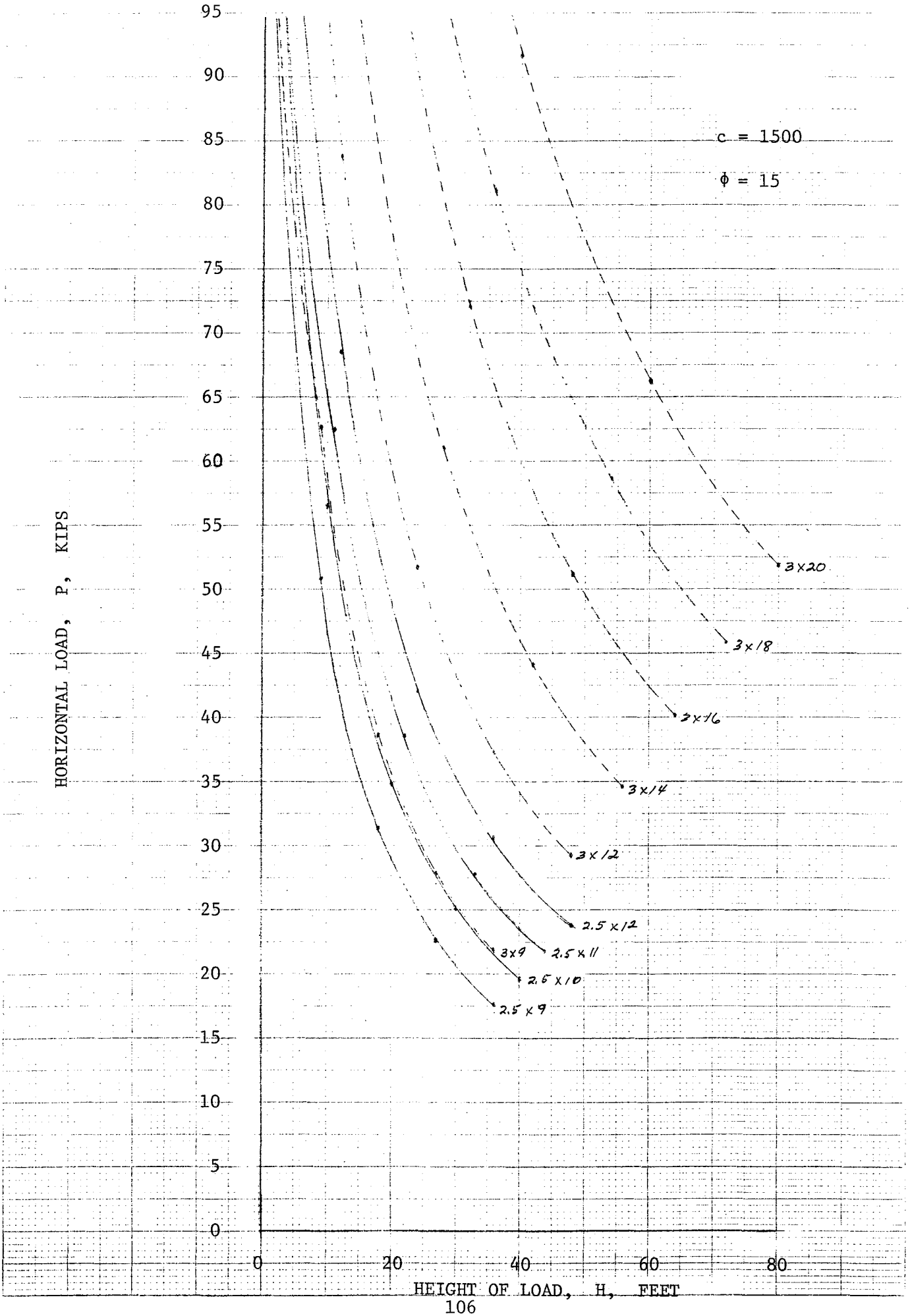
c = 1500
ϕ = 15
3x20
3x18
3x16
3x14
3x12
2.5x12
2.5x11
3x9
2.5x10
2.5x9
HORIZONTAL LOAD, P, KIPS
HEIGHT OF LOAD, H, FEET
0
5
10
15
20
25
30
35
40
45
50
55
60
65
70
75
80
85
90
95
0
20
40
60
80

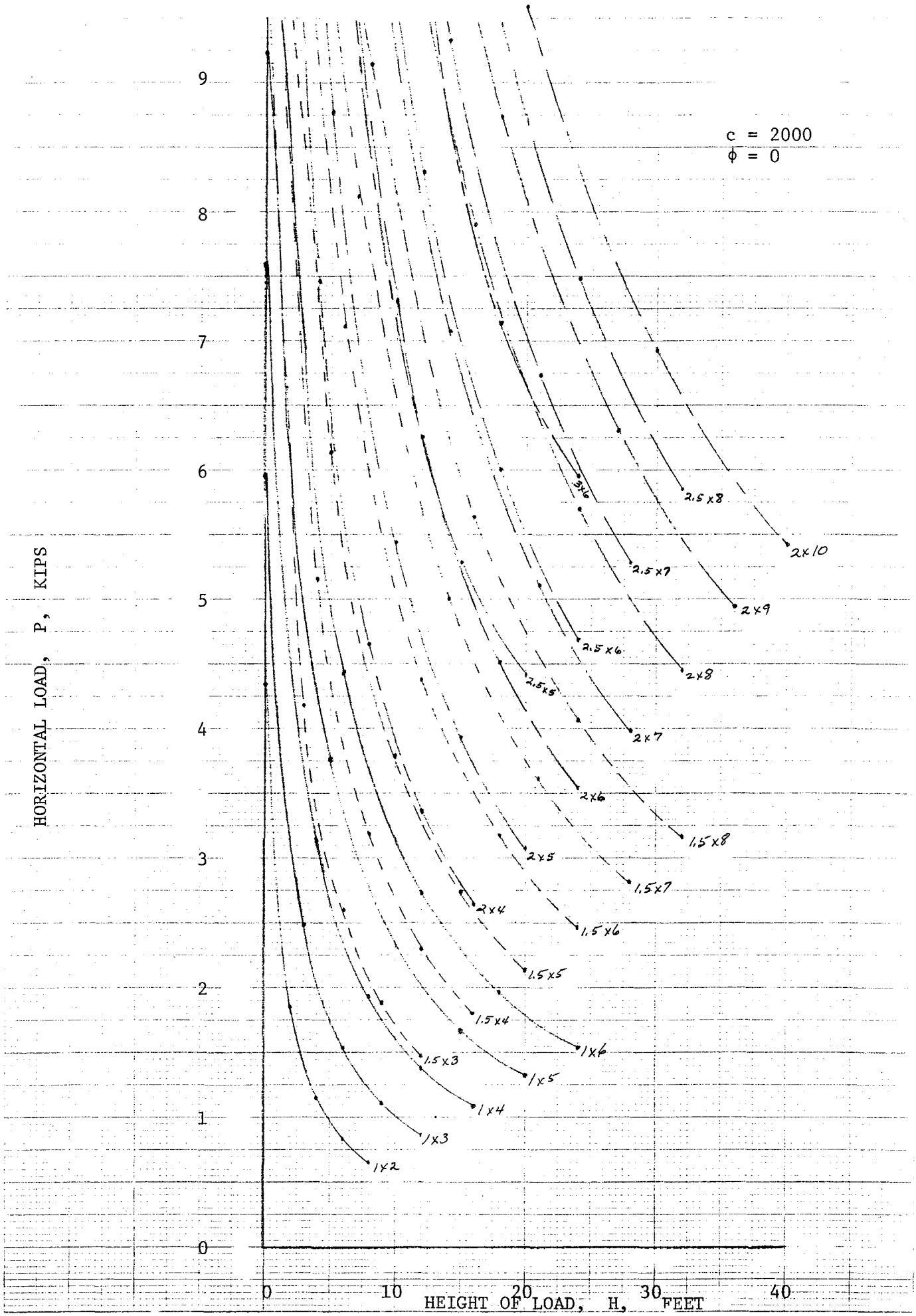
c = 2000
ϕ = 0
HORIZONTAL LOAD, P, KIPS
HEIGHT OF LOAD, H, FEET
0
1
2
3
4
5
6
7
8
9
10
20
30
40
3x6
2.5x8
2.5x7
2x10
2x9
2.5x6
2x8
2.5x5
2x7
2x6
1.5x8
2x5
1.5x7
2x4
1.5x6
1.5x5
1.5x4
1x6
1.5x3
1x5
1x4
1x3
1x2

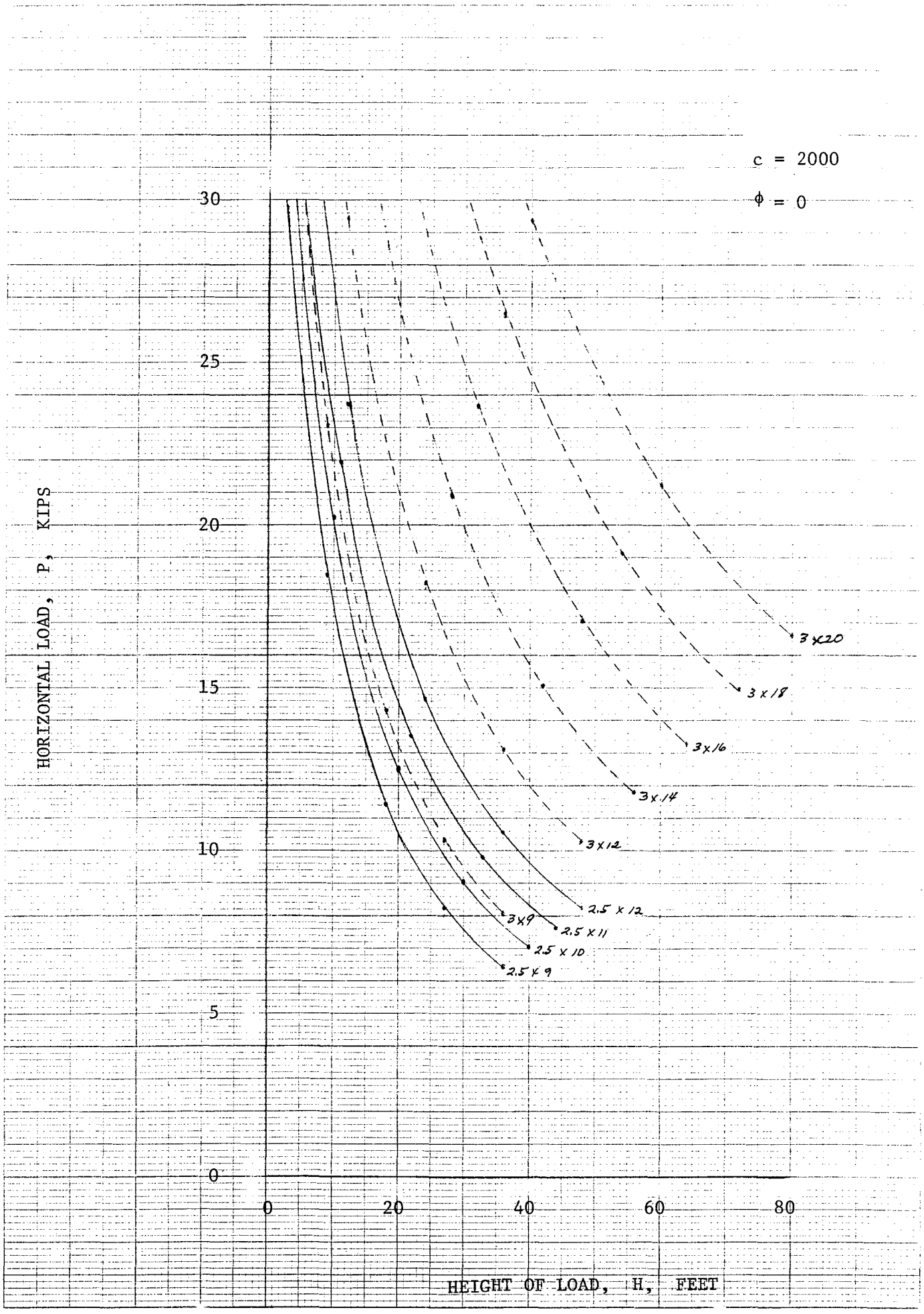
c = 2000
ϕ = 0
30
25
20
15
10
5
0
0
20
40
60
80
HORIZONTAL LOAD, P, KIPS
HEIGHT OF LOAD, H, FEET
3 x 20
3 x 18
3 x 16
3 x 14
3 x 12
2.5 x 12
3 x 9
2.5 x 11
2.5 x 10
2.5 x 9

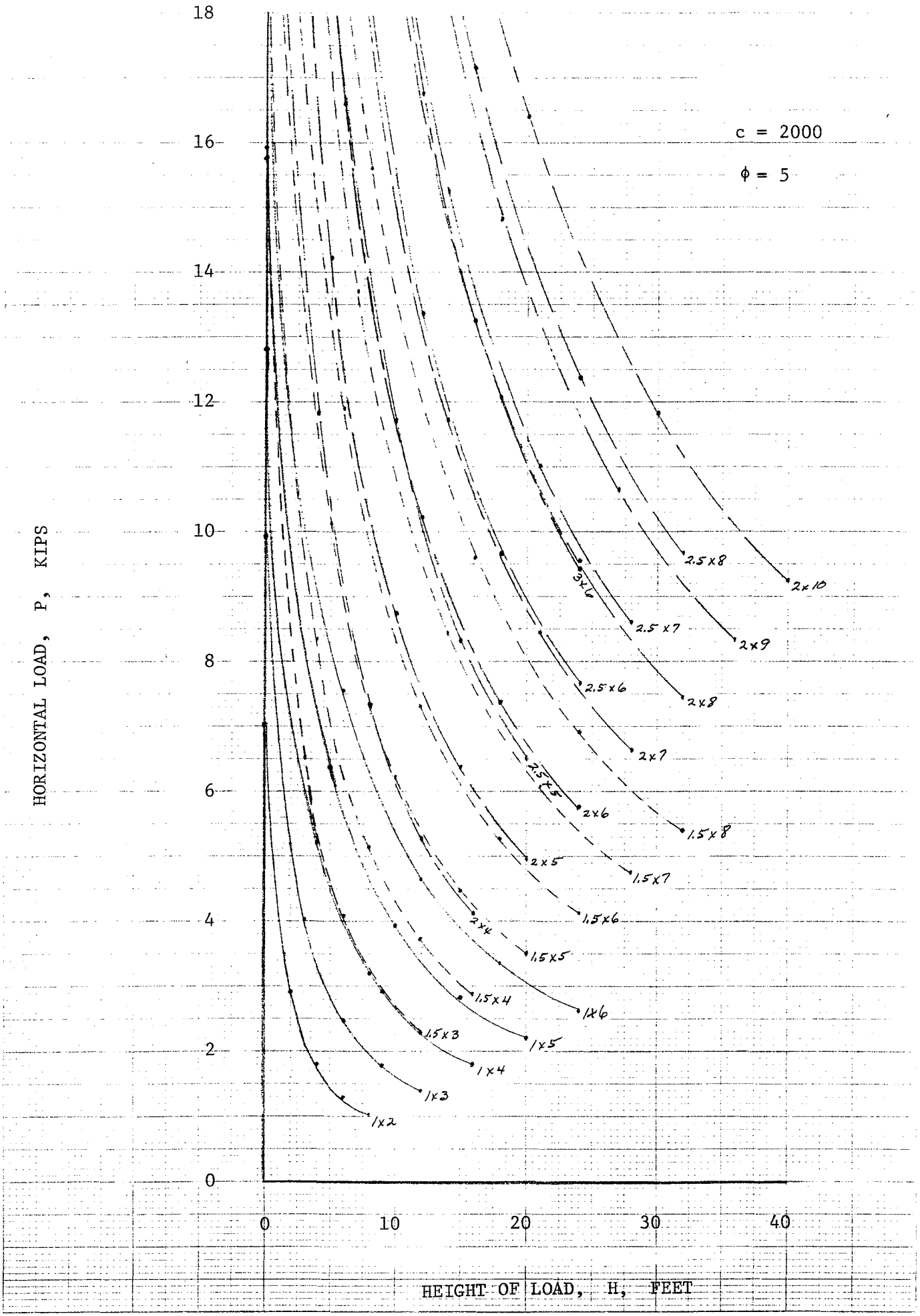
c = 2000
ϕ = 5
HORIZONTAL LOAD, P, KIPS
HEIGHT OF LOAD, H, FEET
0
2
4
6
8
10
12
14
16
18
0
10
20
30
40
1x2
1x3
1x4
1x5
1x6
1.5x3
1.5x4
1.5x5
1.5x6
1.5x7
1.5x8
2x4
2x5
2x6
2x7
2x8
2x9
2x10
2.5x5
2.5x6
2.5x7
2.5x8
3x6

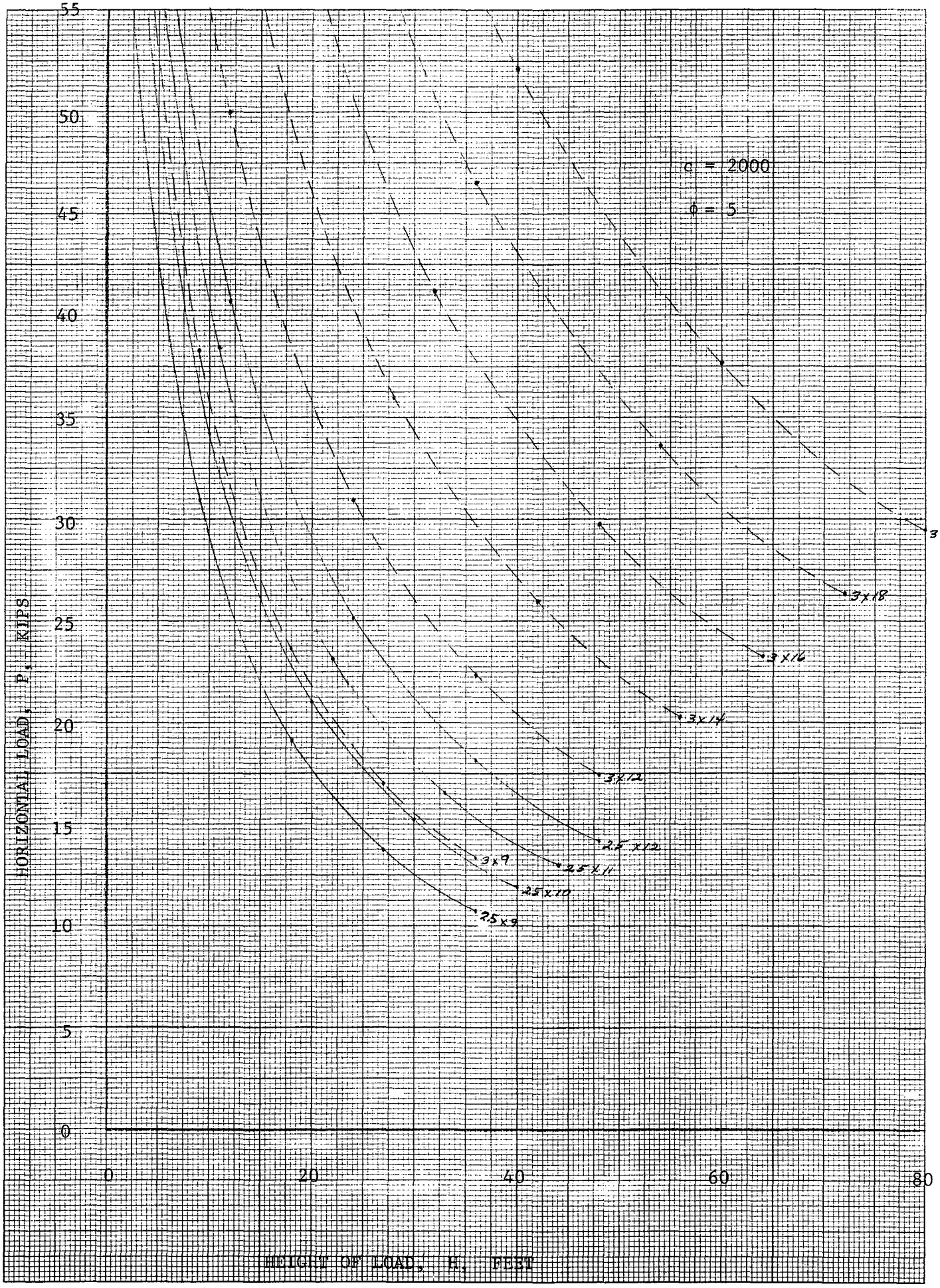

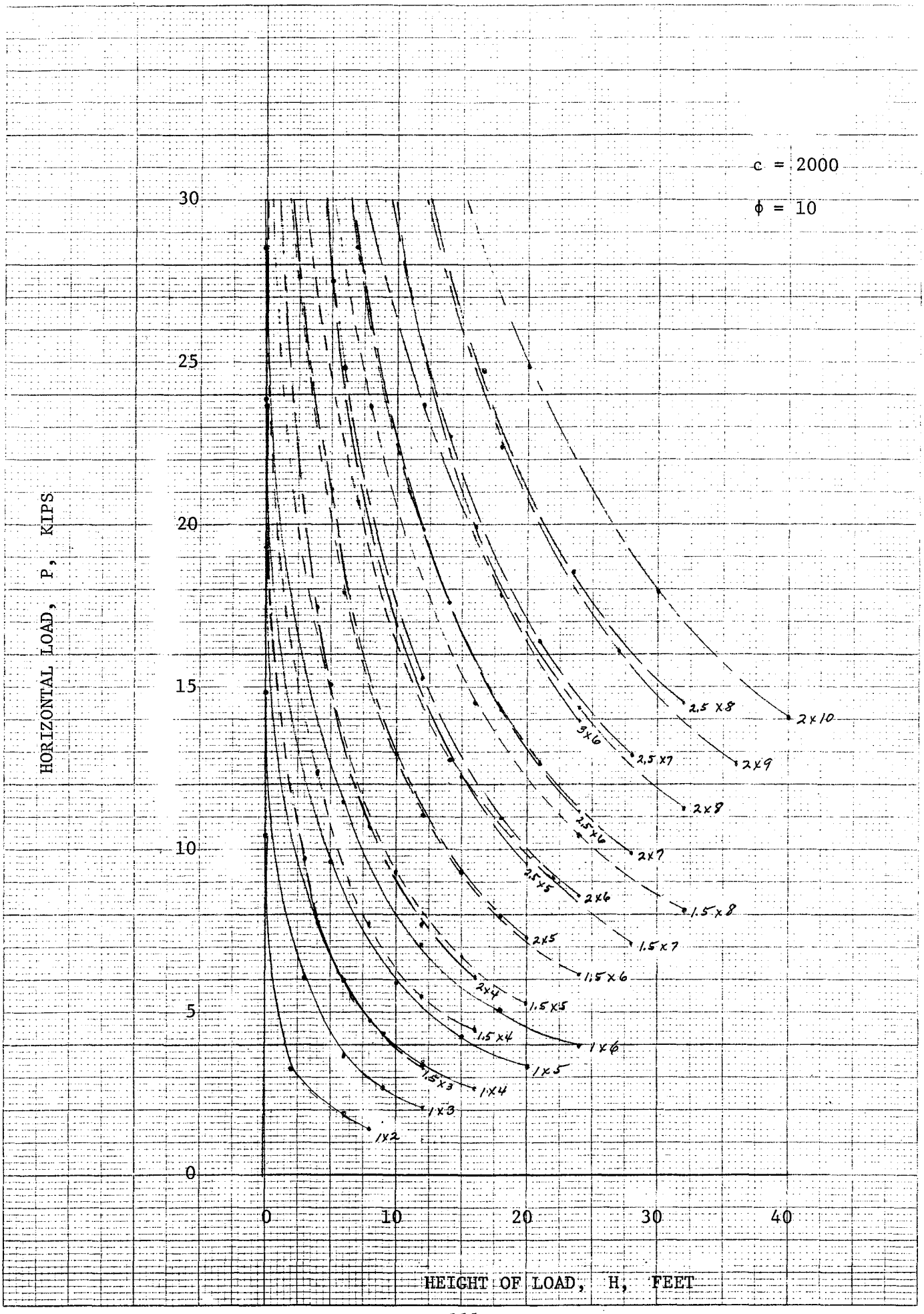
c = 2000
ϕ = 10
HORIZONTAL LOAD, P, KIPS
HEIGHT OF LOAD, H, FEET
0
5
10
15
20
25
30
0
10
20
30
40
2.5 X 8
2 X 10
3 X 6
2.5 X 7
2 X 9
2 X 8
2.5 X 6
2 X 7
2.5 X 5
2 X 6
1.5 X 8
2 X 5
1.5 X 7
1.5 X 6
2 X 4
1.5 X 5
1.5 X 4
1 X 6
1 X 5
1.5 X 3
1 X 4
1 X 3
1 X 2

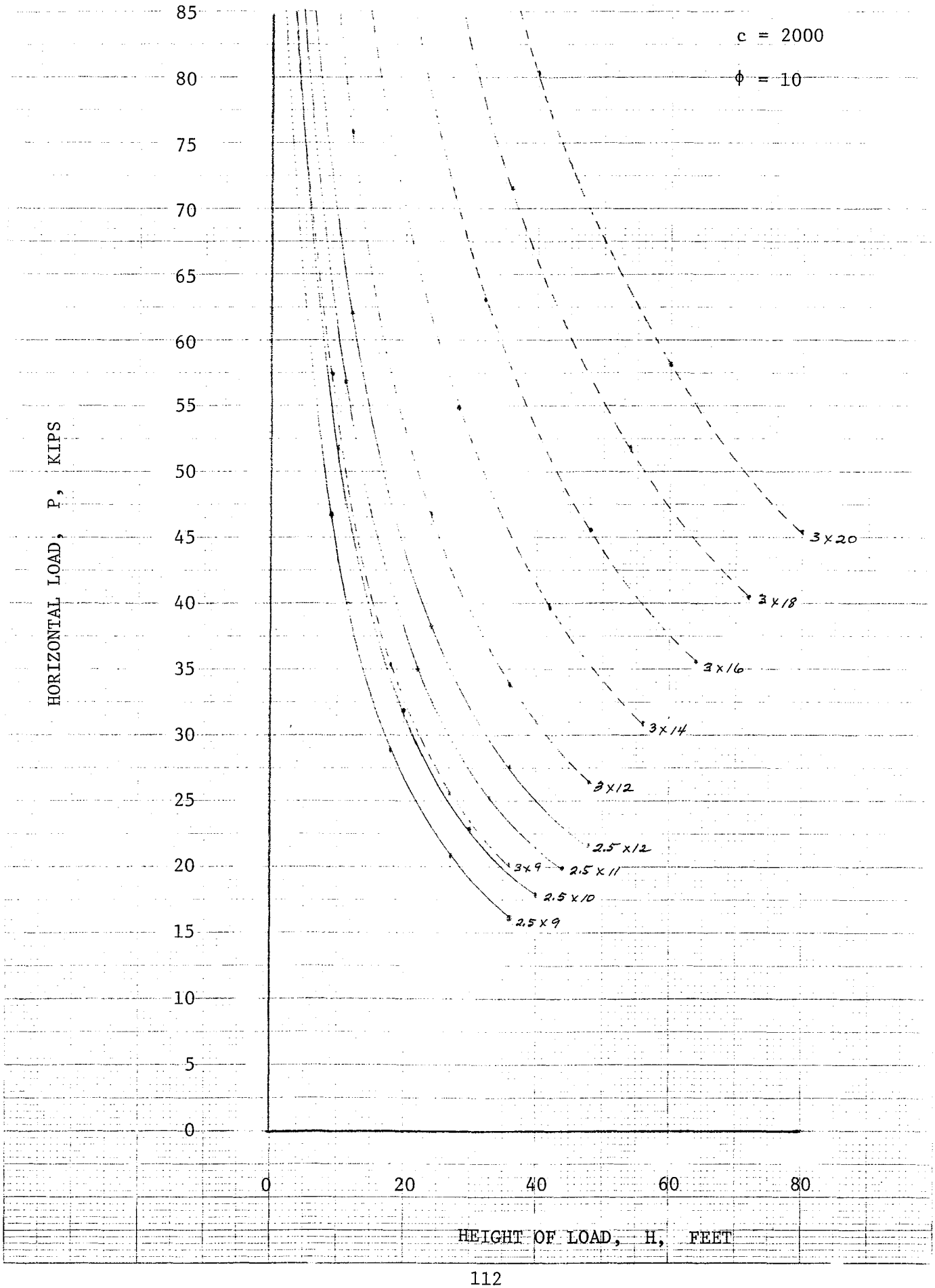
c = 2000
ϕ = 10
3 x 20
3 x 18
3 x 16
3 x 14
3 x 12
2.5 x 12
3 x 9
2.5 x 11
2.5 x 10
2.5 x 9
HORIZONTAL LOAD, P, KIPS
HEIGHT OF LOAD, H, FEET
0
5
10
15
20
25
30
35
40
45
50
55
60
65
70
75
80
85
0
20
40
60
80

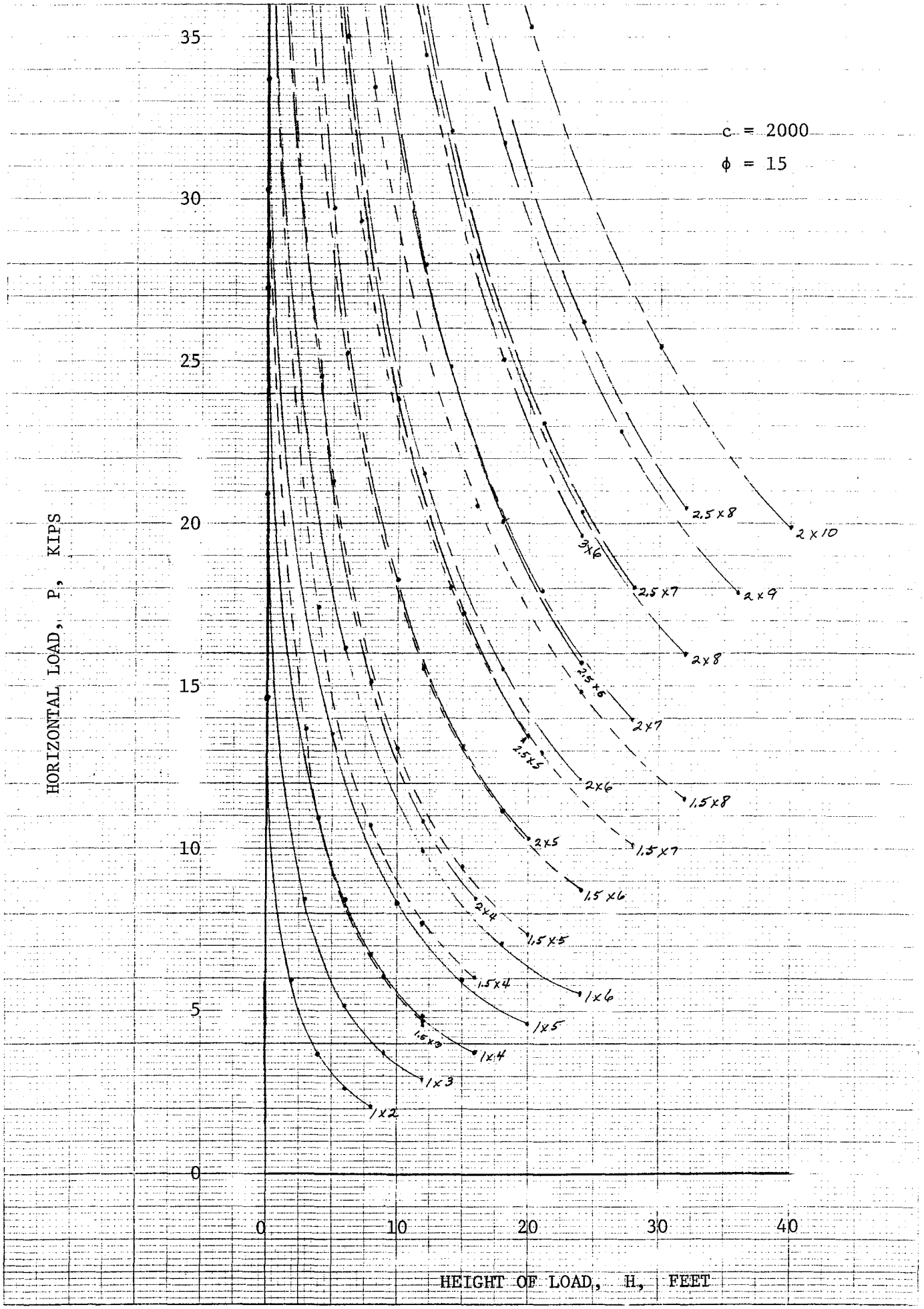
c = 2000
ϕ = 15
HORIZONTAL LOAD, P, KIPS
HEIGHT OF LOAD, H, FEET
0
5
10
15
20
25
30
35
0
10
20
30
40
2 x 10
2.5 x 8
3 x 6
2.5 x 7
2 x 9
2 x 8
2.5 x 6
2 x 7
2.5 x 5
2 x 6
1.5 x 8
1.5 x 7
2 x 5
1.5 x 6
2 x 4
1.5 x 5
1.5 x 4
1 x 6
1 x 5
1.5 x 3
1 x 4
1 x 3
1 x 2

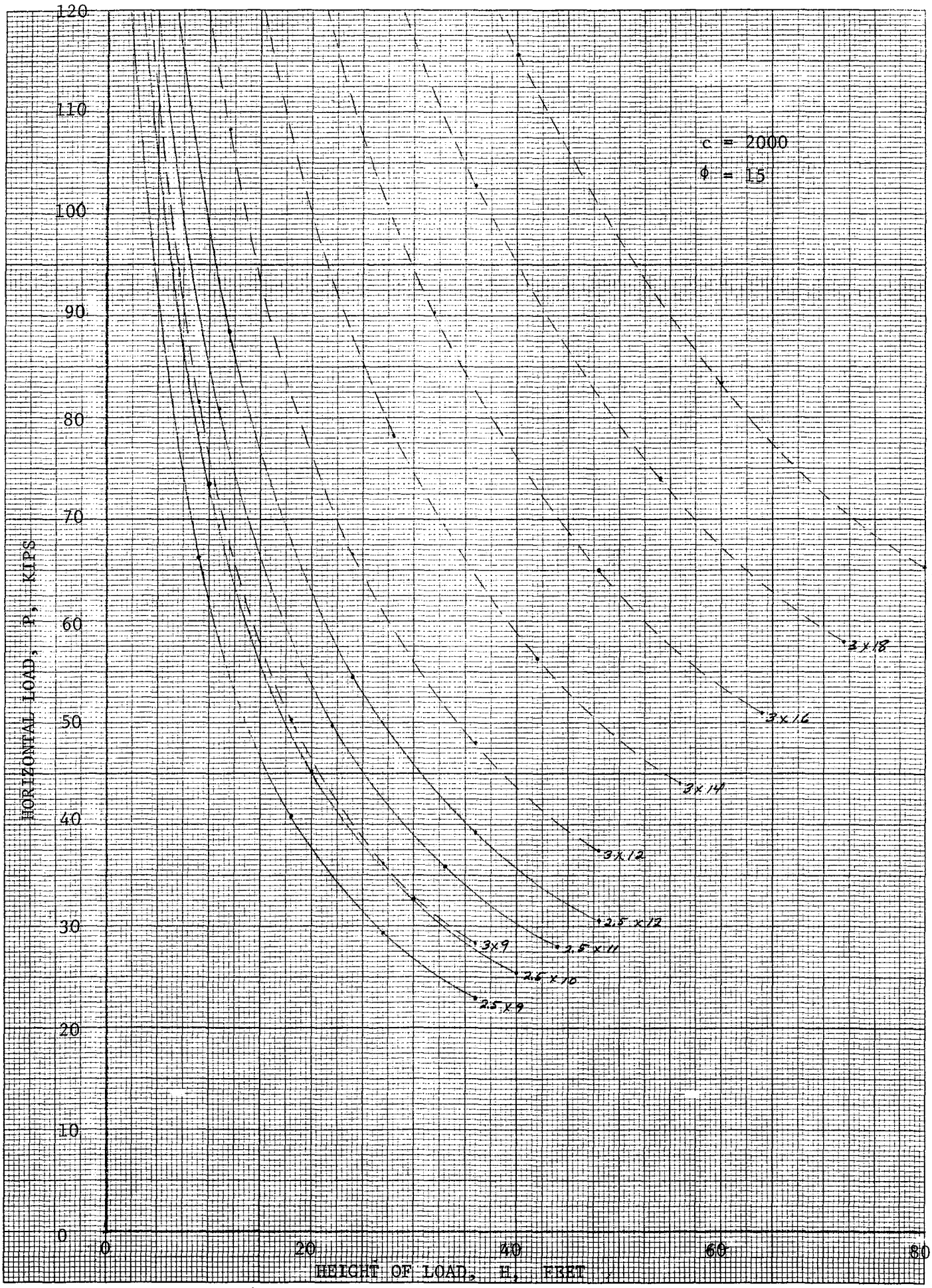

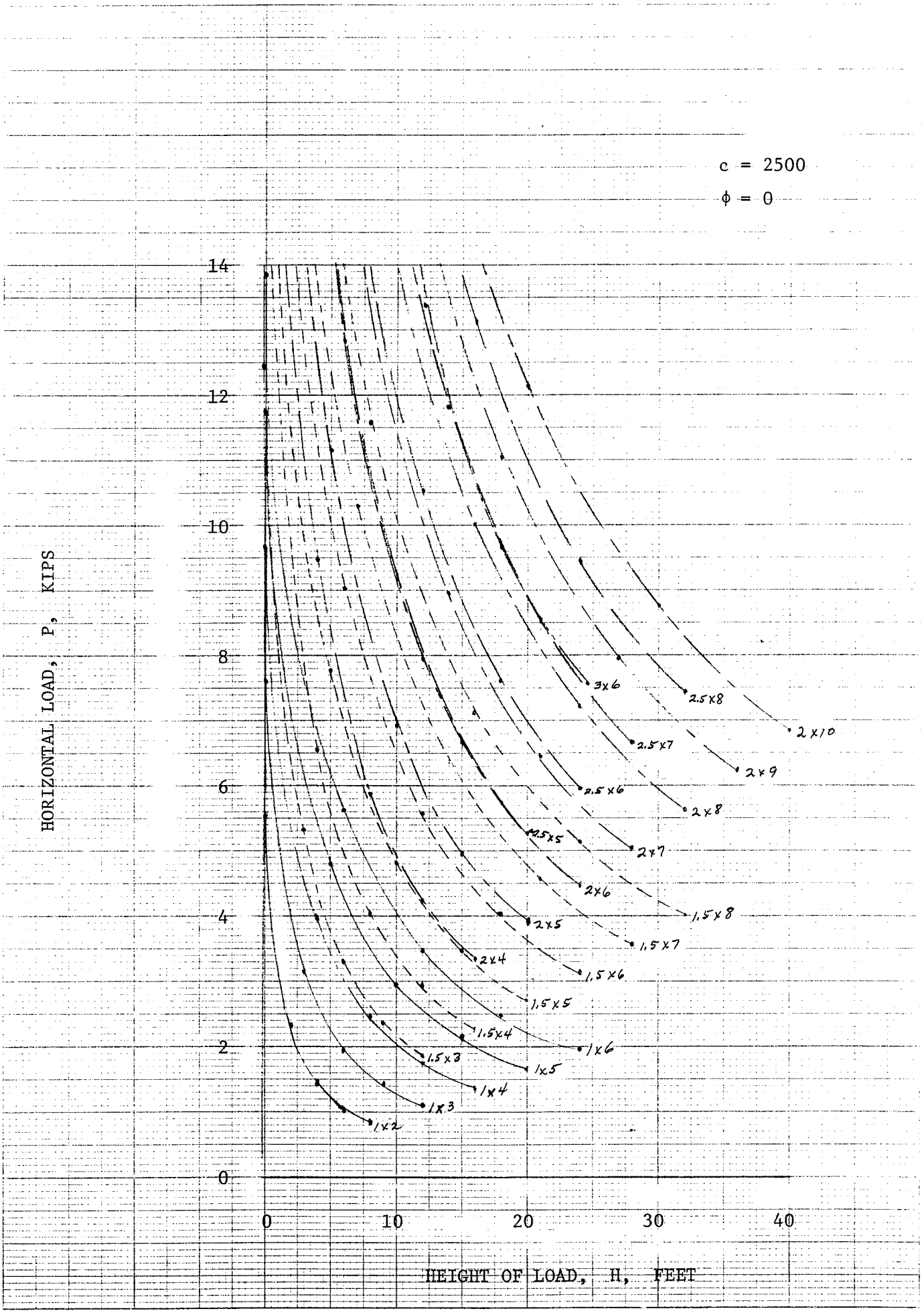
c = 2500
ϕ = 0
HORIZONTAL LOAD, P, KIPS
HEIGHT OF LOAD, H, FEET
0
2
4
6
8
10
12
14
0
10
20
30
40
3x6
2.5x8
2x10
2.5x7
2x9
2.5x6
2x8
2.5x5
2x7
2x6
1.5x8
2x5
1.5x7
2x4
1.5x6
1.5x5
1.5x4
1x6
1.5x3
1x5
1x4
1x3
1x2

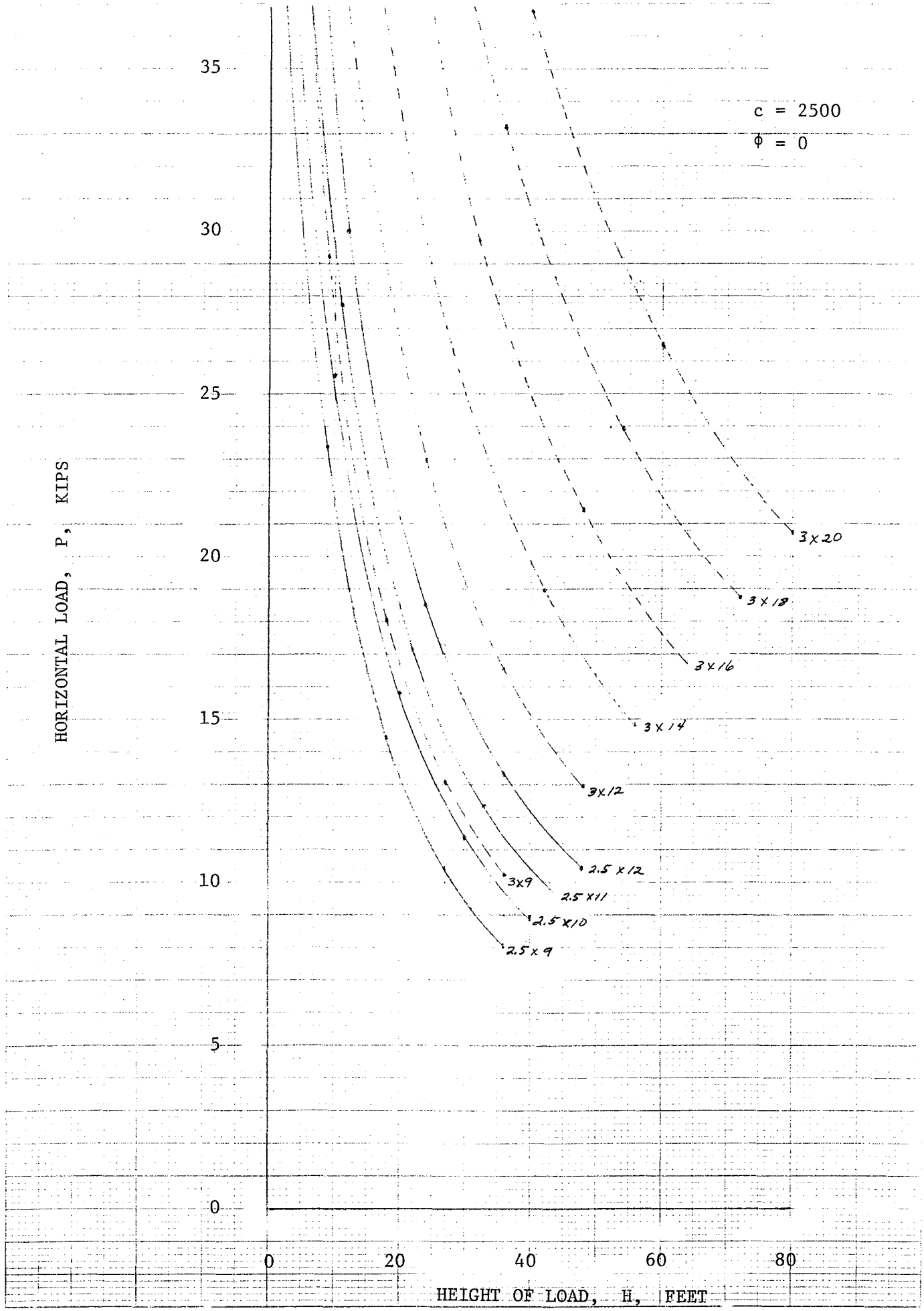
c = 2500
ϕ = 0
3 x 20
3 x 18
3 x 16
3 x 14
3 x 12
2.5 x 12
3x9
2.5 x11
2.5 x10
2.5 x 9
35
30
25
20
15
10
5
0
0
20
40
60
80
HORIZONTAL LOAD, P, KIPS
HEIGHT OF LOAD, H, FEET

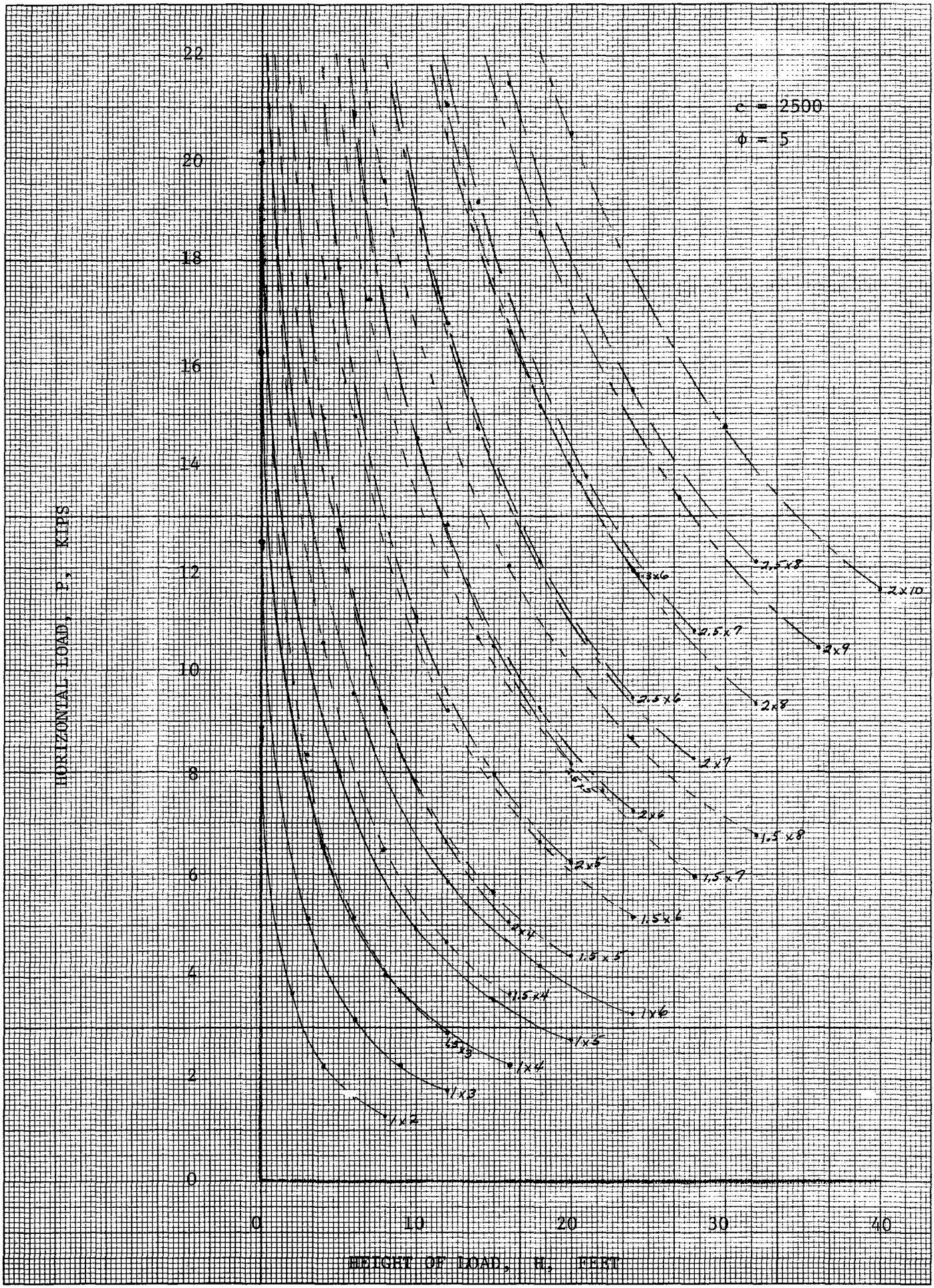

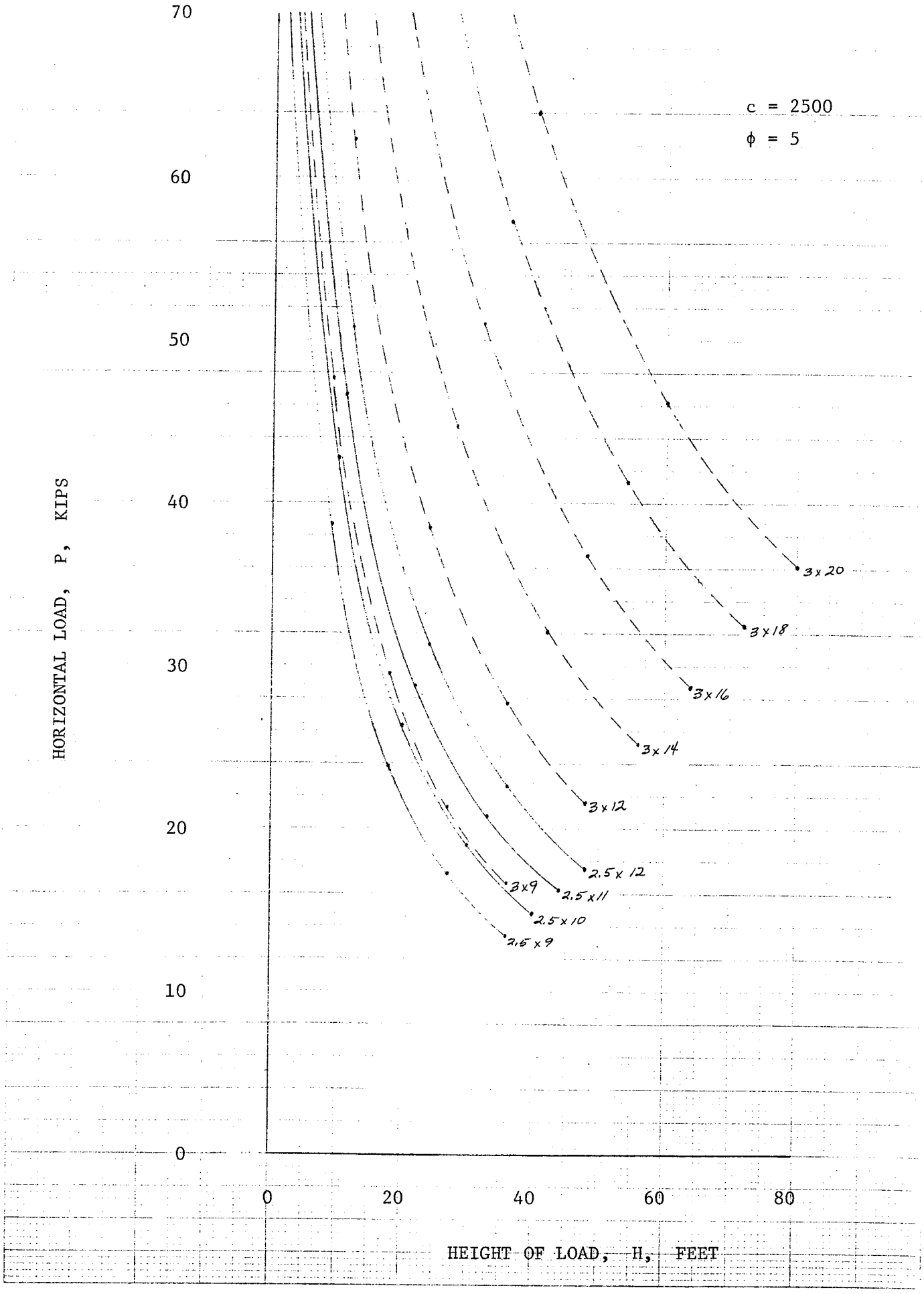
c = 2500
ϕ = 5
3 x 20
3 x 18
3 x 16
3 x 14
3 x 12
2.5 x 12
2.5 x 11
2.5 x 10
2.5 x 9
3 x 9
70
60
50
40
30
20
10
0
0
20
40
60
80
HORIZONTAL LOAD, P, KIPS
HEIGHT OF LOAD, H, FEET

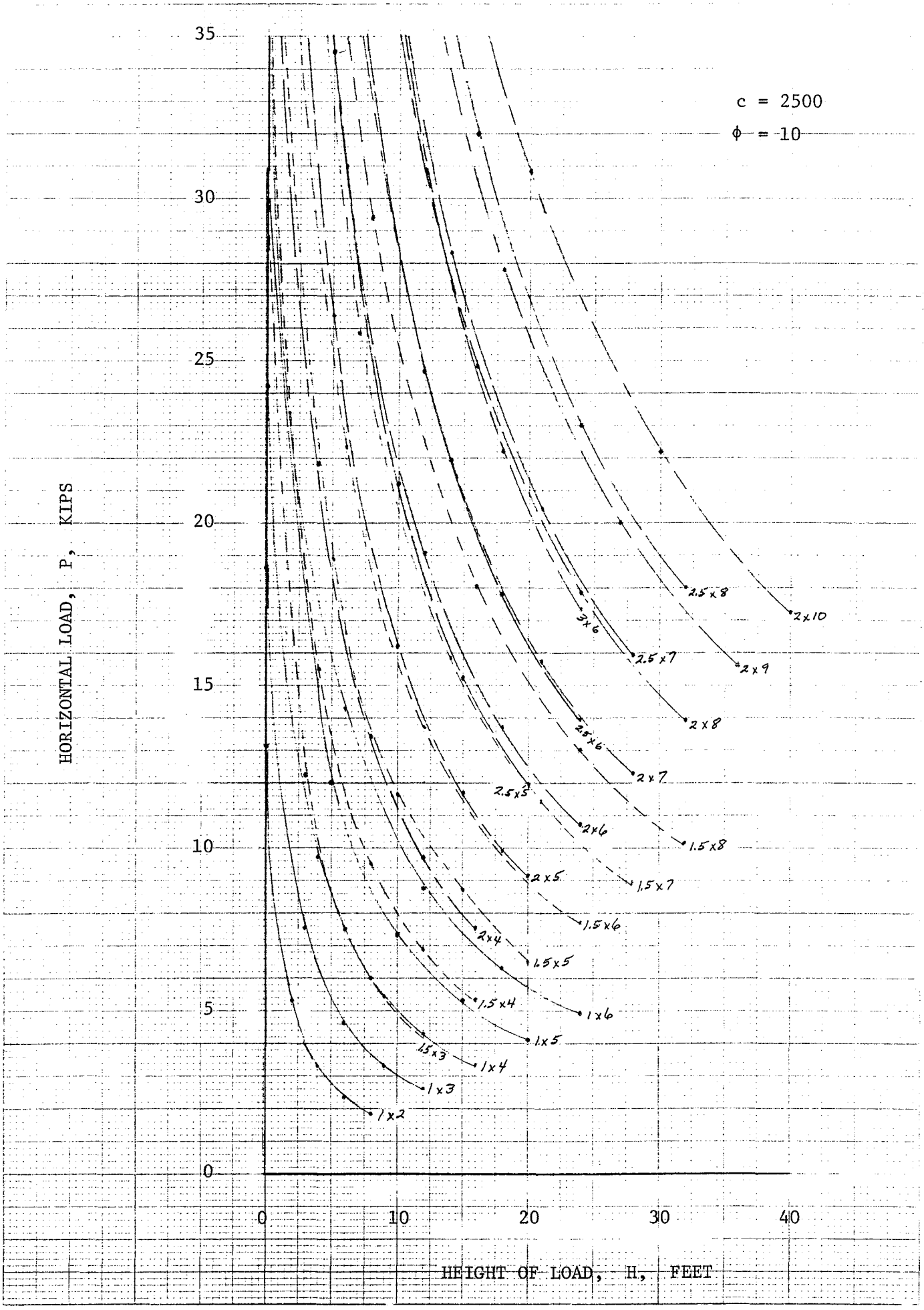
c = 2500
ϕ = 10
HORIZONTAL LOAD, P, KIPS
HEIGHT OF LOAD, H, FEET
0
5
10
15
20
25
30
35
0
10
20
30
40
2x10
2.5x8
3x6
2.5x7
2x9
2x8
2.5x6
2x7
2.5x5
2x6
1.5x8
2x5
1.5x7
1.5x6
2x4
1.5x5
1.5x4
1x6
1x5
1.5x3
1x4
1x3
1x2

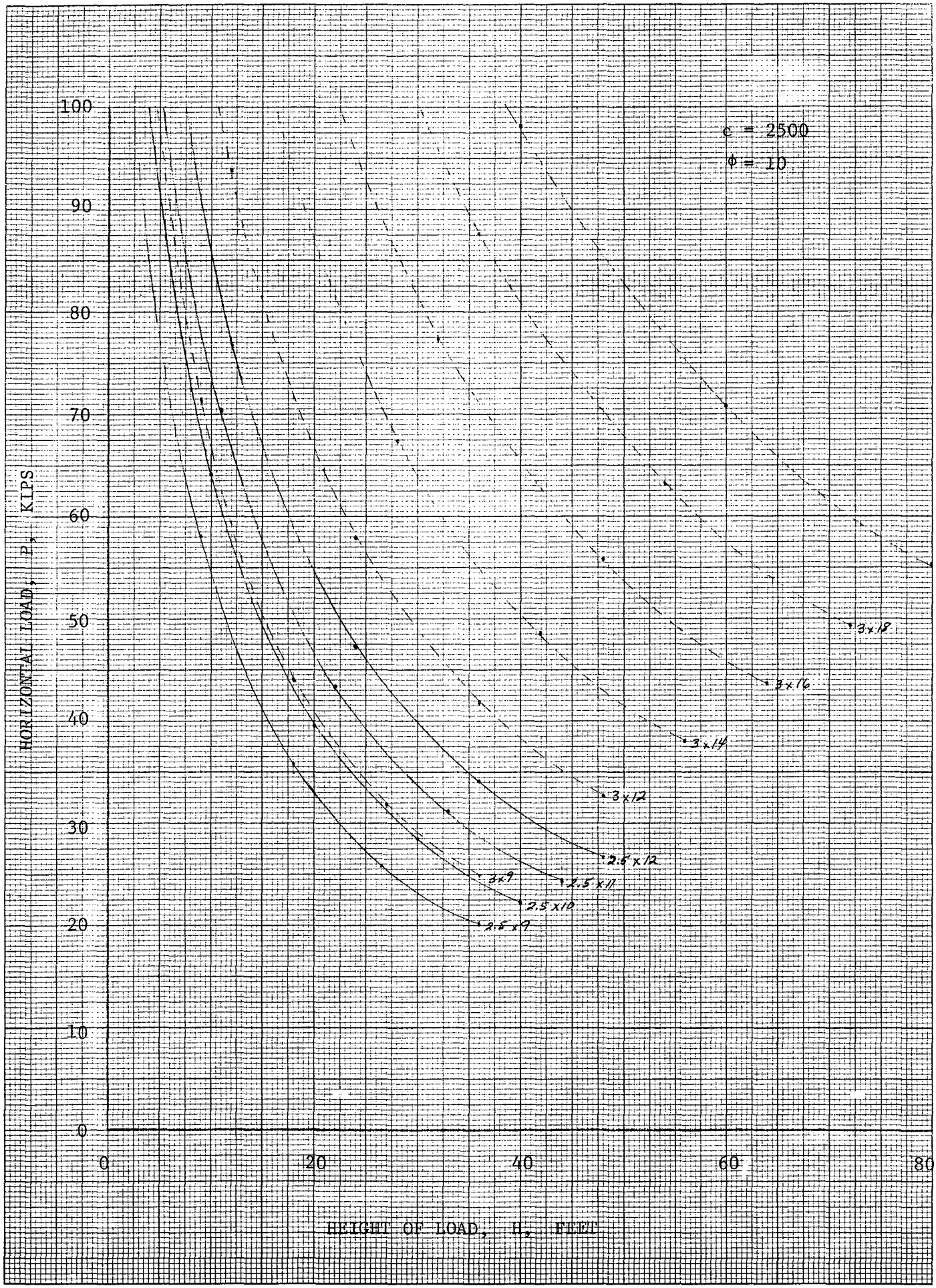

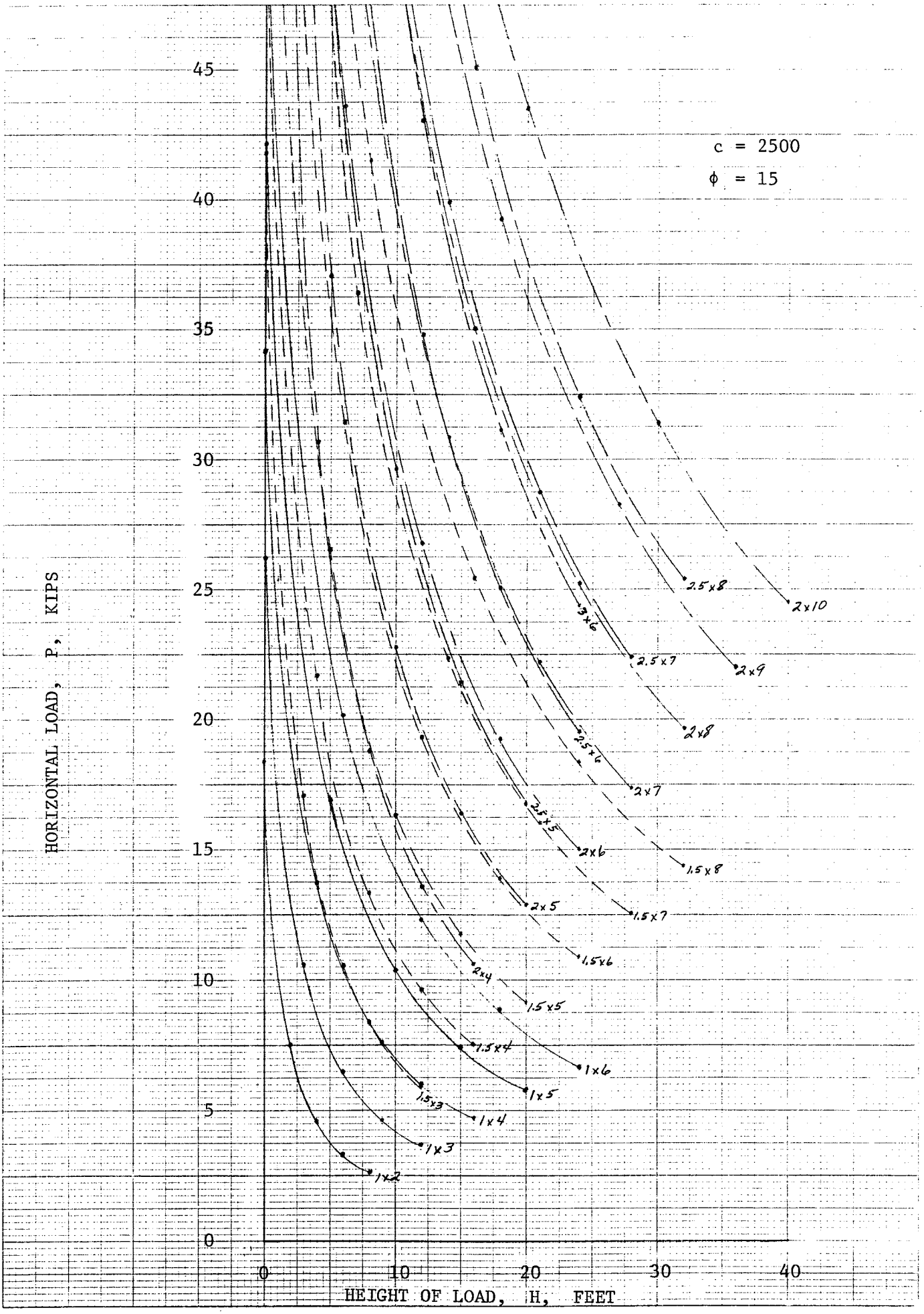
c = 2500
ϕ = 15
HORIZONTAL LOAD, P, KIPS
HEIGHT OF LOAD, H, FEET
0
5
10
15
20
25
30
35
40
45
0
10
20
30
40
2.5x8
2x10
3x6
2.5x7
2x9
2x8
2.5x6
2x7
2.5x5
2x6
1.5x8
2x5
1.5x7
1.5x6
2x4
1.5x5
1.5x4
1x6
1x5
1.5x3
1x4
1x3
1x2

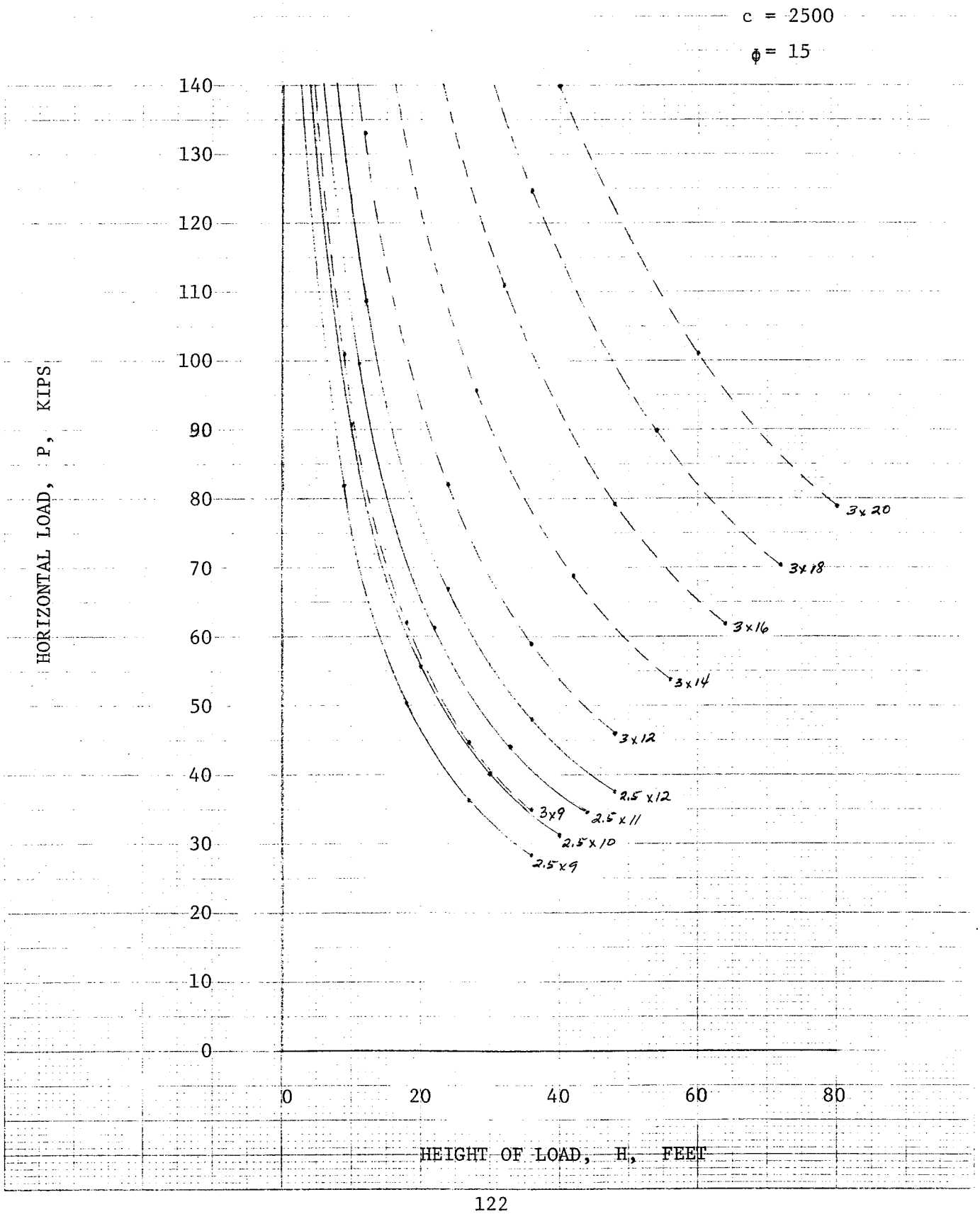
c = 2500
ϕ = 15
HORIZONTAL LOAD, P, KIPS
140
130
120
110
100
90
80
70
60
50
40
30
20
10
0
0
20
40
60
80
HEIGHT OF LOAD, H, FEET
3x20
3x18
3x16
3x14
3x12
2.5x12
2.5x11
3x9
2.5x10
2.5x9

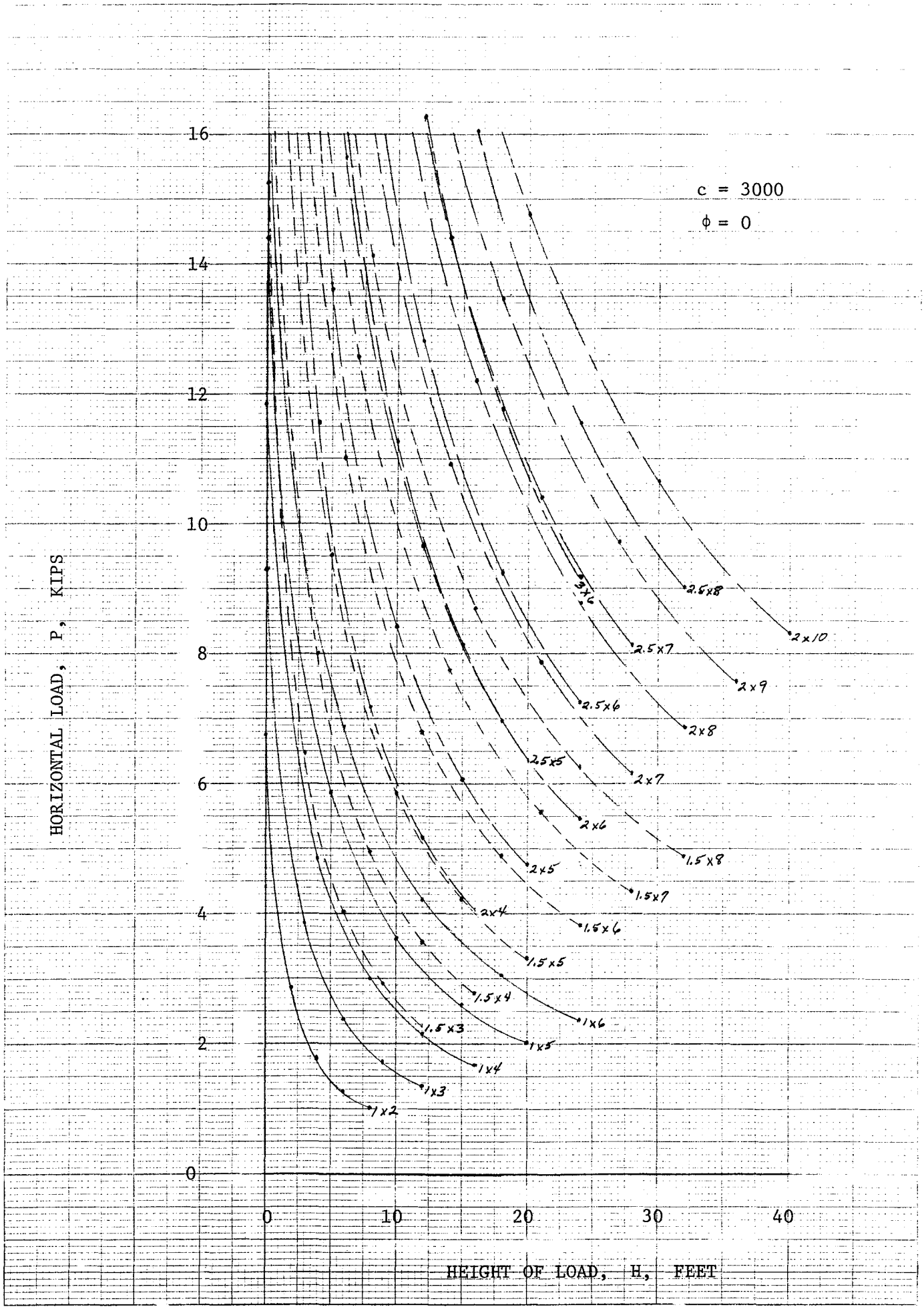
c = 3000
ϕ = 0
HORIZONTAL LOAD, P, KIPS
HEIGHT OF LOAD, H, FEET
0
2
4
6
8
10
12
14
16
0
10
20
30
40
1x2
1x3
1x4
1x5
1x6
1.5x3
1.5x4
1.5x5
1.5x6
1.5x7
1.5x8
2x4
2x5
2x6
2x7
2x8
2x9
2x10
2.5x5
2.5x6
2.5x7
2.5x8

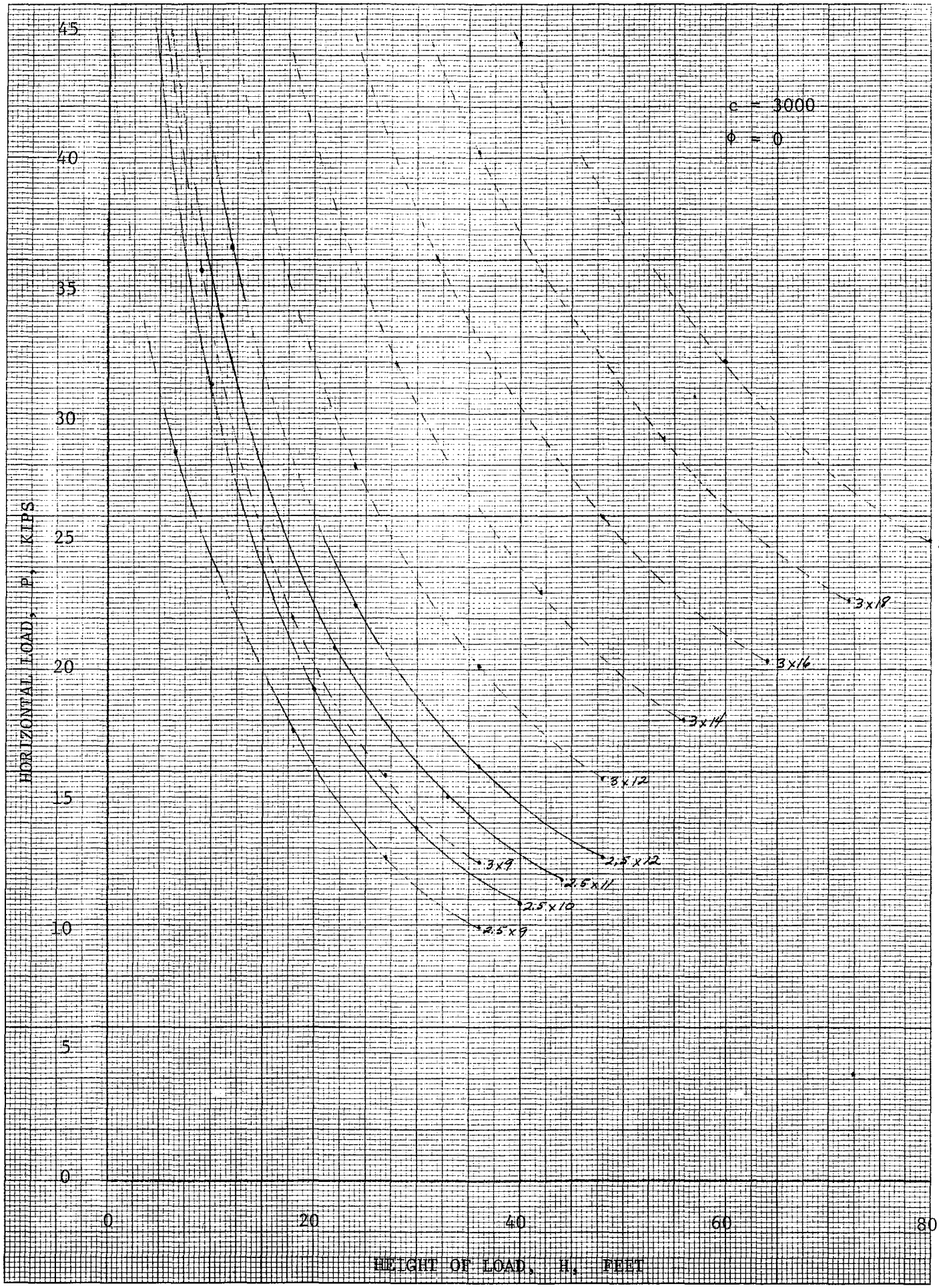

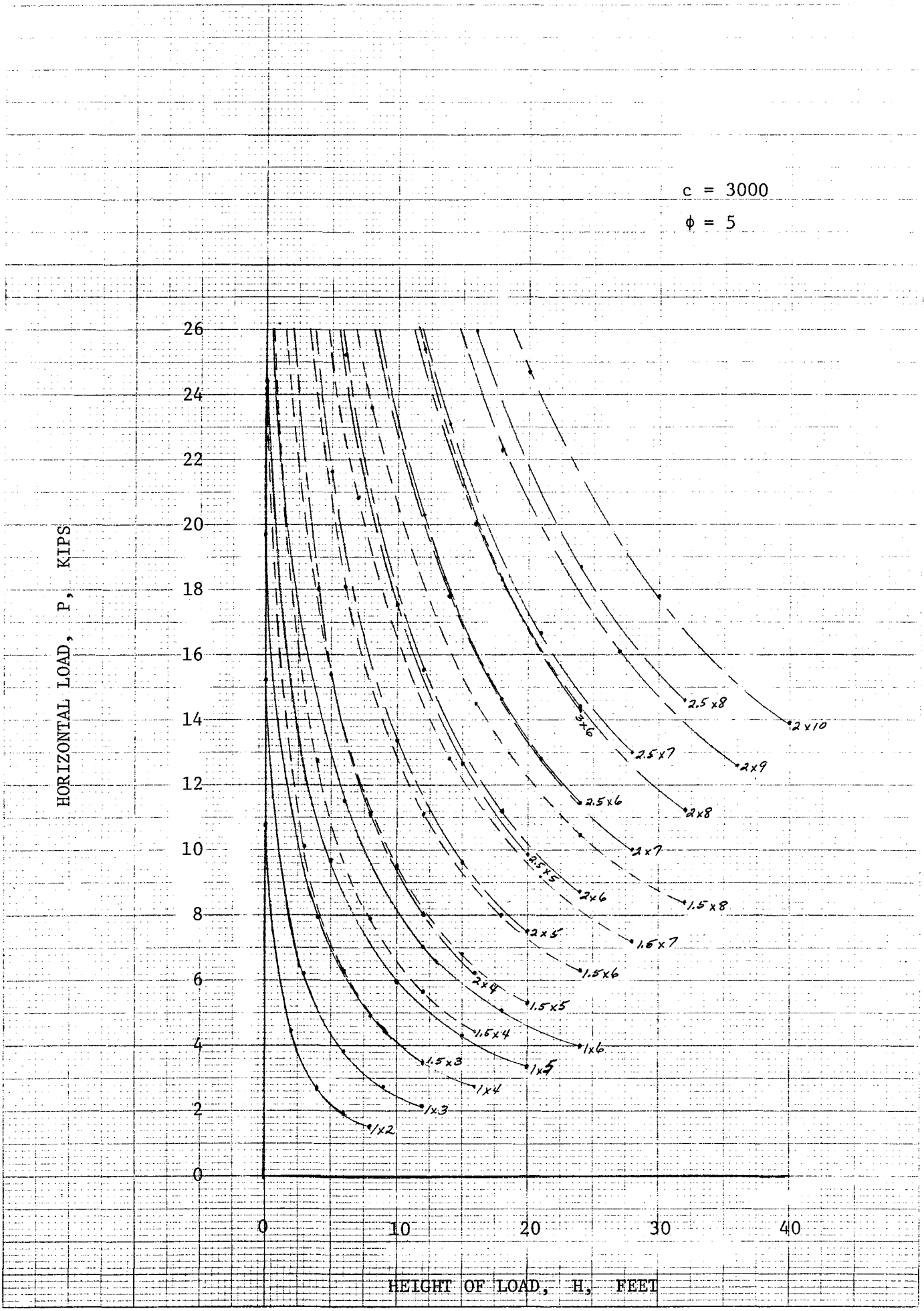
c = 3000
ϕ = 5
HORIZONTAL LOAD, P, KIPS
HEIGHT OF LOAD, H, FEET
0
2
4
6
8
10
12
14
16
18
20
22
24
26
0
10
20
30
40
2x10
2.5x8
3x6
2.5x7
2x9
2.5x6
2x8
2x7
2.5x5
2x6
1.5x8
2x5
1.6x7
1.5x6
2x4
1.5x5
1.5x4
1x6
1.5x3
1x5
1x4
1x3
1x2

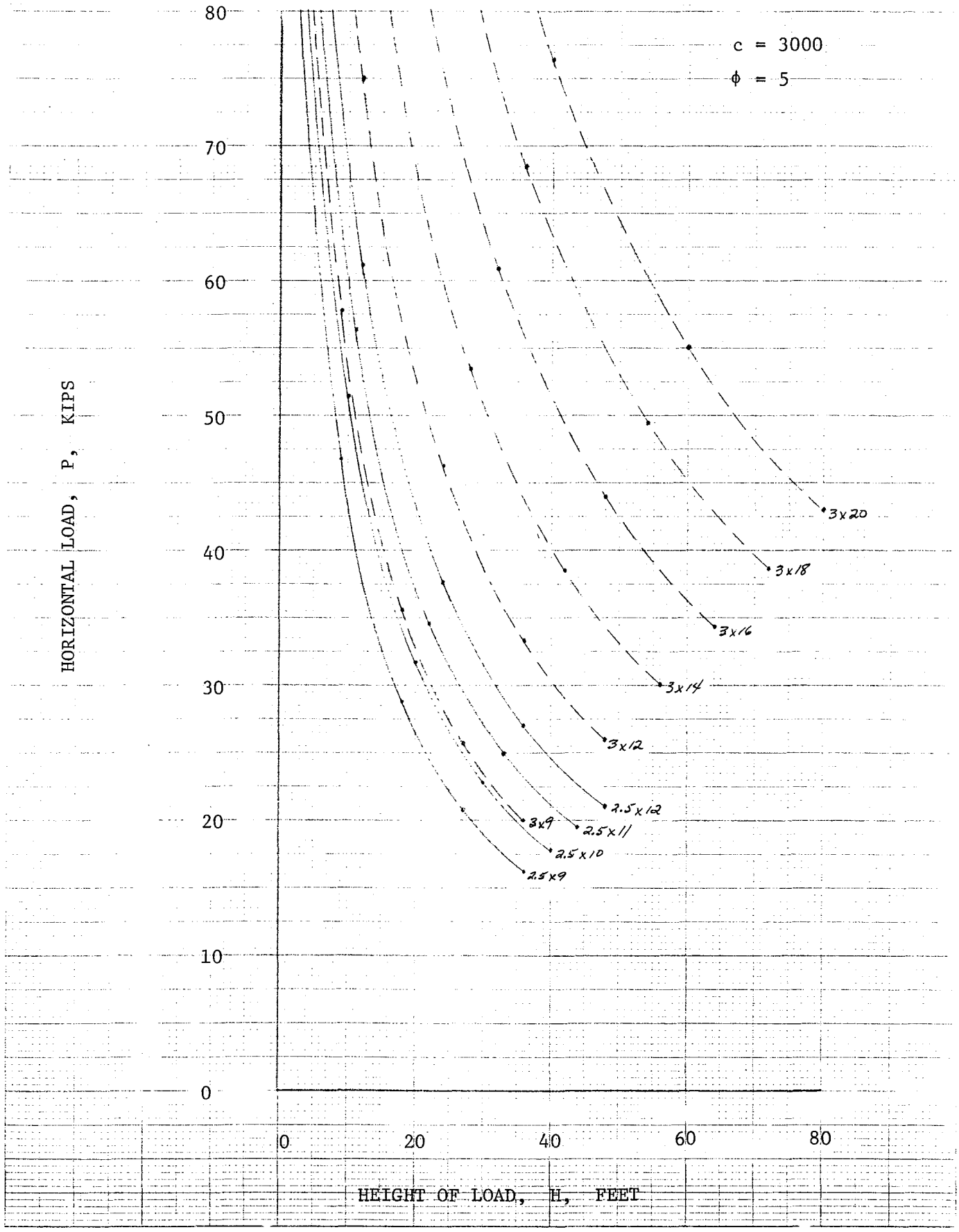
c = 3000
ϕ = 5
3x20
3x18
3x16
3x14
3x12
2.5x12
3x9
2.5x11
2.5x10
2.5x9
80
70
60
50
40
30
20
10
0
0
20
40
60
80
HORIZONTAL LOAD, P, KIPS
HEIGHT OF LOAD, H, FEET

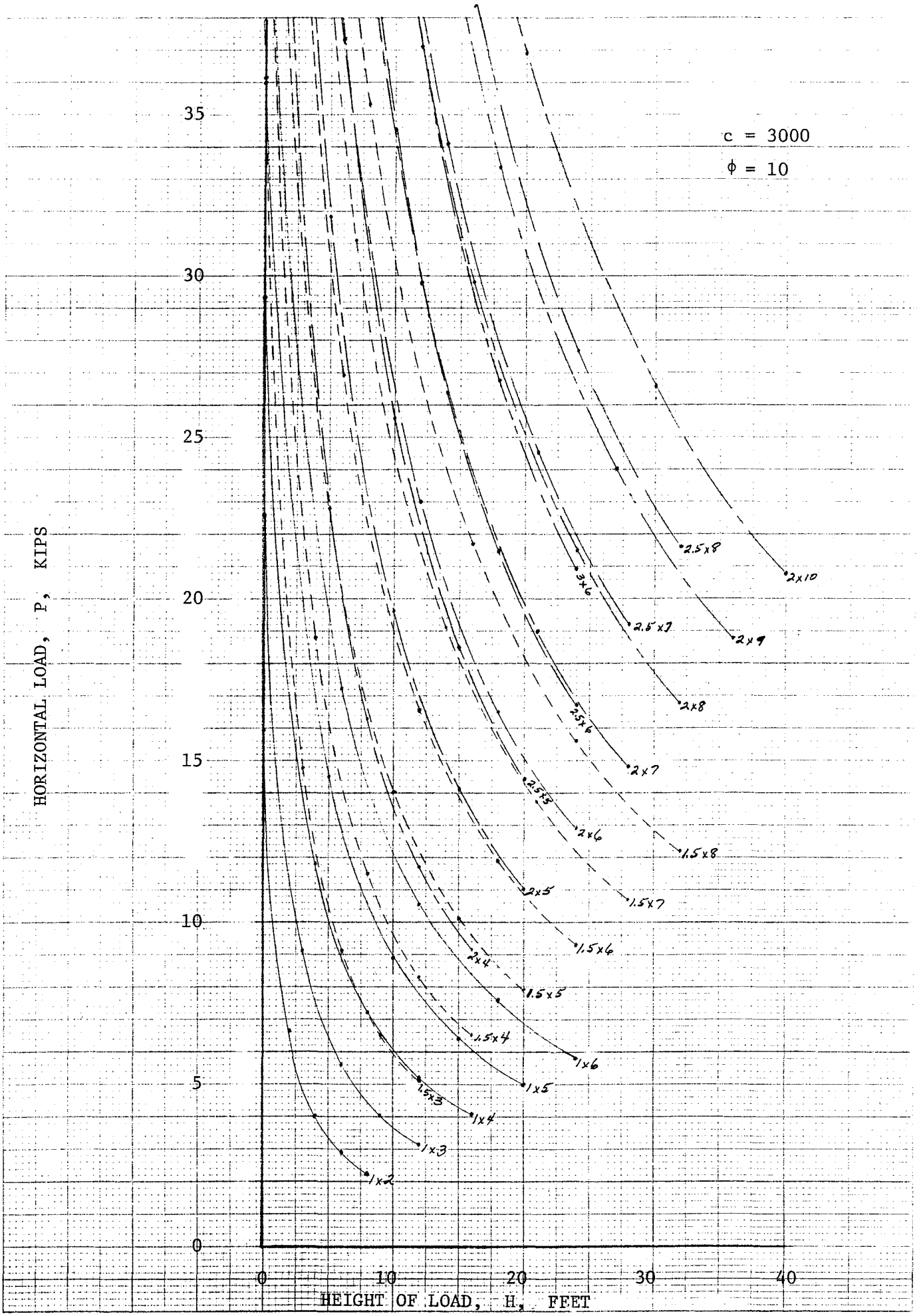
c = 3000
ϕ = 10
HORIZONTAL LOAD, P, KIPS
HEIGHT OF LOAD, H, FEET
0
5
10
15
20
25
30
35
0
10
20
30
40
2x10
2.5x8
2x9
3x6
2.5x7
2x8
2.5x6
2x7
2.5x5
2x6
1.5x8
1.5x7
2x5
1.5x6
2x4
1.5x5
1.5x4
1x6
1x5
1.5x3
1x4
1x3
1x2

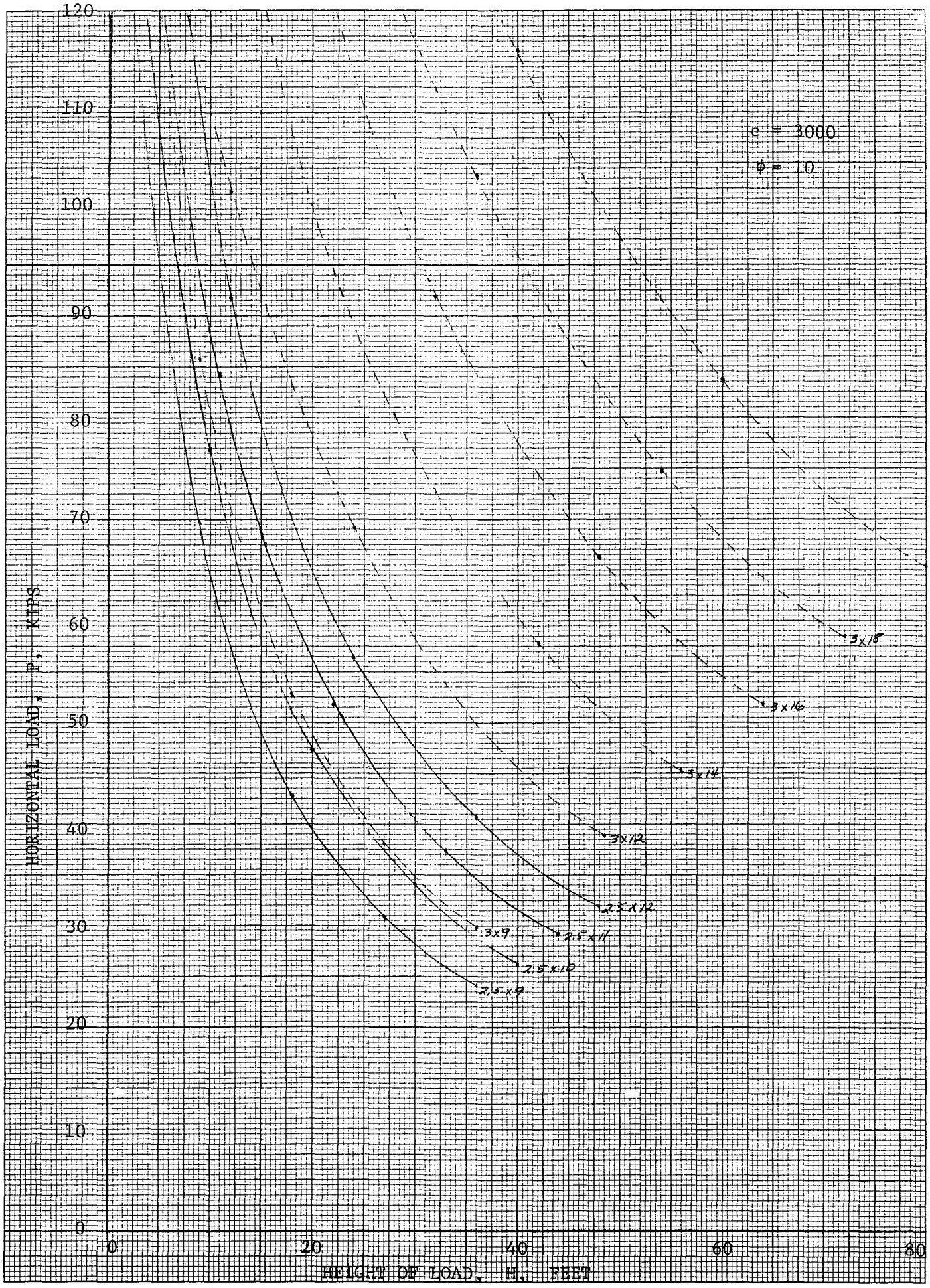

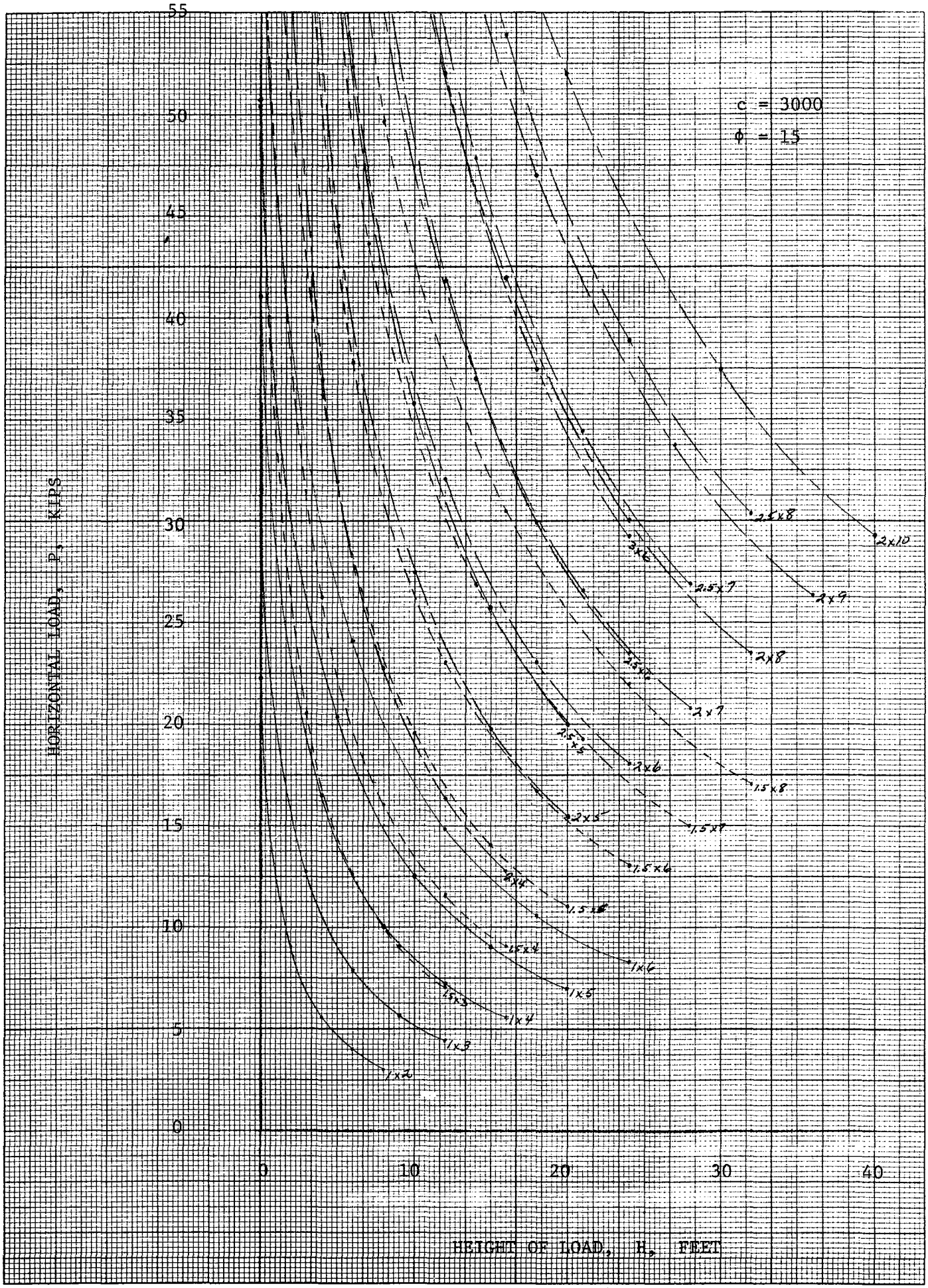

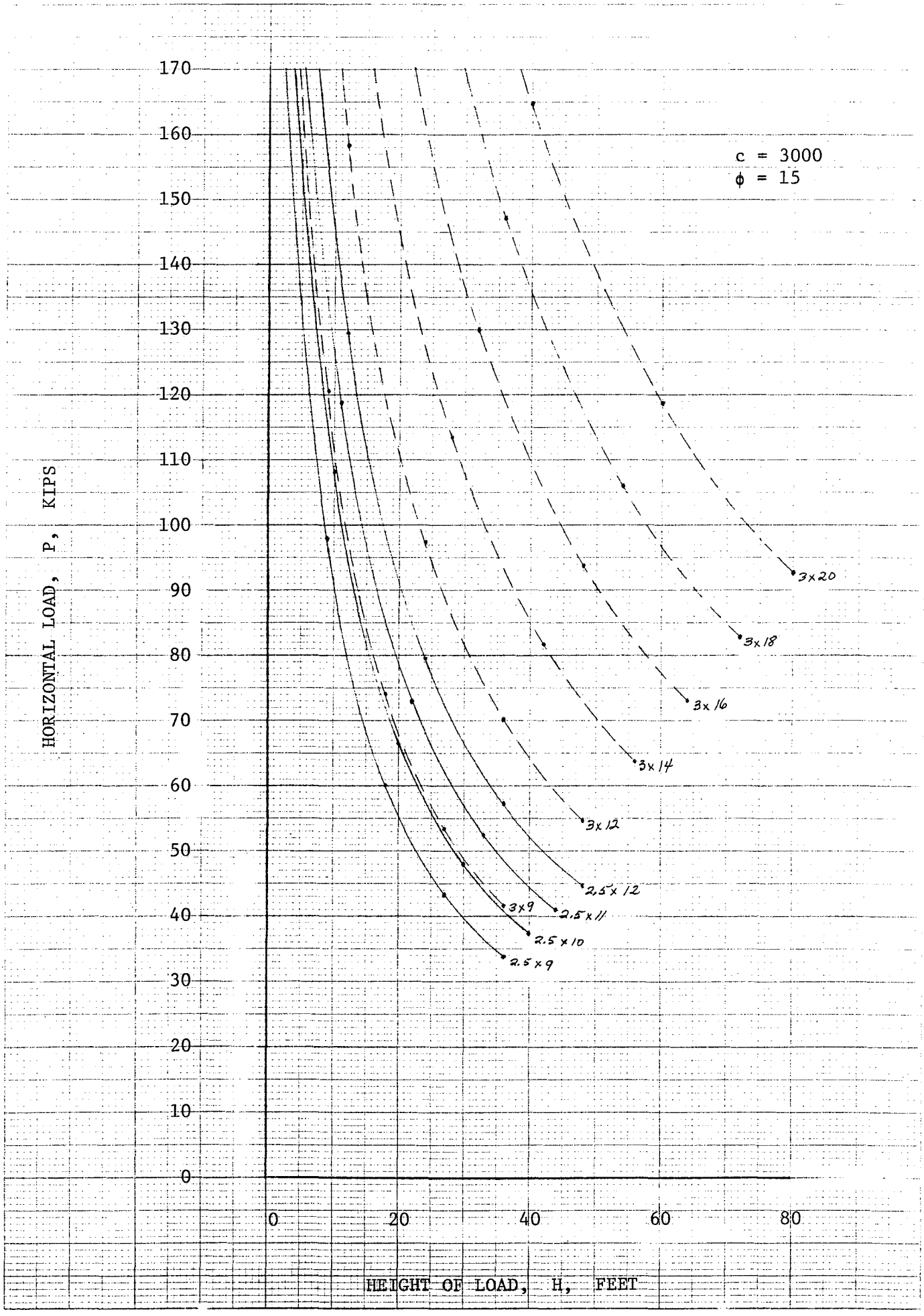
c = 3000
ϕ = 15
3x20
3x18
3x16
3x14
3x12
2.5x12
3x9
2.5x11
2.5x10
2.5x9
HORIZONTAL LOAD, P, KIPS
HEIGHT OF LOAD, H, FEET
0
10
20
30
40
50
60
70
80
90
100
110
120
130
140
150
160
170
0
20
40
60
80

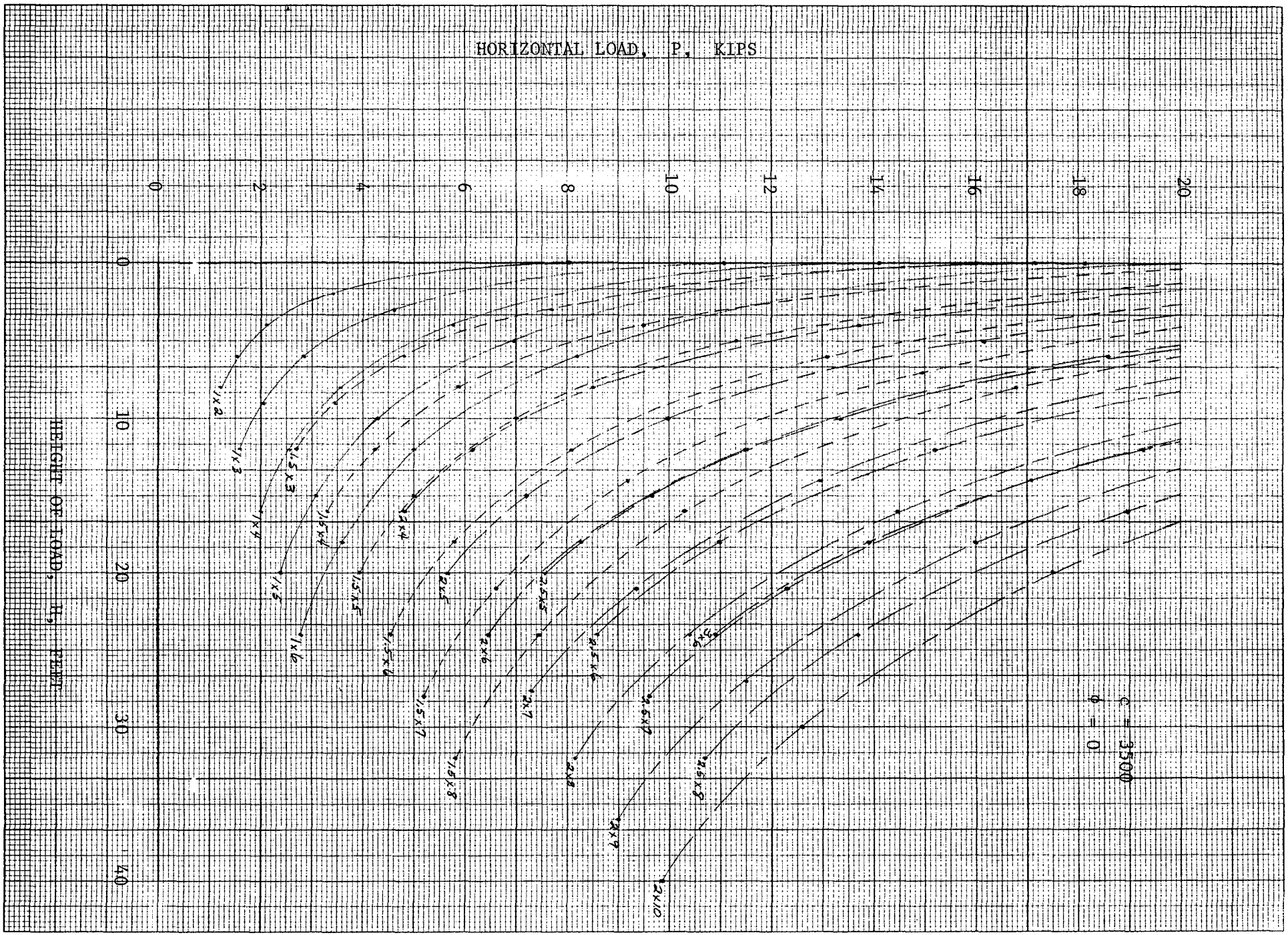
HORIZONTAL LOAD, P, KIPS
HEIGHT OF LOAD, H_p, FEET
$\epsilon = .3500$
$\phi = 0$
1"x2"
1"x3"
1.5"x3"
1"x4"
1.5"x4"
2"x4"
1"x5"
2"x5"
1.5"x5"
1"x6"
2"x6"
1.5"x6"
2"x7"
1.5"x7"
2"x8"
1.5"x8"
2"x9"
2"x10"

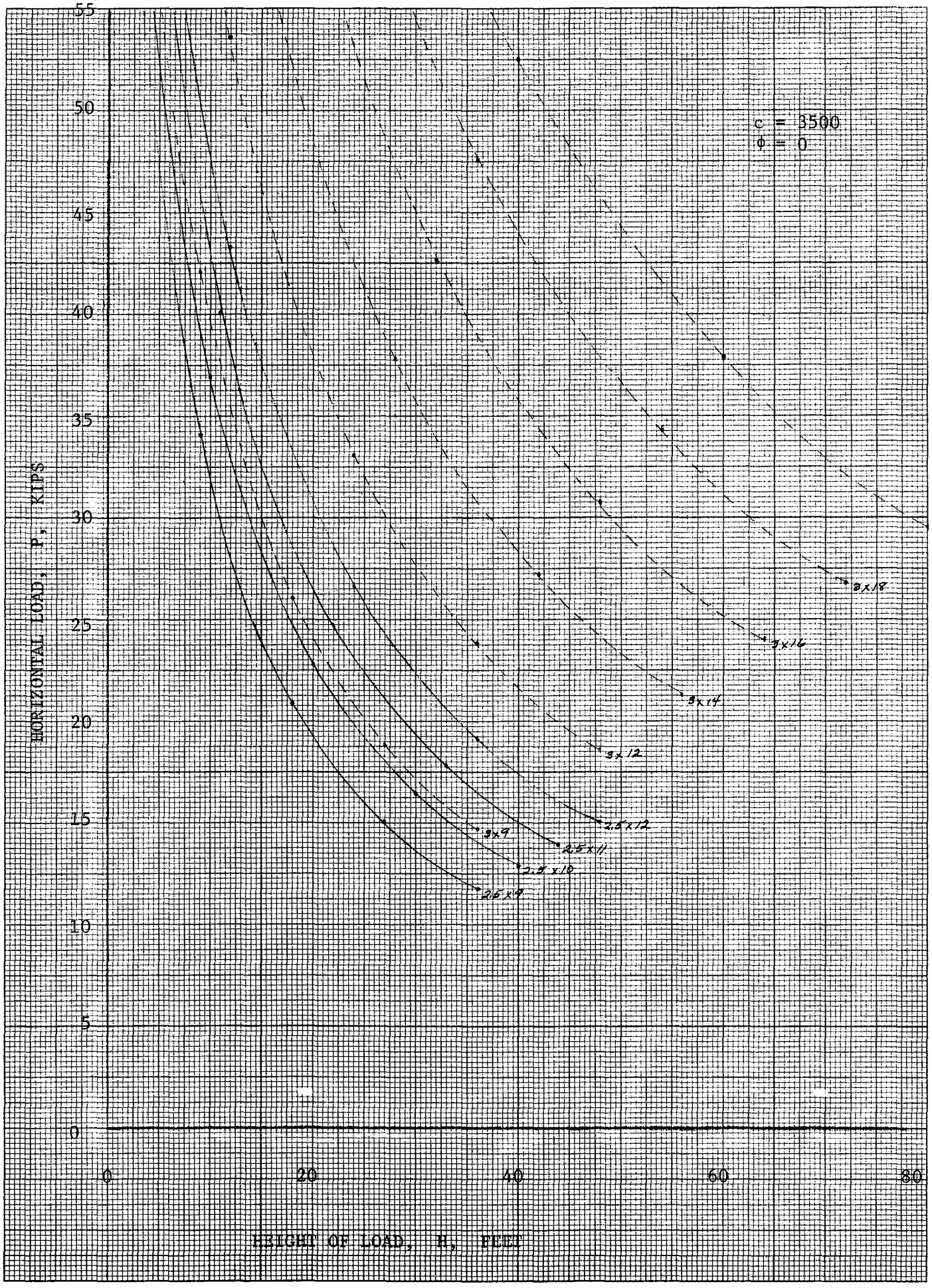

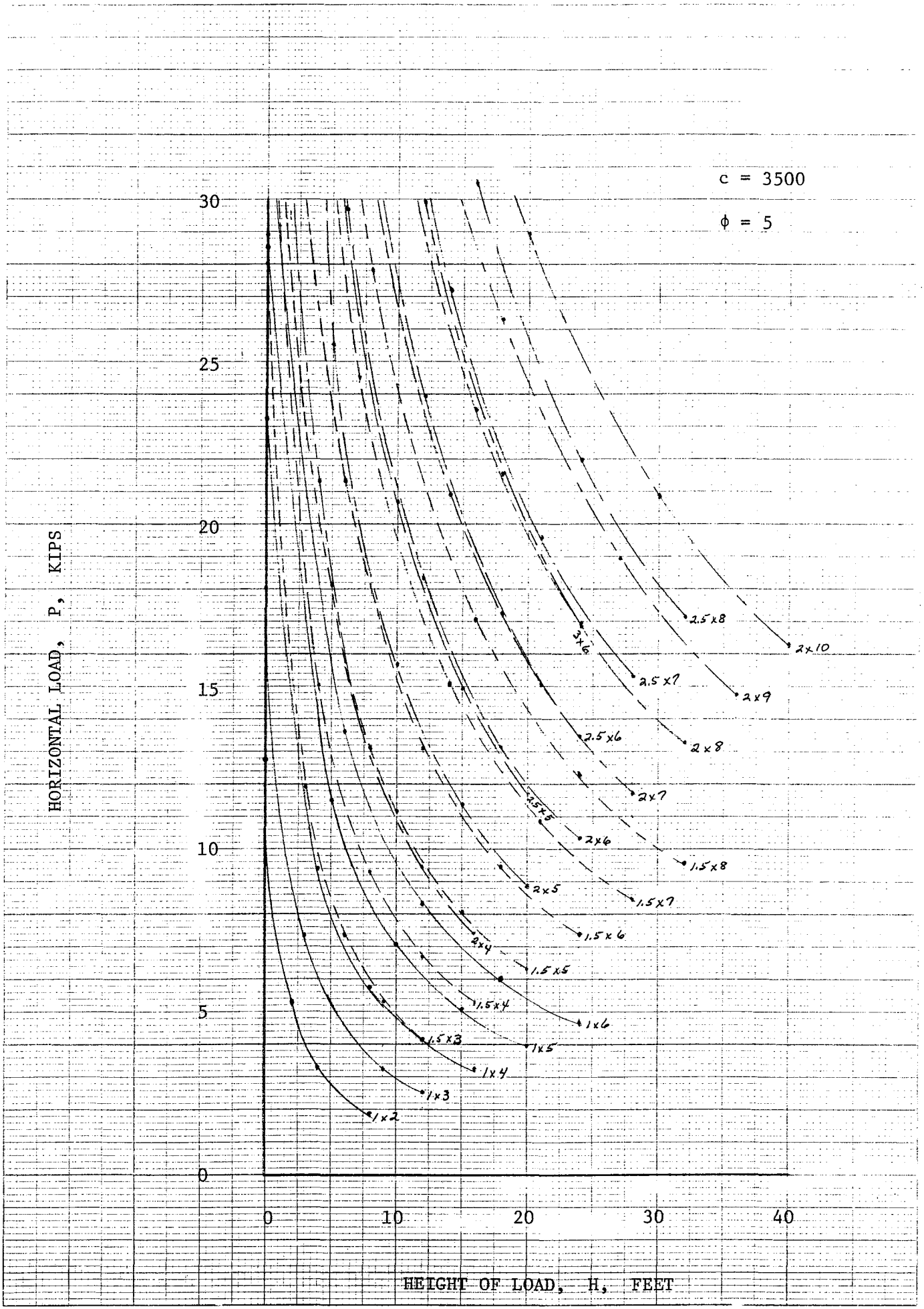
c = 3500
ϕ = 5
HORIZONTAL LOAD, P, KIPS
HEIGHT OF LOAD, H, FEET
0
5
10
15
20
25
30
0
10
20
30
40
2.5x8
2x10
2x6
2.5x7
2x9
2.5x6
2x8
2x7
1.5x5
2x6
1.5x8
2x5
1.5x7
1.5x6
2x4
1.5x5
1.5x4
1x6
1.5x3
1x5
1x4
1x3
1x2

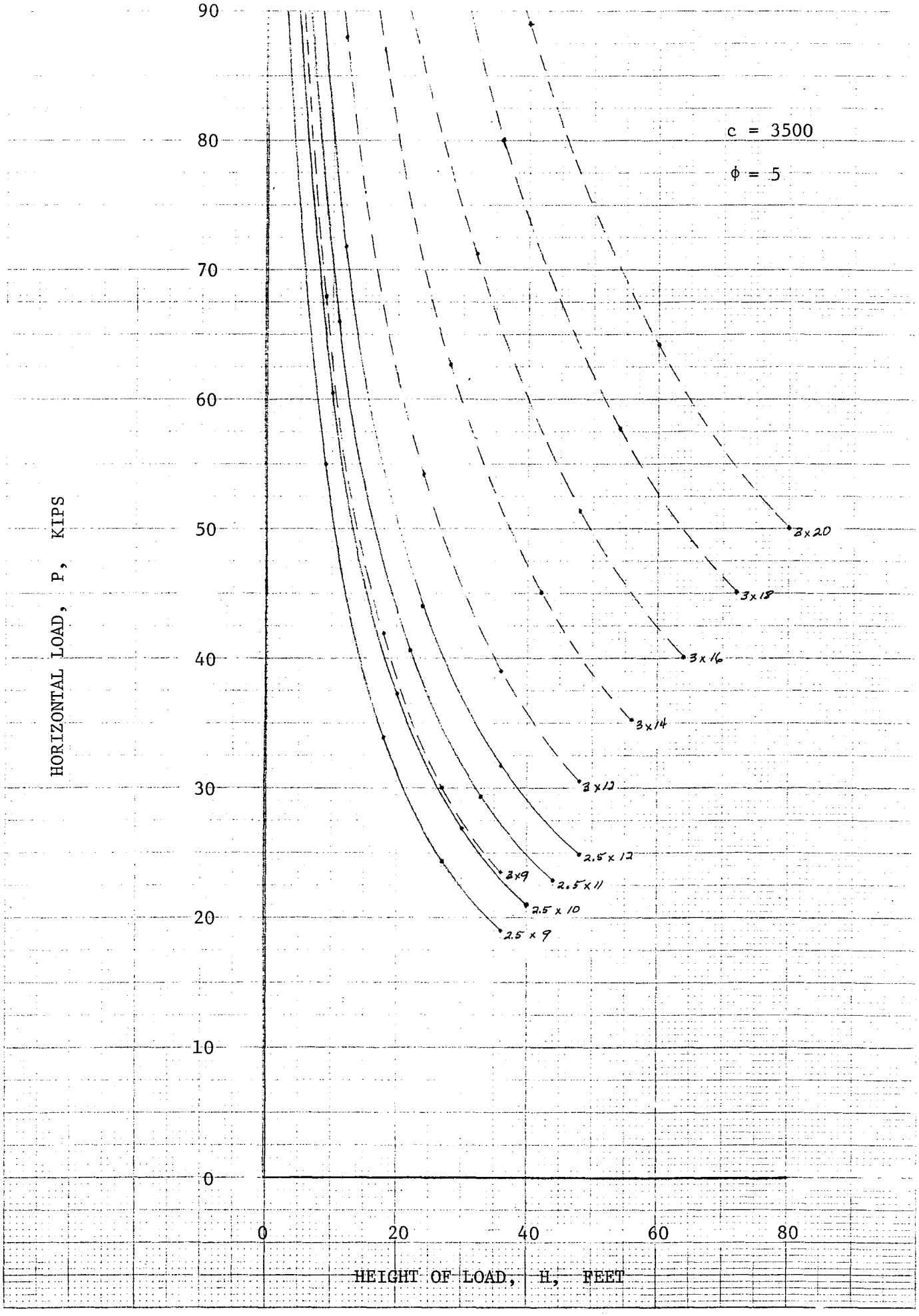
c = 3500
ϕ = 5
3x20
3x18
3x16
3x14
3x12
2.5x12
3x9
2.5x11
2.5x10
2.5x9
HORIZONTAL LOAD, P, KIPS
HEIGHT OF LOAD, H, FEET
0
10
20
30
40
50
60
70
80
90
0
20
40
60
80

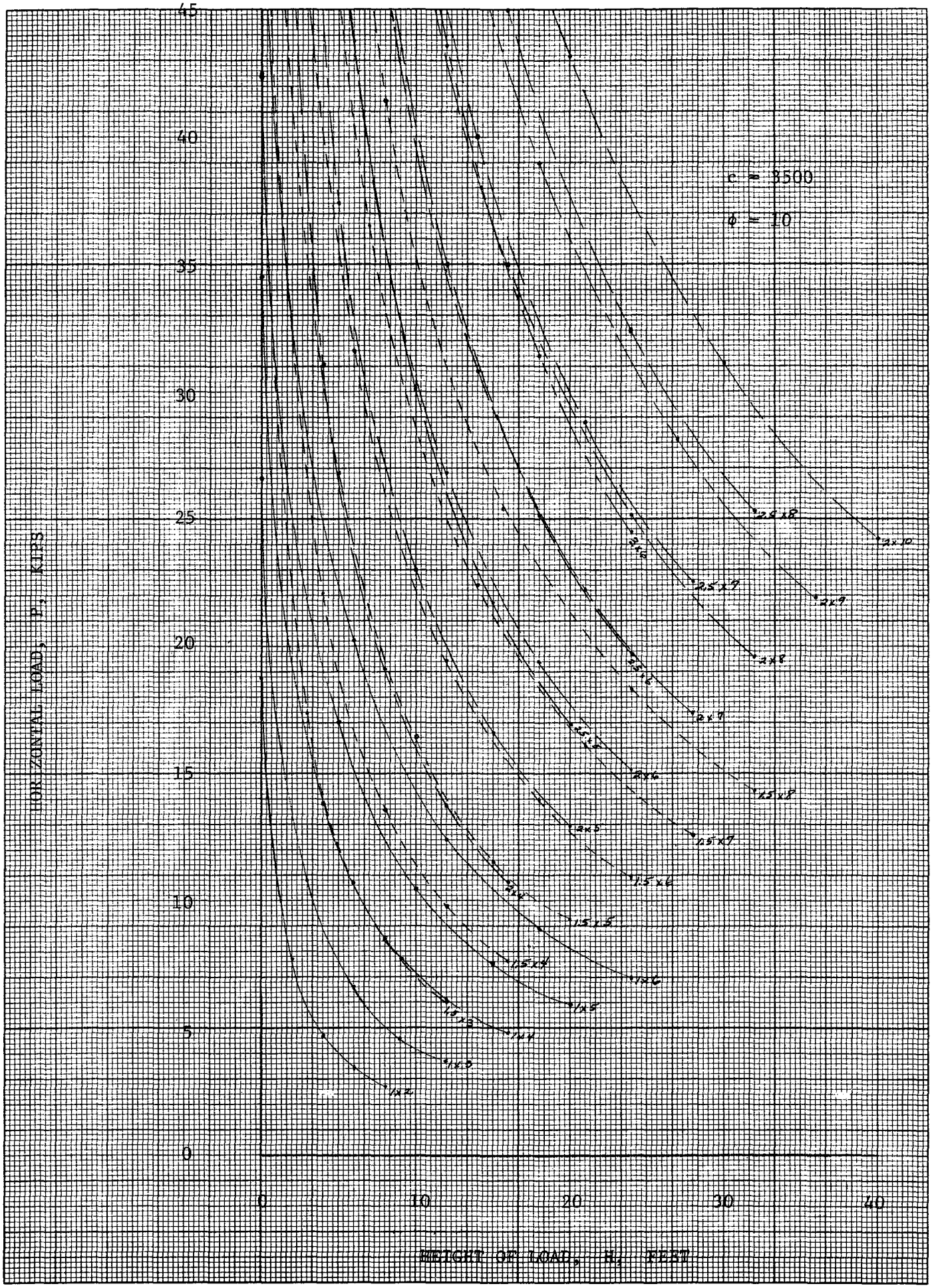

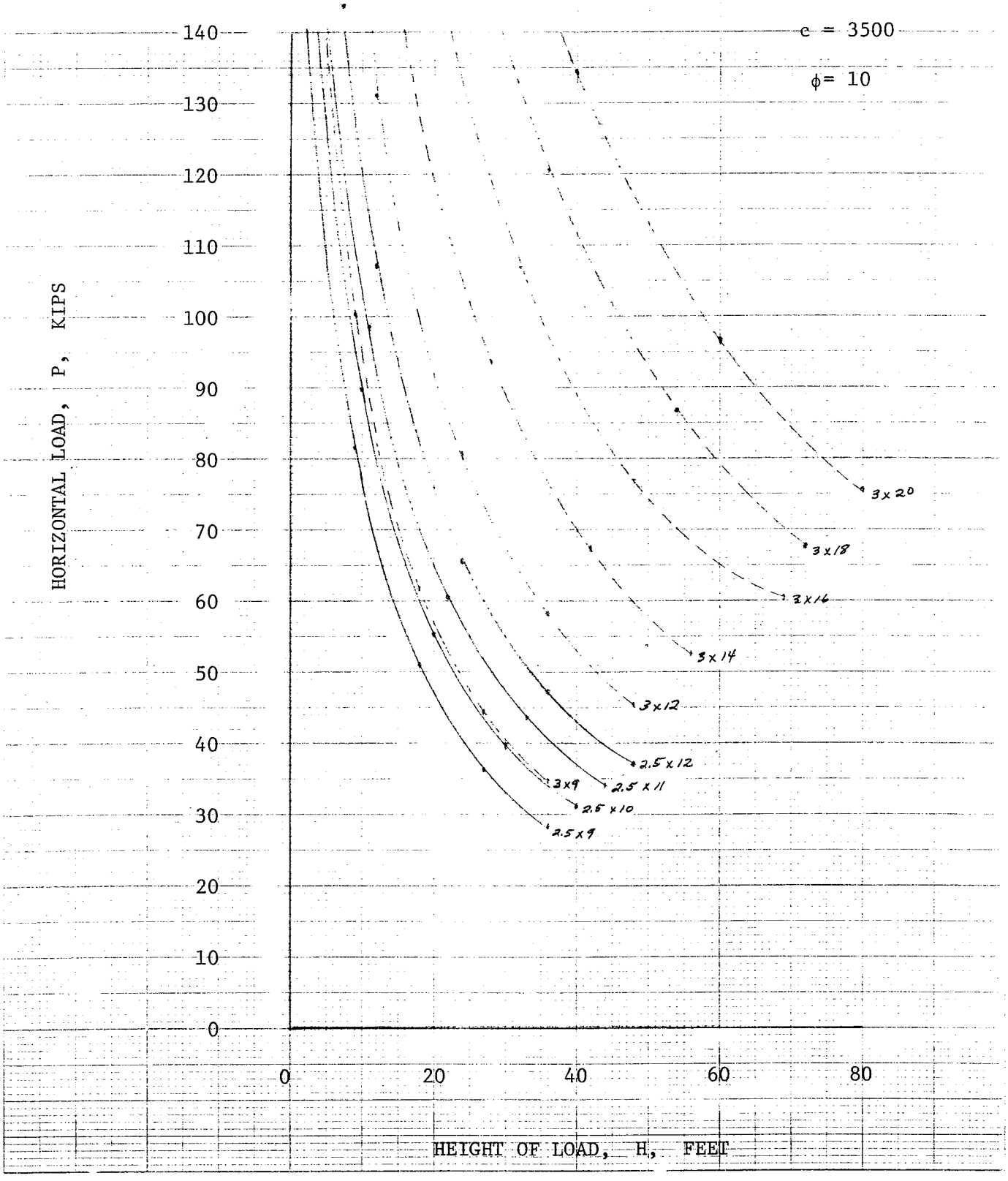
c = 3500
ϕ = 10
HORIZONTAL LOAD, P, KIPS
HEIGHT OF LOAD, H, FEET
140
130
120
110
100
90
80
70
60
50
40
30
20
10
0
0
20
40
60
80
3x20
3x18
3x16
3x14
3x12
2.5x12
3x9
2.5x11
2.5x10
2.5x9

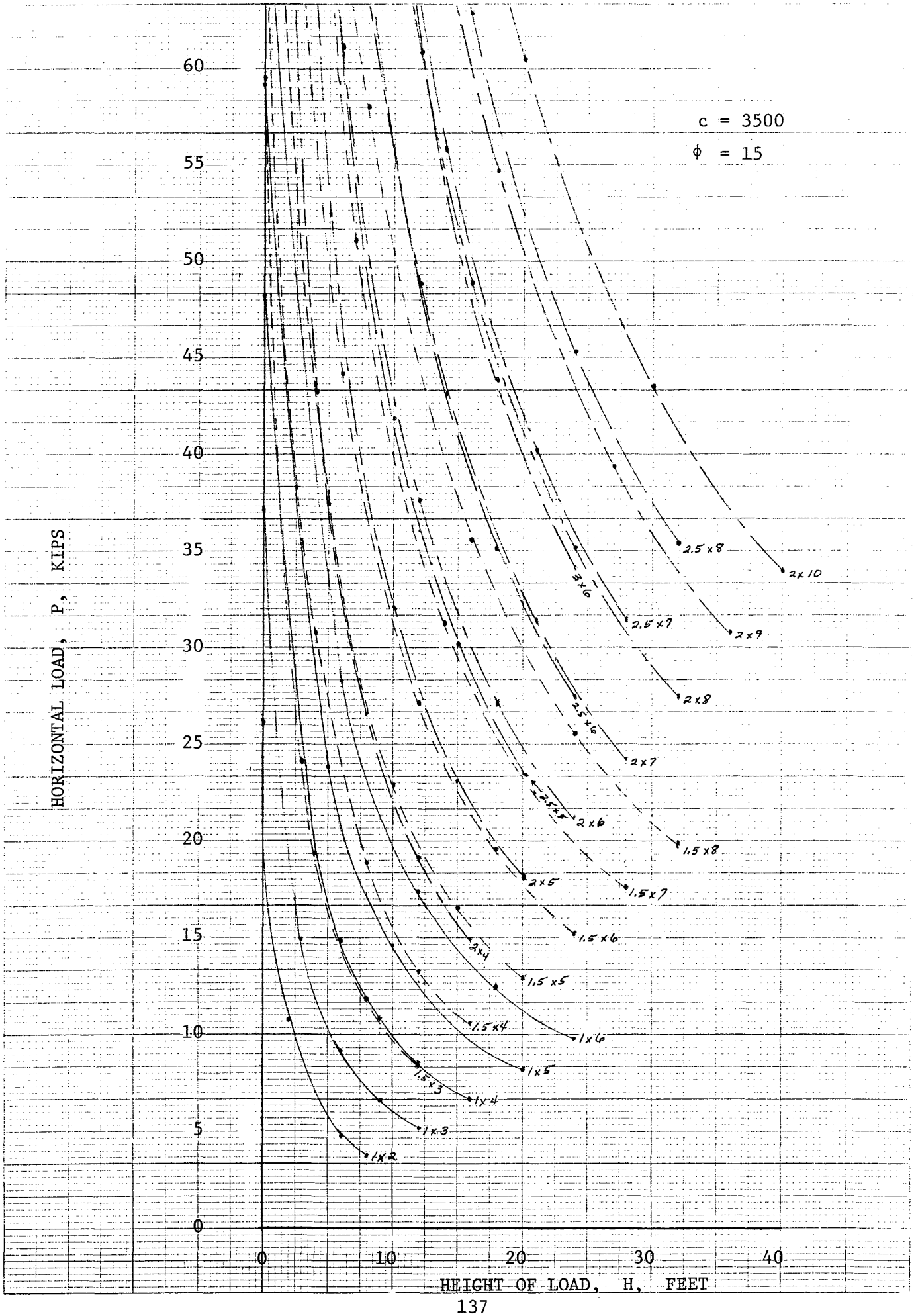
c = 3500
ϕ = 15
HORIZONTAL LOAD, P, KIPS
HEIGHT OF LOAD, H, FEET
0
5
10
15
20
25
30
35
40
45
50
55
60
0
10
20
30
40
2.5x8
2x10
3x6
2.5x7
2x9
2x8
2.5x6
2x7
2.5x5
2x6
1.5x8
2x5
1.5x7
1.5x6
3x4
1.5x5
1.5x4
1x6
1x5
1.5x3
1x4
1x3
1x2

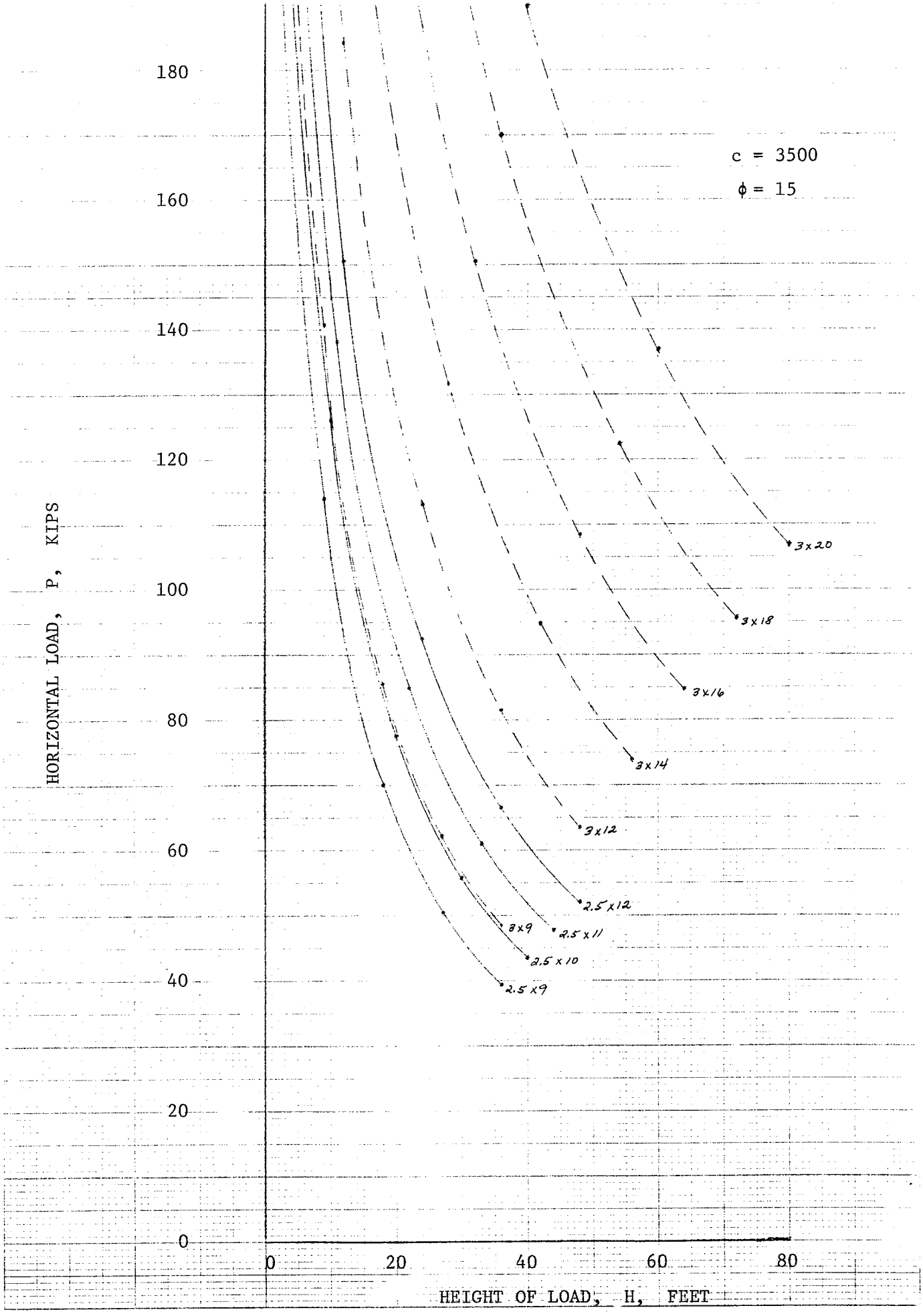
c = 3500
ϕ = 15
3x20
3x18
3x16
3x14
3x12
2.5x12
2.5x11
3x9
2.5x10
2.5x9
HORIZONTAL LOAD, P, KIPS
HEIGHT OF LOAD, H, FEET
0
20
40
60
80
100
120
140
160
180

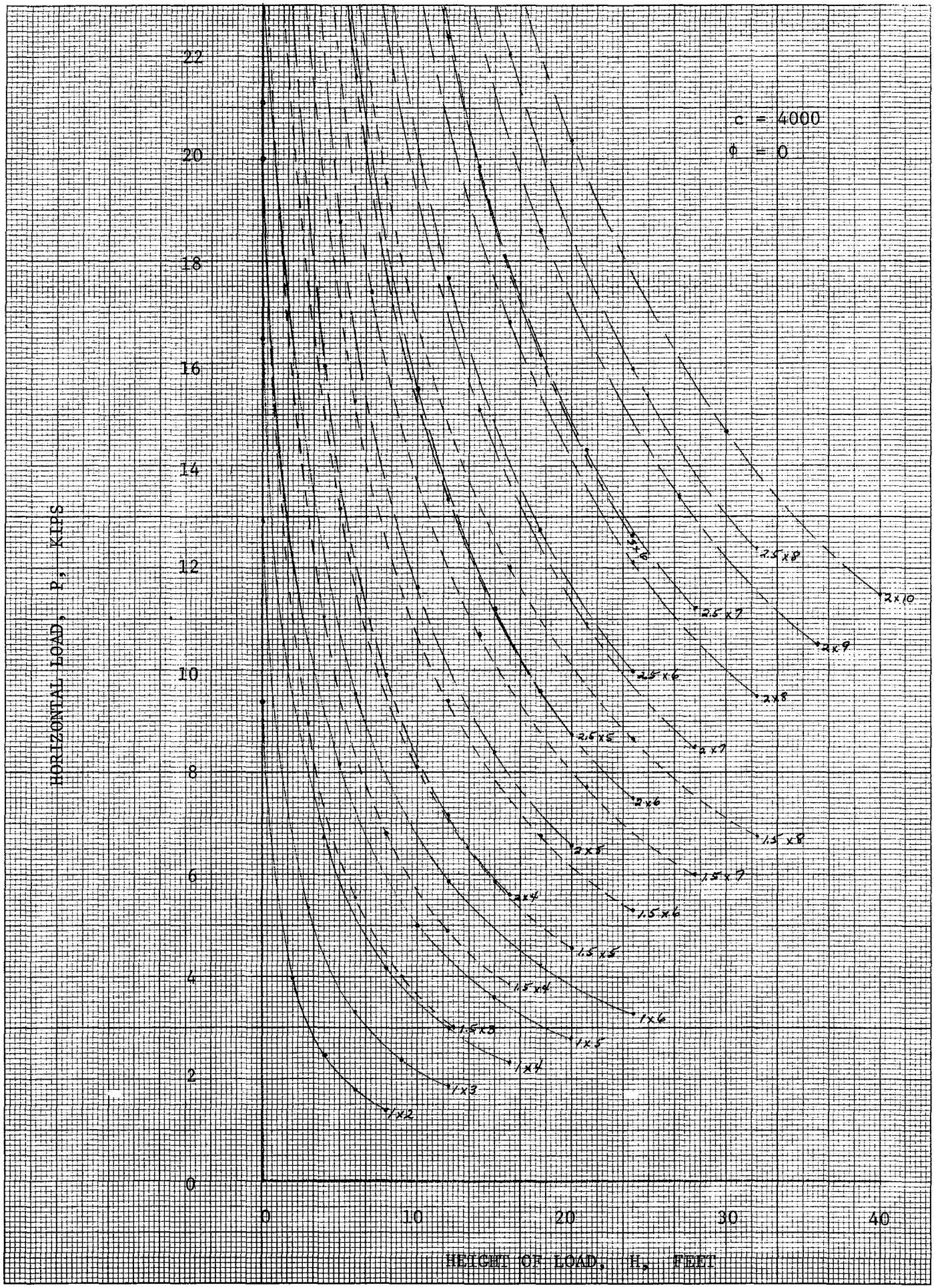

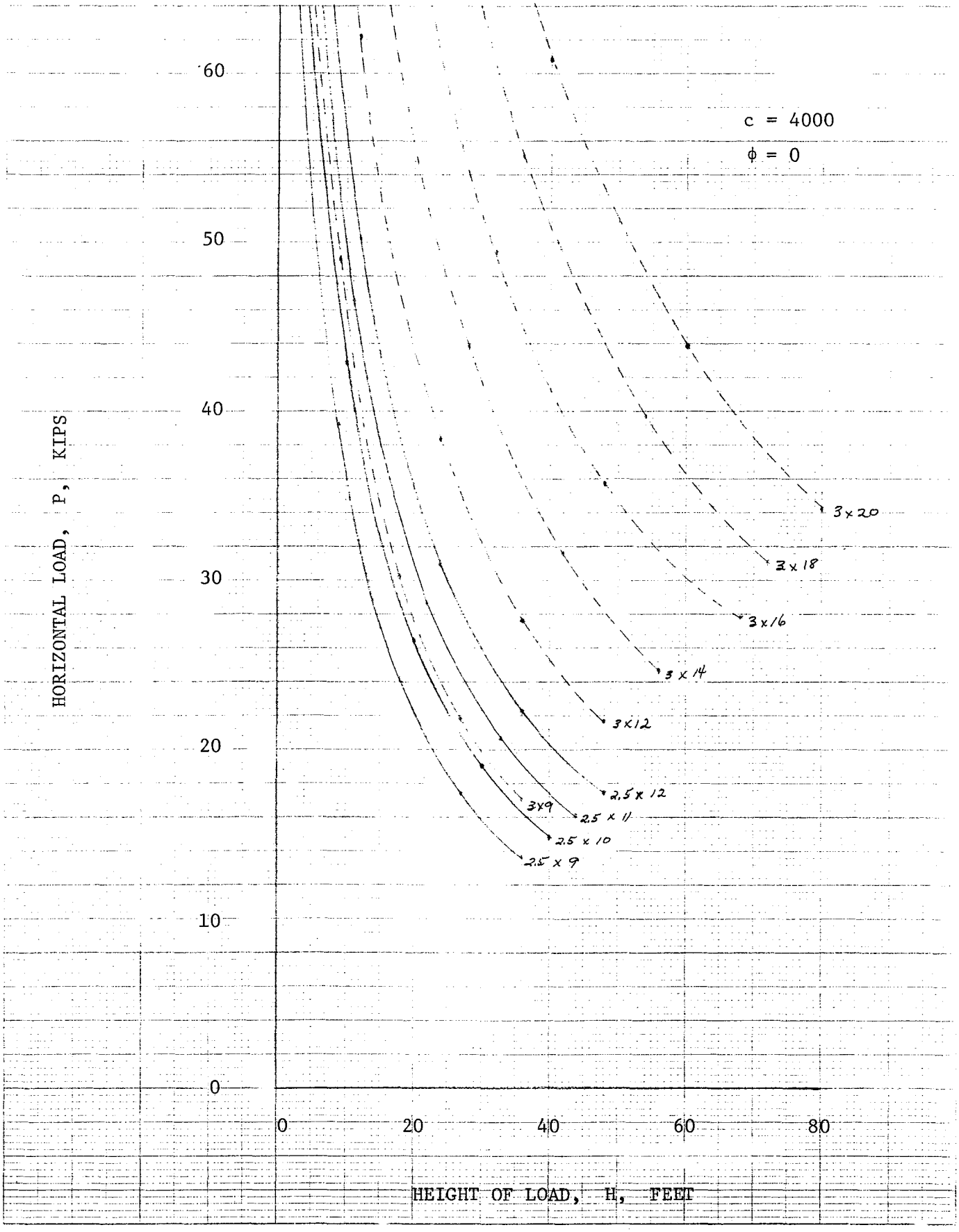
c = 4000
ϕ = 0
3 x 20
3 x 18
3 x 16
3 x 14
3 x 12
2.5 x 12
3 x 9
2.5 x 11
2.5 x 10
2.5 x 9
60
50
40
30
20
10
0
0
20
40
60
80
HORIZONTAL LOAD, P, KIPS
HEIGHT OF LOAD, H, FEET

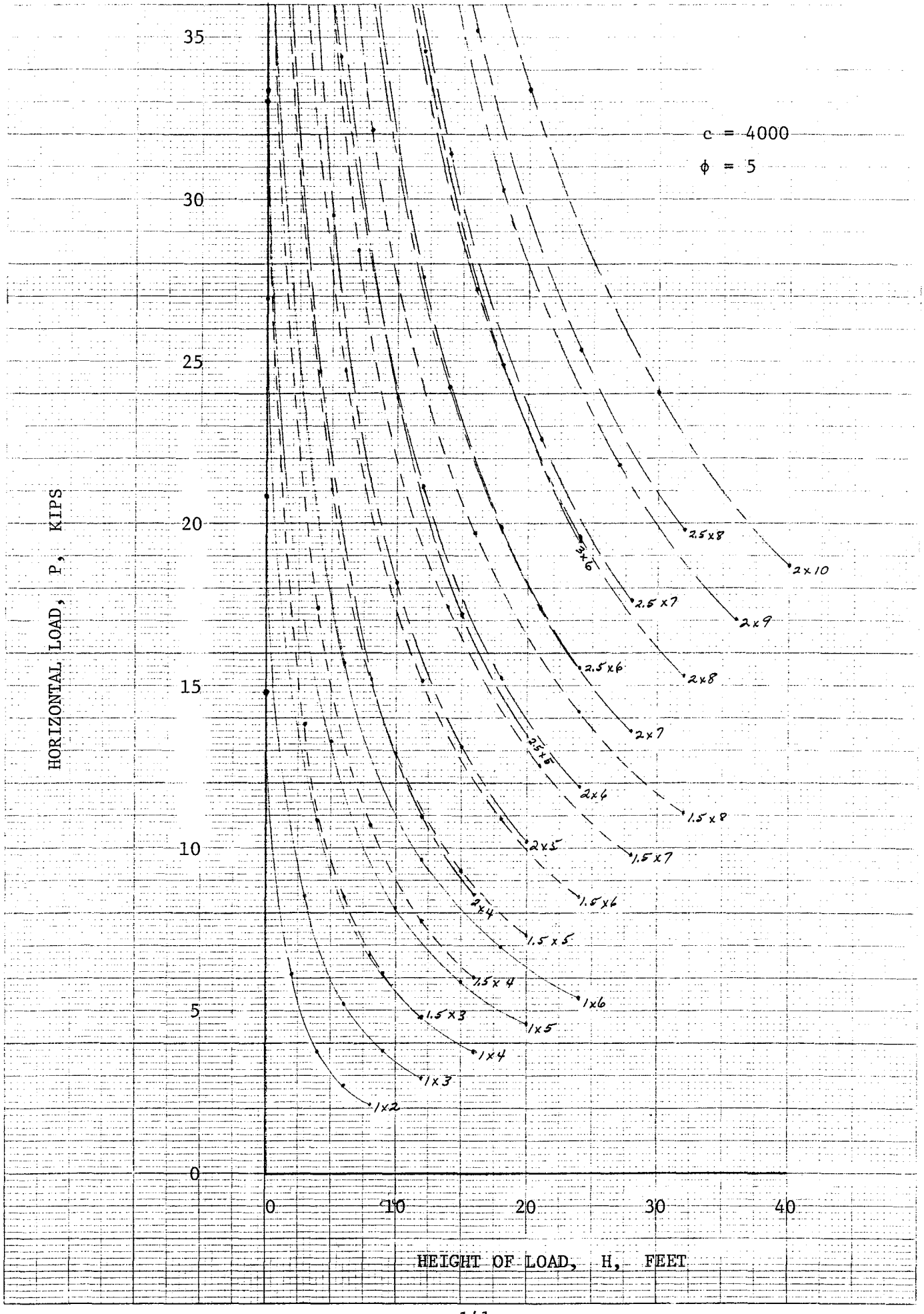
c = 4000
ϕ = 5
35
30
25
20
15
10
5
0
0
10
20
30
40
HORIZONTAL LOAD, P, KIPS
HEIGHT OF LOAD, H, FEET
2.5x8
2x10
3x6
2.5x7
2x9
2.5x6
2x8
2x7
2.5x5
2x6
1.5x8
2x5
1.5x7
1.5x6
2x4
1.5x5
1.5x4
1x6
1.5x3
1x5
1x4
1x3
1x2

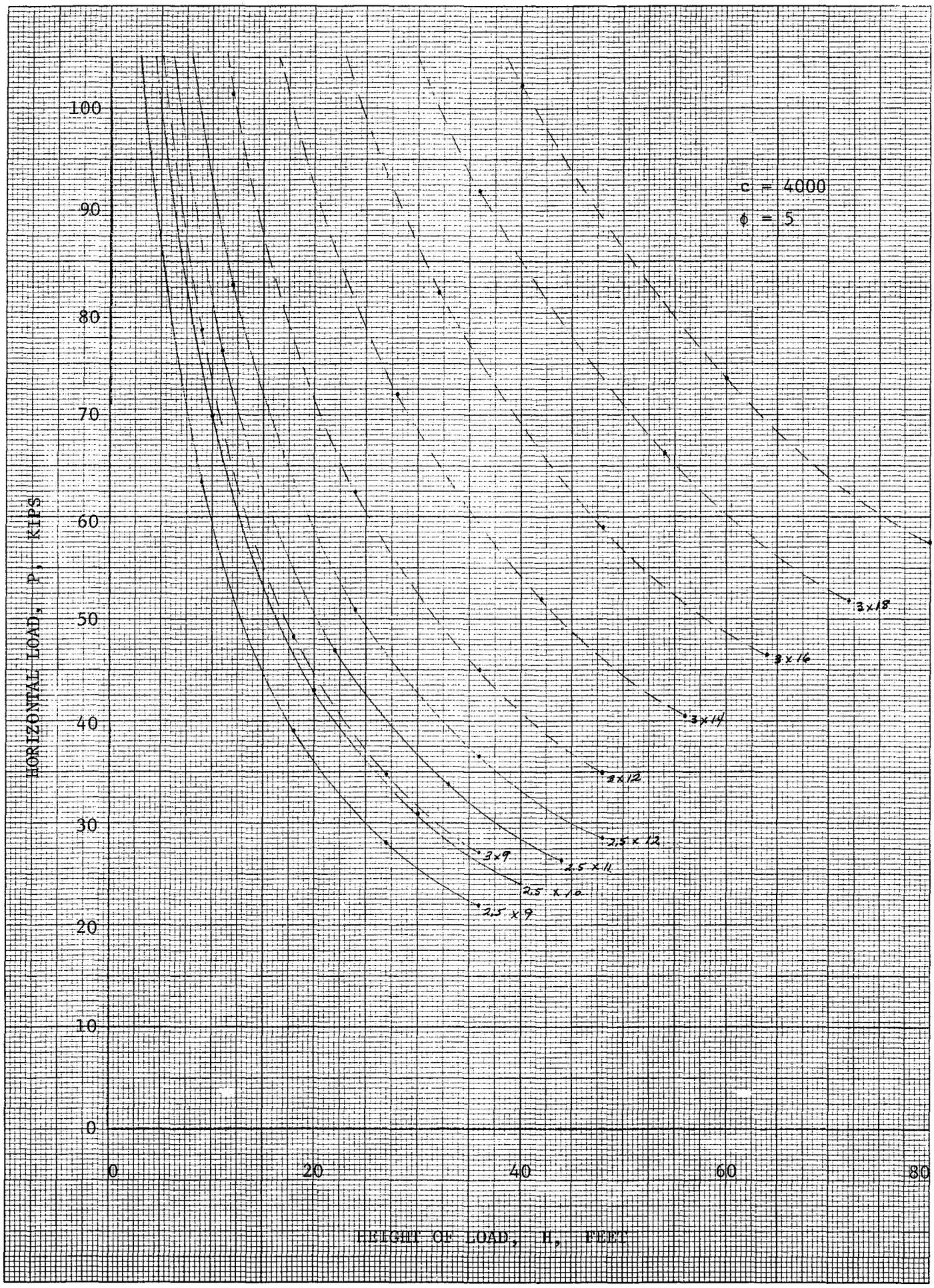

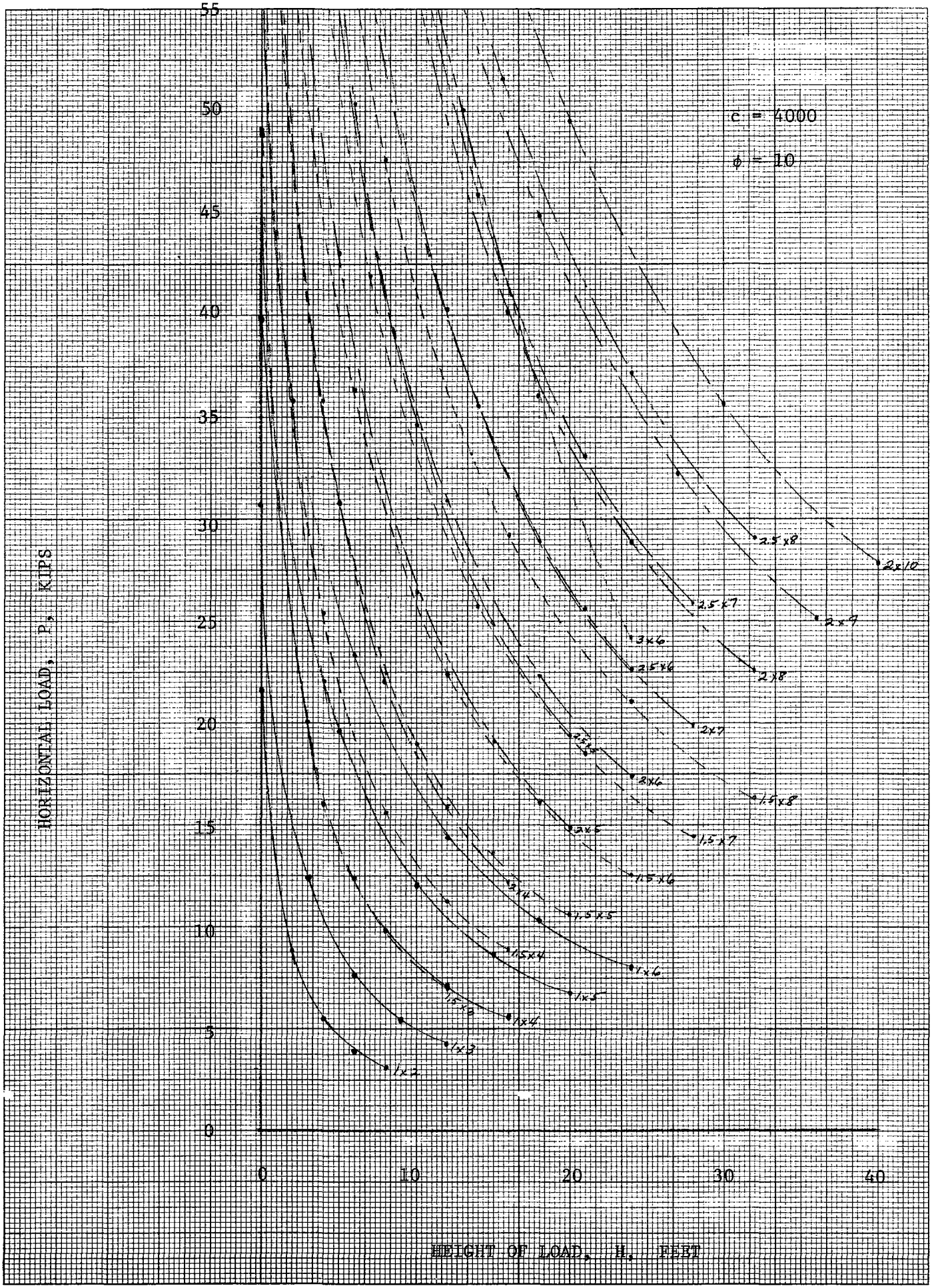

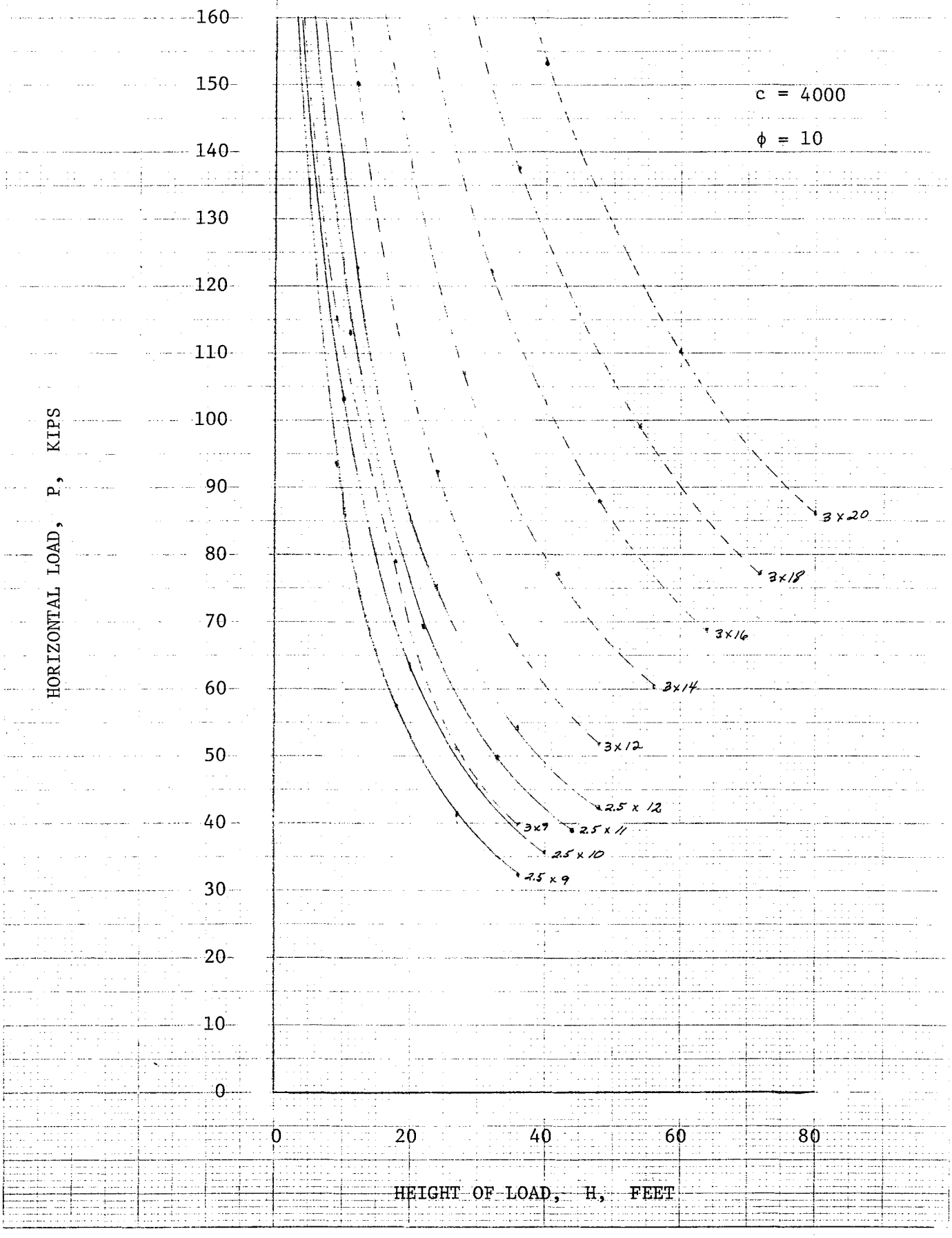
c = 4000
ϕ = 10
3 x 20
3x18
3x16
3x14
3x12
2.5 x 12
3x9
2.5 x 11
2.5 x 10
2.5 x 9
HORIZONTAL LOAD, P, KIPS
160
150
140
130
120
110
100
90
80
70
60
50
40
30
20
10
0
0
20
40
60
80
HEIGHT OF LOAD, H, FEET

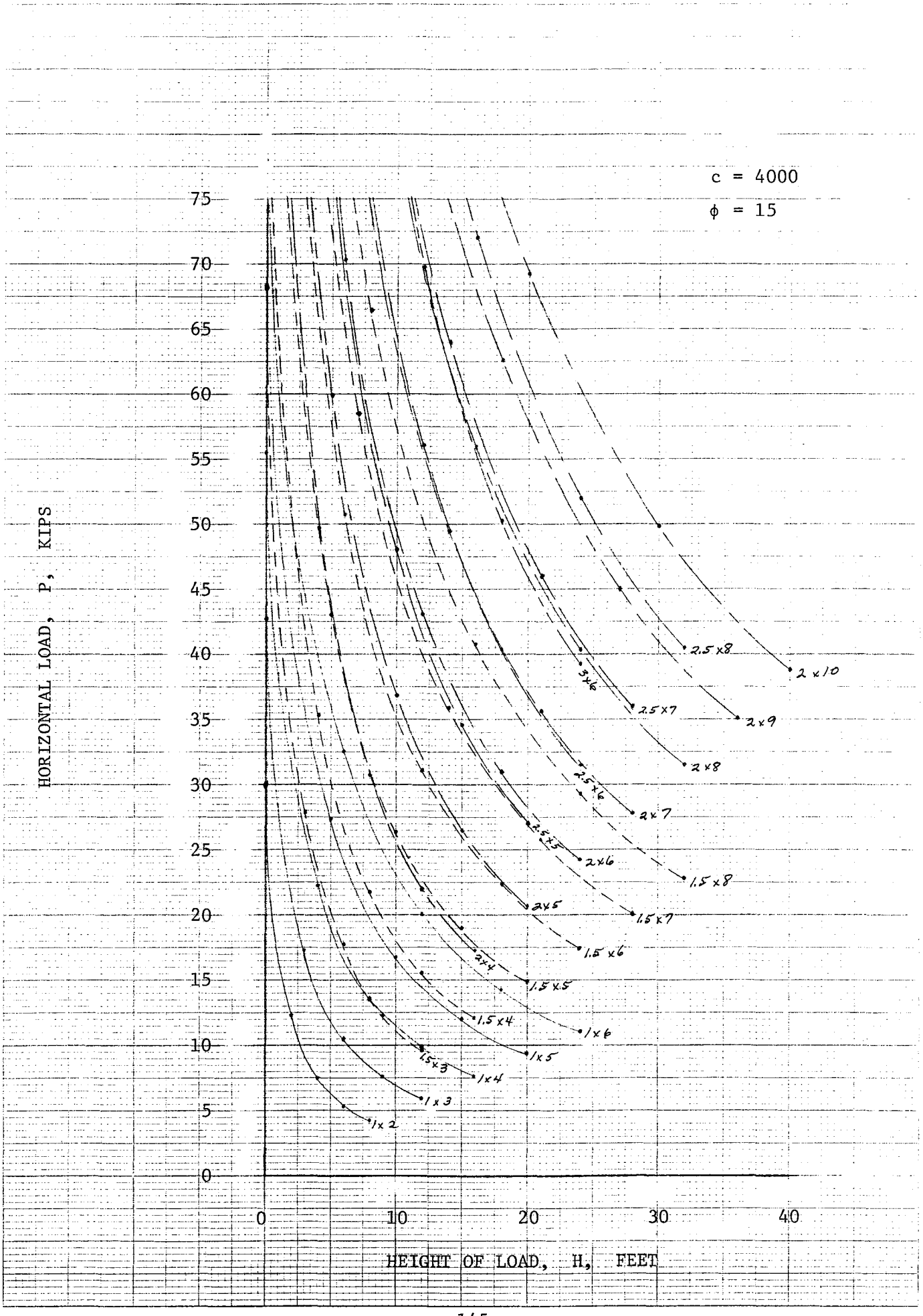
c = 4000
ϕ = 15
HORIZONTAL LOAD, P, KIPS
HEIGHT OF LOAD, H, FEET
0
5
10
15
20
25
30
35
40
45
50
55
60
65
70
75
0
10
20
30
40
2.5x8
2x10
3x6
2.5x7
2x9
2x8
2.5x6
2x7
2.5x5
2x6
1.5x8
2x5
1.5x7
1.5x6
2x4
1.5x5
1.5x4
1x6
1x5
1.5x3
1x4
1x3
1x2

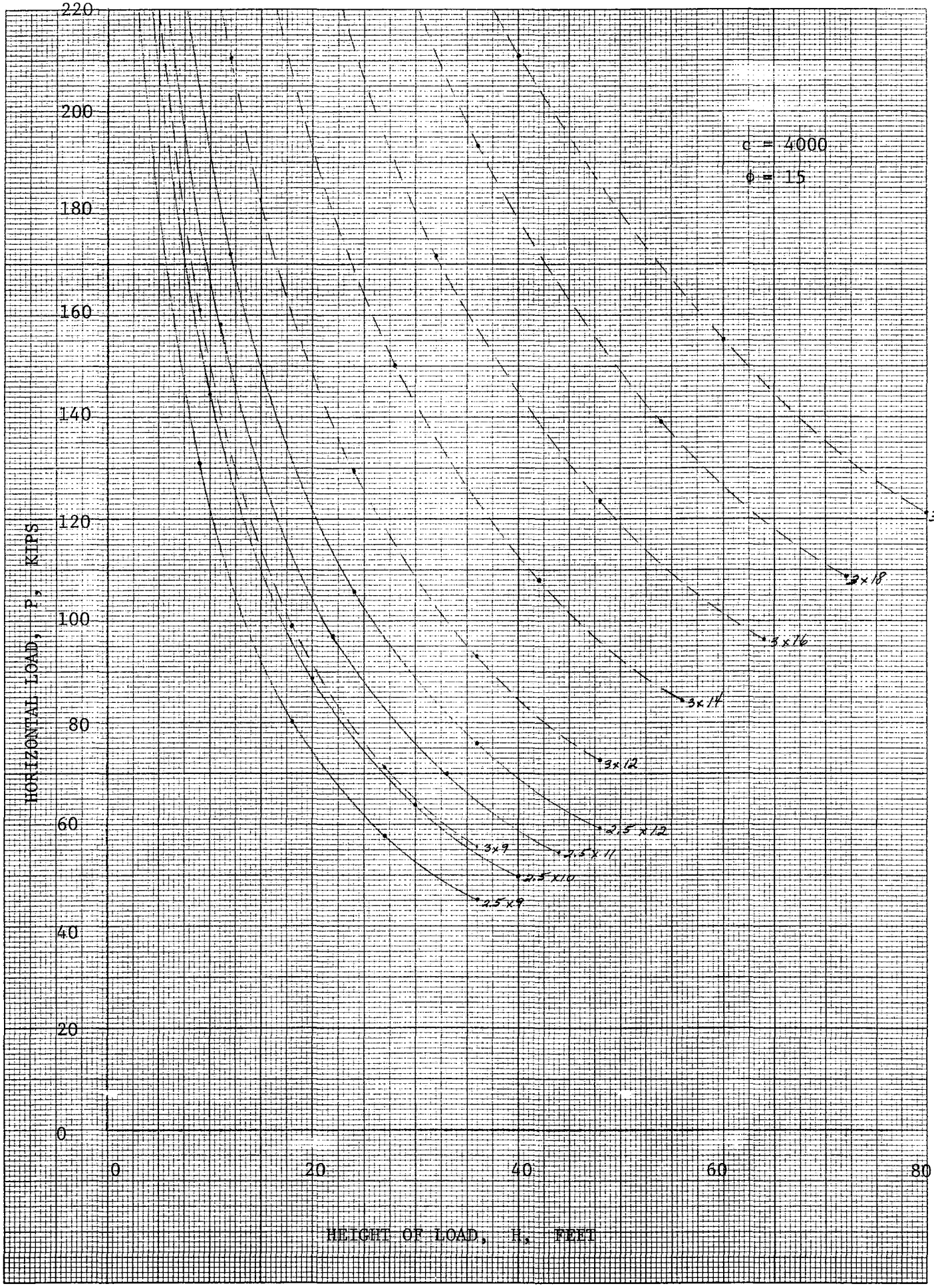

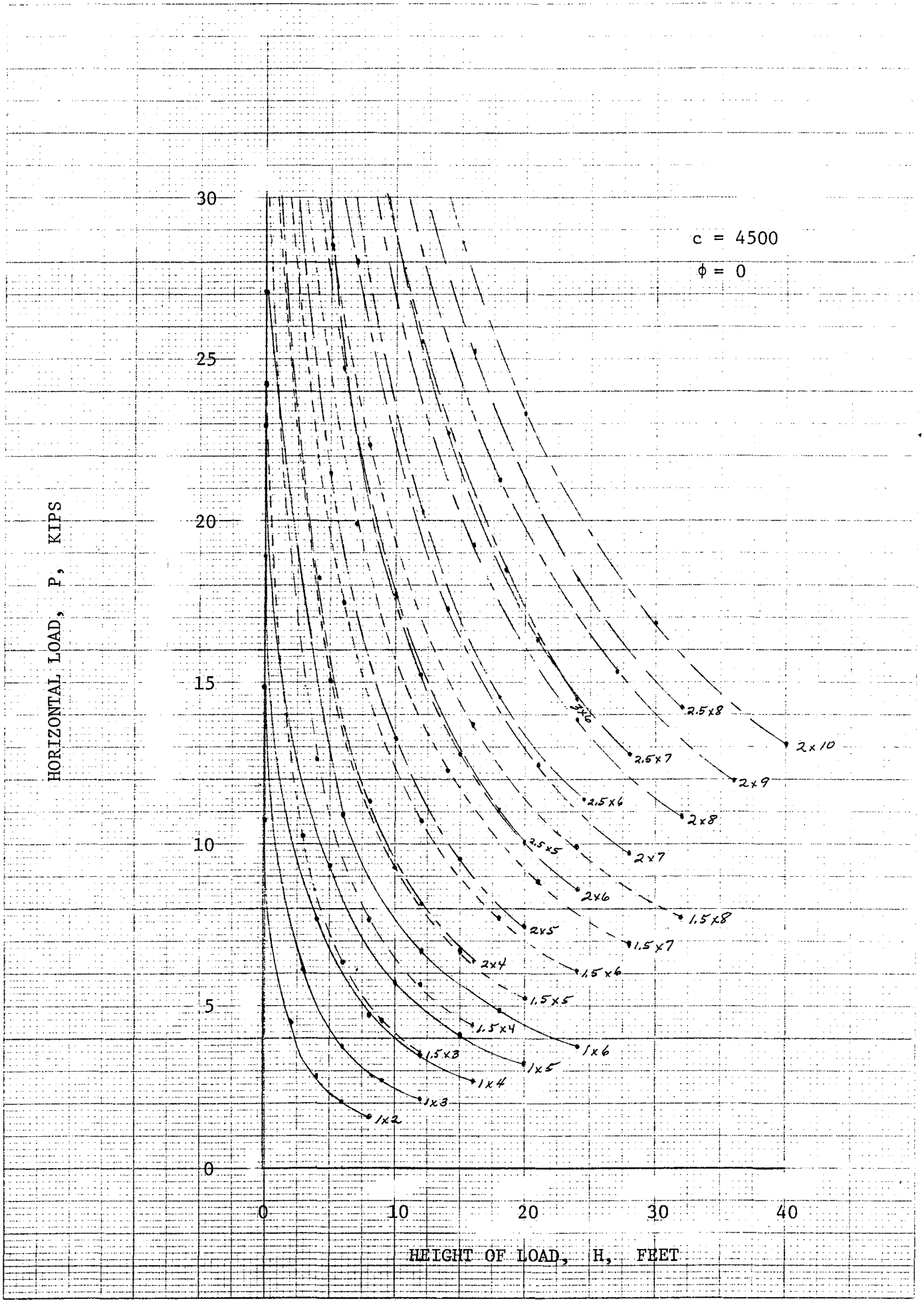
c = 4500
ϕ = 0
HORIZONTAL LOAD, P, KIPS
HEIGHT OF LOAD, H, FEET
0
5
10
15
20
25
30
0
10
20
30
40
2.5x8
2x10
2.5x7
2x9
2.5x6
2x8
2.5x5
2x7
2x6
1.5x8
2x5
1.5x7
2x4
1.5x6
1.5x5
1.5x4
1x6
1.5x3
1x5
1x4
1x3
1x2

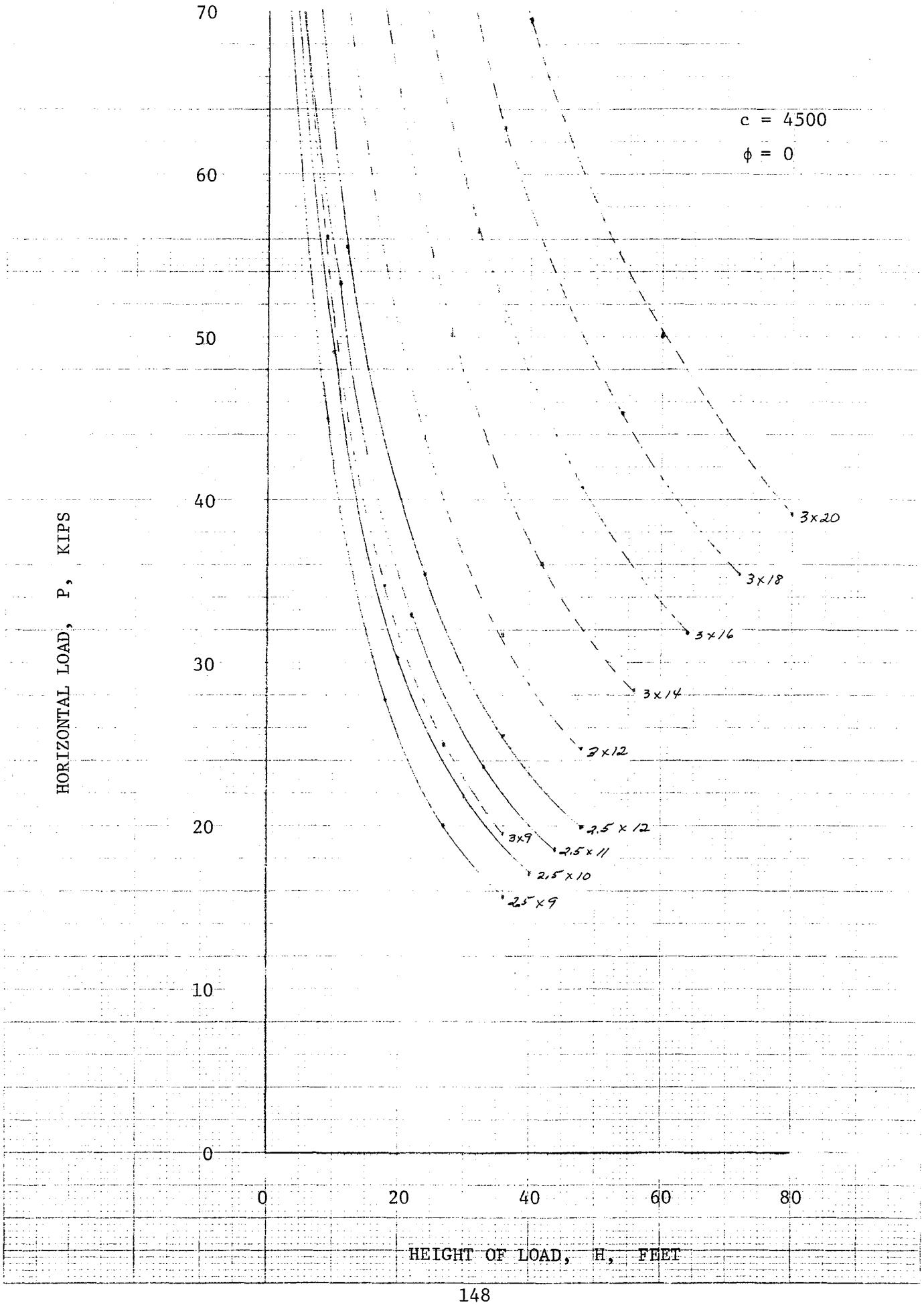
c = 4500
ϕ = 0
3x20
3x18
3x16
3x14
3x12
2.5 x 12
2.5 x 11
2.5 x 10
2.5 x 9
3x9
70
60
50
40
30
20
10
0
0
20
40
60
80
HORIZONTAL LOAD, P, KIPS
HEIGHT OF LOAD, H, FEET

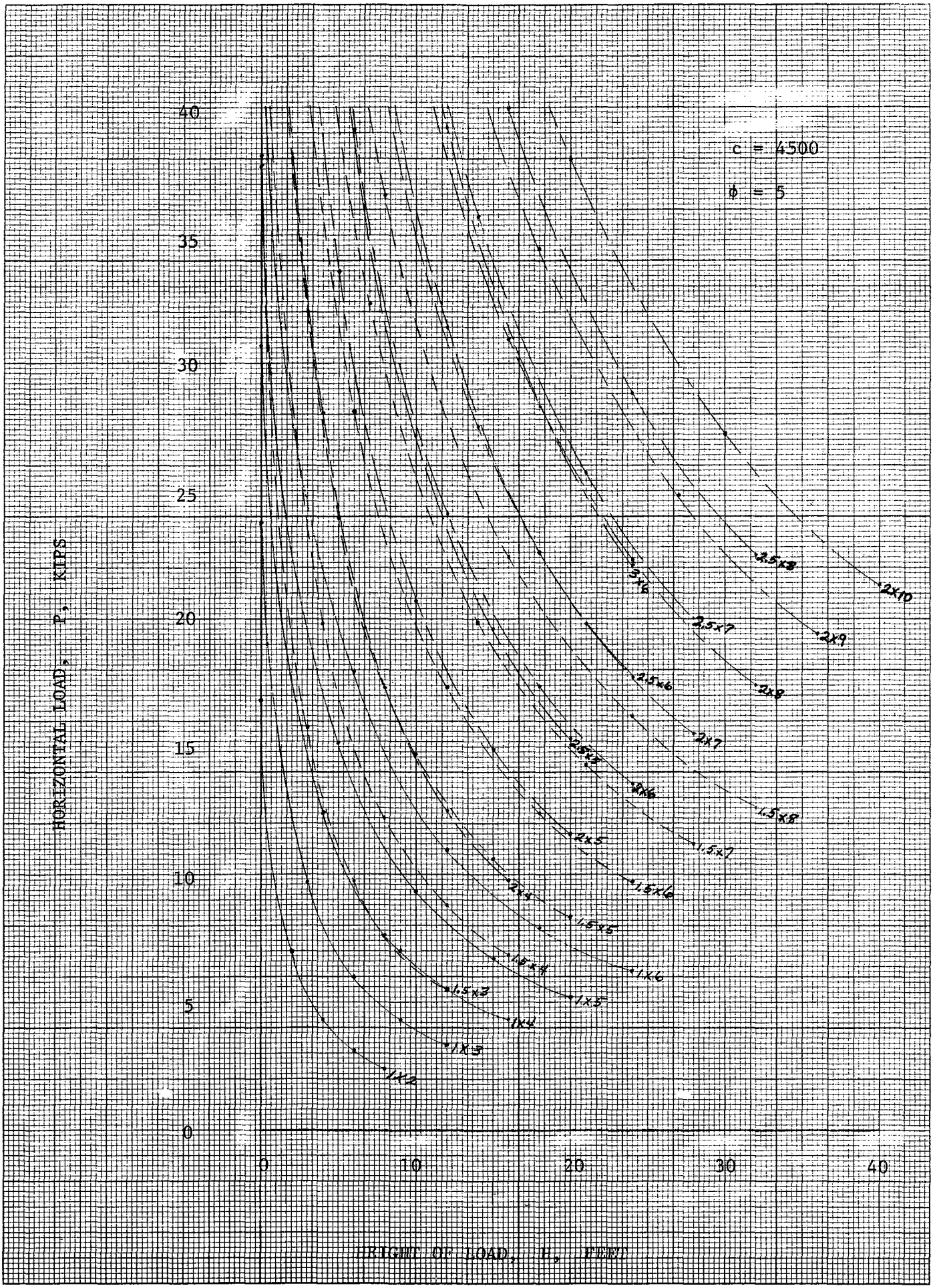

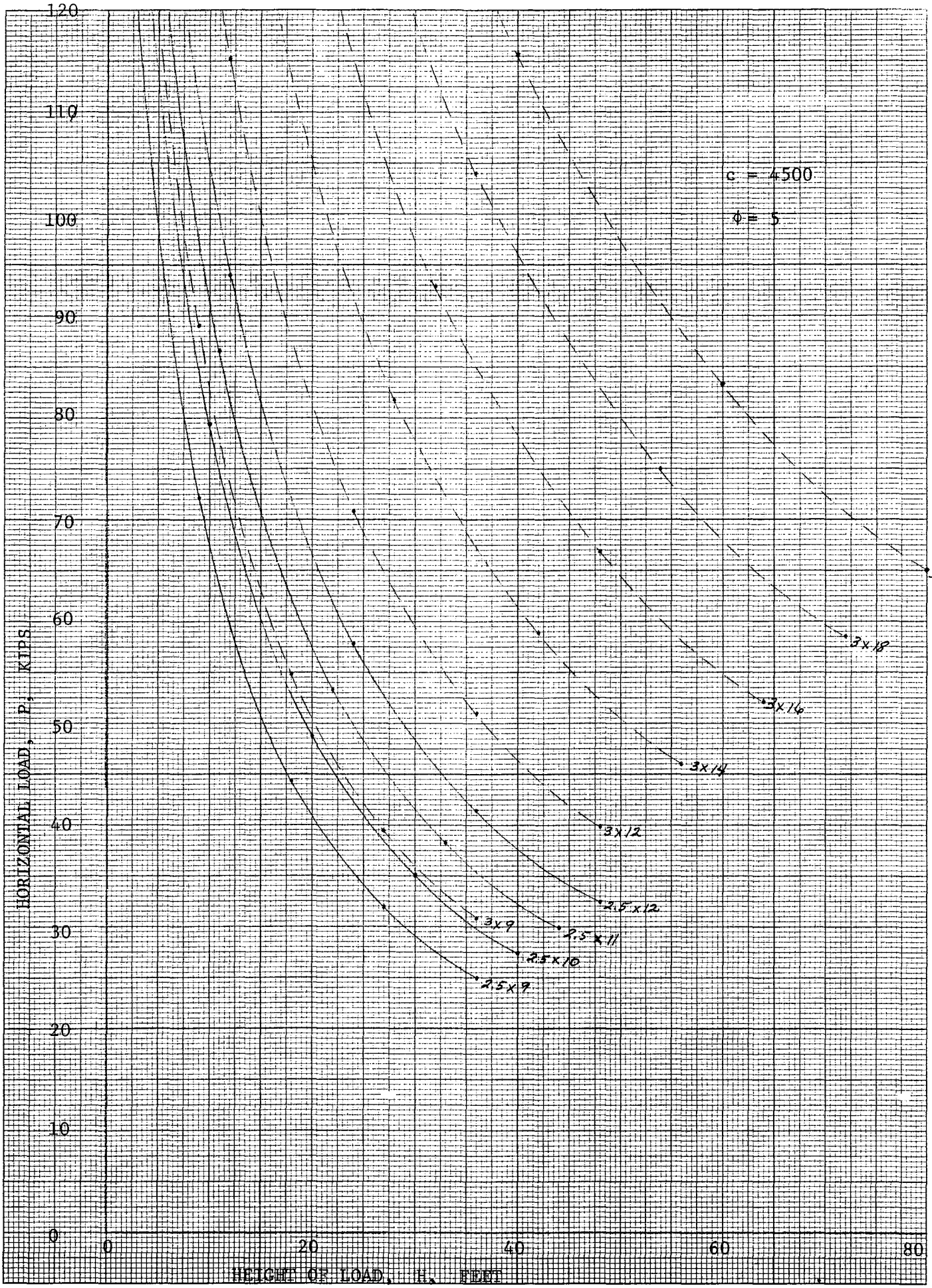

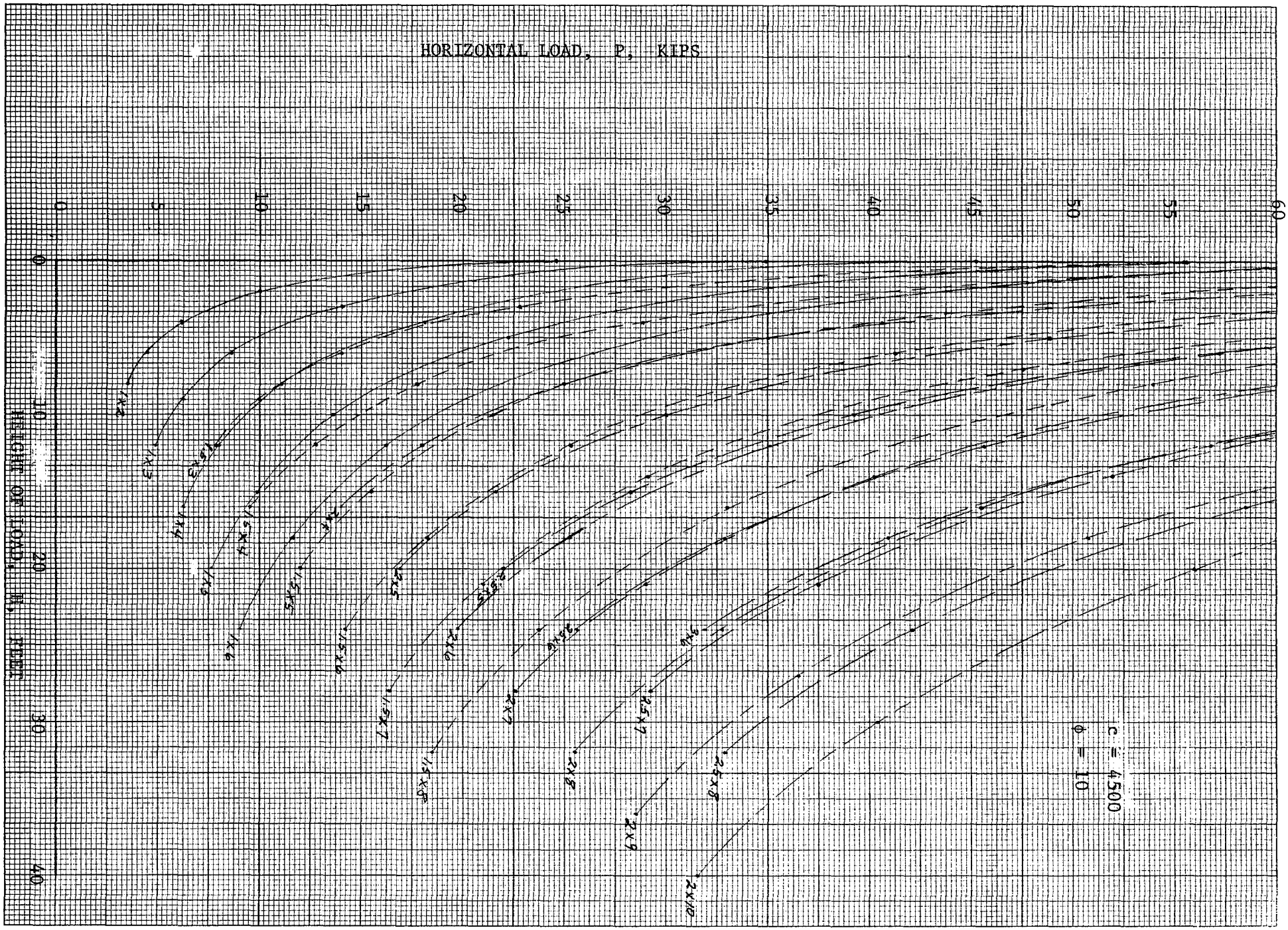
HORIZONTAL LOAD, P, KIPS
0
5
10
15
20
25
30
35
40
45
50
55
60
HEIGHT OF LOAD, H, FEET
0
10
20
30
40
c = 4500
ϕ = 10
2x2
3x3
4x4
5x5
6x6
7x7
8x8
2x4
2.5x5
2.5x6
2.5x7
2.5x8
2x10

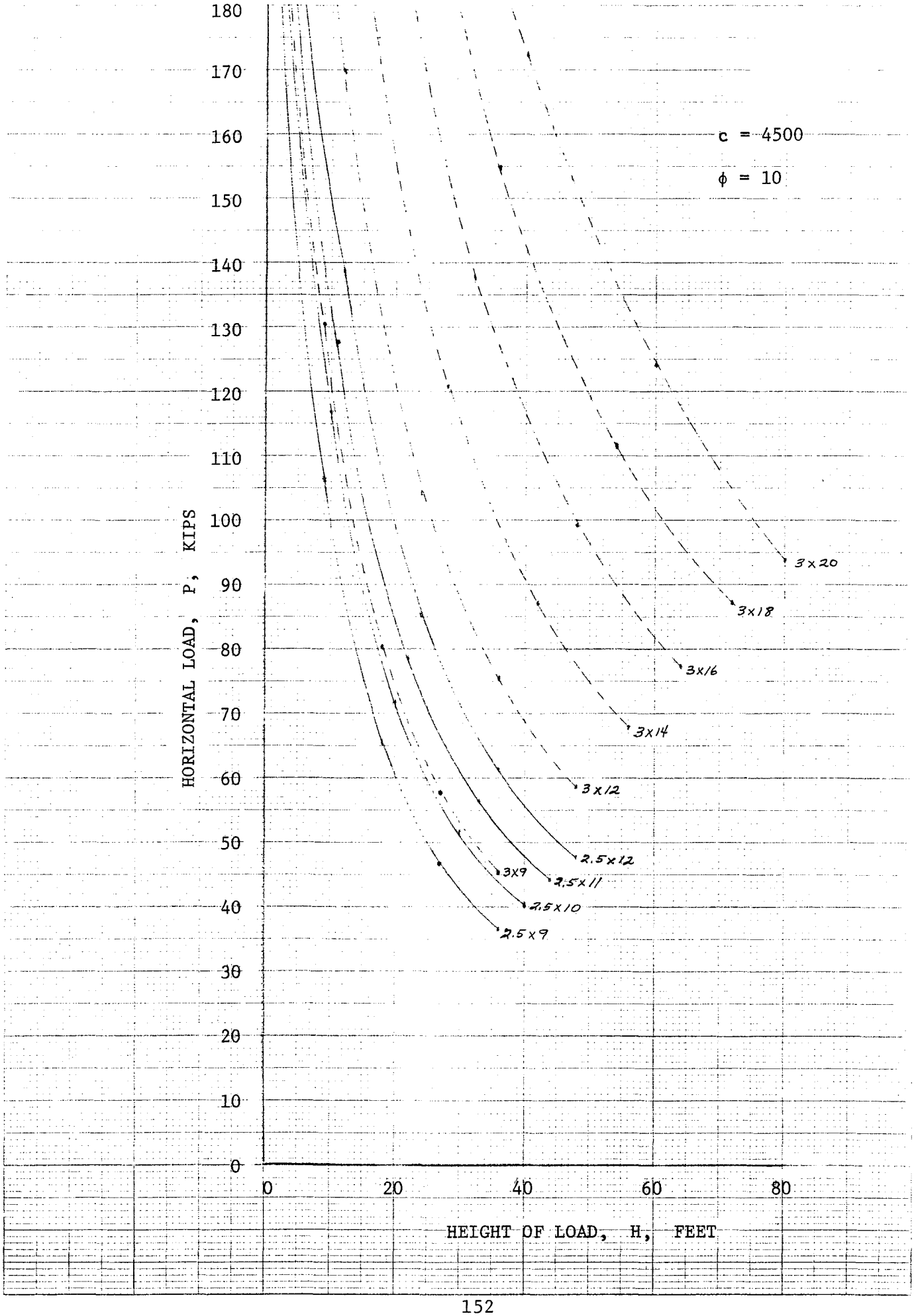
c = 4500
ϕ = 10
3x20
3x18
3x16
3x14
3x12
2.5x12
2.5x11
2.5x10
2.5x9
3x9
HORIZONTAL LOAD, P, KIPS
HEIGHT OF LOAD, H, FEET
0
10
20
30
40
50
60
70
80
90
100
110
120
130
140
150
160
170
180
0
20
40
60
80

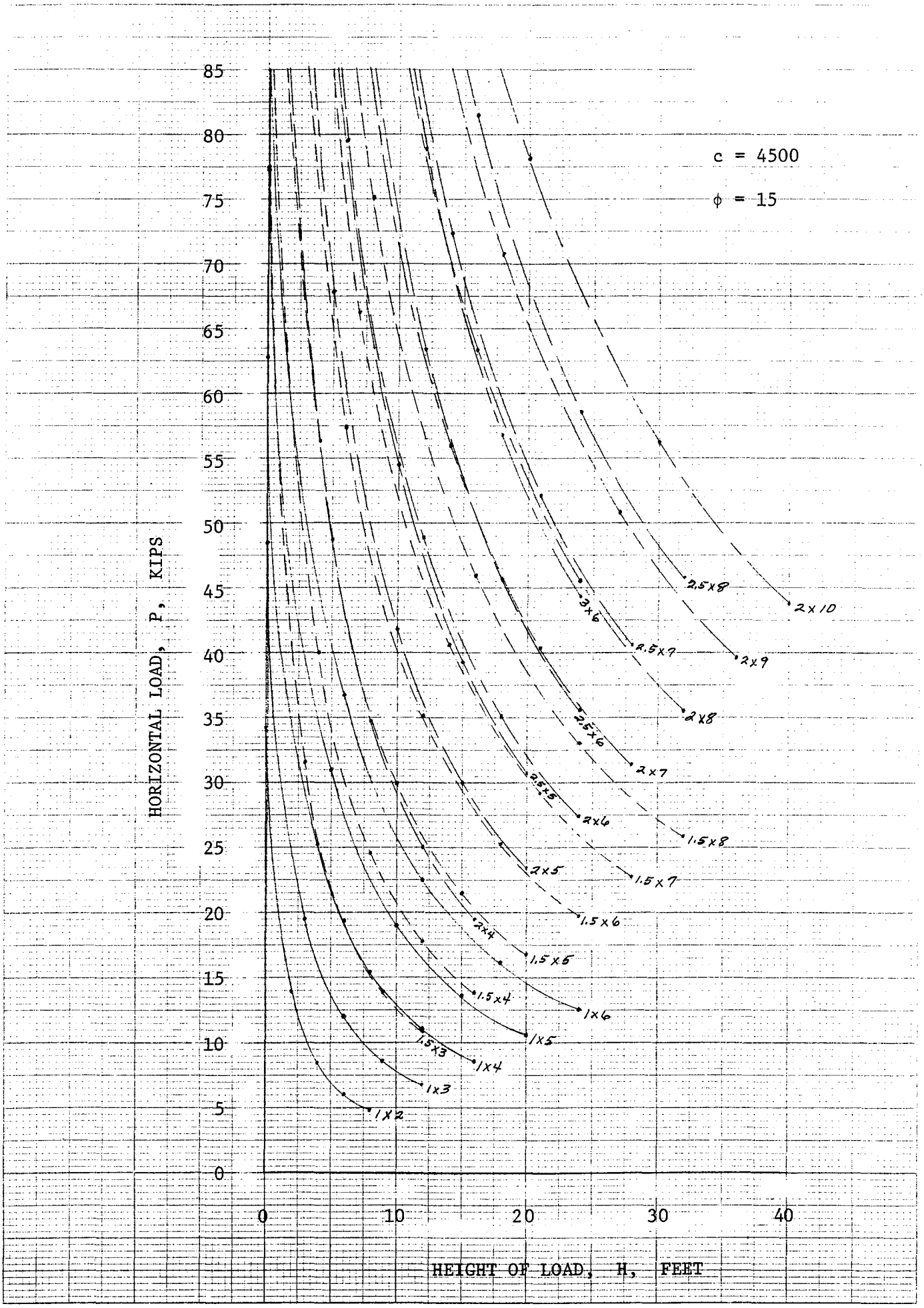
c = 4500
ϕ = 15
HORIZONTAL LOAD, P, KIPS
HEIGHT OF LOAD, H, FEET
0
5
10
15
20
25
30
35
40
45
50
55
60
65
70
75
80
85
0
10
20
30
40
2x10
2.5x8
3x6
2.5x7
2x9
2x8
2.5x6
2x7
2.5x5
2x6
1.5x8
2x5
1.5x7
1.5x6
2x4
1.5x5
1.5x4
1x6
1x5
1.5x3
1x4
1x3
1x2

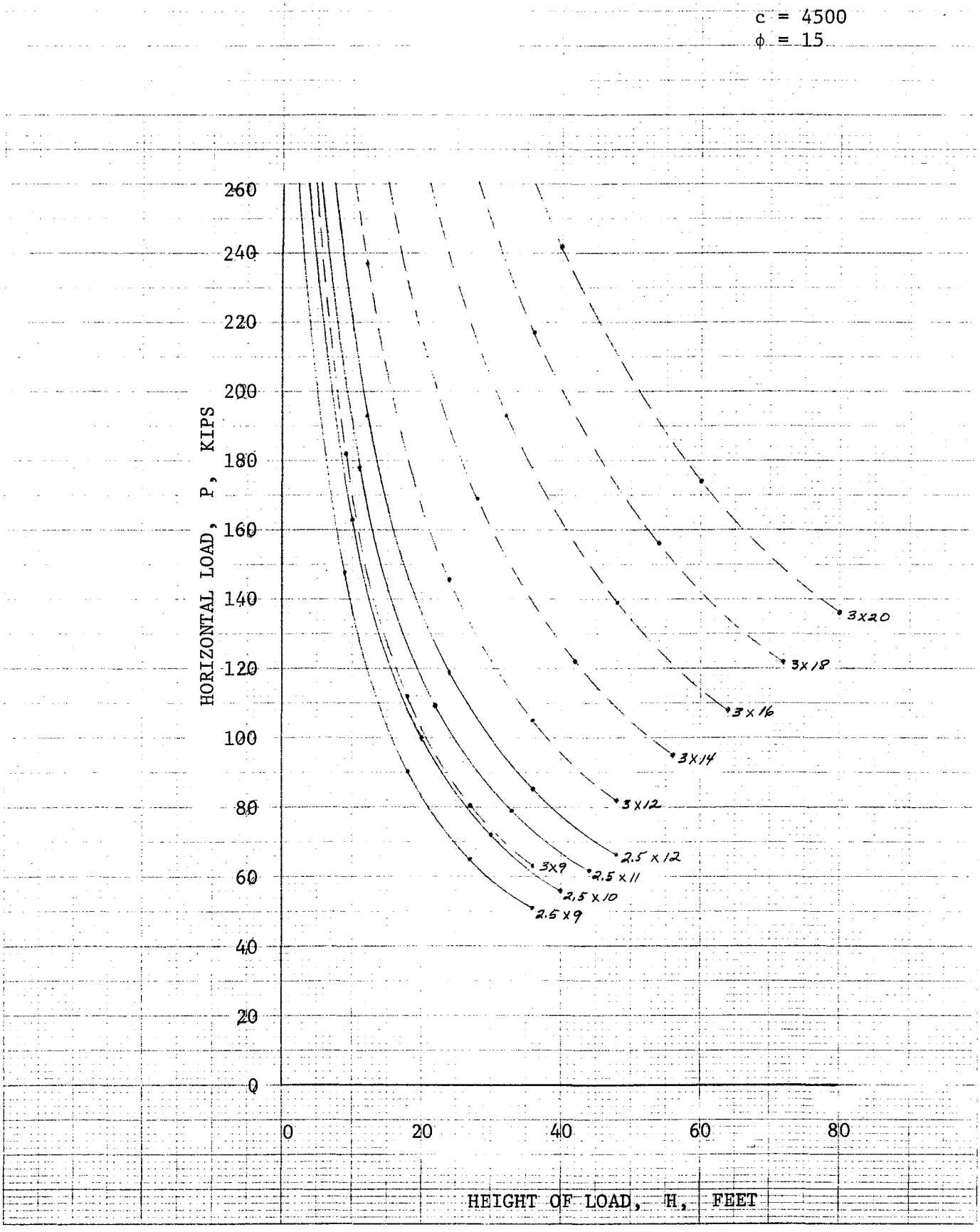
c = 4500
ϕ = 15
HORIZONTAL LOAD, P, KIPS
260
240
220
200
180
160
140
120
100
80
60
40
20
0
0
20
40
60
80
HEIGHT OF LOAD, H, FEET
3X20
3X18
3X16
3X14
3X12
2.5 X 12
3X9
2.5 X 11
2.5 X 10
2.5 X 9

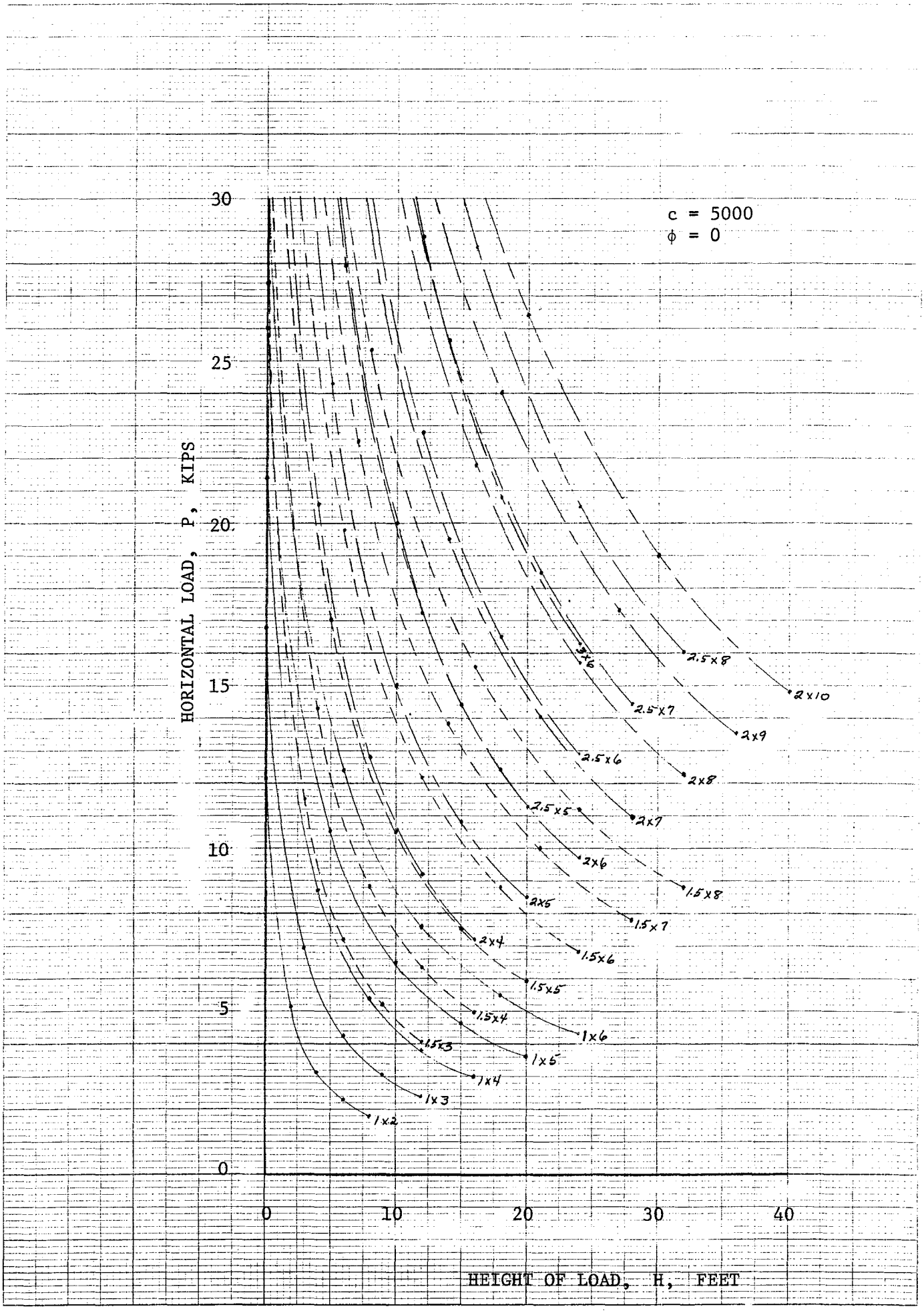
c = 5000
ϕ = 0
HORIZONTAL LOAD, P, KIPS
HEIGHT OF LOAD, H, FEET
0
5
10
15
20
25
30
0
10
20
30
40
1x2
1x3
1x4
1x5
1x6
1.5x3
1.5x4
1.5x5
1.5x6
1.5x7
1.5x8
2x4
2x5
2x6
2x7
2x8
2x9
2x10
2.5x5
2.5x6
2.5x7
2.5x8

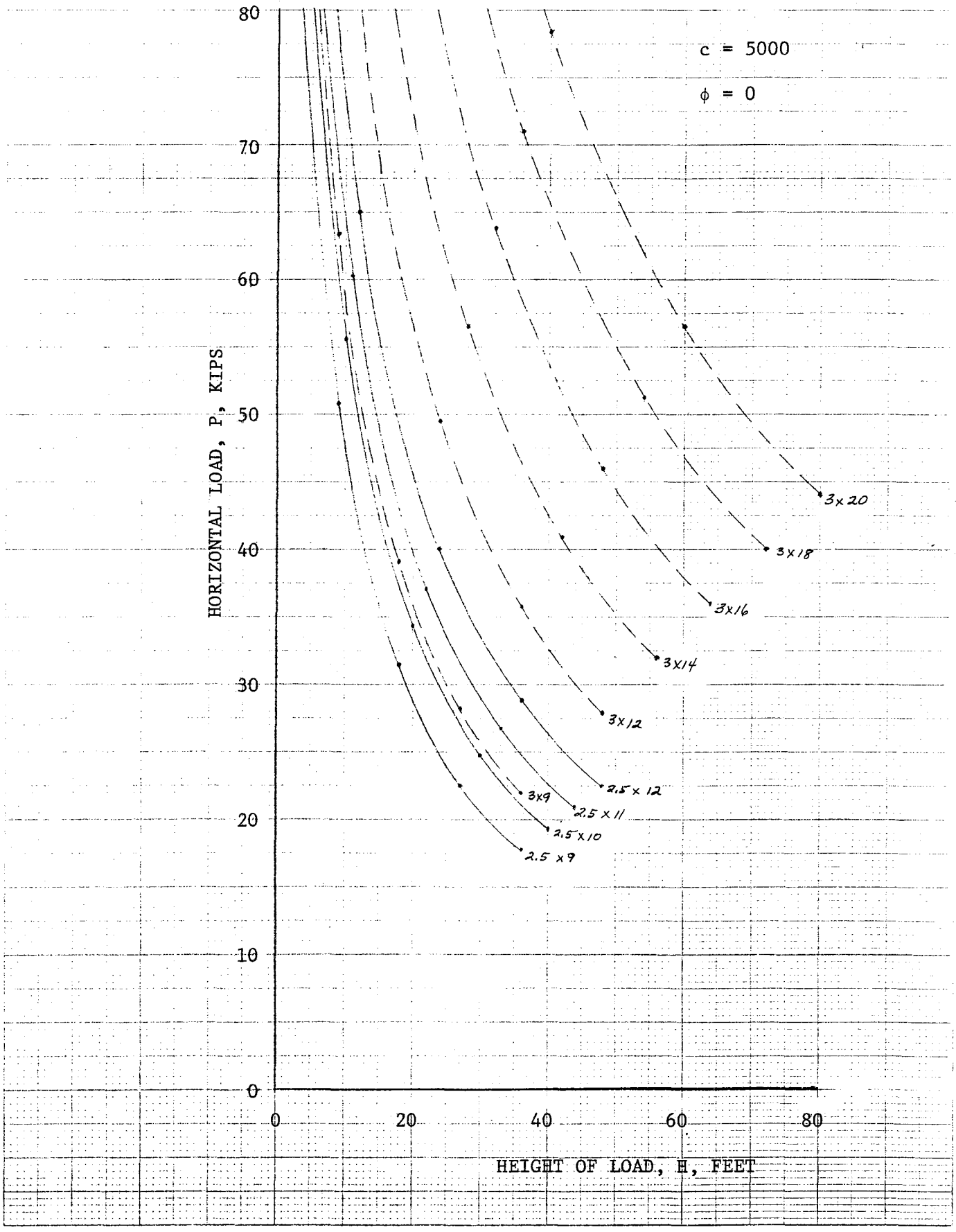
c = 5000
ϕ = 0
3x20
3x18
3x16
3x14
3x12
2.5x12
3x9
2.5x11
2.5x10
2.5x9
HORIZONTAL LOAD, P, KIPS
HEIGHT OF LOAD, H, FEET
0
10
20
30
40
50
60
70
80
0
20
40
60
80

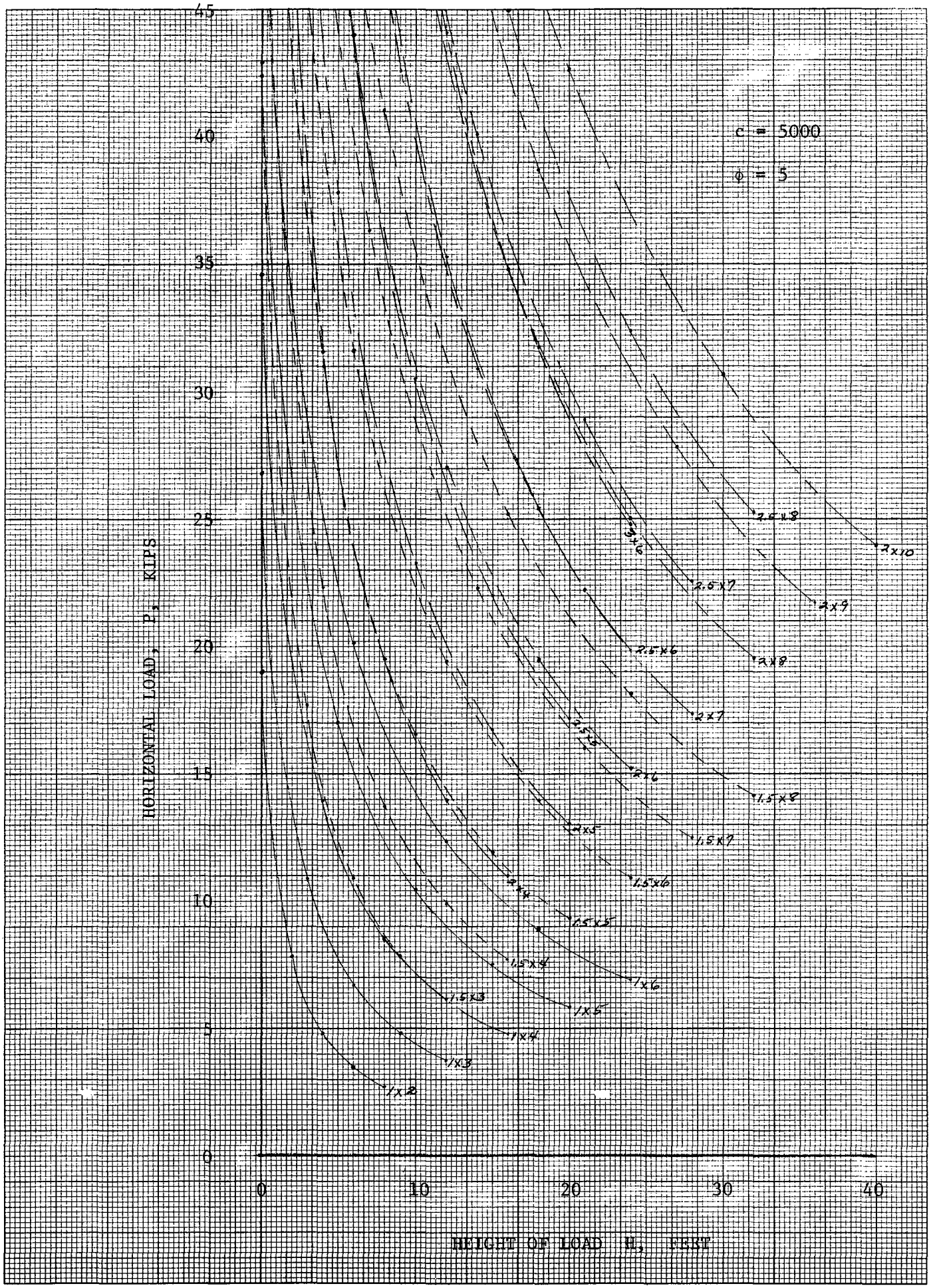

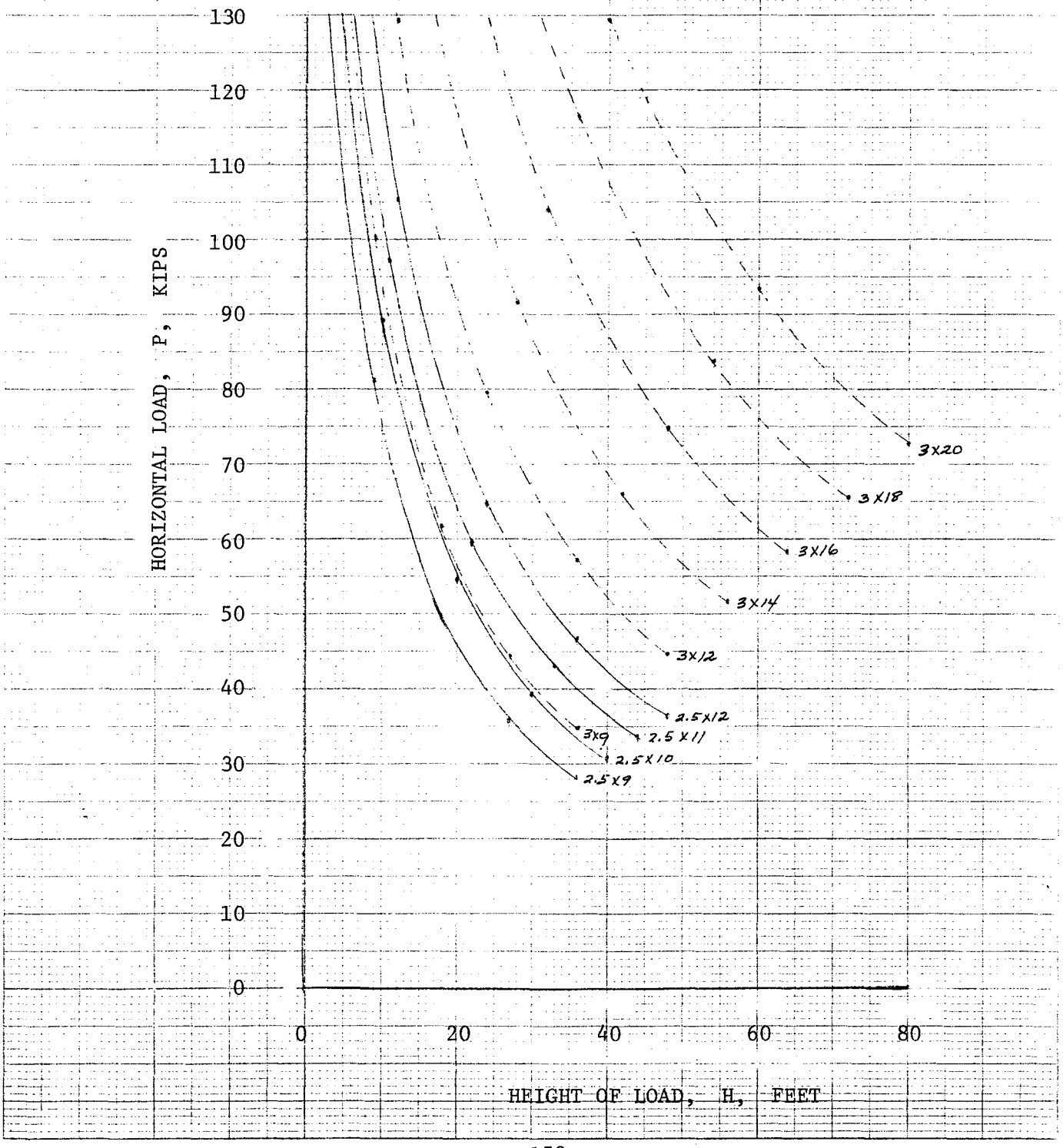
c = 5000
ϕ = 5
HORIZONTAL LOAD, P, KIPS
130
120
110
100
90
80
70
60
50
40
30
20
10
0
0
20
40
60
80
HEIGHT OF LOAD, H, FEET
3X20
3X18
3X16
3X14
3X12
2.5X12
2.5X11
3X9
2.5X10
2.5X9

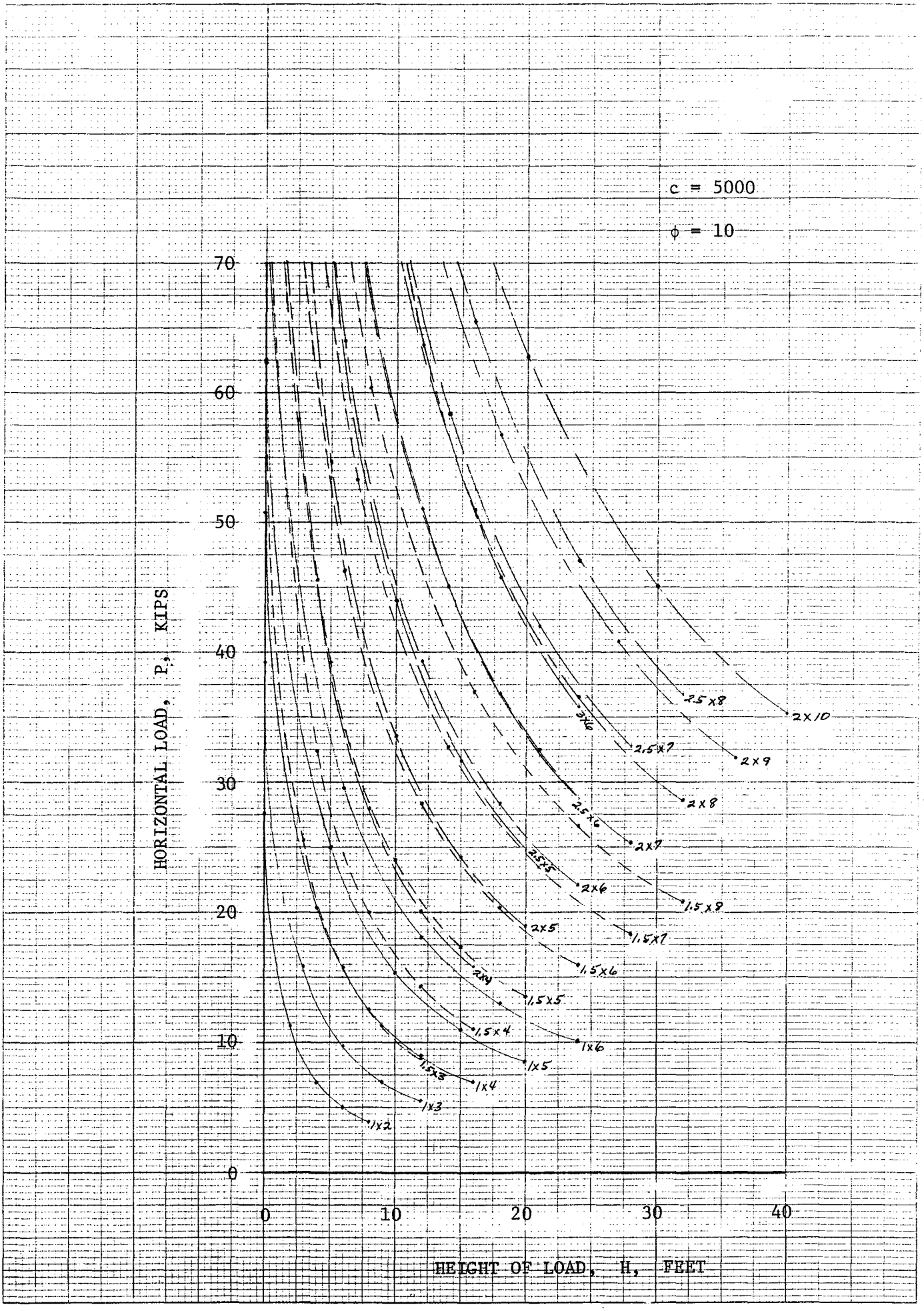
c = 5000
ϕ = 10
HORIZONTAL LOAD, P, KIPS
HEIGHT OF LOAD, H, FEET
0
10
20
30
40
50
60
70
2.5x8
2x10
3x6
2.5x7
2x9
2x8
2.5x6
2x7
2.5x5
2x6
1.5x8
2x5
1.5x7
1.5x6
2x4
1.5x5
1.5x4
1x6
1x5
1.5x3
1x4
1x3
1x2

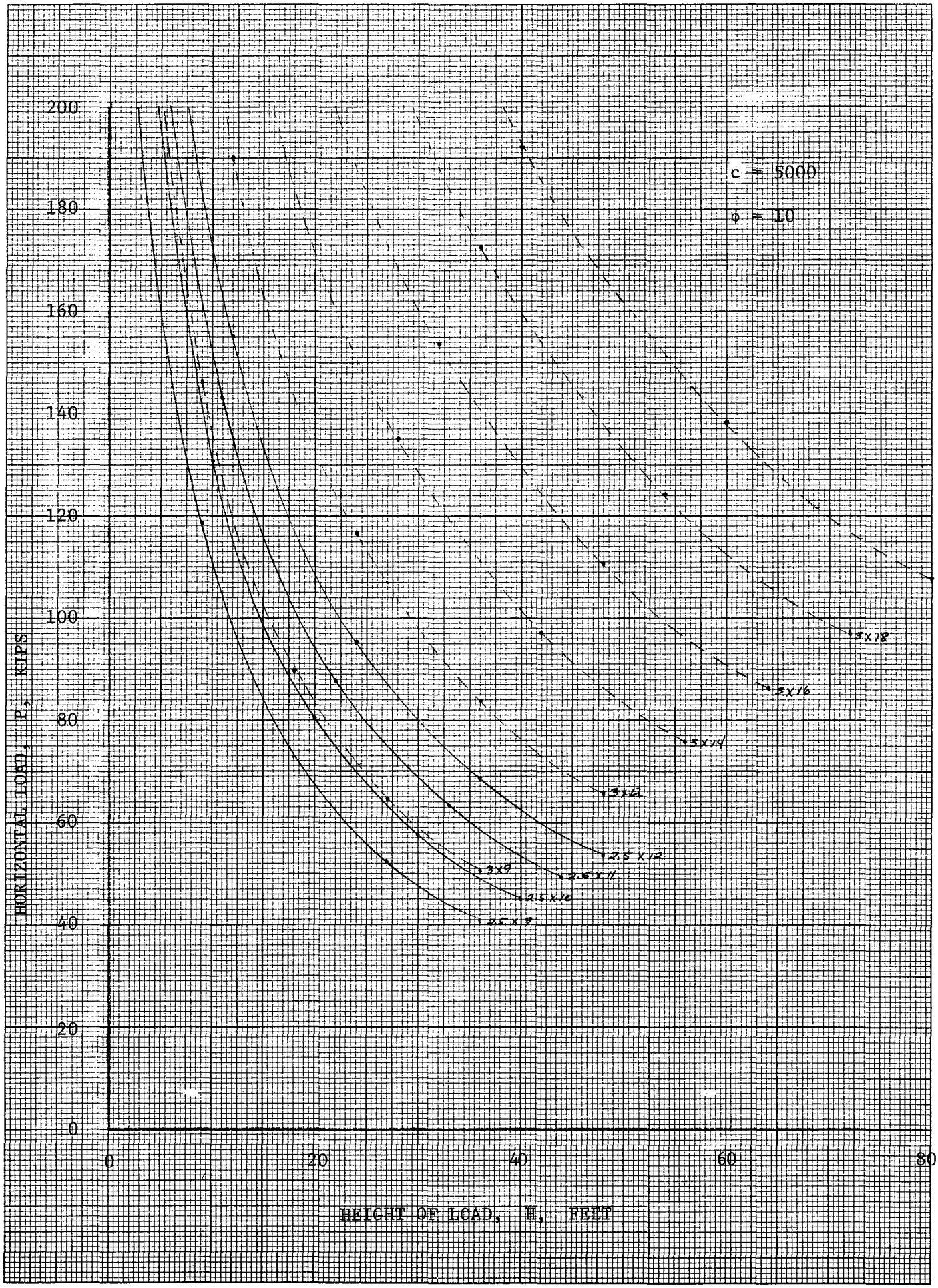

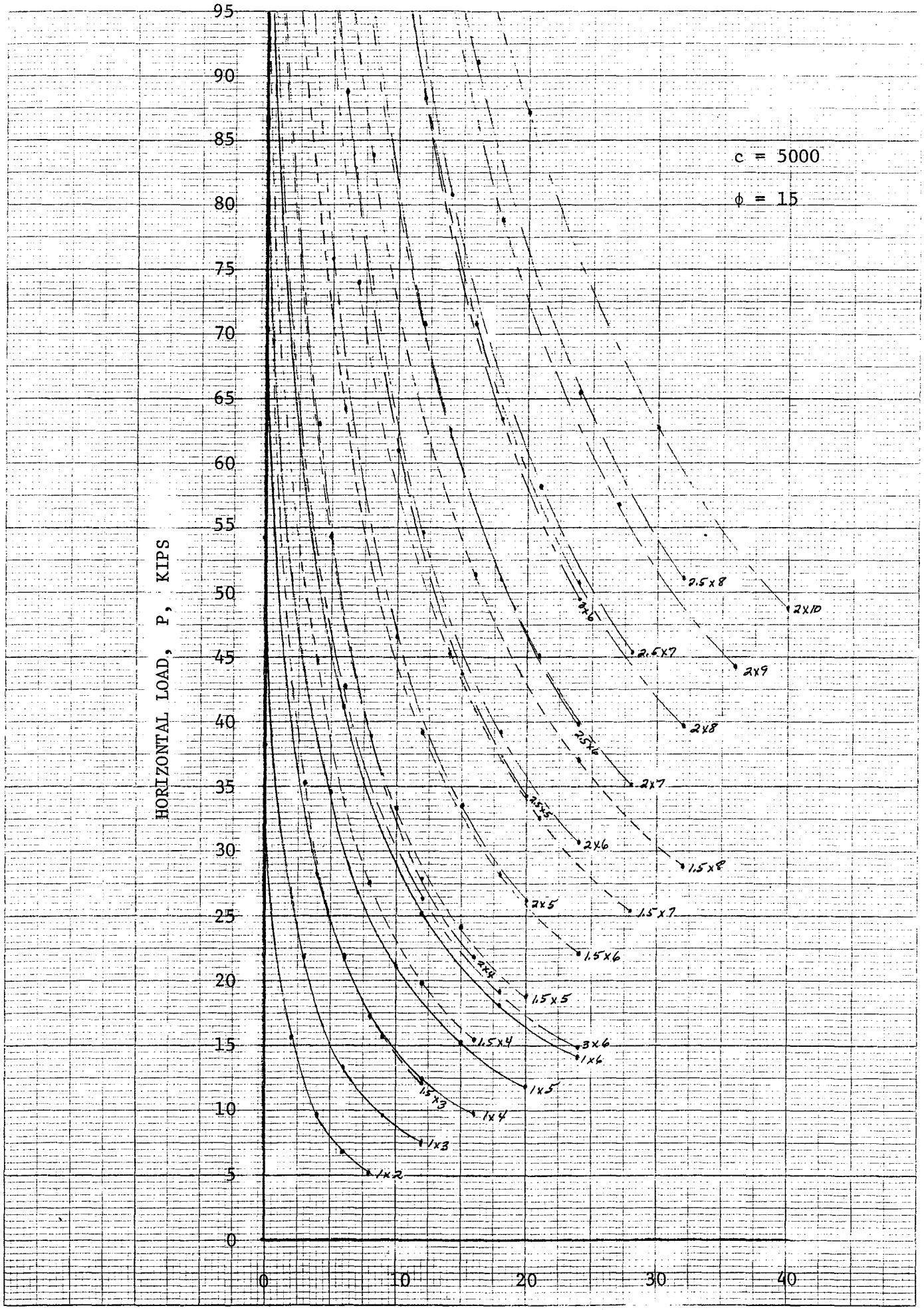
c = 5000
ϕ = 15
HORIZONTAL LOAD, P, KIPS
HEIGHT OF LOAD, H, FEET
95
90
85
80
75
70
65
60
55
50
45
40
35
30
25
20
15
10
5
0
0
10
20
30
40
2.5x8
2x10
2x6
2.5x7
2x9
2x8
2.5x6
2x7
3.5x5
2x6
1.5x8
2x5
1.5x7
1.5x6
2x4
1.5x5
3x6
1.5x4
1x6
1x5
1.5x3
1x4
1x3
1x2

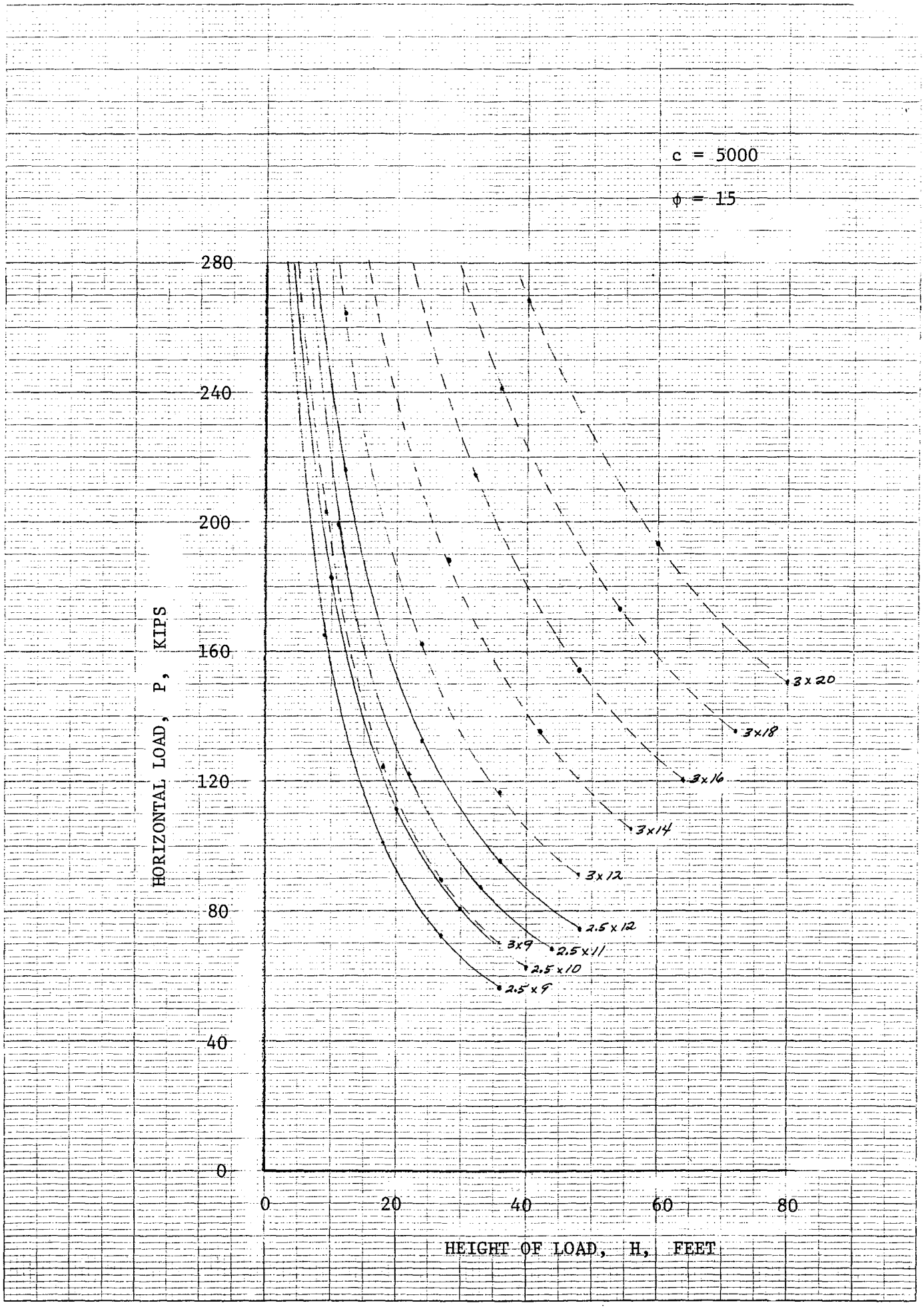
c = 5000
ϕ = 15
280
240
200
160
120
80
40
0
HORIZONTAL LOAD, P, KIPS
0
20
40
60
80
HEIGHT OF LOAD, H, FEET
3x20
3x18
3x16
3x14
3x12
2.5x12
3x9
2.5x11
2.5x10
2.5x9